Proceedings of the

Twenty-Ninth DOE Solar Photochemistry Research Conference

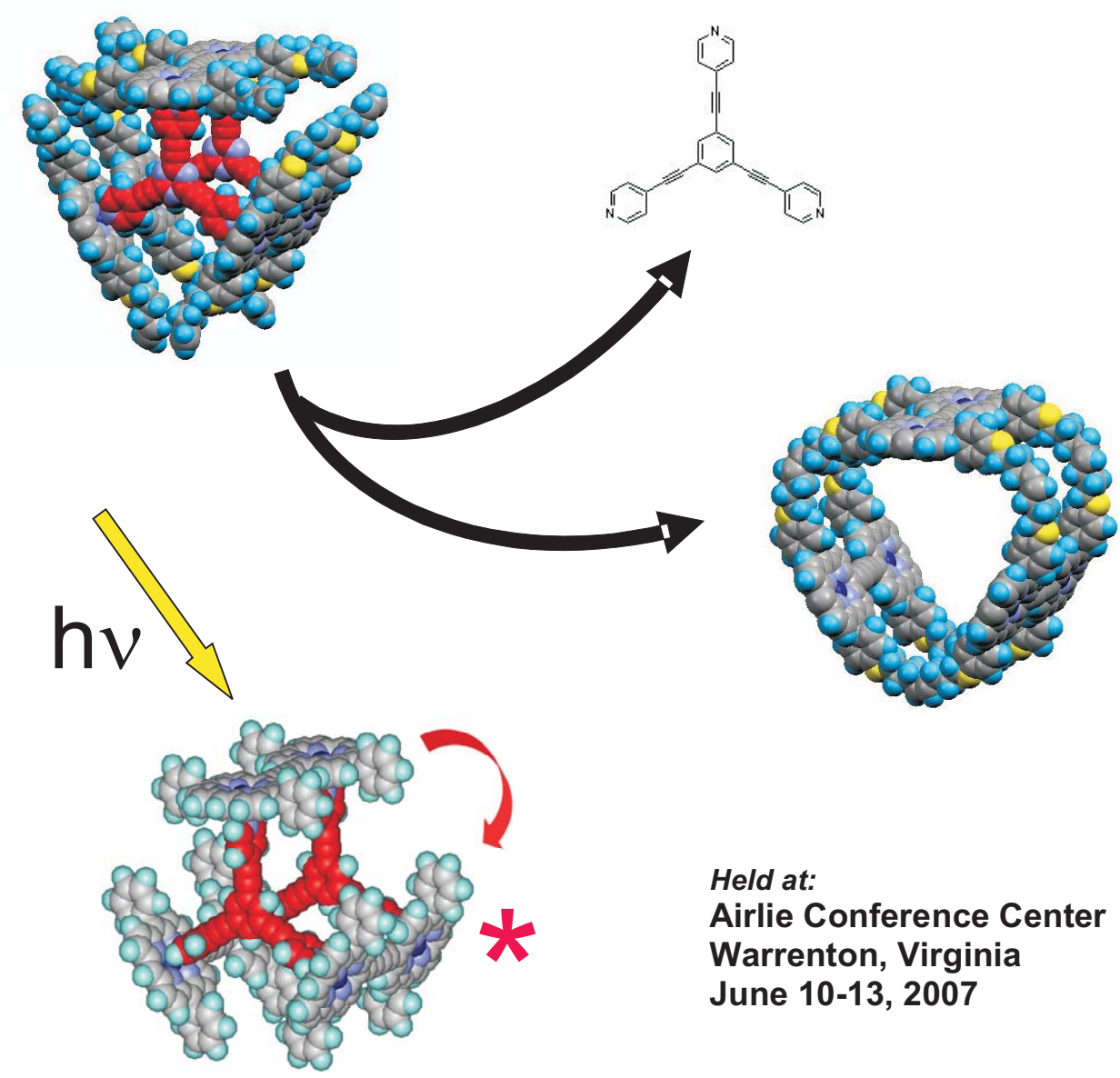

Held at:
Airlie Conference Center
Warrenton, Virginia
June 10-13, 2007

Sponsored by:
Chemical Sciences, Geosciences and Biosciences Division
Office of Basic Energy Sciences
U.S. Department of Energy

Cover Graphics

The figure on the cover portrays prism-shaped assemblies of Zn(II) porphyrins formed through the coordination of three such porphyrin molecules with the triangular triethynylpyridylbenzene and a subsequent covalent linking of the porphyrins with each other around the periphery. The central coordinating molecule can be removed to produce an independent prismatic Zn(II) porphyrin trimer with an enhanced light harvesting capability for use in the spectral sensitization of semiconductor electrodes. Spectroscopic studies of the coordinated porphyrins have shown that a fast energy transfer occurs between the subunits of a trimer unit. (Jospeh Hupp, Northwestern University)

This document was produced under contract number DE-AC05-00OR22750 between the U.S. Department of Energy and Oak Ridge Associated Universities.

FOREWORD

The 29th Department of Energy Solar Photochemistry Research Conference, sponsored by the Chemical Sciences, Geosciences and Biosciences Division of the Office of Basic Energy sciences is being held June 10-13, 2007 at the Airlie Conference Center, in Warrenton, Virginia. The purpose of the meeting is to foster collaboration, cooperation, and the exchange of new information and ideas among grantees and contractors within the Division.

There are many aspects of solar photochemical energy conversion that recommend its exploitation for energy production in a future economy. It may be used to produce fuels, chemicals and electricity through a carbon-neutral pathway and to accomplish those tasks with closed energy cycles and with minimal environmental impact. The DOE solar photochemistry research program supports the study of fundamental processes involved in the capture and conversion of solar energy to chemical or electrical energy. In this endeavor, the program sponsors research across a variety of disciplines in an array of topics. In this proceedings volume are described supported efforts in homogeneous and heterogeneous catalysis for fuel generation, photoelectrochemistry, and basic research in organic and inorganic photochemistry, with an emphasis on light-induced charge transfer. Photosynthetic reaction centers are investigated as models for the design of efficient biomimetic assemblies.

Our special guest plenary lecturer is Professor Frank Willig of the Fritz Haber Institute in Berlin, who will discuss ultrafast electron transfer at dye sensitized semiconductor surfaces from both a theoretical and experimental standpoint. The topical sessions that follow will include presentations on charge separation in supramolecular and photosynthetic-based systems, solar photoconversion in dye sensitized solar cells and in organic polymer constructs, homogeneous photocatalysis, heterogeneous catalysis to produce molecular hydrogen, theory of charge transfer, and the fundamental excitations of quantum particles. The proceedings of this volume include the meeting agenda, abstracts of the 29 formal presentations and forty posters to be presented at the conference, and an address list for the 95 participants.

This proceedings volume is dedicated to Dr. Mary Gress who retired in May of this year after managing the DOE Photochemistry and Radiation Sciences Program for over a quarter of a century. Her personal dedication to the management of this program and her uncompromising standards of excellence in scientific research are the primary reason for the high level of respect given to this program and its grantees. We are grateful for her many years of service. We will miss her leadership and guidance.

I would like to express my appreciation to Lydia Ferguson and the staff of the Airlie Conference Center for their gracious hospitality. Thanks are also due to Sophia Kitts and Margaret Lyday of the Oak Ridge Institute for Science and Education for assistance with the preparation of this volume. I must also thank each of the attendees for their enthusiasm and their spirit of intellectual inquiry that makes this program and this conference a success.

Mark T. Spitler
Chemical Sciences, Geosciences
and Biosciences Division
Office of Basic Energy Sciences

Table of Contents

TABLE OF CONTENTS

Poster Abstracts

Program

29th DOE SOLAR PHOTOCHEMISTRY RESEARCH CONFERENCE

June 10-13, 2007

Airlie Conference Center
Warrenton, Virginia

PROGRAM

Sunday, June 10

5:00 – 11:00 p.m. Reception and Registration
6:30 – 8:00 p.m. Buffet Dinner

Monday Morning, June 11

SESSION I
Plenary Session
Mark T. Spitler, Chair

7:30 a.m. Breakfast, Airlie Dining Room

8:30 a.m. Opening Remarks
Mark Spitler and Eric Rohlfing, Department of Energy

8:45 a.m. Plenary Lecture.
Dynamics of Ultrafast Photoinduced Heterogeneous Electron Transfer
Frank Willig, Fritz Haber Institute, Berlin

9:45 a.m. Coffee Break

SESSION II
Dye Sensitized Solar Cells
Elena Galoppini, Chair

10:15 a.m. Fundamental Studies of Light-Induced Charge Transfer, Energy Transfer, and Energy Conversion with Supramolecular Systems
Joseph T. Hupp, Northwestern University

10:45 a.m. Photoinduced Charge Separation in Molecular Assemblies and Cobalt Polypyridine-Mediated Dye Sensitized Solar Cells
C. Michael Elliott, Colorado State University

11:15 a.m. Tandem Hybrid Solar Energy System
Greg D. Barber, Pennsylvania State University

11:50 a.m. Lunch, Airlie Dining Room

Monday Afternoon, June 11

SESSION III
Solar Photoconversion with Polymers
John R. Miller, Chair

1:00 p.m. Spectroelectrochemistry Studies of Photovoltaic Conjugated Polymers
Paul F. Barbara, University of Texas, Austin

1:30 p.m. Time-Resolved Microwave Photoconductivity Studies of Conjugated Polymer-Nanostructured Heterojunctions
G. Rumbles, National Renewable Energy Laboratory

2:00 p.m. Electronic Defects in π-Conjugated Polymers and their Elimination via Nucleophilic and Electrophilic Addition Reactions
Brian A. Gregg, National Renewable Energy Laboratory

2:30 p.m. Coffee Break

SESSION IV
Molecular Complexes for Energy and Charge Transfer
Michael R. Wasielewski, Chair

3:00 p.m. Photoinduced Charge Separation across Redox Gradients: Organic-Inorganic Composite Dyads with Dendrimeric Sensitizers Bound to Nanocrystalline Semiconductor and Metal Clusters
Marye Anne Fox, University of California, San Diego

3:30 p.m. Photoinduced Energy and Electron Transfer Reactions of Ru(II) and Pt(II) Complexes
Russell Schmehl, Tulane University

4:00 p.m. Solvation and Charge Transfer in Ionic Liquids and Polar Solvents
Mark Maroncelli, Pennsylvania State University

4:30 p.m. Break

SESSION V
Theory of Heterogeneous Charge Transfer
Richard A. Friesner, Chair

5:00 p.m. Theoretical/Computational Probes of Homogeneous and Interfacial Electron Transfer : Electronic Structure and Energetics
Marshall D. Newton, Brookhaven National Laboratory

5:30 p.m Dynamics on the Nanoscale: Time-Domain *ab initio* Studies of Molecule-Semiconductor Interfaces, Quantum Dots and Nanotubes
Oleg Prezhdo, University of Washington

6:30 p.m.. Dinner, Airlie Dining Room

7:30 p.m. Posters (Odd numbers), Jefferson Room
Light Refreshments on Roof Terrace

Tuesday Morning, June 12

7:30 a.m. Breakfast, Airlie Dining Room

SESSION VI
Photoinduced Charge Separation in Photosynthetic-based Systems
Garry Brudvig, Chair

8:30 a.m. Measuring Ultrafast Photosynthetic Function in Single Crystals and Structure in Solution
D. M. Tiede, Argonne National Laboratory

9:00 a.m. Environmental Tuning of Photosynthetic Electron Transfer
Lisa M. Utschig, Argonne National Laboratory

9:30 a.m. Synthetic Analogues of Chlorophylls for Solar-Energy Applications
Jonathan S. Lindsey, North Carolina State University,
David F. Bocian, University of California, Riverside,
and Dewey Holten, Washington University

10:15 a.m. Coffee Break

SESSION VII
Photocatalytic Systems
Daniel G. Nocera, Chair

10:30 a.m. Photoinitiated Electron Collection in Mixed-Metal Supramolecular Complexes: Development of Photocatalysts for Hydrogen Production
Karen J. Brewer, Virginia Polytechnic Institute and State University

11:00 a.m. Polynuclear Photocatalytic Sites on Nanoporous Silica Supports for H_2O Oxidation and O_2 Reduction
Heinz Frei, Lawrence Berkeley National Laboratory

11:30 a.m. Transition Metal-Based Reactions for Photogeneration of Fuels
David C. Grills, Brookhaven National Laboratory

Tuesday Afternoon, June 11

12:15 p.m. Lunch
1:30 p.m. Depart for Winery Expeditions

Tuesday Evening, June 11

SESSION VIII
Charge Separation in Supramolecular Systems
Marye Anne Fox, Chair

5:30 p.m. Supramolecular Structures for Photochemical Energy Conversion
Devens Gust, Thomas A. Moore, and Ana L. Moore
Arizona State University

6:00 p.m. "Electrochemically Wired" Dye-Modified Dendrimers and Semiconductor Nanoparticles in Sol-Gel Films: Toward Vectoral Electron Transport in Hybrid Materials and Solar-Assisted Hydrogen Production
Neal R. Armstrong and Jeffery Pyun
University of Arizona

6:30 p.m. Social Hour, Pavilion
7:30 p.m. Cookout, Pavilion

8:30 p.m. Posters (Even numbers)
Light Refreshments on Roof Terrace

Wednesday Morning, June 13

7:30 a.m. Breakfast

Session IX
Quantum Particles for Solar Photoconversion
Louis E. Brus, Chair

8:30 a.m. Fundamental Photochemical Properties of Single-Wall Carbon Nanotubes
M.J. Heben, National Renewable Energy Laboratory

9:00 a.m. Exciton and Charge Separation Dynamics in Quantum Dot Heterojunctions
David F. Kelley, University of California, Merced

9:30 a.m. Multiple Exciton Generation in Colloidal Semiconductor Nanocrystals and Nanocrystal Arrays for Efficient Solar Energy Conversion
R. J. Ellingson, National Renewable Energy Laboratory

10:00 a.m. Coffee Break

Session X
Novel Photoelectrode Morphology
Neal R. Armstrong, Chair

10:30 a.m. Photoelectrochemistry of Semiconductor Nanowire Arrays
Thomas E. Mallouk, Pennsylvania State University

11:00 a.m. Electrochemical Synthesis of Inorganic Electrodes with Controlled Micro- and Nano-Structures for Use in Solar Energy Conversion
Kyoung-Shin Choi, Purdue University

11:40 a.m. Lunch, Airlie Dining Room

Session XI
Hydrogen Evolution at Photocatalytic Surfaces
Arthur J. Nozik, Chair

12:45 p.m Sunlight-Driven Hydrogen Formation by Membrane-Supported Photoelectrochemical Water Splitting
Nathan S. Lewis, California Institute of Technology

1:15 p.m Fundamental Investigations of Water Splitting on Model TiO_2 Photocatalysts Doped For Visible Light Absorption
M. A. Henderson, Pacific Northwest National Laboratory

1:45 p.m Catalyzed Water Oxidation by Solar Irradiation of Band Gap Narrowed Semiconductors
Etsuko Fujita, Brookhaven National Laboratory

2:15 p.m A Combination Method for Discovery of Water Photoelectrolysis Catalysts
B. A. Parkinson, Colorado State University

2:45 p.m Closing Remarks
Mark Spitler and Richard Greene, U.S. Department of Energy

Session I

Plenary Session

DYNAMICS OF ULTRAFAST PHOTOINDUCED HETEROGENEOUS ELECTRON TRANSFER

Frank Willig*, Lars Gundlach[§], Ralph Ernstorfer[&], V. May[#]

*Fritz-Haber-Institute of the Max-Planck-Society, Faradayweg 4-6, 14195 Berlin, Germany
[§]Chemistry Department, Rutgers University, 73 Warren Street, Newark, NJ 07102-1811, USA
[&]Chemistry Department, University of Toronto, 80 St. George Street, Ontario M5S 3H6, Canada
[#]Institute of Physics, Humboldt University, Newtonstrasse 15, 12489 Berlin, Germany

Electron transfer (ET) is a fundamental reaction ubiquitous in our natural and technical environment. R. Marcus has developed the celebrated classical theory of ET for molecular reactants in a solvent environment where all the vibrational modes are in thermal equilibrium. Several authors have presented perturbative quantum theoretical models for ET. ET at electrodes (HET) plays an important role in fields like electrochemistry, surface science, and catalysis and in devices like batteries and fuel cells. For photo-induced HET (PHET) the molecular reactant state is created via photon absorption. Recently PHET has been utilized to drive an efficient photo-electrochemical solar cell. It is being discussed in the context of future devices for optical data storage and molecular electronics. From the basic science point of view the dynamics of PHET represents a more general case compared to HET of thermalized reactants. In PHET the excited molecule can be photo-generated in a non-thermalized state from where ET can occur ultrafast and prior to the establishment of a thermalized energy distribution. A typical example is shown in the Fig. 1 with an ET time of 9 femtoseconds from the chromophore perylene to TiO_2(110) via the anchor group -COOH. The latter forms a strong chemical bond on the surface. Adsorption of chromophores via their bridge-anchor groups from solution on single crystals was carried out in a special ultra-high-vacuum chamber designed for this purpose [1]. To allow for a meaningful comparison both, 2PPE measurements on single crystals [2] and transient absorption measurements on colloidal layers [3,1] were carried out under ultra-high-vacuum conditions. Selecting a chromophore like perylene with pronounced vibrational structure in the linear absorption spectrum allows for determining the time constant of ultrafast HET already from a fit to the line-broadened linear absorption spectrum of the adsorbed chromophore [4]. For the system shown in Fig. 1 PHET from each excited vibrational level of the chromophore is much faster than energy redistribution and relaxation.

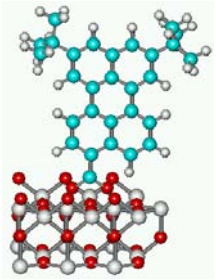

Fig. 1 The chromophore perylene anchored via the carboxylic group on TiO_2 (110). The HET time constant for this system is 9 fs.

Electron transfer can be slowed down by inserting a rigid saturated bridge group like bicyclooctane between the chromophore and the anchor group (Fig. 2). This leads to intermediate HET dynamics where electron transfer and intramolecular vibrational energy redistribution are occurring on comparable time scales. For the system shown in Fig. 2 the ET time is 165 fs.

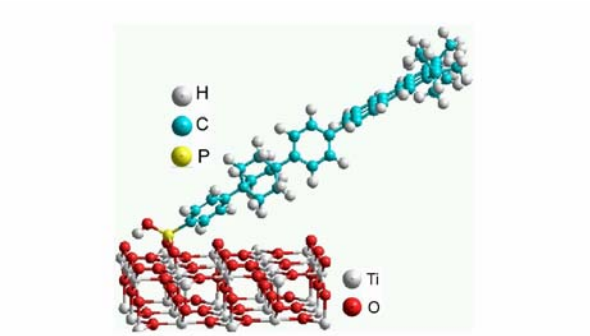

Fig. 2 Insertion of the bicyclooctane bridge groups slows down electron transfer. Surface bonds formed by the phosphonate anchor group lead to an angle of 66˚ of the long axis against the surface normal.

There are two border cases to ultrafast PHET, on one side instantaneous direct optical charge transfer transitions as described by Mulliken for molecular donor-acceptor pairs, and on the other side sufficiently slow HET occurring from thermalized reactants as addressed by Marcus theory. On the surface of a single crystal one can determine the orientation, distance and alignment of the chromophore with respect to the surface plane and the direction of lattice vectors (Fig. 2) [5]**.** Fs-2PPE of ultrafast HET yields the injection time of the excited donor molecule [2]. It can reveal the escape dynamics of the injected electron [6] and important properties like the initial energy distribution and subsequent scattering and escape processes. A satisfactory theoretical model of reduced dimensionality has been developed for describing PHET which correctly predicts the essential observables, in particular also the broad Franck-Condon controlled energy distribution for the injected electron [7,8]. The energetic situation addressed as wide band limit leads to an injection time which is independent of any Franck-Condon factor and is only controlled by the strength of the electronic coupling. Virtues and shortcomings of ultrafast PHET from molecules will be discussed with respect to solar energy conversion.

References

1. R. Ernstorfer, L. Gundlach, S. Felber, W. Storck, R. Eichberger, F. Willig, J. Phys. Chem. B 110 (2006) 25383
2. L. Gundlach, R. Ernstorfer, F. Willig, Progress in Surface Science (2007) in print.
3. B. Burfeindt, T. Hannappel, W. Storck, F. Willig, J. Phys. Chem. 100 (1996) 16463.
4. L. Wang, V. May, R. Ernstorfer, F. Willig, J. Phys. Chem. B 109 (2005) 9589.
5. L. Gundlach, J. Szarko, L.D. Socaciu-Siebert, A. Neubauer, R. Ernstorfer, F. Willig, Phys. Rev. B 75 (2007) 125320.
6. L. Gundlach, R. Ernstorfer, F. Willig, Phys. Rev. B 74 (2006) 035324.
7. S. Ramakrishna, F. Willig, V. May, Phys. Rev. B 62 (2000) R16330.
8. L. Wang, F. Willig, V. May, Molecular Simulations 32 (2006) 765.

Session II

Dye Sensitized Solar Cells

FUNDAMENTAL STUDIES
OF LIGHT-INDUCED CHARGE TRANSFER, ENERGY TRANSFER,
AND ENERGY CONVERSION
WITH SUPRAMOLECULAR SYSTEMS

Joseph T. Hupp
Department of Chemistry
Northwestern University
Evanston, IL 60208

Summary of Project. This project seeks to exploit supramolecular chemistry: a) to interrogate and understand fundamental aspects of light-induced charge transfer and energy transfer, and b) to construct solar energy conversion systems that make use of unique assembly motifs to address key conversion efficiency issues.

Energy and electron transfer in self-assembling light-harvesting structures. We have been exploring dye systems that allow us to harvest a large fraction of the visible and near-IR spectrum. Our attention has been on highly conjugated porphyrin systems similar to those developed by Anderson and coworkers and by Therien and coworkers. These offer much higher extinction coefficients than the standard ruthenium dyes employed in Gratzel cells and much better spectral coverage than conventional porphyrin molecules. At the same time, they feature much lower intersystem crossing yields than do conventional porphyrins, so are much less susceptible to degradation by singlet oxygen.

We have been learning how to organize these promising chromophores into well-defined supramolecular assemblies and are now exploring the fundamental photophysics of such arrays. One example is shown below in simplified form (i.e. solubilizing groups are omitted). In this system we have been able to observe rapid panel-to-panel energy transfer via an unusual approach that exploits singlet-singlet annihilation reactions (collaborative work with Wasielewski at Northwestern). From the study we find that energy transfer is rapid: ca. 2.5 ps. When the panels are further displaced by using a larger trigonal component as a panel organizer (see ligand structure below) we find that energy transfer slows to about 30 ps. Since this is still about two orders of magnitude faster than singlet excited state decay, it is clear that the new structures are capable of functioning effectively as light-harvesting arrays.

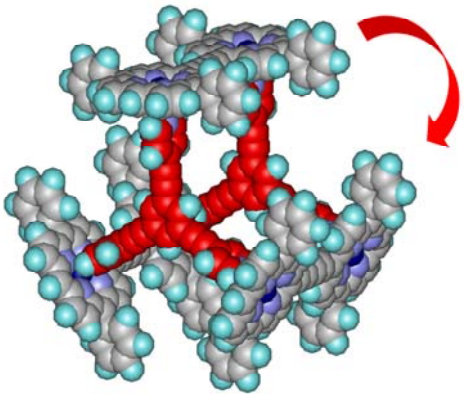

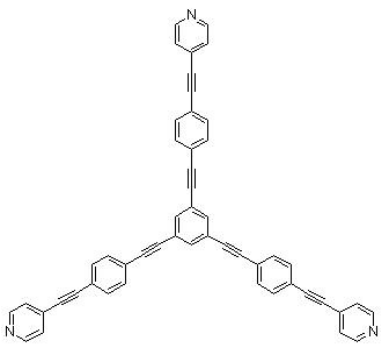

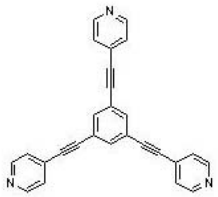

Related work has focused on interrogating electron transfer reactions. In these studies the organizing units have a second function: they serve as electron acceptors. We find that transient DC photoconductivity (TDCP) can be used to distinguish fast recombination from slow recombination. It also can be used to measure directly the true charge separation distance.

Grubbs-type olefin metathesis chemistry has been used to link panels covalently once they are coordinatively organized as prisms. Following covalent linking, the templated units can be removed, leaving the structures intact as established directly by solution-phase x-ray scattering and diffraction (collaborative work with Tiede at Argonne). We find that the prisms can be readily demetallated, with the resulting free-base poly-porphyrinic prisms possessing strikingly different electronic spectral properties. Re-metallation with ions other than Zn(II) is being used to facilitate higher order supramolecular chemistry, e.g. well-defined assembly of multiple prisms into highly oriented super-assemblies. A focus of current work is the reliable multi-point attachment of the assemblies to photoelectrodes.

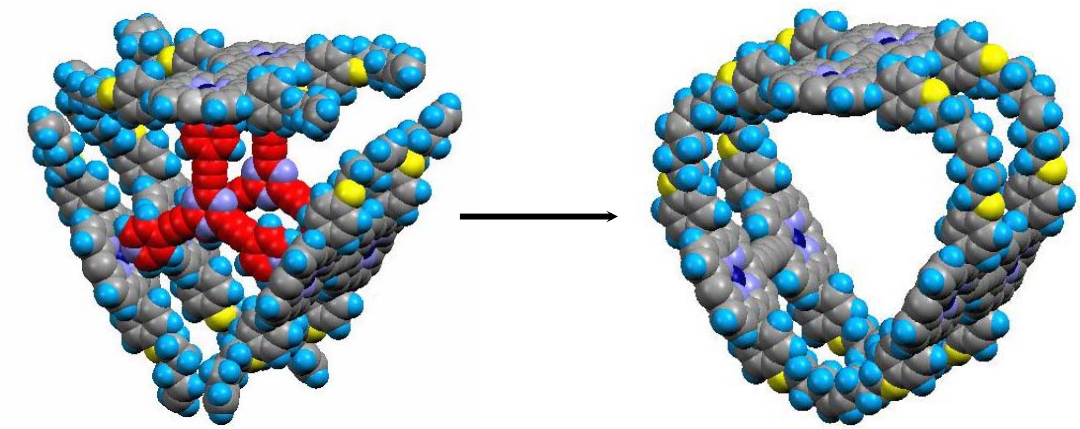

Electrodes. Finally, an issue in synthesis-intensive dye design is the possibility of mismatch of dye excited-state energies with band-edge energies. *Re*design of such dyes to alter their energies is inefficient and often synthetically impractical. Consequently, we are focusing on a new approach: band-edge engineering via composition-controlled fabrication (atomic layer deposition) of high-area mixed-metal-oxide photoelectrodes.

DOE Sponsored Publications 2005-2007

1. "Borderline Class II/III Ligand-Centered Mixed-Valency in a Porphyrinic Molecular Rectangle", P. H. Dinolfo, J. T. Hupp, and S. J. Lee, *Inorg. Chem.*, **2005**, 44, 5789-5797.

2. "Contrasting Electroabsorbance Behavior of Two Borderline Class II/Class III Mixed Valence Systems", P.H. Dinolfo, Robert D. Williams and Joseph T. Hupp, *Chem Phys.*, **2005,** 319, 28-38. (Special Volume in honor of A.M. Kuznetsov)

3. “C- and Z-Shaped Coordination Compounds: Synthesis, Structure and Spectroelectrochemistry of cis- and trans-$[Re(CO)_3(L)]_2$-2,2´-bisbenzimidizolate with L = 4-Phenylpyridine, 2,4´Bipyridine, or Pyridine”, P. H. Dinolfo, K. D. Benkstein, C. L. Stern, and J. T. Hupp, *Inorg. Chem.*, **2005**, 44, 8707-8714.

4. “pH-Dependent Electron Transfer from Re-bipyridyl Complexes to Metal Oxide Nanocrystalline Thin Films”, C. She, N. A. Anderson, J. Guo, F. Liu, W. H. Goh, D. T. Chen, D. Mohler, Z. Q. Tian, J. T. Hupp, and T. Lian, *J. Phys. Chem. B*, **2005**, 109, 19345-19355.

5. "Porphyrin-Containing Molecular Squares: Design and Applications" S. J. Lee and J. T. Hupp, *Coord. Chem. Rev.*, **2006**, *206*, 1710-1723.

6. "Organic Photovoltaics Interdigitated on the Molecular Scale" A. B. F. Martinson, A. M. Massari, S. J. Lee, R. W. Gurney, K. E. Splan, J. T. Hupp, and S. T. Nguyen**,** *J. Electrochem. Soc.*, **2006**, *153*, A527-A532.

7. “The Underlying Spin-Orbit Coupling Structure of Intervalence Charge Transfer Bands in Dinuclear Polypyridyl Complexes of Ruthenium and Osmium” D. M. D’Allessandro, P.H. Dinolfo, M.S. Davies, J. T. Hupp, and F. R. Keene, *Inorg. Chem.*, **2006**, *45*, 3261-3274.

8. “The Effective Electron Transfer Distance in Dinuclear Ruthenium Complexes Containing the Unsymmetrical Bridging Ligand 3,5-bis(2-pyridyl)-1,2,4-triazolate” D. M. D’Alessandro, P. H. Dinolfo, J. T. Hupp, P. C. Junk, and F. R. Keene, *Eur. J. Inorg. Chem.* **2006**, *2006*, 772-783.

9. “Rhenium-linked Multiporphyrin Assemblies: Synthesis and Properties”, J. T. Hupp, *Structure and Bonding* **2006**, *121*, 145-165.

10. “Dynamics of Charge Transport and Recombination in ZnO Nanorod Array Dye Sensitized Solar Cells” A. B. F. Martinson, J. E. McGarrah, M. O. K. Parpia, and J. T. Hupp, *Phys. Chem. Chem. Phys.*, **2006**, *8*, 4655-4659.

11. “Atomic Layer Deposition of In_2O_3 Using Cyclopentadienyl Indium: A New Synthetic Route to Transparent Conducting Oxide Films” J. W. Elam, A. B. F. Martinson, M. J. Pellin, and J. T. Hupp, *Chem. Mater.*, **2006**, *18*, 3571-3578.

12. “A New Class of Mixed-Valence Systems with Orbitally Degenerate Organic Redox Centers Based on Hexa-Rhenium Molecular Prisms” P. H. Dinolfo, V. Coropceanu, J-L. Brédas, and J. T. Hupp, *J. Am. Chem. Soc.*, **2006**, *128*, 12592-12593.

13. "Supramolecular Porphyrinic Prisms: Coordinative Assembly and Solution-phase X-ray Structural Characterization" S. J. Lee, K. L. Mulfort, J. L. O'Donnell, X. Zuo, A. J. Goshe, S. T. Nguyen, D. M. Tiede, J. T. Hupp, *Chem. Commun*., **2006**, *44*, 4581 - 4583.

14. "Rhenium-linked Multiporphyrin Assemblies: Synthesis and Properties" J. T. Hupp, *Structure and Bonding*, E. Alessio Ed., **2006**, *121*, 145-165.

15. "Comparison of Interfacial Electron Transfer Through Carboxylate and Phosphonate Anchoring Groups" C. She, J. Guo, S. Irle, K. Morokuma, D. L. Mohler, F. Odobel, J. T. Hupp, and T. Lian, *J. Phys. Chem. B,* **2007**, ASAP.

16. "ZnO Nanotube Dye-Sensitized Solar Cells" A. B. F. Martinson, J. W. Elam, J. T. Hupp, M. J. Pellin, *Nano Letters*, **2007**, in revision.

17. "Rhenium-linked Multiporphyrin Assemblies: Synthesis and Properties" J. T. Hupp, *Structure and Bonding*, E. Alessio Ed., **2006**, *121*, 145-165.

18. "Novel Photoanode Architectures and Tunneling Barriers" T. W. Hamann, A. B. F. Martinson, J. W. Elam, M. J. Pellin and J. T. Hupp, *ACS Fuel Division Preprints*, **2007**, accepted.

19. "Transparent Conducting Oxides at High Aspect Ratios by ALD" M. J. Pellin, J. W. Elam, J. A. Libera, A. B. F. Martinson, and J. T. Hupp, *J. Electrochem. Soc*., accepted.

DOE-Supported Ph.D. Theses

"Electron Transfer Study of Dye Sensitized Nanocrystalline Metal-Oxide Semiconductors and Design of Multilayered Dye-Sensitizers" Fang Liu, Dept. of Chemistry, Northwestern University, **2006**.

PHOTOINDUCED CHARGE SEPARATION IN MOLECULAR ASSEMBLIES AND COBALT POLYPYRIDINE-MEDIATED DYE SENSITIZED SOLAR CELLS

C. Michael Elliott[a], M. T. Rawls[a], J. M. Weber[a], M. J. Scott, J. J. Nelson, U. E. Steiner[b] , S. Caramori[c], , and C. A. Bignozzi[c]

(a) Department of Chemistry, Colorado State University, Ft Collins CO 80523,
(b) Fachbereich Chemie, Universität Konstanz, D-78457 Konstanz, Germany,
(c) *Dipartimento di Chimica, Università di Ferrara, Via Luigi Borsari 46, 44100 Ferrara*

Molecular Assemblies. It is now well established that photoinduced charge separation can be effected at the molecular level by systems incorporating a chromophore (C), an electron donor(D) and an electron acceptor(A). Often, these systems have low to modest quantum efficiencies for forming charge-separated states (CSS) because the rate of geminate recombination of the initial photoproducts is faster than or, at least comparable with, the rate of charge separation. However, large quantum efficiencies for CSS formation (Φ_{CSS}) can be observed but they are just not particularly common. Furthermore, when they are observed, they are usually associated with a single D-C-A molecule within a series. Donor-chromophore-acceptor molecular assemblies, where the chromophore is a ruthenium bipyridine complex and the donor is an azine (i.e., phenoxazine, phenothiazine or phenoselenazine--represented in the figure to the right), behave qualitatively differently. These assemblies have large quantum efficiencies for charge separated state formation which *extend across the entire class of assemblies*. Irrespective of the details of driving force and, to a large extent, structure, these molecules all form CSSs with almost unity quantum efficiencies. To understand the origin of this large efficiency, we have conducted studies on photoinduced electron transfers in systems consisting of a chromophore-acceptor diad (C-A) and freely diffusing azine donor. Results from these studies clearly show that the donor is not oxidized in a bimolecular event, rather it is in an equilibrium ground-state association with the chromophore prior to photoexcitation. This observation leads to the conclusion that a similar intramolecular C/D association happens in the D-C-A triad assembly and it is this association that is responsible for the near-unity quantum efficiency for charge separation.

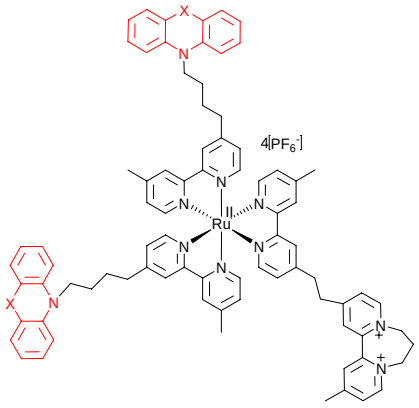

Another notable feature of these particular D-C^{2+}-A^{2+} triads is the magnetic field dependence of their photoinduced CSS decay. Earlier it was established that when D = phenothiazine (i.e., X = S in the structure of the above figure), the cation radical pair comprising the CSS, $D^{+\bullet}$-C^{2+}-$A^{+\bullet}$, is formed with virtually pure triplet spin correlation. Thus, the back electron transfer to form the singlet ground state is effectively spin forbidden. As a result, the CSS decay kinetics exhibit a strong magnetic field dependence. The decay kinetics become strongly biexponential with applied fields as small as a few millitesla. At fields at or above ca. 500 mT, the average lifetime of the

CSS has increased by ca. ×10 relative to zero applied field. In order to more fully understand the spin-chemical aspects of CSS decay, we prepared a series of D-C^{2+}-A^{2+} triads wherein only the heteroatom of the donor was changed from O, S and Se. Across this series of donors, there is only a very modest difference in redox potential (<200 mV) but there is over an order of magnitude difference in spin-orbit coupling for the heteroatom. Investigations of the magnetic field dependence of CSS decay within this series of molecules have allowed us to understand the spin-chemical control of that process.

Electron-Transfer Mediation in Dye Sensitized Solar Cells. Similar to the photo-process operational in molecular assemblies, charge separation across the interface between a photoexcited adsorbed dye molecule and a wide bandgap semiconductor nanoparticle (e.g., TiO_2) comprises the primary photo-event in dye sensitized solar cells (DSSCs). Subsequent to this initial electron transfer, electrons must be shuttled from the cathode to the oxidized dye. Historically, I^-/I_3^- has proven most efficient in this electron-transfer mediation. The I^-/I_3^- couple has ideal kinetic properties: specifically, the regenerative reduction of the dye by I^- is very fast and the recombination of I_3^- with photoinjected electrons in the TiO_2 is extremely slow. On the other hand, I^-/I_3^- has a number of drawbacks. Certain polypyridine Co(II) complexes (e.g., with DTB = 4,4'-di-*t*-butyl-2,2'-bipyridine) have been shown to be reasonably efficient mediators in DSSCs; however, compared to I^-/I_3^-, these complexes generally exhibit slower dye re-reduction and faster recombination with photoinjected electrons. We have examined the issue of sluggish dye^+ reduction by $Co(DTB)_3^{2+}$ by considering mediator mixtures in which a co-mediator, characterized by a fast electron transfer reaction, is used in conjunction with $Co(DTB)_3^{2+}$. The figure to the right shows the recovery kinetics of photooxidized dye (Z907) on mesoporous TiO_2 in contact with several solutions of reductants. Both phenothiazine (PTZ) and ferrocene (Fc), both of which are thermodynamically poorer reductants than $Co(DTB)_3^{2+}$, reduce the photooxidized dye much more rapidly. Yet, because they are weaker reductants, once oxidized, they are rapidly reduced by $Co(DTB)_3^{2+}$ in solution. Therefore, the steady-state concentration of either PTZ^+ or Fc^+ remains quite small and they are unavailable to engage in any parasitic reaction with photoinjected electrons. Such mediator/co-mediator combinations can have a positive impact on cell performance relative to the $Co(DTB)_3^{2+/3+}$ mediator alone.

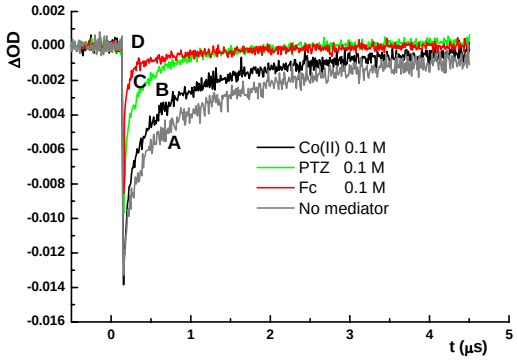

DOE-Supported Publications (2005-2007)

Elliott, CM; Caramori, S; Bignozzi, CA. "Indium-tin oxide electrodes modified with tris(2,2'-bipyridine-4,4'-dicarboxylic acid)iron(II) and the catalytic oxidation of tris(4,4'-di-*tert*-butyl-2,2'-bipyridine)cobalt(II)," Langmuir 21, 3022-3027 (2005).

Cazzanti, Silvia; Caramori, Stefano; Argazzi, Roberto; Elliott, C. Michael; Bignozzi, Carlo Alberto. "Efficient Non-Corrosive Electron-Transfer Mediator Mixtures for Dye Sensitized Solar Cells," J. Amer. Chem. Soc. 128(31), 9996-9997 (2006).

Weber, JM; Rawls, M.T.; MacKenzie, VJ; Limoges BR; Elliott, C.M. "High Energy and Quantum Efficiency in Photoinduced Charge Separation" J. Amer. Chem Soc. 129, 313-320 (2007).

Rawls, M.T.; Kollmannsberger, G.; Elliott, C.M.; Steiner, U.E. Spin Chemical Control of Photoinduced Electron-Transfer Processes in Ruthenium(II)-Trisbipyridine-Based Supramolecular Triads: 2. The Effect of Oxygen, Sulfur, and Selenium as Heteroatom in the Azine Donor," J. Phys. Chem A,Web Release Date: 14-Apr-2007; (Article) DOI: 10.1021/jp070221s.

Scott, M.J.; Nelson, J.J.; Caramori, S.; Bignozzi, C.A.; Elliott, C.M. "*cis*-dichloro-bis(4,4'-dicarboxy-2,2-bipyridine)osmium(II)-Modified Optically Transparent Electrodes: Application as Cathodes in Stacked Dye Sensitized Solar Cells," (submitted April 2007) Inorg. Chem.

TANDEM HYBRID SOLAR ENERGY SYSTEM

Greg D. Barber, Paul G. Hoertz, Neal M. Abrams, Seung-Hyun Lee, Lara I. Halaoui, and Thomas E. Mallouk
Materials Research Institute and Department of Chemistry
Pennsylvania State University
University Park, PA 16802

Our DOE sponsored work has focused on the development of a tandem hybrid solar energy system for photoelectrochemical conversion of sunlight utilizing nanoscale material development to create efficient dye-sensitized titania based solar cells. Our goal is to leverage all aspects of chemistry, materials science, optics, engineering, and manufacturability to develop a 20% efficient generation II photoelectrochemical system for hydrogen and solar energy generation.

Tandem hybrid solar energy system. The continued rapid worldwide growth of the solar industry and expansion of the semiconductor industry has created tremendous price increases in silicon solar product due to a constrained availability of refined polycrystalline silicon. Past DOE reports predict concentrator systems to be the lowest cost solar systems due to their minimal use of solar device area but current concentrator systems only work under direct normal radiation and thus deployment is limited. To increase deployment and lower costs, we have developed a tandem hybrid approach that combines low cost dye sensitized solar cells (DSSCs) built into the reflector of a parabolic Si concentrator system. The DSSCs utilize diffuse and visible light similar to flat plate Si systems while directing near-IR photons to a Si concentrator cell by spectrum splitting mirrors built into the DSSC cells. We have measured an outdoor system level efficiency of 14.3-14.5% using an array of ~1 cm^2 DSSCs interconnected in series-parallel with a Si module placed at the focal point.

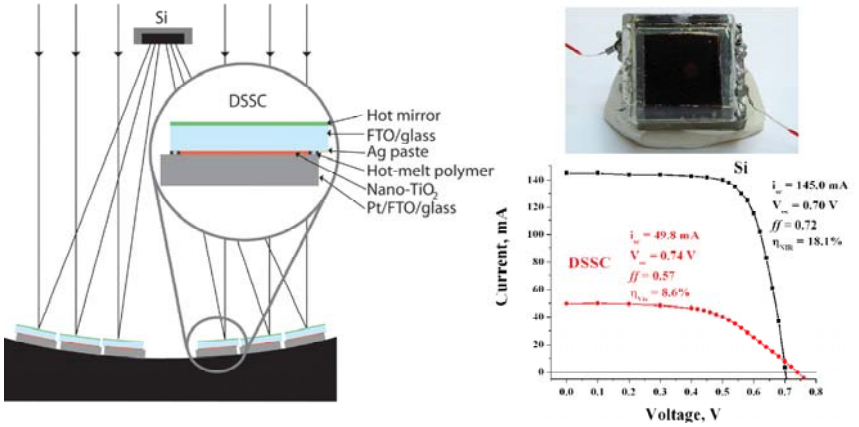

Figure 1. Schematic diagram of the spectrum splitting concentrator cell. Hot mirror coated DSSCs reflect near infrared light onto a Si p-n junction cell (1.2 x 1.2 cm). Insets show a photograph of an individual DSSC and current-voltage curves for the DSSC array and Si cell.

High efficiency Dye Sensitized Solar Cell Development. The major challenge of the construction of the tandem device has been the optimization and reproducibility of individual DSSC performance. Despite many attempts to follow published literature procedures for high

efficiency DSSCs, in the above demonstrations, the DSSCs had an outdoor efficiency of ~5.5% under global radiation loads. The realization of 10% DSSCs reliably from our current level will require the incorporation of a light scattering layer as previously reported by Grätzel et al. and Arakawa et al. These particle based scattering approaches enhance absorption at ~550-700 nm. We use an inverse opal photonic crystal (PC), structure, which is a more efficient scatterer. We have shown that TiO_2 inverse opals enhance 550-700 nm photon absorption in a transparent counter electrode DSSC configuration. The wavelength region at which enhanced backscattering occurs can be tuned by controlling the PC interlayer spacing or the filling fraction during TiO_2 infiltration. We have verified theoretical predictions by Miguez, et al., that DSSCs incorporating photonic crystals offer higher performing cells.

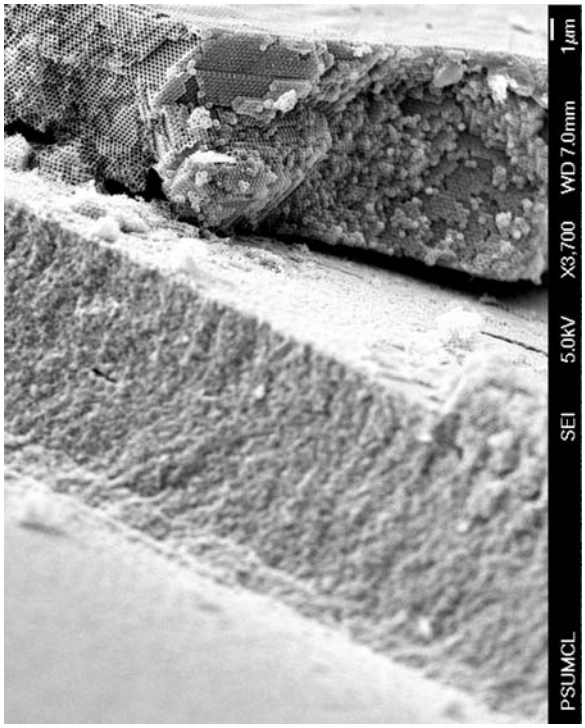

Figure 2. FESEM image of a photonic crystal (top) enhanced DSSC (middle) FTO.

Bonded Titanium Foils to Transparent Conducting Oxides. Published values from the Grimes group at PSU for the splitting of water show titania nanotubes may make the highest performing DSSCs. We have thus been investigating bonding techniques of readily available titanium foils to FTO substrates to enhance manufacturability and complement the work of the Grimes group. Our methods of bonding and preliminary anodization results of titanium bonded to FTO will be presented along with preliminary photoelectrochemical results.

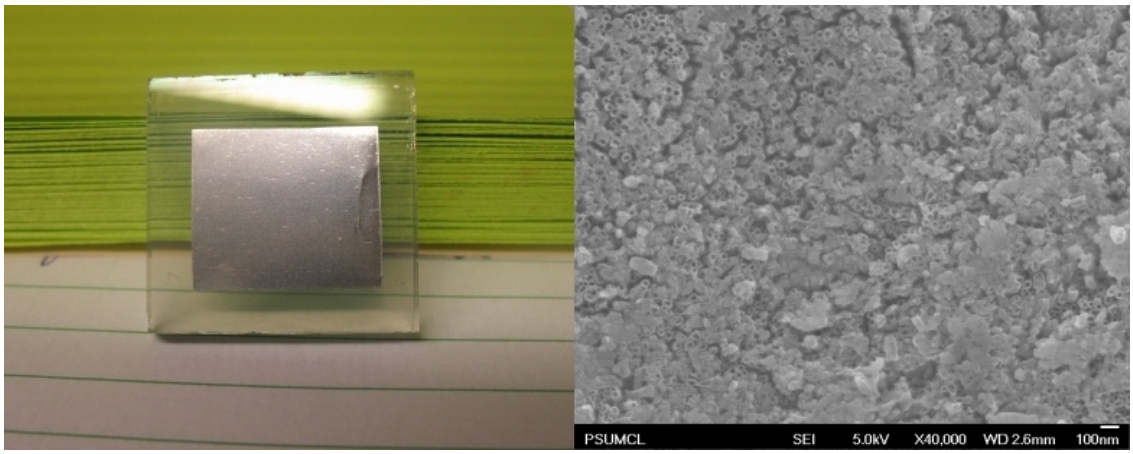

Figure 3. *Left:* Photograph of a titanium foil bonded to a transparent conducting electrode. *Right:* The titanium foil after anodization.

DOE Sponsored Publications 2005-2007

1. “An Efficient Dye-Sensitized Solar Cell-Silicon Hybrid System,” Paul G. Hoertz, Neal M. Abrams, Janine Mikulca, Greg D. Barber, and Thomas E. Mallouk, resubmitted to Science, April 2007.

2. G. D. Barber, T. E. Mallouk, P. G. Hoertz, and S. H. Lee, “Tandem Hybrid Concentrator System,” Provisional Patent Application submitted to U.S. Patent Office, March 2007.

Session III

Polymeric Solar Photoconversion

SPECTROELECTROCHEMISTRY STUDIES OF PHOTOVOLTAIC CONJUGATED POLYMERS

Rodrigo E. Palacios, Fu-Ren F. Fan, Allen J. Bard, and Paul F. Barbara
Department of Chemistry and Biochemistry and the Center for Nano- and Molecular Science and Technology, University of Texas, Austin, TX 78712

We describe an approach to the determination of the thermodynamics and kinetics of electron transfer (eT) to single immobilized molecules based on single molecule spectroelectrochemistry (**SMS-EC**). Such eT reactions are of interest in solar cells, flat-panel displays and chemical sensors.[1-5] The extreme heterogeneity of inorganic/organic interfaces has been a key obstacle to developing a quantitative, molecular-level understanding of such devices. Here we introduce a powerful new technique for studying eT processes at highly heterogeneous interfaces. **SMS-EC** measures electrochemical behavior one molecule at a time, offering for the first time the distribution of key electrochemical variables, e.g. the half-wave potential, $E_{1/2}$, not just the ensemble average. **SMS-EC** is used herein to study the oxidation at an indium tin oxide (ITO) electrode of single molecules of the organic conjugated polymer poly(9,9-dioctylfluorene-*co*-benzothiadiazole) (F8BT), used in solar cells and OLEDs.

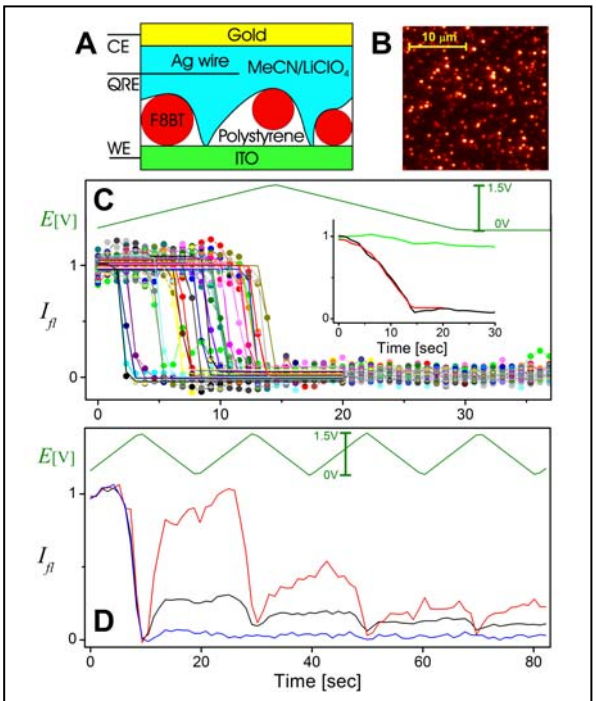

Figure 1. (**A**) SMS-EC cell configuration. (**B**) Wide-field TIRF image for a SMS-EC cell. (**C**) Examples of normalized single-molecule fluorescence-intensity trajectories (data points) that were obtained while applying the bias shown by the top green curve, and corresponding fits ($I_{fl}(t)_i \approx 1/(1+\exp((E-E_{1/2,i})/\delta E)$ with a variable $E_{1/2,i}$ for each molecule and a global δE of < 0.1 eV. Insert: Ensemble average of 200 trajectories (black curve) and of their corresponding fits (red curve). The green curve shows the ensemble average of 200 trajectories obtained at zero bias. (**D**) Ensemble average of normalized single-molecule fluorescence intensity trajectories 20 s time range. The green curve shows the applied bias.

The unique ability of single molecule spectroelectrochemisry, SMS-EC, to unravel complex electrochemical process in heterogeneous media is used to study the oxidation of nanoparticles of the practically important conjugated polymer poly (9,9-dioctylfluorene-*co*-benzothiadiazole) (F8BT). Two main processes have been observed, an irreversible chemical reaction on the surface of the oxidized F8BT nanoparticles, and a reversible hole-injection charging process. The latter occurs primarily by initial injection of shallow (untrapped) holes, but soon after the injection, the holes become deeply trapped. Good agreement between experimental data and simulations strongly supports the presence of deep traps in the studied nanoparticles and highlights the ability of SMS-EC to study deep traps in organic materials at the nanoscale.

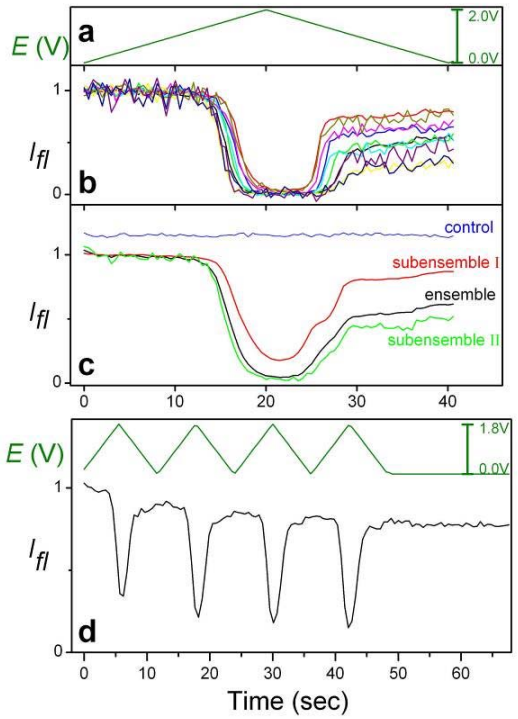

Figure 2. a, Applied bias between working and reference electrodes (*E*). **b,** Examples of normalized single-aggregate fluorescence-intensity trajectories obtained while applying the *E* shown in panel A to a pristine cell. **c,** Ensemble average (50 particles, black curve) and subensembles constructed by sorting the particles based on their intensities. The top 25 highest intensity particles were averaged to give subensemble I (red curve), the remaining particles were averaged to give subensemble II (green curve). The blue curve shows the total ensemble average obtained at 0 volts. **d,** Total ensemble average (black curve) obtained while applying multiple potential cycles (green curve) to a pristine cell.

The discharging process occurs much more slowly than the injection process, and, given the coupling of potential and time during a potential sweep experiment, appears over a much larger potential range (which is also consistent with Fig. 2).This implies that hole injection occurs initially to shallow sites (to produce untrapped holes) but soon after injection, the holes are deeply trapped by either relaxation of the polymer structure (self-trapping) or by transfer from the initial site of hole injection to a deep-trapped hole site. The shape of the $I_{fl}(t)$ data are qualitatively consistent with a highly efficient trapping of the initially injected holes, implying a density for either types of holes that exceeds 10^{21} holes/cm^3. This suggests that deep trapped holes are not rare defect sites, but rather are a relaxed form of the shallow traps. The deep trapping of hole in the present experiments, could in principle be due to charge trapping at the nanoparticle/electrolyte interface. In particular, slow penetration (diffusive mass transport) of negative ions from the electrolyte solution into the surface layer of the nanoparticles could assist the trapping of holes in the film. This is analogous to the operation of super capacitors.

To explore in more detail the formation and decay kinetics of deep traps pulsed bias experiments were performed on nanoparticles samples. Simulations are able to reproduce the two main features associated with the presence of deep traps, i.e. slow intensity recovery after oxidationand a decrease in intensity with increasing pulse duration. When the formation of deep traps is excluded from the model, the resulting simulations (Fig. 3, red curves) can not reproduce these two main features. The good agreement between experimental data and simulations strongly supports the presence of deep traps in the studied nanoparticles and highlights the ability of SMS-EC to study deep traps in organic materials at the nanoscale. A detailed analysis of the "best-fit" simulations indicates that the trapping rate constant is surprisingly slow (k_T= 0.6×10^{-3} (2×10^{-3}) s^{-1}) and only a small fraction (<1%) of the shallow traps are converted to deep traps in a typical SMS-EC experiment. Nevertheless, deeply trapped holes contribute significantly to the SMS-EC data at long time due to the high efficiency of exciton quenching by holes.

We also report on the spectroscopy of isolated chains of important photovoltaic material, P3OT,

in a highly dilute solution in the inert polymer host poly(methyl-methacrylate) (PMMA). This environment permits a detailed analysis of emission transitions in the 1.9-2.2 eV range by suppressing the formation of the lowest energy aggregated form of P3OT. Herein it is observed that the 1.9-2.2 eV band is in fact split into low (red) and high (blue) energy forms in a highly analogous situation to that found for the conjugated polymer MEH-PPV. Another focus of this work is an investigation of the interaction of singlet and triplet excitons in P3OT. The results indicate that, like in MEH-PPV, triplet excitons are highly efficient fluorescence quenchers for P3OT, strongly quenching the fluorescence of the P3OT under even relatively low excitation intensities.

DOE Sponsored Publications 2005-2007

1. Palacios, R. E., Fan, F.-R. F., Bard, A. J. & Barbara, P. F. Single-Molecule Spectroelectrochemistry (SMS-EC). *Journal of the American Chemical Society* **128**, 9028-9029 (2006).

2.Rodrigo Palacios and Paul F. Barbara, Single Molecule Spectroscopy of Poly 3-alkyl-thiophene, *Journal of Fluorescence*, in press.

3. Rodrigo E. Palacios, Fu-Ren F. Fan, Allen J. Bard, and Paul F. Barbara, Spectroelectrochemistry Studies of the Charging and Discharging of Single Conjugated-Polymer Nanoparticles, *Nature Materials*, submitted (final revision).

4. Tieqiao Zhang, Young Jong Lee, Tak W. Kee and Paul F. Barbara, The Mechanism of Electron-Cation Geminate Recombination in Liquid Isooctane *Chem. Phys. Lett.* 403, 4-6, 257 (2005).

5. So-Jung Park; Stephan Link; William L Miller; Andre Gesquiere, and P. F. Barbara; Effect of Electric Field on the Photoluminescence Intensity of Single CdSe Nanocrystals, *Chemical Physics,* submitted.

TIME-RESOLVED MICROWAVE PHOTOCONDUCTIVITY STUDIES OF CONJUGATED POLYMER-NANOSTRUCTURE HETEROJUNCTIONS

G. Rumbles, N. Kopidakis, A.J. Ferguson, X. Ai,
S. Shaheen, T.J. McDonald and M.J. Heben

Chemical and Biosciences Center
National Renewable Energy Laboratory
Golden, Colorado 80401-3393

We have recently established flash photolysis, time-resolved microwave conductivity (TRMC) as a tool for detecting, predominantly, charged carriers that are produced either directly or indirectly from a pulse of light that excites a sample of interest. Over the past year we have applied this technique to a number of specific problems where the light-absorbing system is the conjugated polymer, poly(3-hexylthiophene), P3HT. This polymer has become established as one of the most efficient polymers in excitonic solar cells, where it not only acts as the light absorber and electron donor, but also a good transporter of holes. It is far from ideal as an active component of a photovoltaic device, but it does provide an excellent system for studying the fundamental photochemistry and photophysics that takes place at a junction with an electron acceptor, such as C_{60}, a metal oxide, a colloidal quantum dot, or a single-walled carbon nanotube (SWNT). We have recently studied all four of these chemical systems using the TRMC technique, and the conclusions from these studies will be reported.

The primary step in generating carriers in the bulk heterojunction, excitonic solar cell is the transport and dissociation of a photo-generated exciton into separated charge carriers. Recombination and trapping of these carriers competes with their transport to the external electrodes where they can be used to do useful work. This presentation will discuss three specific examples of electron-acceptor systems: magnesium-doped zinc oxide, a soluble derivative of C_{60} (PCBM), and isolated single-wall carbon nanotubes.

The doping of zinc oxide with magnesium provides a method of raising the conduction band by 400 meV which, presumably, changes the driving force for free carrier separation at the interface. We investigated the impact of Mg doping on the kinetics of photo-induced electron transfer of excitons created in a thin film of P3HT deposited onto the oxide. Increasing the magnesium content from 0-40%, we observed a significant drop in electron mobility. But more surprisingly, we found no good evidence for the dissociation of excitons at the oxide

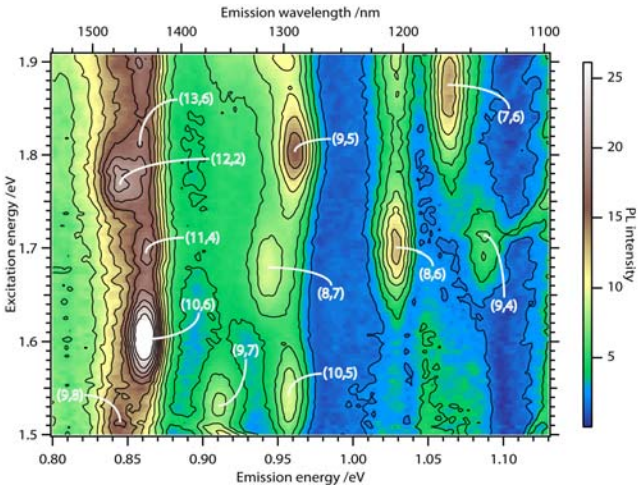

Figure 1 - 2D photoluminescence excitation spectra from a P3HT suspension of HiPCO SWNTs in toluene, showing the roll-up vectors (n,m) of the nanotubes associated with the observed transitions. The colour is proportional to the natural logarithm of the emission intensity and is in arbitrary units.

interface; even for pure ZnO. The production of carriers is an intrinsic property of the P3HT, with the Zn(Mg)O serving only as an electron acceptor.

The inclusion of PCBM is well-known to promote exciton dissociation for a range of conjugated polymers, although P3HT is the preferred choice for device construction, as it has a red-shifted absorption spectrum and is known to be a good transporter of holes. Using TRMC, we have investigated a range of polymer blends that range from 0 to 80 wt% PCBM content. At the low loading of 1 wt%, where disruption of the ordered polymer is not significant, we observe, as expected, a significant increase in carrier production compared to the pure polymer. Like the pure polymer, however, the initial carrier concentration does not increase linearly with excitation density; a phenomenon that has been reported as efficient exciton-exciton annihilation. However, by comparing the results from the PCBM-doped polymer, we have demonstrated that the effect is actually caused by an efficient exciton-hole quenching process that may prove to be a limiting factor in photovoltaic device performance. Further increase in PCBM concentrations does not significantly increase the carrier production process further, but it does have an impact on the long-term recombination kinetics.

C_{60} (and PCBM) is an excellent electron acceptor and, at high concentrations, a reasonable transporter of electrons; however, it is not ideal. Electron mobilities are quite low, the C_{60} network is not perfect, which leads to isolated C_{60} quenching sites, and the inclusion of nanoparticles in the P3HT disrupts the order and hence negatively impacts both the exciton and hole transporting properties. Using SWNTs instead of C_{60} is an attractive proposition, as potentially they can eliminate all the aforementioned issues. But to realize their full potential, samples of specific semi-conducting SWNTs are required; an aspect of the project that is a collaboration with Mike Heben (see Heben abstract), where significant progress in SWNT purification is being made. Using solutions of P3HT, we have successfully isolated SWNTs into organic solvents, where the PL of specific, isolated nanotubes can be uniquely identified (see Figure 1). Using these solutions, thin films were prepared and studied using the TRMC technique (see Figure 2). These are only preliminary studies, but some initial conclusions can be drawn: Like C_{60}, some of the SWNTs promote efficient exciton dissociation, whether the exciton is created in the polymer or the nanotube; also the carrier recombination process is slow. These early results indicate that SWNTs have the potential to replace C_{60} as the electron-acceptor in bulk heterojunction photovoltaic devices.

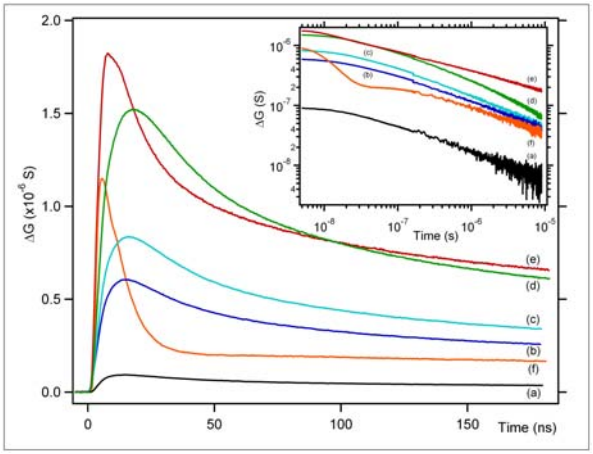

Figure 2 - Time-resolved microwave photoconductivity transients, for times up to 175 ns, for pristine P3HT (a), P3HT:PCBM blends with W_{PCBM} = 0.01 (b), 0.05 (c), and 0.5 (d), and a P3HT:SWNT blend (W_{SWNT} = 0.2) excited at 500 nm (e) and 660 nm (f) – the inset shows a log-log plot of the transients extended to 10 μs.

DOE Sponsored Publications 2005-2007

1. Jorge Piris, Nikos Kopidakis, Dana C. Olson, Sean E. Shaheen, David S. Ginley and Garry Rumbles, **"**The locus of free charge carrier generation in solution-cast $Zn_{1-x}Mg_xO$/poly(3-hexylthiophene) bilayers for photovoltaic applications," *Advanced Functional Materials* (In press).
2. Scholes, G. D.; Rumbles**,** G**.**. "Excitons in Nanoscale Systems," *Nature Materials*. (2006) **5**(9), 683-696.
3. Ai, X., Beard, M.C., Knutsen, K.P., Shaheen, S.E., Rumbles, G., Ellingson, R.J. "Photoinduced charge carrier generation in a poly(3-hexylthiophene) and methanofullerene bulk heterojunction investigated by time-resolved terahertz spectroscopy," *Journal of Physical Chemistry* **2006** 110(50), 25462-2547.
4. Chasteen, S. V.; Harter, J. O.; Rumbles**,** G**.**; Scott, J. C.; Nakazawa, Y.; Jones, M.; Horhold, H. H.; Tillman, H.; Carter, S. A.. "Comparison of Blended versus Layered Structures for Poly(p-phenylene vinylene)-based Polymer Photovoltaics" *Journal of Applied Physics.* (2006) Vol. 99(3).
5. Shaheen, S. E.; Olson, D. C.; White, M. S.; Gregg, B. A.; Rumbles**,** G.; Ginley, D. S.; Collins, R. T. "Morphological Changes of Conjugated Polymers in Nanostructured Environments" Rumbles, G.; Lian, T.; Murakoshi, K., eds., Electron Transfer in Nanomaterials: *Proceedings of the International Symposium on Charge Transfer Processes in Semiconductor and Metal Nanoparticles* held at the 205th Meeting of the Electrochemical Society, 9-14 May 2004, San Antonio, Texas. Electrochemical Society Proceedings Volume 2004-22. Pennington, NJ: The Electrochemical Society, Inc. pp. 443-448.
6. Chasteen, S. V.; Carter, S. A.; Rumbles, G. (2006). "Effect of Broken Conjugation on the Excited State: Ether Linkage in the Cyano-Substituted Poly(p-phenylene vinylene) Conjugated Polymer Poly(2,5,2',5'-tetrahexyloxy-8, 7'-dicyano-di-p-phenylene vinylene)" *Journal of Chemical Physics*. Vol. 124(21), 2006; 6 pp.
7. Mitchell, W. J.; Kopidakis, N.; Rumbles, G.; Ginley, D. S.; Shaheen, S. E. (2005). "Synthesis and Properties of Solution Processable Phenyl Cored Thiophene Dendrimers" *Journal of Materials Chemistry.* , 2005, 4518-4528.
8. Selmarten, D.; Jones, M.; Rumbles**,** G**.**; Yu, P.; Nedeljkovic, J.; Shaheen, S**. "**Quenching of Semiconductor Quantum Dot Photoluminescence by a .π-Conjugated Polymer" *Journal of Physical Chemistry B.* 2005 Vol. 109,; pp. 15927-15932.

ELECTRONIC DEFECTS IN π-CONJUGATED POLYMERS AND THEIR ELIMINATION VIA NUCLEOPHILIC AND ELECTROPHILIC ADDITION REACTIONS

Brian A. Gregg, Dong Wang, Sophie E. Gledhill and Brian Scott
National Renewable Energy Laboratory, Golden, CO 80401

After developing a theoretical understanding of crystalline excitonic semiconductors, XSCs, we are now studying the influence of disorder and electronic defects in XSCs. Defects, including dopants, often control the electronic and photovoltaic properties of semiconductors. Although the study of defects in inorganic semiconductors is a major field of research, almost nothing is known about defects in organic semiconductors. We report here what, to our knowledge, are the first experiments to explore the chemistry of defects in XSCs. We previously studied precisely doped, polycrystalline molecular semiconductors that had only non-covalent disorder. The theoretical model developed from this work should apply equally well to the more commonly employed amorphous polymeric XSCs. To test this prediction, we initiated a study of amorphous π-conjugated polymers which exhibit both covalent and non-covalent disorder.

Both types of disorder generate electronic states in the bandgap, that is, chemical sites more prone to either oxidation or reduction than most sites. In a disordered solid, the reactivity of a specific chemical moiety such as a double bond will depend strongly on its local environment. If it exists in an electric field-free location in an unperturbed geometry, its reduction and oxidation potentials will match those of the conduction (CB) and valence bands (VB), respectively. If it resides in a weakly perturbed environment, it will lie in a shallow state near one of the band edges (see Figure). This is often the case with non-covalently disordered systems in which only Van der Waals bonds and other weak interactions are perturbed. But covalent disorder involves the bending and/or twisting of a conjugated covalent bond. This can generate electronic states deep inside the bandgap, that is, chemical sites that are highly unstable relative to their unperturbed counterparts.

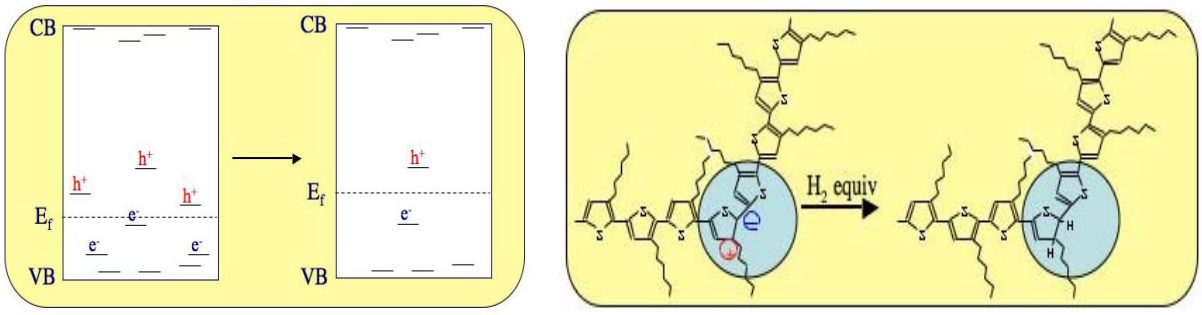

Figure. The effects of chemically annealling defects shown in a band diagram (left) and in a chemical cartoon (right).

The population of electrons or holes (anions or cations) in the intragap states is determined by the relative energetic position of the state relative to the Fermi level (E_f) and

by the chemical nature of the state: some states may be either positive or neutral, while others may be negative or neutral. The figure shows some uncharged (empty) states near both conduction band and valence band caused by non-covalent disorder, as well as some charged states representing deeply trapped electrons and holes caused by covalent disorder. As shown, the electrons are more deeply trapped than the holes resulting in an XSC that will act p-type even though it is not purposely doped.

The presence of charged defects in all but the most perfect semiconductor crystals is well established in the field of conventional inorganic semiconductors but has been hitherto ignored in the study of XSCs. Many physical descriptions of XSC films still assume that dark currents result from carriers injected at the electrodes, but this is true only for insulators and XSCs with purely non-covalent disorder, not for most π-conjugated polymers. This mistaken assumption leads to the common treatment of dark currents by the space-charge-limited current (SCLC) model. We have recently criticized this approach and shown experimentally that dark currents in π-conjugated polymers are better interpreted as Poole-Frenkel currents, consistent with our general model.

More recently we have employed electrophilic and nucleophilic addition chemistry first, to demonstrate the presence of these charged defect sites and second, to modify their concentration and electrical properties. Detailed chemical analysis of the treated polymers, unfortunately, is not feasible since the charged defects occur in molar ratios of only $10^{-5} - 10^{-4}$ —large enough to dominate the electronic properties of the solid, but small enough to be chemically indistinguishable. Defects in semiconductors have historically been characterized by their electrical properties while their chemical nature was only inferred.

Nucleophiles such as methoxide ion (and hydride ion) react with poly(3-hexylthiophene) and poly(dialkoxy phenylenevinylene) in solution as well as in solid thin films. This reaction eliminates some of the reactive defect sites in the polymer, presumably by adding CH_3O^- to partially cationic sites and H^+ (during workup) to the conjugate anionic sites. These reactions cannot energetically occur in the pristine material and should thus occur only at defect sites where the atomic energy levels are substantially perturbed. Since this reaction removes both electrons and holes equally, it moves the Fermi level toward the middle of the gap as evidenced by an increase in activation energy for the current ($E_{a,j}$) and decrease in conductivity (σ). This procedure also increases the exciton diffusion length (L_{ex}) and exciton lifetime (τ_{ex}). Charge carrier mobility (μ) measurements are in progress.

Treatment of the polymers with electrophiles such as dimethyl sulfate gives very different results. In this case, anionic sites are (presumably) attacked by the methyl cation while the sulfate anion, instead of bonding with the cationic site, serves as its counterion. This reaction thus eliminates bound electrons, exchanging them for sulfate anions, while leaving the holes (cations) untouched. It is equivalent to a classical p-type doping process. It results in movement of the Fermi level closer to the valence bandedge (decreasing $E_{a,j}$), and in an increase in σ and L_{ex}, while τ_{ex} decreases.

These studies should ultimately reveal the criteria necessary to improve organic photovoltaic cells.

DOE Sponsored Publications 2004-2007

1. Gregg, B. A., Chen, S. G., Cormier, R. A., "Coulomb Forces and Doping in Organic Semiconductors", invited review, *Chem. Mater*. **2004**, *16*, 4586-4599.

2. Gregg, B. A., "Toward a Unified Treatment of Electronic Processes in Organic Semiconductors", *J. Phys. Chem. B*, **2004**, *108*, 17285-17289.

3. Gregg, B. A. "The Photoconversion Mechanism of Excitonic Solar Cells", invited review, *MRS Bulletin*, **2005**, 30, 20-22.

4. Gregg, B. A., "Coulomb Forces in Excitonic Solar Cells" in "Organic Solar Cells: Mechanisms, Materials and Devices", Sun, S. and Sariciftci, S, Eds., Marcell Dekker, **2005**, 139-159.

5. Chen, S.-G., Stradins, P., Gregg, B. A. "Doping Highly Ordered Organic Semiconductors: Experimental Results and Fits to a Self-Consistent Model of Excitonic Processes, Doping, and Transport", *J. Phys. Chem. B*. **2005**, *109*,13451-13460.

6. Gledhill, S. E., Scott, B., Gregg, B. A. "Organic and Nano-structured Composite Photovoltaics: An Overview", invited review, *J. Mater. Res.* **2005**, 20, 3167-3179.

7. Gregg, B. A., Gledhill, S. E. and Scott, B. "Can True Space-Charge-Limited Currents Be Observed in π-conjugated Polymers?", *J. Appl. Phys.* **2006** 99, 116104.

8. Gregg, B. A., "Organic Photovoltaic Cells with an Electric Field Integrally-Formed at the Heterojunction Interface", US Patent No. US 7,157,641 B2, Jan. 2, 2007.

Session IV

Molecular Complexes for Energy and Charge Transfer

PHOTOINDUCED CHARGE SEPARATION ACROSS REDOX GRADIENTS: ORGANIC-INORGANIC COMPOSITE DYADS WITH DENDRIMERIC SENSITIZERS BOUND TO NANOCRYSTALLINE SEMICONDUCTOR AND METAL CLUSTERS

Marye Anne Fox, James K. Whitesell, and Linyong Zhu
Department of Chemistry and Biochemistry
University of California, San Diego
La Jolla, CA 92093

Achieving long-lived charge separation in integrated arrays containing photosensitizers, and electron donors and acceptors bound to semiconductor nanoparticulate arrays has been an important objective for over a decade. When a donor (D) is physically separated from an acceptor (A), absorption of light can initiate an electron cascade that results in a separated ion pair, irrespective of whether D or A is excited (Scheme 1). (1-2)

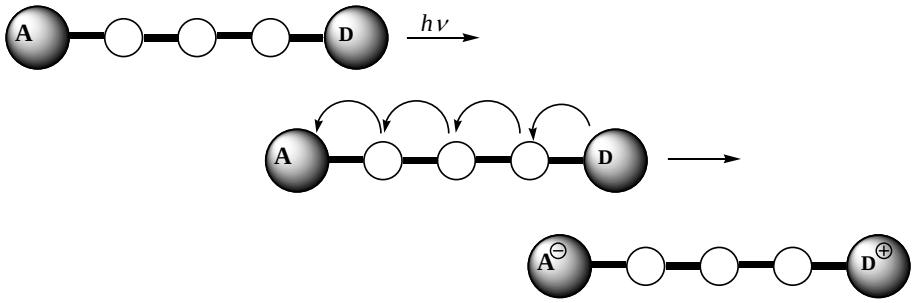

Scheme 1. Generation of a separated ion pair by a photoinduced electron cascade.

Recently, we have prepared a range of such arrays as key components for solar photoconversion as well as biotechnology and photonic applications. These involve self-assembled arrays of increasing complexity, allowing three-dimensionally disposed multilayer interactions. These arrays also include dendrimers as the distinguishing structural building blocks. These photoactive integrated systems have a regular, highly-branched, three-dimensional architecture in which the distance separating D and A can be varied synthetically. (3-5) Structural modifications of these units also include variation of the photophysical and redox properties of the core, bridging layers, and terminal groups. These modifications result in a large array of dendritic molecules with potential applications for light harvesting (Scheme 2).

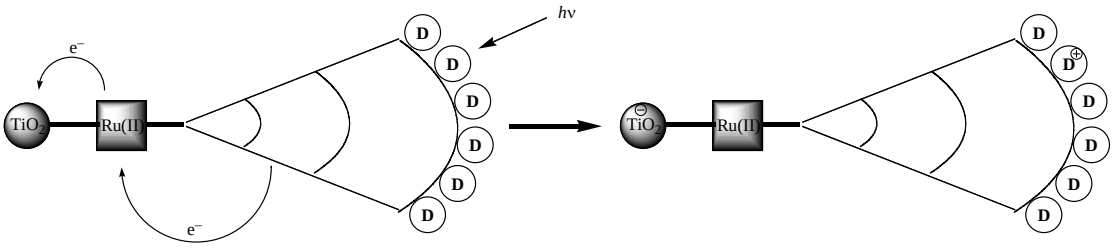

Scheme 2. Photoinduced charge separation in a dendritic sensitized composite array.

We have synthesized a class of photoactive nanocomposite dendrimers containing multiple phenothiazine units and a single ruthenium (II) complex bound to a semiconductor or metal cluster (Scheme 3). In this series, we have found that the key parameter that controls the rate of charge transfer at the dendrimer/TiO_2 interface is the spatial separation between the sensitizer and the inorganic core. In addition, we have achieved remarkably long-lived charge separation by virtue of spatial retardation of charge-recombination. (6-7) Both parameters are adjustable by varying the spatial separation through increasing generations of the dendrimeric scaffold.

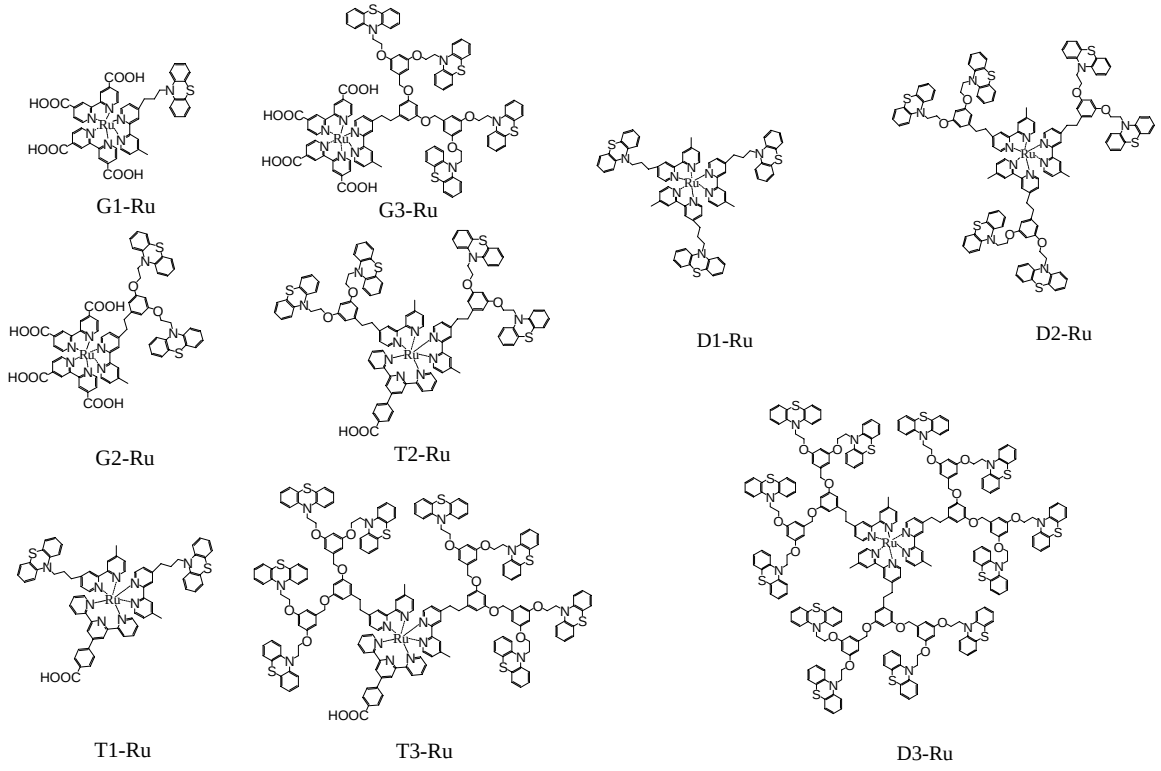

Scheme 3. Structure of ruthenium (II) : phenothiazine dendimer.

References

1. Tao Gu, James K. Whitesell, and Marye Anne Fox, "Energy Transfer from a Surface-bound Arene to the Gold Core in ω-Fluorenylalkane-1-thiolate Monolayer Protected Gold Clusters," *Chem. Mater*. **2003**, *15*, 1358.

2. K.R. Gopidas, James K. Whitesell, and Marye Anne Fox, "Metal Core– Organic Shell Dendrimers as Unimolecular Micelles," *J. Am. Chem. Soc.* **2003**, *46*, 14168.

3. K.R. Gopidas, J.K. Whitesell, and Marye Anne Fox, "Nanoparticle-Cored Dendrimers: Synthesis and Characterization," *J. Amer. Chem. Soc.* **2003**, *125*, 6491.

4. Marina Canepa, Marye Anne Fox, and James K. Whitesell, “The Influence of Core Size on Electronic Coupling in Shell-Core Nanoparticles: Gold Clusters Capped by Pyrenoxylalkylthiolate,” *Photochem. Photobiol. Sci.* **2003**, *2*, 1177.

5. K.R. Gopidas, J.K. Whitesell, and Marye Anne Fox, “Palladium Nanoparticle-Cored Dendrimers as Chemical Catalysts,” *Nano Lett.* **2003** *3*, 1757.

6. Jian Zhang, J.K. Whitesell, and Marye Anne Fox, "Photophysical Behavior of Pyrenyl Probes of Differently Sized Colloidal Gold Clusters Capped with Monolayers of an Alkylstilbenethiolate," *J. Phys. Chem.* **2003**, *107*, 6051.

7. Tao Gu, Tong Ye, John D. Simon, James K. Whitesell, and Marye Anne Fox, "Subpicosecond Transient Dynamics in Gold Nanoparticles Encapsulated by a Fluorophore-Terminated Monolayer," *J. Phys. Chem.* **2003**, *107*, 1765.

Recent DOE Sponsored Publications

1. Tao Gu, James K. Whitesell, and Marye Anne Fox, “Electrochemical Charging of a Fullerene-Functionalized Self-Assembled Monolayer on Au (111),” *J. Org. Chem.* **2004**,*69*, 4075-4080.

2. Mariana Rusa, James K. Whitesell, and Marye Anne Fox, “Controlled Fabrication of Gold/Polymer Nanocomposites with a Highly Structured Poly(*N*-acylethyleneimine) Shell,” *Macromolecules* **2004**, *37*, 2766-2774.

PHOTOINDUCED ENERGY AND ELECTRON TRANSFER REACTIONS OF RU(II) AND PT(II) COMPLEXES

Kalpana Shankar, Duraisamy Kumaresan, Heidi Hester, Kristi Lebkowsky and Russell Schmehl
Department of Chemistry
Tulane University
New Orleans, LA, 70118

Over the past two years we have focused on two principal areas: ligand-ligand energy transfer in multimetallic Ru(II) complexes and the photophysical and photoredox behavior of Pt(II) terpyridyl complexes. The latter chemistry is focused on the possibility of exploiting the reactivity of one electron oxidized or reduced Pt(II) complexes to catalyze net two electron processes.

Ligand-ligand energy transfer processes: The idea of this work is that transition metal complex centers could act as light harvesting chromophores to sensitize bridging ligand triplet excited states in polymetallic complexes and excitation energy migration along the length of the linear polymetallic array would be through the linked ligand localized excited states (figure below).

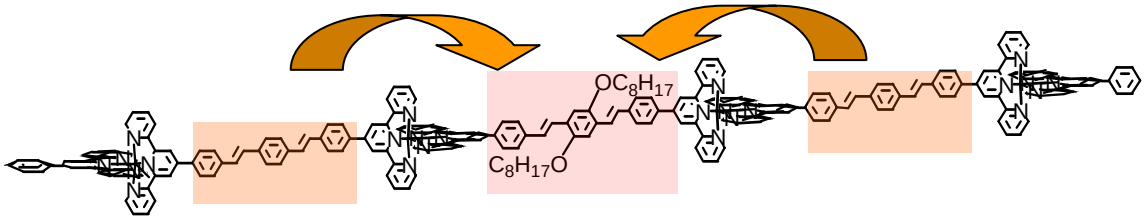

The structures of bis-terpyridyl ligands with slightly different distyrylbenzene bridges is shown below. By preparing complexes of the type [(tpy)Ru(tpvpvpt)Ru(tpvp(OR)vpt)Ru(tpvpvpt) Ru(tpy)]$^{8+}$, excitation energy migration from an excited state localized on the tpvpvpt ligand to the tpvp(OR)vpt ligand can be monitored using transient absorption spectroscopy.

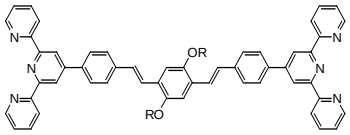

tpvp(OR)vpt

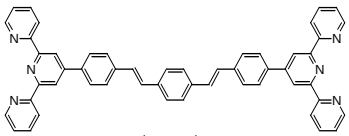
tpvpvpt

In the bimetallic complex [(tpy)Ru(tpvpvpt)Ru(tpy)]$^{4+}$, the rate constant for relaxation of the tpvpvpt localized triplet excited state is 3.8 x 10^6 s^{-1}. The alkoxy derivative, [(tpy)Ru(tpvpORvpt)Ru(tpy)]$^{4+}$ has a decay rate constant of 1.2 x 10^5 s^{-1} for relaxation of the ligand localized triplet state.

Excitation energy migration in [(tpy)Ru(tpvpvpt)Ru(tpvp(OR)vpt)Ru(tpvpvpt) Ru(tpy)]$^{8+}$ involves initial excitation of the Ru(II) complex MLCT excited states followed by rapid (< 100 ps) energy migration to sensitize the ligand localized triplets on both the bridging ligands and then subsequent, much slower, energy migration from the higher energy bridging ligand triplet state to the central bridging ligand triplet state as above.

Spectroscopically we were able to distinguish this relatively subtle process by the fact that the excited state lifetime of the donor tpvpvpt intraligand triplet is much shorter than that of the tpvpORvpt acceptor. Figure 1 shows the overall transient spectrum and the ground state spectrum for this complex and figure 2 shows transient decays obtained at 525 nm, where only the tpvpvpt bridging ligand triplet state absorbs and at 630 nm, where both the triplets absorb.

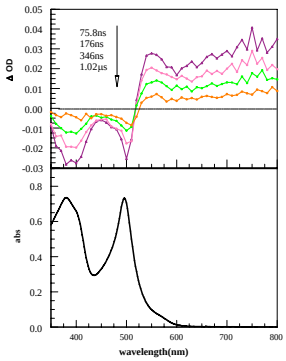

Excited State Absorption spectrum (top) and Ground State Absorption Spectrum(bottom) of $[(mpt)Ru2VRu2V(OR)Ru2VRu(mpt)]^{8+}$ $(PF_6)_8$ in MeCN (λ_{exc}=505nm)

Figure 1

The collected decays were evaluated using global analysis and the result is that the rate constant for energy migration from the tpvpvpt triplet to the tpvpORvt triplet is significantly slower than the decay of the tpvpvpt triplet state (3.8×10^6 s^{-1}). Potential explanations for this will be discussed.

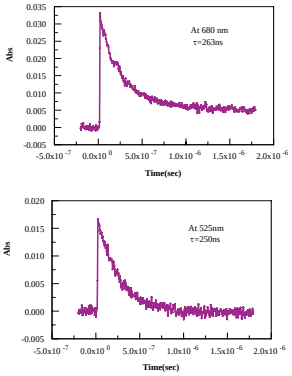

Figure 2

Photoinduced Electron Transfer Reactions of Pt(II) Complexes: We have also recently investigated intra- and intermolecular photoinduced electron transfer in complexes containing terpyridine ligands. These complexes have attracted considerable recent interest because derivatives have been prepared that have relatively long (>100 ns) excited state lifetimes. For instance terpyridyl Pt(II) complexes having modified terpyridyl ligands and/or aryl acetylide ligands as the fourth ligand fall into this class. There are a number of characteristics of these complexes that make them particularly interesting for photophysical investigation. First, the one electron oxidation is irreversible as disproportionation leads to formation of six coordinate Pt(IV) complexes. Photochemical approaches provide a means to make the Pt(III) species through a photoredox reaction and examine its reactivity. Also, many square planar Pt(II) complexes tend to aggregate in solution and their photophysical behavior changes because of Pt-Pt interactions in the ground state of the complexes.

Recently we have investigated the photoredox reactions of several (L)Pt(II) terpyridyl complexes (L= Cl, CN, aryl acetylide, pyridine) and have determined excited state potentials for one electron reduction via Rehm-Weller analysis. We are working on one electron oxidation processes for some of the complexes, but the excited state oxidation is kinetically slow and traditional luminescence quenching approaches may not be practicable.

More recently we began investigating the complex $[(ND\text{-}tpy)Pt(II)Cl]^+$, easily prepared from bis-benzonitrile Pt(II) chloride and the ND-tpy ligand shown below. NMR experiments reveal that the complex is aggregated in solution at room temperature but, upon heating to 90 ^{0}C in DMSO-d_6, a clean spectrum for the monometallic complex is obtained. Upon cooling heated DMSO solutions gel formation occurs. Further examination of the gels by TEM, SEM and small angle x-ray scattering reveals that the complex forms extended rods of several microns in length and 100-200 nm in diameter. The observed spacing between diffraction planes, presumed to be stacked Pt(II) complexes, yielded an interplanar spacing of 1.4 nm. The emerging picture of the aggregation is that *both* the ND and Pt complex form stacked layers. Transient spectroscopic investigations of the Pt(II) complex reveal that excitation of the complex in what could best be described as suspended gels reveals formation of a long lived transient that clearly resembles the reduced ND. At this point we are investigating this system more carefully to more clearly understand the relationship between aggregation and charge separation and also the fate of the one electron oxidized Pt complex.

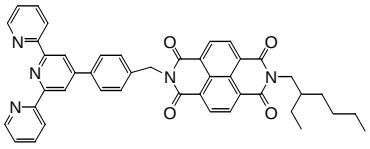

DOE Sponsored Publications 2005-2007

1. G. Christian Balazs, Andre del Guerzo and Russell H. Schmehl "Photophysical Behavior and Intramolecular Energy Transfer in Os(II) Diimine Complexes Covalently Linked to Anthracene," J. Photochem. Photobiol. Sci., **2005**,*4*, 88-94 .

2. Soma Chakraborty, Thaddeus J. Wadas, Heidi Hester, Russell Schmehl and Richard Eisenberg, "Platinum Chromophore Based Systems for Photoinduced Charge Separation: A Molecular Design Approach for Artificial Photosynthesis," Inorg. Chem. , **2005,** *44*, 6865-6878.

3. Soma Chakraborty, Thaddeus J. Wadas, Heidi Hester, Christine Flaschenreim, Russell Schmehl and Richard Eisenberg, "Synthesis, Structure, Characterization and Photophysical Studies of a New Platinum Terpyridyl-Based Triad with Covalently Linked Donor and Acceptor Groups," Inorg. Chem., **2005**, *44*, 6284-6293.

4. Mauricio Cattaneo, Florencia Fagalde , Néstor E. Katz, Ana María Leiva, Bárbara Loeb and Russell Schmehl, "Enhancement of Metal-to-Metal Coupling at a Considerable Distance by Using 4-pyridinealdazine as a Bridging Ligand in Polynuclear Complexes of Rhenium and Ruthenium," Inorg. Chem., **2006**, *45*, 127-136.

5. Xian-yong Wang, Andre del Guerzo, Sujoy Baitalik, Gerald Simon and Russell Schmehl "The Influence of Bridging Ligand Electronic Structure on the Photophysical Properties of Noble Metal Diimine and Triimine Light Harvesting Systems," Photosynthesis Research, **2006,** *87*, 83-103. (invited)

6. María G. Mellace, Florencia Fagalde, Néstor E. Katz, Heidi Hester, and Russell Schmehl , "Photophysical Properties of the Photosensitizer $[Ru(bpy)_2(5\text{-}CNphen)]^{2+}$ and intramolecular quenching by complexation of Cu(II).," J. Photochem. Photobiol., A: Chem., **2006**, *181*, 28-32,

7. Rupesh Narayana-Prabhu and Russell H. Schmehl, "Photoinduced Electron Transfer Reactions of Pt(II) Terpyridyl Acetylide Complexes: Reductive Quenching in a Hydrogen Generating System," Inorg. Chem., **2006**, *45*, 4319-21.

8. Xian-Yong Wang, Rupesh Narayana Prabhu, Russell H. Schmehl and Marcus Weck, "Polymer-Based Tris-2-phenylpryidine Iridium Complexes," Macromolecules, **2006**, *39*, 3140-46.

9. Xian-Yong Wang, Andre del Guerzo, Hari Tunuguntla, Russell H. Schmehl "Photophysical Behavior of Ru(II) and Os(II) terpyridyl phenylene vinylene complexes: Perturbation of MLCT State by Intraligand Charge Transfer State," Res. Chem. Intermed., **2007**, *33*, 63-77.

10. Duraisamy Kumaresan, Kalpana Shankar, Srivathsa Vaidya and Russell H. Schmehl "Photochemistry and Photophysics of Coordination Compounds: Osmium," Topics in Current Chemistry, in press (invited review).

11. Kosho Akatsuka, Yasuo Ebina, Masaru Muramatsu, Heidi Hester, Russell H Schmehl, Takayoshi Sasaki, Masa-aki Haga "Photoelectrochemical Properties of Alternating Multilayer Films Composed of Titania Nanosheets and Zn Porphyrins," Langmuir, in press.

12. Kalpana Shankar and Russell H. Schmehl "Synthetic Design Controls the Excited State Photoprocesses in Tetrametallic Ruthenium(II) Terpyridyl Complex" submitted.

13. Duraisamy Kumaresan and Russell H. Schmehl "Synthesis and Aggregation Influences on the Photo-induced Electron Transfer Studies of a Bis(terpyridine) Iron(II) Complex Donor bridged to a Naphthalene Diimide Acceptor," in preparation.

14. Duraisamy Kumaresan, Kristi Lebkowski and Russell H. Schmehl "Gel Formation and Intramolecular Photoredox Reactivity of a Pt(II) Terpyridyl Naphthalene Diimine Chromophore-Acceptor Complex," in preparation.

SOLVATION AND CHARGE TRANSFER IN IONIC LIQUIDS AND POLAR SOLVENTS

Mark Maroncelli, Sergei Arzhantsev, and Hui Jin
Department of Chemistry
The Pennsylvania State University
University Park, PA 16802

Project Scope: The goal of our DOE-funded research is to understand the dynamic coupling between photo-induced charge transfer within a solute and its solvent environment. A component of this work involves understanding how time-dependent emission spectra report on this coupling. During the past three years we have developed an experimental setup for measuring complete time-resolved emission spectra[2] which is now in its 2nd generation, measured solvation and charge-transfer dynamics of several fluorescent probes in conventional solvents[1,3,5], and explored the nature of solvation energetics and dynamics in room-temperature ionic liquids[4,6-9].

Kerr-Gated Emission (KGE) Spectroscopy: We have been developing KGE spectroscopy as a method for acquiring complete time-resolved emission spectra of conventional fluorophores with subpicosecond time resolution. Several other groups are also working on this technique and have reported time resolution of ~100 fs for solutes having lifetimes of a few ps or less. We have shown that by accepting somewhat poorer time resolution (400 fs) one can extend such measurements to conventional fluorophores with ns excited-state lifetimes. We have employed this method in a number of studies described below. An example of recent data are provided in Fig. 1, which shows spectra of DCS (see structure) in an ionic liquid. The time evolution in this case simply reflects solvation dynamics. We have recently replaced the collection optics in the KGE spectrometer with an improved system based on an axial Schwarzchild collection scheme developed by Niko Ernsting. We are now in the process of testing this system and I hope to report on the improved performance of this 2nd generation setup in my talk.

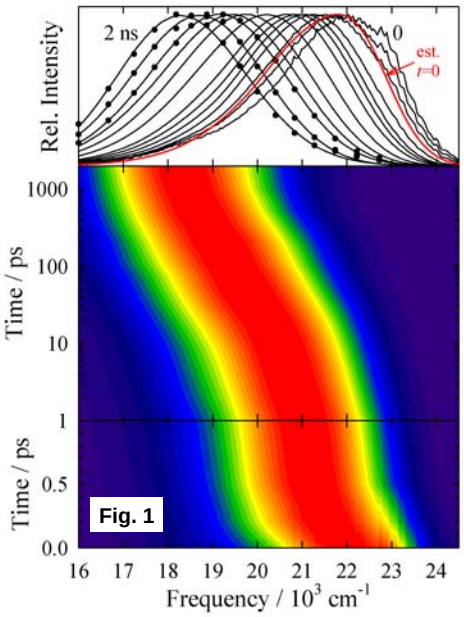

Fig. 1

CT Dynamics of Fluorescent Probes: Studies of the spectral dynamics of the solutes illustrated on the following page are in various stages of completion. The $S_0 \leftrightarrow S_1$ transitions of all of these solutes involve substantial charge transfer from an amino (aniline) donating group to a cyano (benzonitrile) accepting group, making these solutes highly solvatochromic. In DCS a single excited state dominates the spectroscopy so that only the effects of solvent relaxation are observed after excitation. As a result DCS provides an excellent probe of polar solvation comparable in most respects to benchmark solute coumarin 153. Dramatic variations in the

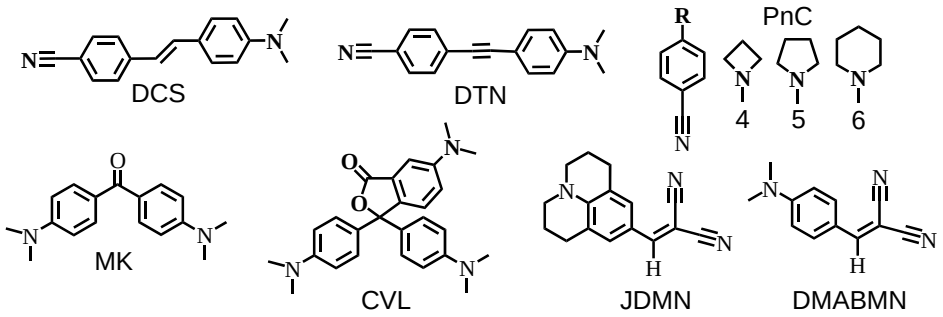

radiative rates of DTN and MK show that these two solutes undergo ultrafast barrierless reactions to CT states after excitation in polar solvent. The PnC series and CVL exhibit dual emission in some solvents which reflects emission from equilibrated locally excited and charge-transferred states. We have extensive experimental results on DTN and the PnC molecules and have developed semi-empirical models to relate their emission dynamics to time-dependent solvation. We are currently extending this work to MK and CVL, partly in order to check the generality of our modeling and partly because of the advantages the latter molecules offer for studying ionic liquids. Finally, we have recently begun systematic studies of the malononitriles DMABMN and JDMN, whose excited state dynamics mainly involve ultrafast internal conversion as a result of twisting about the double bond. These latter molecules are used as local friction/viscosity probes and are also of interest for studies in ionic liquids.

Solvation in Ionic Liquids: The majority of our work during the past two years has involved measuring the time-dependence of solvation in ionic liquids. Using the probe DCS and both the KGE and time-correlated single photon counting (TCSPC) techniques, we have measured the complete solvation response in six varied ionic liquids. As illustrated by the data in Fig. 2, the solvation dynamics in ionic liquids are remarkably distributed in time. Most of the relaxation occurs via a process that is reasonably represented by a stretched exponential time dependence (β~0.4) covering the range 1 ps – 10 ns.

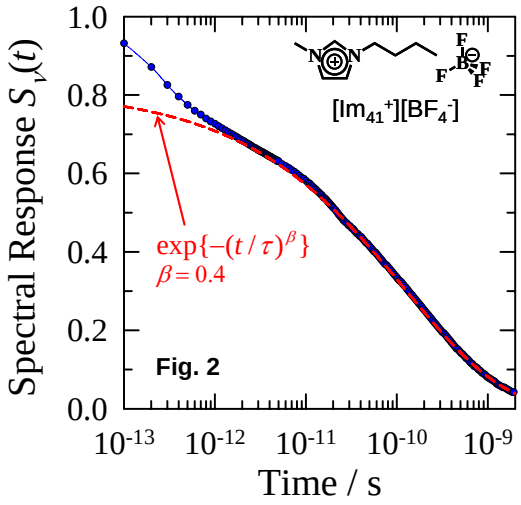

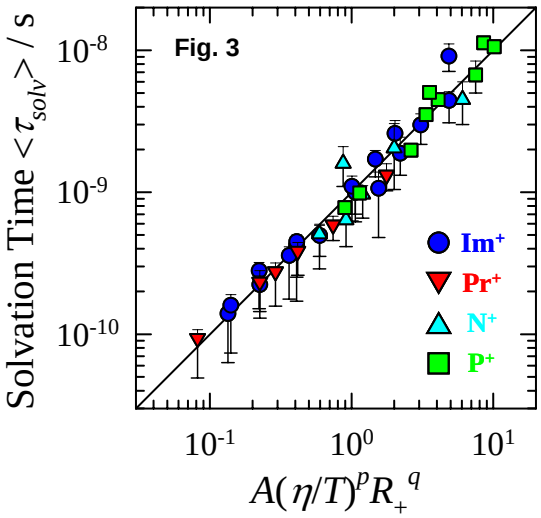

There is also a subpicosecond component which accounts for a modest fraction of the relaxation at the earliest times. The amplitudes and time constants of this latter component are reasonably correlated to inertial characteristics of the ions. The integral time of the slower, dominant component scales with bulk viscosity, which implies the involvement of structural relaxation of the surrounding solvent. TCSPC measurements in 21 different ionic liquids (Fig. 3) underscore this behavior and also indicate some relationship to cation size. At this point we have

largely completed the empirical characterization of solvation dynamics in ionic liquids, but we do not yet have a good understanding of what molecular motions are responsible for these dynamics or how to model them theoretically. We are currently performing molecular dynamics simulations on simplified model ionic liquids that should enable us to develop such an understanding. We are also beginning to measure the kinetics associated with charge transfer and internal conversion of the solutes previously discussed in ionic liquids with an eye toward learning how the slow and highly distributed solvation response influences charge transfer in these interesting solvents.

DOE Sponsored Publications 2005-2007

1. K. Dahl, R. Biswas, N. Ito, and M. Maroncelli, "Solvent Dependence of the Spectra and Kinetics of the LE→CT Reaction in Three Alkylaminobenzonitriles," *J. Phys. Chem. B* **109**, 1563-1585 (2005).

2. S. Arzhantsev and M. Maroncelli, "Design and Characterization of a Femtosecond Spectrometer Based on Optical Kerr Gating," *Appl. Spectrosc*. **59**, 206-220 (2005).

3. Min Liu, Naoki Ito, Mark Maroncelli, David H. Waldeck, Anna M. Oliver, and Michael N. Paddon-Row, "Solvent Friction Effect on Intramolecular Electron Transfer," *J. Am. Chem. Soc*. **127**, 17867-17876 (2005).

4. Sergei Arzhantsev, Hui Jin, Naoki Ito, and Mark Maroncelli, "Observing the Complete Solvation Response of DCS in Imidazolium Ionic Liquids, from the Femtosecond to the Nanosecond Regimes," *Chem. Phys. Lett*. **417**, 524-529 (2006).

5. Sergei Arzhantsev, Klaas A. Zachariasse, and Mark Maroncelli, "The Photophysics of trans-4-Dimethylamino-4'-Cyanostilbene and its use as a Solvation Probe," *J. Phys. Chem. A* **110**, 3454-3470 (2006).

6. Sergei Arzhantsev, Hui Jin, Gary A. Baker, Naoki Ito, and Mark Maroncelli, "Solvation Dynamics in Ionic Liquids, Results from ps and fs Emission Spectroscopy," in *Femtochemistry VII, Fundamental Ultrafast Processes in Chemistry, Physics, and Biology* , A. W. Castleman, Jr. and Michele L. Kimble eds. (Elsevier B.V. Ltd., 2006), p. 225-234.

7. Sergei Arzhantsev, Hui Jin, Gary Baker, and Mark Maroncelli, "Measurement of the Complete Solvation Response in Ionic Liquids," *J. Phys. Chem. B* **111**, ASAP (2007).

8. Hui Jin, Gary A. Baker, Sergei Arzhantsev, Jing Dong, and Mark Maroncelli, "Survey of Solvation and Rotational Dynamics of Coumarin 153 in a Broad Range of Ionic Liquids and Comparisons to Conventional Solvents," *J. Phys. Chem. B* **111**, in press (2007).

9. Hui Jin, Bernie O'Hare, Jing Dong, Sergei Arzhantsev, Gary A. Baker, James F. Wishart, Alan J. Benesi, and Mark Maroncelli, "Physical Properties of Ionic Liquids Consisting of the Bis(trifluoromethylsulfonyl)imide Anion with Various Cations and the 1-Butyl-3-Methyl Imidazolium Cation with Various Anions," submitted to *J. Phys. Chem. B* (5/07).

Session V

Theory of Heterogeneous Charge Transfer

THEORETICAL/COMPUTATIONAL PROBES OF HOMOGENEOUS AND INTERFACIAL ELECTRON TRANSFER: ELECTRONIC STRUCTURE AND ENERGETICS

Marshall D. Newton

Chemistry Department, Brookhaven National Laboratory
Upton, New York 11973-5000

An array of theoretical and computational techniques are enlisted in the mechanistic analysis of a number of electron transfer (ET) processes, thermal and optical, homogeneous and interfacial. The calculations include electronic structure and molecular level (as well as continuum) treatment of nuclear modes. Complementing the well-known Franck-Condon (FC) control of nonadiabatic ET kinetics for weakly-coupled donor (D) and acceptor(A) sites, alternative ET mechanisms are considered, which involve tradeoffs among a number of competing electronic and nuclear degrees of freedom (governed by their respective timescales). The latter, including molecular and collective medium modes, may modulate electronic coupling and may lead to several types of rate-determining step (rds) in dynamical regimes beyond the simple two-state transition state theory model. Mediation of ET tunneling via molecular spacers is examined for homogeneous and interfacial systems, and comparison is also made with transport in conductive junctions involving the same spacer units.

A unified mechanistic analysis has been completed for interfacial ET between a gold electrode and a ferrocene redox group mediated by variable-length (ℓ~10-40 nm) oligomers of three distinct types: oligogmethylene (OM(n)), oligo phenylenevinylene (OPV(n)), and oligo phenyleneethynylene (OPE(n)), where n is the number of spacer units. Some general mechanistic conclusions from analysis of the experimental data, based on kinetic models and electronic structure as well as conformational and reorganization energy calculations, are as follows: (1) insensitivity with respect to concentration of redox-active oligomers, nature of diluent, electrolyte, and spacer substituent, but with a *striking exception*: CH_3 substitution on OPE phenylene groups; (2) all activated processes involve common transition state (TS), characterized primarily by solvent reorganization associated with ET at the redox group; (3) irrespective of the rds, all actual ET events are *via* direct tunneling between electrode and redox group; (4) global exponential decay of the log of the prefactor with respect to ℓ is *not* observed for *any* system (OM(n), OPV(n), or OPE(n)): OM exhibits an adiabatic plateau below ℓ~10 Å, OPV is nearly flat for ℓ < 25 Å (adiabatic), and the nonmonotonic behavior of OPE (n) is most likely influenced by variation in torsion angle distributions.

The reorganization of electronic charge *at* (as distinct from the transport *through*) interfaces involves a number of specific issues related to the geometrical and electronic structure at the interface, eg, as in metal-organic interfaces comprised of close-packed monolayer films. Taking the interface associated with a phenylthiolate (PT) self-assembled monolayer (SAM) film-modified metal electrode interface (111 Au or Cu), we have exploited DFT band structure techniques to examine the interfacial charge redistribution in terms of the charge distributions of the isolated individual components of the interfacial assembly, with the goal of characterizing the electronic nature of the S atom linker (eg, 'thiolate' ($-RS^-$) vs 'thiyl' ($-RS^\bullet$) ?). A major

contribitution to the net surface dipole (related to the work function) is the electronic promotion at the S atom sites accompanying formation of the film. The results also imply significant interference effects between direct through-space (TS) and indirect substrate-mediated interactions of adsorbate molecules. A unique feature of the organic thiolate/substrate interface is attributed to the presence of two quasi-degenerate S radical states, leading to large dispersion effects (transverse k components) in partially occupied bands. These special electronic effects are not expected for closed shell 'contact' linker groups such as $-NH_2$ or –NC.

Solvent influence on precursor complex formation for bimolecular ET is an important example of the role of nuclear modes in controlling ET mechanisms. The paramagnetic [1:1] encounter complex $(TCNE)_2^{-}\bullet$ has been established experimentally as the precursor in the self-exchange between the tetracyanoethylene (TCNE) acceptor (A) and its radical-anion as the donor (D) in polar solvents.The spectroscopically observed intervalence absorption band of the dimeric $(TCNE)_2^{-}\bullet$ has been analyzed with the aid of Mulliken-Hush theory, revealing sizable coupling (H_{DA} = 1000 cm^{-1}) between the TCNE moieties. Ab initio quantum-mechanical computations of both the reorganization energy and H_{DA} imply a significant role of solvent in determining the encounter geometries, yielding structures appreciably displaced from the face-to-face contact calculated in the gas phase and observed in related dimeric dianion crystal structures. Electronic structure calculations employing a continuum reaction field are currently underway, in efforts to model the dependence of the electronic coupling and precursor structure on solvent polarity.

The main structural and electronic factors controlling intramolecular dissociative electron transfer in a homologous D-peptide-A systems have been investigated by an integrated computational procedure based on a density functional theory, its time-dependent extension, and the polarizable continuum model. The calculations identify the electronic states involved in the process, including intermediate bridge states, and how they are perturbed by the orientation of the donor and the acceptor with respect to the peptide chain and by the presence of the solvent. A semiquantitative estimate of the overall rate constant in reasonable agreement with experiment is obtained by direct quantum mechanical evaluation of all the terms entering a generalized Marcus equation. The results indicate a kinetic regime near the nonadiabatic/adiabatic boundary.

DOE Sponsored Publications 2005-2007

1. Theory of torsional non-Condon Electron Transfer: A Generalized Spin-Boson Hamiltonian and its Non-adiabatic Limit Solution, Seogjoo Jang and Marshall D. Newton, *J. Chem. Phys*. **122**, 24501 (2005).

2. A Theoretical Investigation of Charge Transfer in Several Substituted Acridinium Ions, J. Lappe, Robert J. Cave, M. D. Newton, and I.V. Rostov, *J. Phys. Chem. B* **109**, 6610 (2005).

3. Intermolecular Electron Transfer Mechanisms via Quantitative Stuctures and Ion-Pair Equilibria for Self-Exchange of Anionic (Dinitrobenzenide) Donors, S.V. Rosokha, J.M. Lu, M.D. Newton, and J.K. Kochi, *J. Am. Chem. Soc.* **127**, 7411 (2005).

4. Electronic structure of S-C_6H_5 self-assembled monolayers on Cu(111) and Au(111) substrates, V. Perebeinos and M. D. Newton, *Chem. Phys.* **319**, 159 (2005).

5. Single Molecule Electron Transfer Dynamics in Complex Environments: A Model Simulation Study, Vitor B.P.Leite, Luciana C.P. Alonso, Marshall Newton, and Jin Wang, *Phys. Rev. Letts.* **95**, 11830 (2005).

6. Mulliken-Hush Elucidation of the Encounter (Precursor) Complex in Intermolecular Electron Transfer via Self–Exchange of Tetracyanoethylene Anion-Radical, S.V. Rosokha, M.D. Newton, M. Head-Gordon, and J.K. Kochi, *Chem. Phys.* **324**, 117 (2006).

7. Activation Entropy of Electron Transfer Reactions, A. Milischuk, D. V. Matyushov, and M. D. Newton, *Chem. Phys*. **324**, 172 (2006).

8. A Simple Comparison of Interfacial Electron-Transfer Rates for Surface-Attached and Bulk Solution-Dissolved Redox Moieties, John F. Smalley, Marshall D. Newton, and Stephen W. Feldberg, *J.Electroanal.Chem* **589**, 1 (2006).

9. A Parameter Free Quantum Mechanical Approach to the Calculation of Electron Transfer Rates for Large Systems in Solution, Roberto Improta, Vincenzo Barone , and Marshall D. Newton, *ChemPhysChem* **7**, 1211 (2006).

10. Dissociative Electron transfer in D-peptide-A systems: Results for Kinetic Parameters from a Density Functional/polarizable Continuum Model, Vincenzo Barone, Marshall D. Newton, and Roberto Improta, *J. Phys. Chem. B* **110**, 12632 (2006).

11. Closed Form Expressions of Quantum Electron Transfer Rates Based on the Stationary Phase Approximation, Seogjoo Jang and Marshall D. Newton, *J. Phys. Chem. B* **110**, 18996 (2006).

12. Interfacial Bridge-mediated Electron Transfer: Mechanistic Analysis Based on Electrochemical Kinetics and Theoretical Modeling, Marshall D. Newton and John F. Smalley, *Phys. Chem. Chem. Phys.* **9**, 555 (2007).

13. The Role of Dielectric Continuum Models in Electron Transfer: Theoretical and Computational Aspects, Marshall Newton, In "*Continuum Solvation Models in Chemical Physics: From Theory to Applications"*, Eds., B. Mennucci and R. Cammi, John Wiley & Sons, Ltd., New York, *in press.*

14. Multichromophoric Førster Resonance Energy Transfer from B800 to B850 in the Light Harvesting Complex 2: Evidence for Subtle Energetic Optimization by Purple Bacteria, Seogjoo Jang, Marshall D. Newton, and Robert J. Silbey *J. Phys. Chem., in press.*

.

DYNAMICS ON THE NANOSCALE:
TIME-DOMAIN *ab initio* STUDIES
OF MOLECULE-SEMICONDUCTOR INTERFACES, QUANTUM DOTS
AND NANOTUBES

Oleg Prezhdo
Department of Chemistry
University of Washington
Seattle, WA 98195-1700

Fundamental mechanisms of the excitation energy flow in novel materials for solar hydrogen production are investigated in a series of theoretical studies with emphasis on the simulation in real time, at the atomistic level, and in direct connection with experiment. The state-of-the-art computational approaches most recently developed in our group are applied to several closely related photovoltaic systems that hold a great promise for light harvesting, charge separation and solar-driven generation of molecular hydrogen. With a wealth of time-resolved experimental data on the electron transfer (ET) dynamics available in these systems, the mechanisms responsible for the charge transport and energy relaxation are not yet established or remain controversial. Our expertise in nonadiabatic molecular dynamics and time-dependent density functional theory (DFT) allows us to address the fundamental aspects of the photoexcitation dynamics. Particular attention is given to:

• **Ultrafast charge separation, relaxation and recombination at the organic-inorganic interface that drives the dye-semiconductor solar cell (DSSC).** DSSC is one of the most promising alternatives to the traditional SCs due to inexpensive components and high photocurrents. The proposed mechanisms for the electron injection have vastly different implications for the system properties, and the Marcus ET theory is not generally applicable. Our group reported the first real-time atomistic simulation of the DSSC ET.

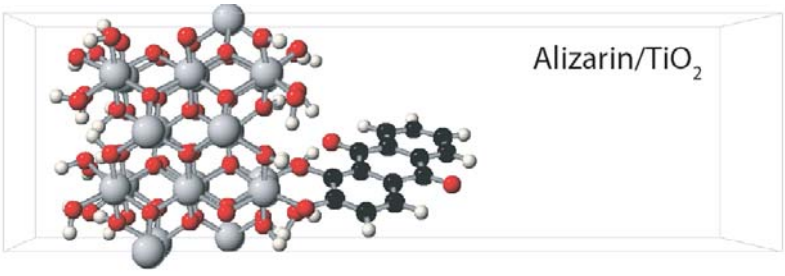

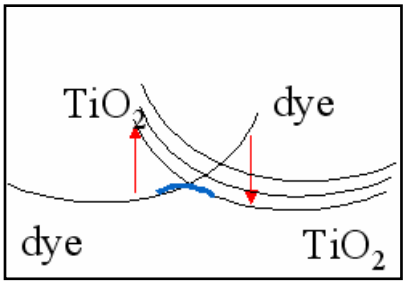

The analysis of the structure, electronic properties and electron-vibrational dynamics in the chromophore-TiO_2 systems allowed us to formulate the general principles characterizing the interface. The photoexcited states were classified into three types, including states deep inside the TiO_2 conduction band (CB), in which efficient ET was possible even with weak chromophore-semiconductor coupling; new low energy photoexcited localized in the surface, which was possible only with strong coupling; and chromophore excited states near the TiO_2 CB edge that could inject into the low density region of the CB minimizing energy loss. Real-time modeling was particularly valuable, since the ET occurred on ultrafast time-scales and showed a variety of individual events that could not be made apparent by an average rate description. Currently we are investigating the relaxation of the injected electron inside the TiO_2 CB, the

back ET from TiO_2 to the chromophore, the ET from the surface to the electrolyte, and the regeneration of the neutral chromophore by ET from the electrolyte to alizarin.
Additionally, we have initiated and will continue studies of the following novel materials:

• **Quantum dots (QD)** have a great potential to replace molecular donors, are tunable with size, form better heterojunctions with conductors, and have a unique possibility to produce photon-to-electron yields greater than one, increasing photocurrent, and to utilize hot carriers, increasing photovoltage. These goals can be achieved by slowing carrier relaxation as evidenced by recent experiments. The competition between the relaxation and productive processes is investigated.

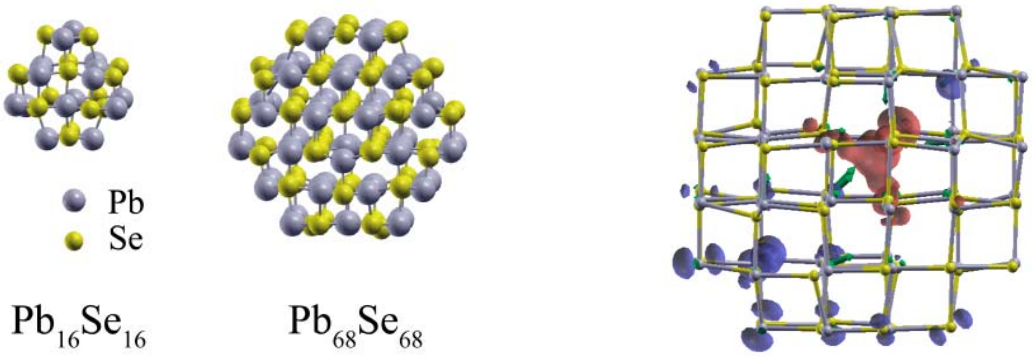

We were the first group to study the phonon-induced relaxation dynamics of charge carriers in a PbSe QD by ab initio DFT in the time-domain. The energy exchanged during individual transitions was typically greater than the characteristic phonon energy, indicating that the transitions were multiphonon. This relatively symmetric vibrational relaxation of electrons and holes proceeded on a picosecond time scale, much slower than the ultrafast carrier multiplication that was reported recently in relation to improved solar power conversion.

• **Carbon nanotubes (CNT)** can serve as electron acceptors in SC assemblies, possess good chemical stability and large surface area suitable for modification with multifunctional groups. CNTs are exceptional molecular wires, resilient to current-induced failure. Understanding of the electron dynamics mechanisms in CNTs is a key to their use for solar hydrogen production.

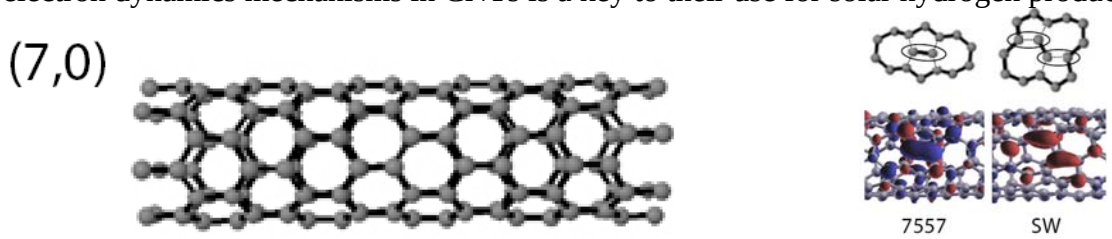

We simulated the electron and hole relaxation in the (7,0) zigzag semiconducting CNT in time domain using a surface-hopping DFT. Following a photoexcitation the excitons decayed to the Fermi level on characteristic subpicosecond time scales. The relaxation was primarily mediated by the high-frequency longitudinal optical (LO) phonons. Hole dynamics were more complex than the electron dynamics: in addition to the LO phonons, holes coupled to lower frequency breathing modes and decayed over multiple time scales.
The studies carried out at the atomistic level reproduce the experimental time-scales and provide detailed insights into the ET dynamics. In addition to the applications described above we continue development of new theoretical and simulation tools.

DOE Sponsored Publications 2005-2007

Book Chapters:

1. O. V. Prezhdo, W. R. Duncan, C. F. Craig, S. V. Kilina and B. F. Habenicht "Photoexcitation dynamics on the nanoscale" in Book *Quantum dynamics of complex molecular systems*, Springer, 2006
2. W. R. Duncan, W. Stier and O. V. Prezhdo "Ab Initio Simulations of Photoinduced Molecule-Semiconductor Electron Transfer" in Book *Nanomaterials: Design and Simulation*, Elsevier, 2006
3. O. V. Prezhdo and W. R. Duncan "Ultrafast heterogeneous electron transfer" in Book *Analysis and Control of Ultrafast Photoinduced Reactions*, Springer, 2007

Review:

4. W. R. Duncan and O. V. Prezhdo, "Theoretical Studies of Photoinduced Electron Transfer in Dye-Sensitized TiO2", *Ann. Rev. Phys. Chem.* **58** 143 (2007)

Articles in Peer Review Journals:

5. A. V. Luzanov and O. V. Prezhdo, "Analysis of multiconfiguratinal wavefunctions in terms of hole-particle distributions", *J. Chem. Phys.*, **124**, 224109 (2006)
6. A. V. Luzanov and O. V. Prezhdo, "Hole-particle characterization of coupled-cluster singles and doubles and related models", *J. Chem. Phys.* **125**, 154106 (2006)
7. Yu. V. Pereverzev, O. V. Prezhdo, "Force-induced deformations and stability of biological bonds", *Phys. Rev. E.* **73** 050902(R) (2006)
8. Hideyuki Kamisaka, Svetlana V. Kilina, Koichi Yamashita, and Oleg V. Prezhdo, "Ultrafast vibrationally-induced dephasing of electronic excitations in PbSe quantum dots", *Nano Lett.* **6** 2295 (2006)
9. B. F. Habenicht, C. F. Craig, O. V. Prezhdo, "Electron and hole relaxation dynamics in a semiconducting carbon nanotube", *Phys. Rev. Lett.* **96**, 187401 (2006)
10. O. V. Prezhdo, "A quantum-classical bracket that satisfies the Jacobi identity", *J. Chem. Phys. – Rapid. Comm.* **124**, 201104 (2006)
11. Yu. V. Pereverzev, O. V. Prezhdo, "Universal laws in the force-induced unraveling of biological bonds", *Phys. Rev. E.* **75**, 011905 (2007)
12. O. V. Prezhdo, "Reply to "Comment on 'A quantum-classical bracket that satisfies the Jacobi identity' " *J. Chem. Phys.* **126**, 057102 (2007)
13. Dmitri S. Kilin, Kiril Tsemekhman, Oleg V. Prezhdo, Eduard I. Zenkevich, Christian v. Borczyskowski, "Ab initio study of exciton transfer dynamics from a core–shell semiconductor quantum dot to a porphyrin-sensitizer", *J. Photochem-Photobiol. A*, in press
14. Svetlana V. Kilina, Colleen F. Craig, Dmitri S. Kilin, Oleg V. Prezhdo "Ab initio time-domain study of phonon-assisted relaxation of charge carriers in a PbSe quantum dot ", *J. Phys. Chem. C*, in press
15. Walter R. Duncan, Colleen Craig, Oleg V. Prezhdo, "Time-domain ab initio study of charge relaxation and recombination in dye-sensitized TiO2", *J. Am. Chem. Soc.*, submitted
16. Dmitri S. Kilin, Oleg V. Prezhdo, Michael Schreiber, "Photoinduced vibrational coherence transfer in molecular dimers", *J. Chem. Phys.*, submitted

Session VI

Photoinduced Charge Separation in Photosynthetic-Based Systems

MEASURING ULTRAFAST PHOTOSYNTHETIC FUNCTION AND STRUCTURE IN SINGLE CRYSTALS AND IN SOLUTION

D. M. Tiede[1], L. Huang[1,2], G. P. Wiederrecht[2], D. H. Hanson[3], L. Utschig[1], O. Poluektov[1], X. Zuo[1], K. Attenkofer[4], and L. X. Chen[1]
[1]Chemistry Division, [2]Center for Nanoscale Materials, [3]Biosciences Division, and [4]Advanced Photon Source
Argonne National Laboratory
Argonne, Illinois, 60439

Bio-inspired photosynthetic energy research is aimed at the resolution of fundamental mechanisms for optimized energy and electron transfer function in photosynthetic proteins, and the utilization of this information for the design and syntheses of advanced materials for solar energy conversion. A key feature of natural photosynthesis is the tuning of energy and electron transfer pathways by tailored, dynamically adapting protein matrices. A problem for correlating photosynthetic structure with function arises from the fact that high-resolution structures are typically determined in crystals where configurational dynamics can differ from those in solution, while detailed function analyses are typically determined in solution or other non-crystalline states. For photosynthetic proteins this raises questions on how well solution phase reaction dynamics map onto crystal coordinates, and re-enforces the need to develop high-resolution, time-resolved structural approaches for characterization of bio-inspired photosynthetic materials in non-crystalline states. We have begun to tackle the challenge of directly correlating bio-inspired photosynthetic function with structure by using micro-focused ultrafast optical techniques to measure photochemical activity in crystals, while using continuous and time-resolved synchrotron x-ray techniques to characterize biological and biomimetic molecular structure and structural dynamics in solution.

Ultrafast Photosynthetic Function in Crystals. Optical studies on single photosynthetic crystals offer the significant advantage of allowing polarized excitation and detection measurements to be made along fixed, well-defined molecular directions. For example, figure 1 shows polarized ground-state absorption spectra for the wild-type *Rhodobacter sphaeroides* reaction center (RC) compared to extinction coefficient-weighted optical transition moments for the cofactors calculated from the crystal structure and projected onto the crystal ***a*** and ***c*** axes. These projections show that several of the otherwise overlapping RC cofactor transition moments

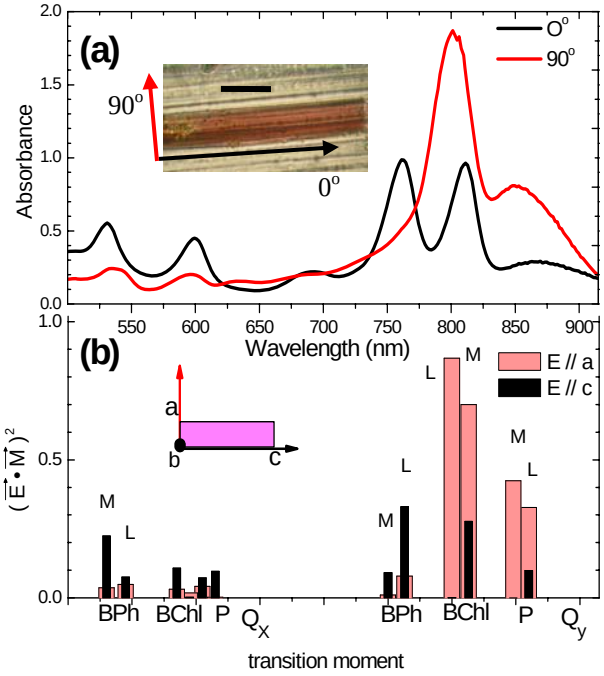

Figure 1. (a) Polarized ground state absorption spectra of a single reaction center crystal with light polarized parallel (black line) and perpendicular (red line) to the long axis of the crystal. (b) Extinction coefficient weighted projections of the optical transition moments calculated from the $P2_12_12_1$ unit cell.

can be resolved selectively along the individual crystal facets. For example, the Q_y transition for the bacteriochlorophyll (Bchl) associated with the L-protein subunit of the special pair (P) makes a unique projection along the crystal ***c*** axis, while the Q_y transitions for both Bchls comprising P contribute to absorption along the other axes. Comparison of the optical absorption for P recorded along these different crystal directions show surprising shifts suggesting that the optical transitions forming P are not degenerate as previously thought. Similarly, optical spectra and crystal projections show that the Q_y transitions of the accessory Bchl in the M-subunit and bacteriopheophytin in the L-subunit are also viewed selectively along the crystal ***c*** axis. Femtosecond transient absorbance spectra of photosynthetic reaction center crystals were found to vary with excitation wavelength and dichroic selection of cofactors for initial excitation, and show altered kinetics compared to solution state samples. This work establishes a foundation for correlating ultrafast electron transfer to crystallographic RC structures, and for mapping photochemical pathways coupled to individual cofactors. Future work is planned for extending photochemical function mapping by imaging energy transfer in photosynthetic 2-D arrays using ultrafast scanning near-field optical capabilities at the Center for Nanoscale Materials.

X-ray Structure Characterization in Solution. Bio-inspired, self-assembling supramolecular materials are increasingly being designed for applications in solar energy conversion and storage. However, the dynamic features of these molecular materials typically preclude structural analyses using crystallographic techniques. This makes *in-situ* structural characterization a critical challenge. We have developed techniques that combine wide-angle solution X-ray scattering (WAXS) measured to better than 2 Å spatial resolution with atomistic simulation to provide a new experimental approach for the characterization of supramolecular solution state structure. Comparisons between experimental scattering patterns measured for a range of proteins, DNA, metal coordination complexes, and host-guest assemblies show WAXS and corresponding pair distribution function (PDF) patterns to be sensitive to supramolecular conformation, dynamics, and solvation. For example, a comparison of experimental scattering and PDF patterns for γ-cyclodextrin (figure 2) show features characteristic of the host structure, configurational broadening, and solvation. In current work we are testing the ability of WAXS to serve as a benchmark for quantitative evaluation molecular dynamics simulations. The ability to provide an experimental marker for supramolecular dynamics and solvation that is directly connected to coordinate models represents a new opportunity for resolving structural dynamics coupled to light-induced charge separation in natural and artificial host matrices. Towards this end we are extending the WAXS technique to include pump-probe techniques at the Advanced Photon Source. Future work is planned for combining time-resolved WAXS, x-ray spectroscopy, and magnetic resonance data to achieve a more complete picture of structural reorganization resolved during the time-course of solar energy conversion function.

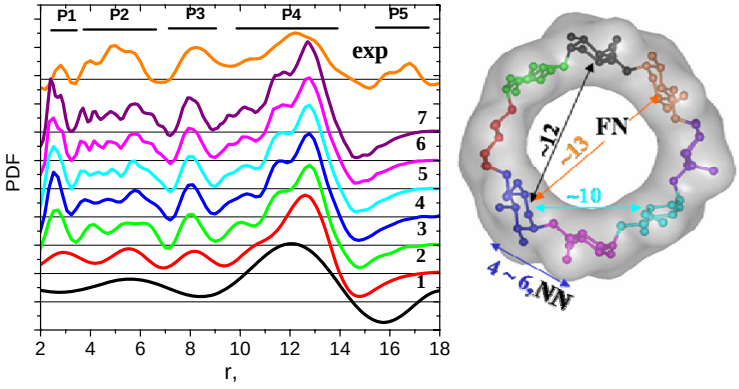

Figure 2. Experimental PDF measured for γ-cyclodextrin with 1.0 Å spatial resolution (top) compared to PDF calculated from a coordinate model with resolution varying from 6 Å (1) to 0.4 Å (7).

DOE Sponsored Publications 2005-2007

1. Femtosecond Spectroscopy of Single Photosynthetic Reaction Center Crystals from *Rhodobacter sphaeroides,* L. Huang, G. P. Wiederrecht, S. Schlesselman, C. Xydis, P.D. Laible, D. K. Hanson, D.M. Tiede, J. Am. Chem. Soc., *submitted.*
2. molX: A Computer Program for Simulating Solution Molecular X-ray Scattering, X. Zuo, A.J. Goshe, R. Zhang, D. M. Tiede, J. Appl. Cryst., *submitted.*
3. X-ray Scattering for Bio-Molecule Structure Characterization, D. M. Tiede and X. Zuo, in "Biophysical Methods in Photosynthesis" Vol 2, (J. Matysik and T.J. Aartsma, eds.) Kluwer/Springer, *in press*.
4. Solution-phase structural characterization of supramolecular assemblies by high-angle molecular diffraction, J.L. O'Donnell, X. Zuo, A.J. Goshe, L. Sarkisov, R. Q. Snurr, J. T. Hupp, D. M. Tiede, J. Am. Chem. Soc. 129, 1578-1585 (2007).
5. Charge Separation and Surface Reconstruction : A Mn2+ Doping Study, Saponjic, Z.V.; Dimitrijevic, N.M.; Poluektov O.G.; Chen, L.X.; Wasinger, E.; Welp, U.; Tiede, D.M.; Zuo, X. and Rajh, T. *J. Phys. Chem. B,* 110 (50), 25441-25450 (2006).
6. Supramolecular Porphyrinic Prisms: Coordinative Assembly and Preliminary Solution-phase X-ray Structural Characterization , S.J. Lee, K. L. Mulfort, J. L. O'Donnell, X. Zuo, A. J. Goshe, S. T. Nguyen, J. T. Hupp, and D. M. Tiede, *Chem. Comm.* 4581 - 4583 (2006).
7. Linearly Polarized Emission of an Organic Semiconductor Nanobelt, Datar, A.; Balakrishnan, K.; Yang, X.; Zuo, X.; Huang, J.; Oitker, R.; Yen, M.; Zhao, J.; Tiede, D. M.; Zang, L., *J. Phys. Chem. B* 110: 12327-12332 (2006).
8. X-ray Diffraction "Fingerprinting" of DNA Structure in Solution for Quantitative Evaluation of Molecular Dynamics Simulation, X. Zuo, G. Gui, K.M. Merz, L. Zhang, F.D. Lewis, and D.M. Tiede, *Proceed. Natl. Acad. Sci. USA*, 103(10) 3534-3539 (2006).
9. Self-assembly of Photofunctional Cylindrical Nanostructures Based on Perylene-3,4:9,10-bis(dicarboximide), Sinks, L. E.; Rybtchinski, B.; Iimura, M.; Jones, B. A.; Goshe, A.J.; Zuo, X.; Tiede, D.M; Li, X.; Wasielewski, M.R.; *Chemistry of Materials* 17: 6295-6303(2005).
10. Low-Temperature Interquinone Electron Transfer in Photosynthetic Reaction Centers from Rhodobacter sphaeroides and Blastochloris viridis: Characterization of Q_B^- States by High-Frequency Electron Paramagnetic Resonance (EPR) and Electron-Nuclear Double Resonance (ENDOR), L.M. Utschig, M.C. Thurnauer, D.M. Tiede, and O.G. Poluektov, *Biochemistry*, 44(43), 14131-14142 (2005).
11. Multi-Scale Modeling of Titanium Dioxide: Controlling Shape With Surface Chemistry, A. Barnard, Z. Saponjic, D. Tiede, T. Rajh, L. Curtiss, *Reviews on Advanced Materials Science*, 10(1) 21 -27 (2005).
12. Excited State Dynamics and Structures of Functionalized Phthalocyanines. 1. Self-Regulated Assembly of Zinc Helicenocyanine, L.X. Chen, G.B. Shaw, D.M. Tiede, X. Zuo, P. Zapol, P.C. Redfern, L.A. Curtiss, T. Sooksimauang, and B.Mandal, *J. Phys. Chem.* **106** 16598 – 16609 (2005).

13. DNA as Helical Ruler: Exciton-Coupled Circular Dichroism in DNA Conjugates, F.D. Lewis, L. Zhang, X. Liu, X. Zuo, D.M. Tiede, H. Long, and G.C. Schatz, *J. Am. Chem. Soc.*, **127** (41), 14445 – 14062 (2005).

14. Shaping Nanoscale Architectures through Surface Chemistry, Z. V. Saponjic, N. M. Dimitrijevic, D. M. Tiede, A. Goshe, X. Zuo, L. X. Chen, A. S. Barnard, P. Zapol, L. Curtiss, and T. Rajh, *Advanced Materials*, **17** (8), 965-971 (2005).

15. Resolving Conflicting Crystallographic and NMR Models for Solution-State DNA with Molecular Solution X-ray Diffraction, X. Zuo and D. M. Tiede, *J. Am. Chem. Soc.*, **127**(1), 16-17 (2005).

ENVIRONMENTAL TUNING OF PHOTOSYNTHETIC ELECTRON TRANSFER

Lisa M. Utschig, David M. Tiede, and Oleg G. Poluektov
Chemistry Division
Argonne National Laboratory
Argonne, IL 60439

Photosynthetic reaction center (RC) proteins serve as unique examples of molecular systems in which both the molecular charge carriers (cofactors) and the surrounding media are tuned for optimized solar energy conversion. Crystal structures of the RCs from purple photosynthetic bacteria, and photosystems I and II (PSI, PSII) of cyanobacteria and higher plants reveal specifically tailored protein environments that act as "smart matrices", dynamically adjusting to promote directional electron transfer, stabilize charge separation, and enable coupling to secondary reactions, i.e. proton transfer or electron transfer to secondary electron acceptors. Our recent work is directed at understanding the function of localized protein environments in tuning light-driven electron transfer. Our experimental approach utilizes both specialized "spin-edited" (i.e., samples that involve isotopic labeling and/or native paramagnetic metal ion extraction or replacement) samples and multi-frequency (including high magnetic field (HF)) pulsed electron paramagnetic resonance (EPR) techniques. A highlight of this work is our recent discovery of intrinsic transition metal ion sites in PSI from cyanobacteria.

Metal ion binding to Photosystem I. In previous work, we showed that Zn^{2+} binding to a surface metal site in bacterial RCs modulates the terminal proton-coupled electron transfer reactions. Our discovery of this Zn^{2+} site is proving to be an important paradigm and has led others to show that Zn^{2+} binding modulates proton gateways in several other proteins. Our experience with metal binding in the bacterial RC has lead to the recent discovery of an intrinsic Zn^{2+} site on the Photosystem I reaction center. In certain purification protocols for PSI from *Synechococcus* cyanobacteria, at least 1 mol equiv of Zn^{2+} is isolated per PSI molecule. To our knowledge, there have been no reports of other first row transition metal ions binding to PSI. Photosystem I is a large, membrane protein complex composed of 12 protein subunits and 127 cofactors (Figure 1) that catalyzes the light driven electron transfer across the membrane from plastocyanin located in the lumen to ferredoxin in the stroma. In PSI, photoexcitation of the primary electron donor, P, (a dimer of chlorophyll molecules) initiates sequential electron transfer through two spectroscopically identified electron acceptors, A_0, a chlorophyll molecule, and A_1, a phylloquinone. From A_1^- the electron is transferred to the [4Fe-4S] cluster F_X, and

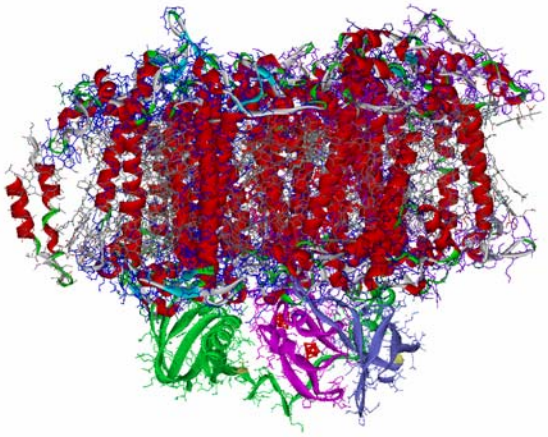

Figure 1 The Photosystem I Reaction Center. Stromal subunits involved in ferredoxin docking and where metal ion binding is predicted to occur are colored green (D), magenta (C), and blue (E). The terminal [4Fe-4S] centers F_A and F_B are located in subunit C.

further to F_A and F_B, two iron-sulfur clusters held within an extrinsic protein subunit.

The role of the Zn^{2+} in PSI remains a mystery. The effect of Zn^{2+} in bacterial RCs does not readily provide clues, as the protein structures and terminal electron transfer steps are quite different between PSI and the bacterial RC. In bacterial RCs, Zn^{2+} binding modulates $Q_A^-Q_B \rightarrow Q_AQ_B^-$ electron transfer and proton uptake at Q_B. The sequential electron transfer steps in PSI terminate at two iron-sulfur clusters instead of terminating at two functionally distinct quinone acceptors and no proton uptake mechanisms have been invoked for PSI function. Metal binding to a protein alters the mobility of metal ligands and the surrounding region of the polypeptide as well as changes electrostatic environments. Does metal ion tuning of structural or electrostatic protein environments influence PSI function? Our working hypothesis is that metal ions bind at the acceptor end of PSI, the most solvent exposed and flexible region of the protein.(Figure 1) We are employing bioinorganic techniques to closely examine the metal ion binding to PSI. The formation of F_A^- and F_B^- in the presence and absence of metal ions is being studied with X-band EPR, and metal ion induced effects on the primary radical pair $P^+A_1^-$ are being studied with HF EPR. Electron spin-echo envelope modulation (ESEEM) spectroscopy was used to probe the coordination environment of Cu^{2+}-substituted PSI and strongly coupled ^{14}N nuclei from a single histidine ligand was observed. Inspection of the crystal structure indicates two potential histidine ligands on the acceptor side of PSI. Preliminary extended x-ray absorption (EXAFS) spectra have been obtained of Zn-PSI. The influence of metal ions on the docking reaction of ferredoxin to PSI will be examined in future work.

Protein conformational changes linked to electron transfer. In the bacterial RC, photoinitiated electron transfer terminates in the electron transfer between two quinone molecules, Q_A and Q_B. The heterogeneous kinetics, temperature trends, and pH dependencies of the $Q_A^-Q_B \rightarrow Q_AQ_B^-$ reaction show that this interquinone electron transfer is intimately linked to a complex conformational landscape. Observed alterations of reaction kinetics by illumination while cooling have been linked to trapping the RC in altered conformations induced by charge separation. We have developed a method, based on monitoring matrix electron nuclear double resonance (ENDOR) lines, to explore the physical basis for the dramatic variation in low temperature $Q_A^-Q_B \rightarrow Q_AQ_B^-$ electron transfer. No differences in the protein structure near Q_B^- or reorientation (within 5^o) of Q_B^- was observed for HF pulsed D-band (130 GHz) matrix ENDOR spectra of "active" and "inactive" $P^+Q_B^-$ conformational states.

These results reveal a remarkably enforced local protein environment for Q_B in its reduced semiquinone state and suggest that the conformational change that controls reactivity resides beyond the Q_B local environment. It is possible that light-induced changes trapped at low temperature are located in the protein environment near Q_A. We have observed reorganization of the protein environment to accommodate the donor-acceptor charge separated state $P^+Q_A^-$ in dark adapted samples. We plan to extend these studies to examine the relaxation response of the protein surrounding Q_A^- in RC samples that have been freeze trapped in the light. In addition, we will be characterizing the quinone protein environments and interquinone electron transfer reactions in crystals. We have obtained the first crystals of RCs that have the non-heme iron biochemically removed and replaced with Zn^{2+}. Removal of the non-heme Fe^{2+} is essential for observing Q_A^- and Q_B^- radical species with EPR. Configurational dynamics will differ in the crystalline environment vs. solution environment, allowing us to resolve dynamic features correlated to photosynthetic electron transfer.

DOE Sponsored Publications 2005-2007

1. Utschig, L. M., Thurnauer, M. C., Tiede, D., and Poluektov, O. G. "Low Temperature Interquinone Electron Transfer in Photosynthetic Reaction Centers from *R. sphaeroides* and *B. viridis*: Characterization of Q_B^- States by High-Frequency EPR and ENDOR," *Biochemistry*, 2005, *44*, 14131-14142.
2. Poluektov, O. G., Utschig, L. M., Dubinskij, A. A. and Thurnauer, M.C. "Electron Transfer Pathways and Protein Response to Charge Separation in Photosynthetic Reaction Centers: Time-Resolved High-field ENDOR of the Spin-Correlated Radical Pair $P_{865}^+Q_A^-$", *J. Am. Chem. Soc.*, 2005, *127*, 4049-4059.
3. Poluektov, O. G., Paschenko, S. V., Utschig, L. M., Lakshmi, K. V., and Thurnauer, M. C. "Bidirectional Electron Transfer in Photosystem I: Direct Evidence from High-Frequency Resolved EPR", *J. Amer. Chem. Soc.* 2005, *127*, 11910-11911.
4. Link, G., Poluektov, O. G., Utschig, L. M., Lalevee, J., Yago, T., Weidner, J.-U., Thurnauer, M. C. and Kothe, G. "Structural Organization in Photosynthetic Proteins as Studied by High-Field EPR of Spin-Correlated Radical Pair States," *Magn. Res. in Chem.,* 2005*, 43, S103-S109*.
5. Dubinskij, A. A., Utschig, L. M., and Poluektov, O. G. "Spin-Correlated Radical Pairs: Differential Effect in High-Field ENDOR Spectra", *Appl. Magn. Reson.*, 2006, *30*, 269-286.
6. Poluektov, O. G., Utschig, L. M., Thurnauer, M. C., and Kothe G. "Exploring Hyperfine Interactions in Spin-Correlated Radical Pairs from Photosynthetic Proteins: High-Frequency ENDOR and Quantum Beat Oscillations", *Appl. Magn. Reson.*, in press
7. Heinen, U., Utschig, L. M., Poluektov, O. G., Link, G., Ohmes, E., Thurnauer, M. C., Kothe, G. Structure of the Charge Separated State $P^+Q_A^-$ in the Photosynthetic Reaction Centers of *Rhodobacter sphaeroides* by Quantum Beat Oscillations and High-Field Electron Paramagnetic Resonance: Evidence for Light-Induced QA- Reorientation," *J. Am. Chem. Soc.*, submitted.
8. Poluektov, O. G. and Utschig, L. M. "Protein Environments and Electron Transfer Processes Probed with High-Frequency ENDOR" In *The Purple Photosynthetic Bacteria*: *Genetics, Molecular Biology, Biochemistry and Biophysics*, Hunter, C. N., Thurnauer, M. C., and Beatty, J. T., Eds., Springer, Dordrecht, in press.

SYNTHETIC ANALOGUES OF CHLOROPHYLLS FOR SOLAR-ENERGY APPLICATIONS

Jonathan S. Lindsey[1], David F. Bocian,[2] and Dewey Holten[3]

[1]Department of Chemistry, North Carolina State University, Raleigh, NC 27695
[2]Department of Chemistry, University of California Riverside, Riverside, CA 92521
[3]Department of Chemistry, Washington University, St. Louis, MO 63130

A long-term goal of our program is to design, synthesize, and characterize synthetic molecular architectures for efficient solar-energy conversion. One recent effort in this regard concerns understanding the effects of substituents on the spectra of synthetic chlorins. This work exploits recent advances in synthetic methodology that have made possible systematic studies of the properties of the chlorin macrocycle as a function of diverse types and patterns of substituents. We have examined the spectral, vibrational, and excited-state decay characteristics for a set of synthetic chlorins. The chlorins bear substituents at the 5,10,15 (meso) positions, or the 3,13 (β) positions, and include 24 zinc chlorins, 18 free base analogues, and one free base or zinc oxophorbine. The oxophorbine contains the keto-bearing isocyclic ring (ring E) present in the natural photosynthetic pigments (e.g., chlorophyll a). The substituents examined include acetyl, ethynyl, formyl, phenyl, and vinyl.

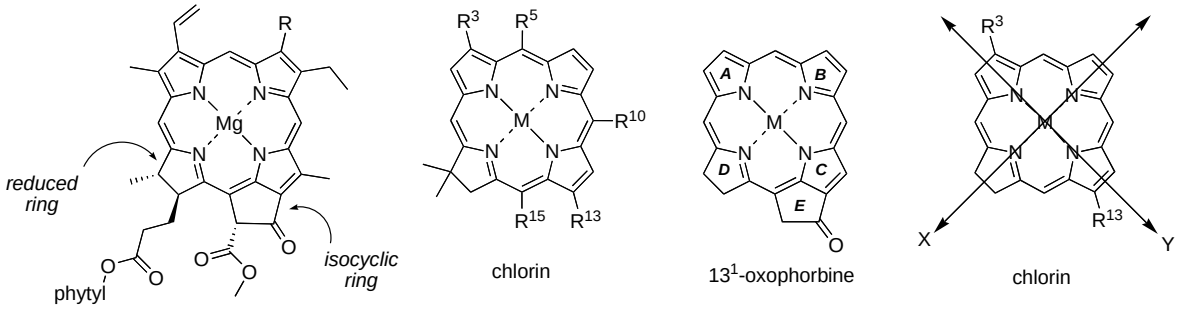

Chlorophyll *a* (R = CH_3)
Chlorophyll *b* (R = CHO)

One motivation for this work is to understand the origin of the intensities and spectral positions of the major absorption bands of chlorophylls. While chlorophyll *a* is a chlorin, a synthetic chlorin lacking any substituents exhibits a quite different absorption spectrum. The substituents in the synthetic chlorins cause no significant perturbation to the structure of the chlorin macrocycle, as evidenced by the vibrational properties investigated using resonance Raman spectroscopy. In contrast, the fluorescence properties are significantly altered by substituents. For example, the fluorescence wavelength maximum, quantum yield, and lifetime for a zinc chlorin bearing 3,13-diacetyl and 10-mesityl

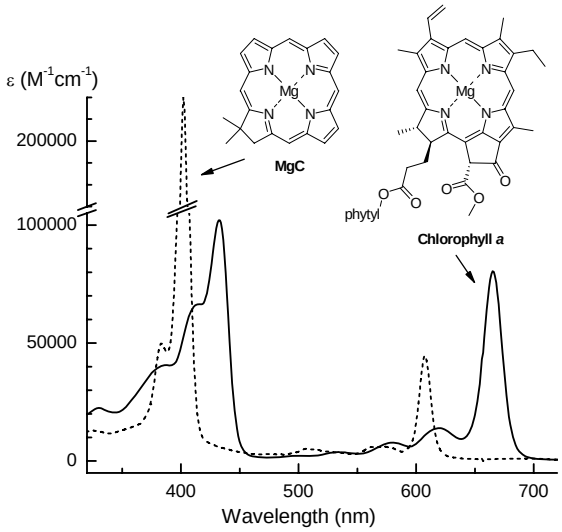

groups (662 nm, 0.28, 6.0 ns) differ substantially from those of the parent unsubstituted chlorin (602 nm, 0.062, 1.7 ns). Each of these properties of the lowest singlet excited state can be progressively stepped between these two extremes by incorporation of different substituents. These perturbations are associated with significant changes in the rate constants of the decay pathways of the lowest excited singlet state. In this regard, the zinc chlorins with the red-most fluorescence also have the greatest radiative decay rate constant, and are expected to have the fastest nonradiative internal conversion to the ground state. Nonetheless, these complexes have the longest singlet-excited-state lifetime. The free base chlorins bearing the same substituents exhibit similar fluorescence properties. Such combinations of factors render the chlorins suitable for a range of applications wherein tunable coverage of the solar spectrum and long-lived excited states are desired.

Density functional theory calculations were carried out to probe the effects of the types and positions of substituents on the characteristics (energies, electron distributions) of the frontier molecular orbitals. A general finding is that the 3,13 positions are more sensitive to the effects of auxochromes than the 5,10,15 positions. The auxochromes investigated (acetyl > ethynyl > vinyl > aryl) cause a significant red shift and intensification of the Q_y band upon placement at the 3,13 positions, whereas groups at the 5,10,15 positions result in much smaller red shifts that are accompanied by a decrease in relative Q_y intensity. In addition, the calculated substituent-induced shifts on the HOMO and LUMO energies track the trends in the measured first oxidation and reduction potentials, respectively. The calculations show that the LUMO is shifted more by substituents than the HOMO, which derives from differences in the electron densities of the two orbitals at the substituent sites.

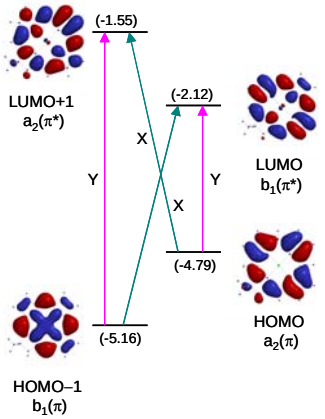

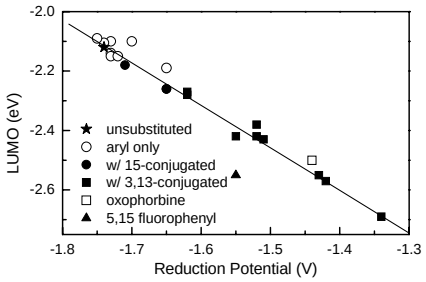

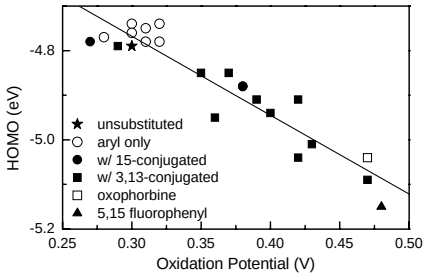

The trends in the substituent-induced effects on the wavelengths and relative intensities of the major features (B_y, B_x, Q_x, Q_y) in the near-UV to near-IR absorption bands are well accounted for using Gouterman's four-orbital model, which incorporates the effects of the substituents on the HOMO–1 and LUMO+1 in addition to the HOMO and LUMO. Collectively, the results and analysis provide insights into the effects of substituents on the optical absorption, redox, and other photophysical properties of the chlorins. These insights form a framework that underpins the rational design of chlorins for applications in solar-energy conversion. Towards this goal, a synthetic chlorin with a tether for surface attachment was utilized along with a bacteriochlorin and three porphyrins in a study of the effects of macrocycle reduction and type of surface tether on photocurrent production in regenerative solar cells. Future goals are to design self-assembling chlorins and bacteriochlorins for solar conversion.

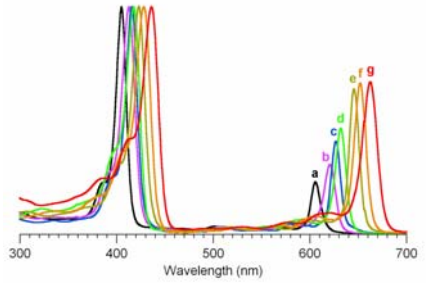

DOE Sponsored Publications 2005-2007:

1. "Structural Control of the Photodynamics of Boron-Dipyrrin Complexes," Kee, H. L.; Kirmaier, C.; Yu, L.; Thamyongkit, P.; Youngblood, W. J.; Calder, M. E.; Ramos, L.; Bocian, D. F.; Scheidt, W. R.; Birge, R. R.; Lindsey, J. S.; Holten, D. *J. Phys. Chem. B* **2005**, *109*, 20433–20443.

2. "Synthesis of Dipyrrin-Containing Architectures," Muthukumaran, K.; Zaidi, S. H. H.; Yu, L.; Thamyongkit, P.; Calder, M. E.; Sharada, D. S.; Lindsey, J. S. *J. Porphyrins Phthalocyanines* **2005**, *9*, 745–759.

3. "Synthesis of a New *trans*-A_2B_2 Phthalocyanine Motif as a Building Block for Rodlike Phthalocyanine Polymers," Youngblood, W. J. *J. Org. Chem*. **2006**, *71*, 3345–3356.

4. "Mechanisms, Pathways, and Dynamics of Excited-State Energy Flow in Self-Assembled Wheel-and-Spoke Light-Harvesting Architectures," Song, H.-E.; Kirmaier, C.; Yu, L.; Bocian, D. F.; Lindsey, J. S.; Holten, D. *J. Phys. Chem. B* **2006**, *110*, 19121–19130.

5. "Effects of Multiple Pathways on Excited-State Energy Flow in Self-Assembled Wheel-and-Spoke Light-Harvesting Architectures," Song, H.-E.; Kirmaier, C.; Yu, L.; Bocian, D. F.; Lindsey, J. S.; Holten, D. *J. Phys. Chem. B* **2006**, *110*, 19131–19139.

6. "Theoretical Solar-to-Electrical Energy-Conversion Efficiencies of Perylene-Porphyrin Light-Harvesting Arrays," Hasselman, G. M.; Watson, D. F.; Stromberg, J. S.; Bocian, D. F.; Holten, D.; Lindsey, J. S.; Meyer, G. J. *J. Phys. Chem. B* **2006**, *110*, 25430–25440.

7. "Effects of Substituents on Synthetic Analogues of Chlorophylls: Synthesis, Vibrational Properties and Excited-State Decay Characteristics," Kee, H. L.; Kirmaier, C.; Tang, Q.; Diers, J. R.; Muthiah, C.; Taniguchi, M.; Laha, J. K.; Ptaszek, M.; Lindsey, J. S.; Bocian, D. F.; Holten, D. *Photochem. Photobiol*. **2007**, *83*, in press.

8. "Effects of Substituents on Synthetic Analogues of Chlorophylls: Redox Properties, Optical Spectra and Electronic Structure," Kee, H. L.; Kirmaier, C.; Tang, Q.; Diers, J. R.; Muthiah, C.; Taniguchi, M.; Laha, J. K.; Ptaszek, M.; Lindsey, J. S.; Bocian, D. F.; Holten, D. *Photochem. Photobiol*. **2007**, *83*, in press.

9. "Meso-^{13}C-Labeled Porphyrins for Studies of Ground-State Hole Transfer in Multiporphyrin Arrays," Thamyongkit, P.; Muresan, A. Z.; Diers, J. R.; Holten, D.; Bocian, D. F.; Lindsey, J. S. *J. Org. Chem.* **2007**, *72*, submitted.

10. "Tracking Electrons and Atoms in a Photoexcited Metalloporphyrin," Chen, L. X.; Zhang, X.; Wasinger, E. C.; Attenkofer, K.; Jennings, G.; Muresan, A. Z.; Lindsey, J. S. *Science* **2007**, submitted.

11. "Examination of Tethered Porphyrin, Chlorin, and Bacteriochlorin Molecules in Mesoporous Metal-Oxide Solar Cells," research groups of D. F. Bocian, D. Holten, J. S. Lindsey, and G. J. Meyer (to be submitted April 2007).

12. "Synthesis and Photophysical Characterization of Porphyrin, Chlorin, and Bacteriochlorin Molecules Bearing Tethers for Surface Attachment," research groups of D. F. Bocian, D. Holten, and J. S. Lindsey (to be submitted April 2007).

Session VII

Photocatalytic Systems

PHOTOINITIATED ELECTRON COLLECTION IN MIXED-METAL SUPRAMOLECULAR COMPLEXES: DEVELOPMENT OF PHOTOCATALYSTS FOR HYDROGEN PRODUCTION

Karen J. Brewer, Mark Elvington, Ran Miao, Shamindri Arachchige
Department of Chemistry
Virginia Tech, Blacksburg, VA 24061-0212

Supramolecular complexes used in this forum are large molecular assemblies built of smaller sub-units. Each sub-unit contributes properties to the supramolecular assembly, allowing the assembly to display complex functions. The coupling of multiple charge transfer light absorbing (LA) units in combination with an electron collector (EC) provides light activated collection of reducing equivalents, photoinitiated electron collection. Supramolecular assemblies coupling two ruthenium light absorbers through bridging ligands (BL) to a central Rh core have been constructed and shown to undergo photoinitiated electron collection at the Rh center. These Rh centered supramolecular complexes are capable of producing H_2 from H_2O when excited in the presence of an electron donor.

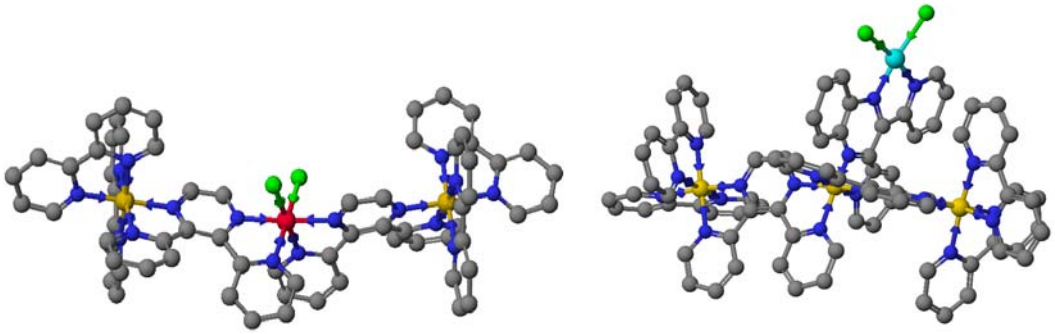

$[(bpy)_2Ru(dpp)RhCl_2(dpp)Ru(bpy)_2]^{5+}$ $[\{(bpy)_2Ru(dpp)\}_2Ru(dpq)PtCl_2]^{6+}$

Figure 1. *Mixed-Metal Supramolecular Photocatalysts for H_2 Production from H_2O.*

Systems have also been developed that couple multiple Ru based LAs to an organic EC attached to a catalytically active Pt site. The system $[\{(bpy)_2Ru(dpp)\}_2Ru(dpq)PtCl_2]^{6+}$ has also been shown to produce H_2 when excited with visible light in the presence of electron donors. These supramolecular complexes display unique reactivity using a single molecule to absorb light, collect reducing equivalents and catalyze H_2 production.

The ability to most effectively use a supramolecular structural motif for solar hydrogen production will depend on the development of an understanding of the factors governing this multi-electron photochemistry. We are exploring the impact of sub-unit variation on the basic chemical and photochemical properties of this class of molecules. The terminal bpy ligands, the polyazine bridging ligands and the halides coordinated to the reactive Rh and Pt centers can all be easily varied within this molecular architecture.

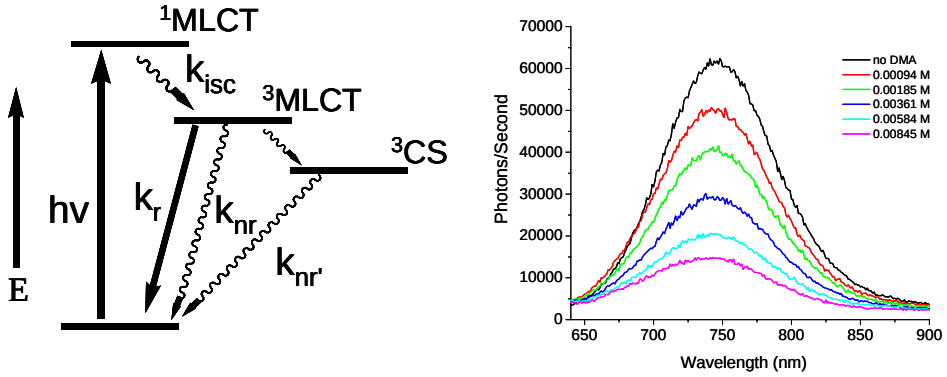

Figure 2. *State diagram for a mixed-metal supramolecular photocatalyst for H_2 production $[\{(bpy)_2Ru(dpp)\}_2Ru(dpq)PtCl_2](PF_6)_6$ and emission quenching by dimethylaniline of the ^{3}MLCT emission.*

The covalent attachment of a PTZ electron donor to produce $[(PTZpbpy)_2Ru(dpp)](PF_6)_2$ has recently been accomplished and this new chromophore-electron donor dyad can be coupled to our supramolecular H_2 photocatalysts. A study of the factors impacting basic redox properties, spectroscopic properties, photochemical properties, electron collection and hydrogen production using a supramolecular motif will be described.

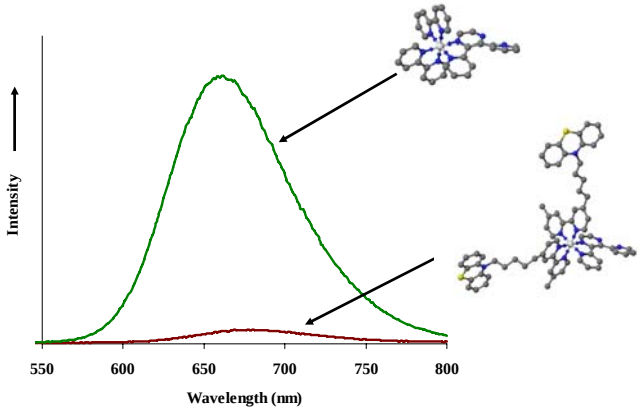

Figure 3. *Relative emission intensity of absorbance matched samples of $[(bpy)_2Ru(dpp)](PF_6)_2$ and $[(PTZpbpy)_2Ru(dpp)](PF_6)_2$ showing the reduction of the ^{3}MLCT emission upon the incorporation of the PTZ electron donor sub-unit.*

DOE Sponsored Publications 2005-2007

1. "A Structurally Diverse Mixed-Metal Complex with Mixed-Bridging Ligands $[\{[(bpy)_2Os(dpp)]_2Ru\}_2(dpq)](PF_6)_{12}$," Ran Miao, Karen J. Brewer, *Inorg. Chem.Commun.* **2007**, *10*, 307-312.
2. "Supramolecular Complexes as Photoinitiated Electron Collectors: Applications in Solar Hydrogen Production," Mark Elvington, Jared R. Brown, David F. Zigler, Karen J. Brewer, *Proceedings of the SPIE, Optics and Photonics, Solar Hydrogen and Nanotechnology* **2006**, *Proc. of SPIE Vol. 6340*, 63400W1-13. Invited Paper.
3. "Electrochemistry," Mark Elvington, Karen J. Brewer, *Encyclopedia of Inorganic Chemistry*, Robert Scott Editor, Wiley and Sons, **2007**, in press.
4. "A Donor-Chromophore Complex Containing the Polyazine Bridging Ligand 2,3-bis(2-pyridyl)pyrazine," Shamindri M. Arachchige, Karen J. Brewer, *Inorg. Chem. Commun.* **2007**, submitted for publication
5. "Rhodium Centered Mixed-Metal Supramolecular Complex as a Photocatalyst for the Visible Light Induced Production of Hydrogen," Mark C. Elvington, Jared Brown, Shamindri M. Arachchige, Karen J. Brewer, **2007**, submitted for publication.
6. "A Mixed-Metal Ru(II),Pt(II) Supramolecular Complex as a Photocatalyst for the Visible Light Production of H_2 from H_2O," Ran Miao, Karen J. Brewer, **2007**, manuscript in preparation.

POLYNUCLEAR PHOTOCATALYTIC SITES ON NANOPOROUS SILICA SUPPORTS FOR H_2O OXIDATION AND CO_2 REDUCTION

Heinz Frei
Physical Biosciences Division, Lawrence Berkeley National Laboratory
Berkeley, CA 94720

The purpose of this project is to develop robust artificial systems for the synthesis of fuels and chemicals from abundant sources like carbon dioxide and water using sunlight as energy source. Using inert nanoporous solids as high surface area supports, we have developed methods over the past few years for assembling well-defined 'molecular', all-inorganic units that function as visible light photocatalysts for demanding reduction and oxidation reactions. In this approach, each photocatalytic site consists of a binuclear metal charge-transfer unit that acts as a visible light electron pump for a driving multi-electron transfer catalyst. The synthetic methods offer inherent flexibility for selecting pairs of transition metals that optimize visible light absorption characteristics, potentials and charge-transfer properties of the photo-redox sites, a crucial requirement for efficiently driving multi-electron transfer catalysts. The high surface area of the nanoporous support is essential for achieving sufficient density of photocatalytic sites to assure maximum utilization of incident photons, and the nanostructured features provide ways of ultimately separating reduced from oxidized species on the nanoscale.

Binuclear Charge-Transfer Units as Visible Light Electron Pumps

We have assembled and covalently anchored in the 30 Angstrom diameter pores of a mesoporous silica material (MCM-41) binuclear units consisting of a group 4 metal (Ti, Zr) linked via an oxo-bridge to a d^{10} or an s^2 metal (Cu^I or Sn^{II}) that renders the unit colored (e.g. Ti-O-Cu^I, Ti-O-Sn^{II}, or Zr-O-Cu^I). These moieties possess metal-to-metal charge-transfer (MMCT) transitions that absorb deep in the visible. In the case of the material featuring anchored Zr-O-Cu^I groups, excitation of the MMCT chromophore led to the reduction of CO_2 gas loaded into the pores to CO by a single photon process, while Cu^I was oxidized to Cu^{II}. Photoreduction of CO_2 to CO is the most demanding of three sequential 2-electron transfer steps for the conversion to methanol.

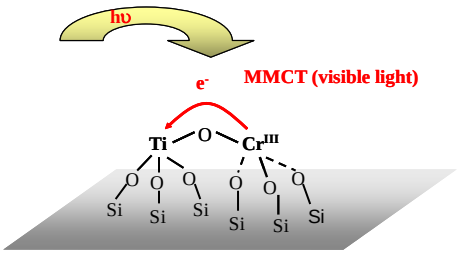

In order to close the photocatalytic cycle, the oxidized donor center needs to be reduced to its initial oxidation state using water as electron source. Hence, units need to be synthesized in which the d^{10} (s^2) donor center is replaced by a metal center that has sufficient oxidizing power to drive a multi-electron catalyst for water oxidation with visible light. Ti-O-Ce^{III}, Ti-O-Co^{II}, Ti-O-Mn^{II} and Ti-O-Cr^{III} sites have been assembled on silica nanopore surfaces. By exploiting selective redox coupling or acidity differences of surface hydroxyl groups, preferential linkage of the donor precursor (e.g. $Co^{II}(NCCH_3)_4$) to Ti rather than formation of isolated metal centers or metal oxide clusters of one or the other metal was achieved. For each system, the MMCT chromophore absorbs visible light, with some extending as far as 700 nm, and the oxidized donor has a positive potential that is sufficient for driving a multi-electron water oxidation catalyst. Evidence for oxo-bridged structures and details about covalent surface anchoring and metal coordination were derived from optical, FT-

IR, FT-Raman, XANES and EPR spectroscopic studies. Moreover, redox reactions induced by MMCT excitation confirm that the units operate as photocatalytic sites.

Visible Light-Driven Water Oxidation at Ir Oxide Catalyst in Nanoporous Silica

We have assembled a photocatalytic unit consisting of an iridium oxide nanocluster that serves as an efficient multi-electron transfer catalyst for water oxidation coupled to a single Cr^{VI} center embedded in the silica nanopore surface. The unit affords water oxidation with blue and green light. The Cr^{VI}-O ligand-to-metal charge-transfer transition acts as a single photon electron pump extracting one electron at the time from the Ir oxide cluster that, in turn, catalyzes the oxidation of water. FT-Raman, FT-IR, optical and high-resolution transmission electron microscopy coupled with X-ray spot analysis allowed structural characterization of individual assembly steps of the photocatalytic unit. This is the first example of visible light-driven oxygen evolution from H_2O by a multi-electron transfer catalyst coupled to a molecular chromophore (a single metal center in this case). At the same time, we are assembling units featuring biomimetic Mn dimer cores. These units will allow us to gain the most detailed understanding of the structural, energetic and electron transfer properties of the linkages between catalytic core and charge transfer pump. The use of surface-anchored metal centers as charge-transfer chromophores for driving water oxidation is the first step in coupling the oxygen evolving catalyst to a binuclear charge transfer pump. The latter offers the flexibility needed for the selection of donor metal and oxidation state to match redox potentials and optimize directional charge flow from catalyst to chromophore, and between the charge transfer units of the two half reactions.

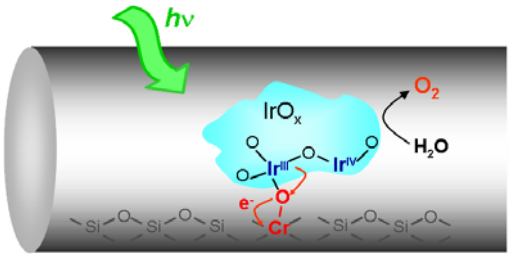

Monitoring Elementary Processes in Nanoporous Solids by Time-Resolved FT-IR Spectroscopy

Understanding of elementary redox steps and the behavior of emerging products in nanoporous photocatalytic assemblies is essential for developing efficient solar to chemical energy conversion systems. We are using transient step-scan and rapid-scan FT-IR absorption spectroscopy to monitor processes inside the nanopores. Recent studies have focused on the behavior of CO molecules, the 2-electron reduction product of CO_2, to determine the kinetics and identify the limiting steps of escape from the nanoscale channels. The goal is to identify nanoporous supports with structures that offer rapid escape from the catalytic sites in order to minimize back reaction. Monitoring of CO inside MCM-41 silica by its infrared band at 25 nanosecond resolution revealed that the molecules leave the 30 Angstrom channels within 500 microseconds at room temperature. The fast rate implies that the escape of the reduced product will not be rate limiting in this nanoporous photoconversion system. The infrared band profile showed that CO molecules interact, O or C end-on, with surface silanol (SiOH) groups or with siloxane oxygens (SiOSi) of the silica surface as they diffuse through the nanopores. This is the first insight into adsorption sites and diffusion kinetics of a small molecule in mesopores under reaction conditions. We have expanded the time-resolved transient IR method to studies of reactions in liquids using the ATR technique with the goal of capturing reaction intermediates of light-driven water oxidation in nanoporous photocatalytic systems. The high sensitivity of the method for mechanistic studies of photochemical reactions of liquids in silica nanopores has been demonstrated.

DOE Sponsored Publications 2005-2007

1. W. Lin, H. Han, and H. Frei. CO_2 Splitting by H_2O to CO and O_2 under UV Light in TiMCM-41 Silica Sieve. *J. Phys. Chem. B* **108,** 18269 (2005).

2. W. Lin and H. Frei. Photochemical CO_2 Splitting by Metal-to-Metal Charge-Transfer Excitation in Mesoporous $ZrCu^{I}$-MCM-41 Silicate Sieve. *J. Am. Chem. Soc.* **127**, 1610-1611 (2005).

3. W. Lin and H. Frei. Anchored Metal-to-Metal Charge-Transfer Chromophores in Mesoporous Silicate Sieve for Visible Light Activation of Ti Centers. *J. Phys. Chem. B* **109**, 4929-4935 (2005).

4. W. Lin and H. Frei. Bimetallic Redox Sites for Photochemical CO_2 Splitting in Mesoporous Silicate Sieve. *Cont. Rend. Sci.* **9**, 207 (2005).

5. J.F. Cahoon, M.F. Kling, K.R. Sawyer, H. Frei, and C.B. Harris. 19-Electron Intermediates in the Ligand Substitution of $CpW(CO)_3^{\cdot}$ with a Lewis Base. *J. Am. Chem. Soc.* **128**, 3152-3153 (2006).

6. H. Frei. Selective Hydrocarbon Oxidation in Zeolites (Perspective Article). *Science* **313**, 309-310 (2006).

7. Nakamura and H. Frei. Visible Light-Driven Water Oxidation by Ir oxide Clusters Coupled to Single Cr Centers in Mesoporous Silica. *J. Am. Chem. Soc.* **128**, 10668-10669 (2006).

8. L.K. Andersen and H. Frei. Dynamics of CO in Mesoporous Silica Monitored by Time-Resolved Step-Scan and Rapid-Scan FT-IR Spectroscopy. *J. Phys. Chem. B* **110**, 22601-22607 (2006).

9. H. Han and H. Frei. Visible Light Absorbing Ti-Co Metal-to-Metal Charge-Transfer Sites on Mesoporous Silica Surface. *Microporous Mesoporous Mater.* **98**, 000 (2007).

10. H. Han, L.K. Andersen, and H. Frei. Applications of Transition Metal Oxide-Based Photocatalysts for CO_2 Reduction and H_2O Oxidation. In *Environmentally Benign Catalysts*; Anpo, M., Ed.; Springer, New York.

11. G. Mul, W.A. Wasylenko, and H. Frei. Time-Resolved FT-IR (ATR) Monitoring of Visible Light-Induced Oxidation of Liquid Cyclohexene in Vanadium TUD-1 Silica Sieve". *J. Phys. Chem. C*, submitted.

TRANSITION METAL-BASED REACTIONS FOR PHOTOGENERATION OF FUELS

David C. Grills, Carol Creutz and Etsuko Fujita
Chemistry Department
Brookhaven National Laboratory
Upton, NY 11973-5000

The goal of our research is to gain a fundamental understanding of the processes involved in the chemical conversion of solar energy. The long-term storage of solar energy as fuels or valuable chemicals could potentially help to solve the problem of our rapidly depleting fossil-fuel reserves. The processes involved require efficient coupling of light absorption, photo-induced electron transfer, and chemical transformations, including bond-forming and cleavage reactions. We have been focusing on factors controlling the bond formation rates between photoproduced metal-based intermediates and substrates in the early stages of photoreduction processes, especially those involving the photoreduction of CO_2. We have broadened our studies to include the photochemical activation of small molecules such as H_2, C_2H_4, CH_4, CO, other gaseous hydrocarbons, and N_2 because of their relevance to our future energy needs, energy conservation, and environmental concerns. New emphases in our program are the study of the photoinduced reduction of CO_2 in supercritical CO_2, and the investigation of hydride transfer mechanisms for the reduction of CO_2 and other molecules.

Direct Measurements of Rate Constants and Activation Volumes for the Binding of Small Molecules to $W(CO)_3(PCy_3)_2$: Theoretical and Experimental Studies. Thermodynamic and kinetic parameters for the binding of small molecules to the agostically stabilized *mer,trans*-$W(CO)_3(PCy_3)_2$ (**W**) have been investigated directly by transient spectroscopy. 355 nm excitation of solutions containing **W**-L (L = H_2, D_2, N_2, C_2H_4 and CH_3CN) resulted in the photo-ejection of L and the formation of **W**. A combination of ns UV-vis flash photolysis and time-resolved step-scan FTIR spectroscopy was used to spectroscopically characterize the photoproduct, **W** and directly measure the rate constants for binding of the ligands L to **W** to reform **W**-L under pseudo-first order conditions. From these data, equilibrium constants for the binding of L to **W** were estimated. The UV-vis flash photolysis experiments were also performed as a function of pressure in order to determine the activation volumes, $\Delta V^{\ddagger}$, for the reaction of **W** with L. Small activation volumes ranging from -7 to +3 cm^3 mol^{-1} were obtained, suggesting that despite the crowded W center, an interchange mechanism between L and the agostic W···H-C interaction of one of the PCy_3 ligands (or a weak interaction with a solvent molecule) at the W center takes place in the transition state. Density functional theory (DFT) calculations were performed at the B3LYP level of theory on **W** with/without the agostic

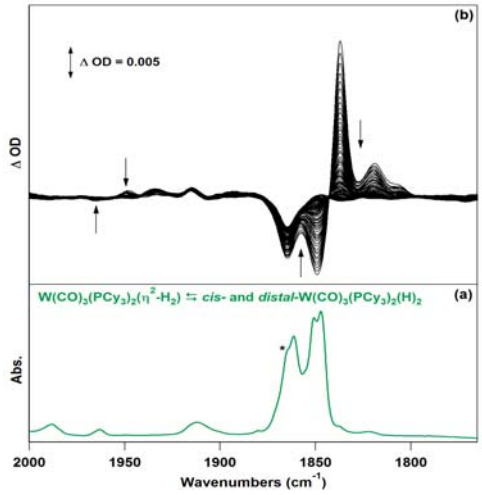

(a) FTIR of **W**-H_2 in hexane under 1.8 atm H_2, showing six overlapped ν(CO) bands due to the equilibrium mixture of **W**-(H_2), **W**-*distal*-$(H)_2$ and **W**-*cis*-$(H)_2$; * = contamination by **W**-CO. (b) Step-scan FTIR spectra recorded between 2 and 192 μs following 355 nm excitation. Arrows show directions of band decay and recovery following excitation.

C-H interaction of the PCy_3 ligand and also on the series of model complexes, *mer*,*trans*-$W(CO)_3(PH_3)_2L$ (**W'**-L, where L = H_2, N_2, C_2H_4, CO and *n*-hexane). These calculations indicate an entropy effect that favors agostic $W^{\cdots}H$-C interaction over a solvent σ C-H interaction by 8-10 kcal mol^{-1}. (DCG, EF with J.T. Muckerman and R. v. Eldik)

Reactivities of Re(dialkyldiimine)$(CO)_3$ in Re-Re Bond Formation: Towards the Photoreduction of CO_2 in Supercritical CO_2. The photoinduced catalytic reduction of CO_2 to CO (and if possible beyond) is an important process that has received significant attention. The family of catalysts based on the $Re(CO)_3(\alpha$-diimine) moiety have been shown to catalyze CO_2-to-CO reduction, but rather inefficiently. Our mechanistic and kinetic investigations of this process indicated that one reason for the inefficiency could be the polar coordinating solvent binding to a vacant site at the catalyst, thus hindering reaction with CO_2. We therefore prepared the new dinuclear complex, $[Re(dnb)(CO)_3]_2$ (dnb = 4,4'-dinonyl-2,2'-bipyridine), and it's mononuclear form, $Re(dnb)(CO)_3Cl$, both of which are soluble in non-coordinating solvents such as hexane. $[Re(dnb)(CO)_3]_2$ is thermochromic in hexane, being pink at room temperature and green at low temperature. We are investigating electronic and structural changes associated with this thermochromic behavior. We are also investigating the solvent-dependent photophysics and photochemistry of the excited states and ground state of these species in detail. Pulsed 532 nm excitation of a hexane solution of $[Re(dnb)(CO)_3]_2$ resulted in the cleavage of the Re-Re bond and formation of the active, 17-electron metal-based radical species, $Re(dnb)(CO)_3$, which was monitored by UV-vis flash photolysis and transient FTIR spectroscopy. These results indicate that the dimerization rate constants are ~10^9 and ~200 M^{-1} s^{-1} in hexane and THF, respectively, supporting our hypothesis that the elimination of coordinating solvents will dramatically enhance the reactivity of CO_2 reduction catalysts. This has paved the way to our current investigations, which involve the use of high-pressure supercritical CO_2 ($scCO_2$) as a solvent, to determine the Re-Re dimerization rate and binding rate of CO_2 in $scCO_2$. The high concentration of CO_2 in $scCO_2$ should lead to enhanced reactions rates with CO_2. (DCG, EF)

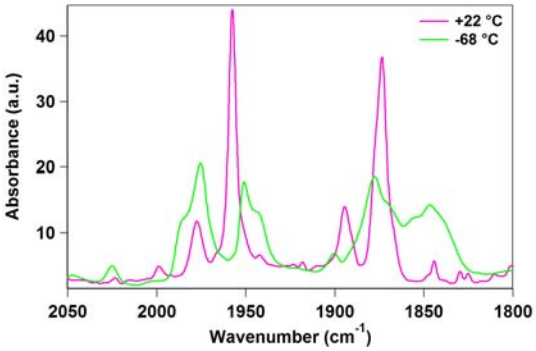

FTIR spectra of $[Re(dnb)(CO)_3]_2$ in hexane at 22 ºC (pink) and -68 ºC (green).

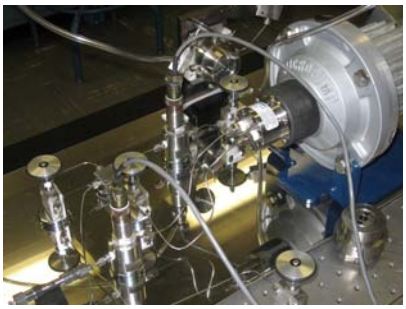
High-pressure apparatus for experiments in $scCO_2$ solution.

Hydride Transfer Reactions. We have recently begun investigating new bioinspired hydride transfer catalysts based on ruthenium complexes with NAD^+/NADH functional model ligands. These have the potential to act as photocatalysts in hydride transfer reactions to generate fuels from solar energy. Hydride transfer from $Ru(terpy)(bpy)H^+$ to CO_2 in water is also the subject of an ongoing investigation. See more details on this latter reaction in the poster given by Carol Creutz. (NAD^+/NADH studies: EF with J. T. Muckerman, D. Polyansky and K. Tanaka; $Ru(terpy)(bpy)H^+$ studies: CC with M. Chou)

DOE Sponsored Publications 2005-2007

1. Reactions of Hydroxylmethyl and Hydride Complexes in Water: Synthesis, Structure and Reactivity of a Hydroxymethyl-Cobalt Complex, C. Creutz, M. H. Chou, E. Fujita, and D. J. Szalda, *Coord. Chem. Rev.* **2005**, *249*, 375-390.
2. Carbon-to-Metal Hydrogen Atom Transfer: Direct Observation Using Time-Resolved Infrared Spectroscopy, J. Zhang, D. C. Grills, K.-W. Huang, E. Fujita, and R. M. Bullock, *J. Am. Chem. Soc.* **2005**, *127*, 15684-15685.
3. Interfacial Charge-Transfer Absorption: Semiclassical Treatment, C. Creutz, B. S. Brunschwig, and N. Sutin, *J. Phys Chem. B* **2005**, *109,* 10251-10260.
4. Transition State Characterization for the Reversible Binding of Dihydrogen to Bis(2,2'-bipyridine)rhodium(I) from Temperature- and Pressure-Dependent Experimental and Theoretical Studies, E. Fujita, B. S. Brunschwig, C. Creutz, J. T. Muckerman, N. Sutin, D. J. Szalda, and R. van Eldik, *Inorg. Chem.* **2006**, *45*, 1595-1603.
5. Kinetic Studies of the Photoinduced Formation of Transition Metal-Dinitrogen Complexes Using Time-Resolved Infrared and UV-vis Spectroscopy, D. C. Grills, K.-W. Huang, J. T. Muckerman, and E. Fujita, *Coord. Chem. Rev.* **2006**, *250*, 1681-1695.
6. Efficient Synthesis of Os-Os dimers: $[Cp(CO)_2Os]_2$, $[Cp^*(CO)_2Os]_2$, and $[(^iPr_4C_5H)(CO)_2Os]_2$, and Computational Studies on the Relative Stabilities of Their Geometrical Isomers, J. Zhang, K. -W. Huang, D.J. Szalda, and R. M. Bullock, *Organometallics* **2006**, *25*, 2209-2215.
7. Direct Measurements of Rate Constants and Activation Volumes for the Binding of H_2, D_2, N_2, C_2H_4 and CH_3CN to $W(CO)_3(PCy_3)_2$: Theoretical and Experimental Studies with Time-Resolved Step-Scan FTIR and UV-vis Spectroscopy, D. C. Grills, R. van Eldik, J. T. Muckerman, and E. Fujita, *J. Am. Chem. Soc.* **2006**, *128*, 15728-15741.
8. Interfacial Charge Transfer Absorption: Application to Metal-Molecule Assemblies, C. Creutz, B. S. Brunschwig, and N. Sutin, *Chem. Phys.* **2006**, *324*, 244-258.
9. Interfacial Charge-Transfer Absorption: 3. Application to Semiconductor-Molecule Assemblies, C. Creutz, B. S. Brunschwig, and N. Sutin, *J. Phys Chem. B* **2006**, *110,* 25181-25190.
10. Henry Taube: Inorganic Chemist Extraordinaire, C. Creutz, P. C. Ford, and T. J. Meyer, *Inorg. Chem.* **2006**, *45*, 7059-7068.
11. Characterization of Transient Species and Products in Photochemical Reactions of $Re(dmb)(CO)_3Et$ with and without CO_2, K. Shinozaki, Y. Hayashi, B. S. Brunschwig, and E. Fujita, *Res. Chem. Intermed.* **2007**, *33*, 27-36.
12. Carbon Dioxide Reduction by Pincer Rhodium η^2-Dihydrogen Complexes: Hydrogen Binding Modes and Mechanistic Studies by Density Functional Theory Calculations, K.-W. Huang, J. H. Han, C. B. Musgrave, and E. Fujita, *Organometallics*, **2007**, *26*, 508-513.
13. Photochemical and Radiolytic Production of an Organic Hydride Donor with a Ru(II) Complex Containing an NAD^+ Model Ligand, D. Polyansky, D. Cabelli, J. T. Muckerman, E. Fujita, T. Koizumi, T. Fukushima, T. Wada, and K. Tanaka, *Angew. Chem. Int. Ed*. **2007**, online Early View in advance of print.
14. Theoretical Investigation of the Binding of Small Molecules and the Intramolecular Agostic Interaction at Tungsten Centers with Carbonyl and Phosphine Ligands, J. T. Muckerman, E. Fujita, C. D. Hoff, and G. J. Kubas, *J. Phys. Chem. B* in press.
15. Generation of Ru(II)-Semiquinone-Anilino Radical Through Deprotonation of Ru(III)-Semiquinone-Anilido Complex, Y. Miyasato, T. Wada, J. T. Muckerman, E. Fujita, and K. Tanaka, *Angew. Chem. Int. Ed.* submitted.

Session VIII

Charge Separation in Supramolecular Systems

SUPRAMOLECULAR STRUCTURES FOR PHOTOCHEMICAL ENERGY CONVERSION

Devens Gust, Thomas A. Moore, Ana L. Moore
Department of Chemistry and Biochemistry
Arizona State University
Tempe, AZ, 85287

The long-term goal of this research is to explore the basic chemistry and photophysics of approaches to "artificial photosynthesis" that employ synthetic organic molecules as light-harvesting antennas, electron donors, and electron accepting species. The research will yield design principles that will form the basis of new solar energy technologies for production of electricity and fuels. Research during the last two years has focused on the interactions of synthetic antenna systems with artificial reaction center components and ways to control the light gathering process. Two general types of antenna systems will be discussed: those based on hexaphenylbenzene as an organizing principal and those based on carotenoid polyenes.

Hexaphenylbenzene as a structural core for antenna-reaction center complexes. Hexaphenylbenzene has proven to be a useful material for organizing antenna and reaction center components. It is relatively rigid, and allows control of interchromophore distances and angles. It provides interchromophore separations and electronic coupling interactions that permit ultrafast migration of singlet excitation energy among components. Finally, it is synthetically versatile, so that a variety of antenna motifs may be examined.

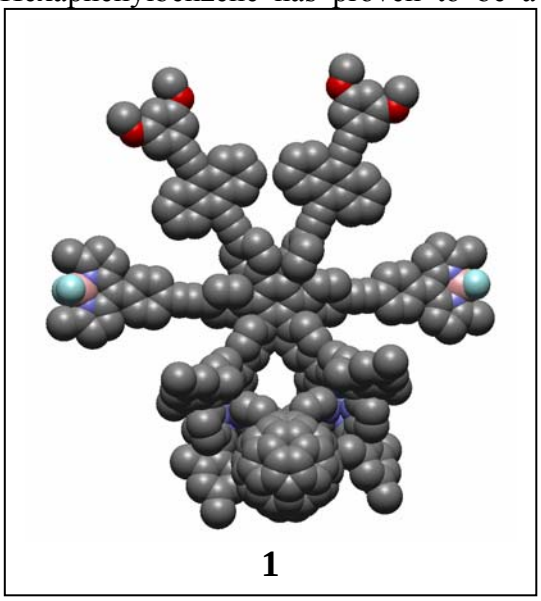

1

Heptad structure **1**, for example, features two bisphenylethynylanthracene (BPEA) antenna moieties, two borondipyrromethene (BDPY) antennas, and two zinc porphyrins bound to the hexaphenylbenzene core. The BPEA species absorb around 450 nm, at slightly longer wavelengths than the porphyrin Soret band. The BDPY chromophores absorb in the 510-nm region, and the porphyrin Q-bands at longer wavelengths. Thus, the molecule absorbs throughout most of the visible spectrum. Excitation of BPEA is followed by energy migration to the BDPY, and then on to the porphyrin in ≤20 ps, in a funnel-like fashion. Some excitation also migrates directly to the porphyrins on a similar time scale.

The zinc porphyrins associate with a dipyridylfullerene derivative (binding constant = 7.3×10^4 M^{-1} in *o*-difluorobenzene). The resulting heptad demonstrates photoinduced electron transfer from the porphyrin to the fullerene with a time constant of ~3 ps, and the charge-separated state has a lifetime of 230 ps.

A variety of other model antenna-reaction center structures based on hexaphenylbenzene also demonstrate energy transfer from antenna moiety to porphyrin by multiple pathways.

Carotenoid polyenes in artificial photosynthesis. The role of carotenoid pigments in photosynthesis is enigmatic; they harvest solar energy for driving photosynthesis and are important components of mechanisms that down-regulate photosynthesis. Under down-regulated conditions light energy collected by these pigments is later dissipated as heat. By studying model systems we have found electrochemical and spectroscopic determinants that control energy flow between carotenoid and tetrapyrrole pigments. This work has set the stage for understanding this paradox of carotenoid function in natural systems.

Transient absorption spectroscopy on a series of artificial light harvesting dyads made up of a zinc phthalocyanine (Pc) covalently linked to carotenoids with 9, 10 or 11 conjugated carbon-carbon double bonds (dyads **2**, **3** and **4**, respectively) allowed assessment of the energy transfer and excited-state deactivation pathways of the strongly allowed carotenoid S_2 state as a function of the conjugation length. Following excitation, the carotenoid S_2 state rapidly relaxes to the S^* and S_1 states. In all systems we detected a new pathway of energy deactivation within the carotenoid manifold, in which the S^* state acts as an intermediate state in the $S_2 \rightarrow S_1$ internal conversion pathway on a sub-ps timescale. In dyad **4**, a novel type of collective carotenoid-Pc electronic state was observed which might correspond to a carotenoid excited state(s)–Pc Q-band exciplex. The exciplex is only observed upon direct carotenoid excitation and is nonfluorescent. In dyad **2**, two carotenoid singlet excited states, S_2 and S_1, contribute to singlet-singlet energy transfer to Pc, making the process very efficient (>90 %), while for dyads **3** and **4** the S_1 energy transfer channel is precluded and only S_2 is capable of transferring energy to Pc. In the latter two systems, the lifetime of the first singlet excited state of Pc is dramatically shortened compared to **2** and a model Pc, indicating that the carotenoid acts as a strong quencher of the phthalocyanine excited-state energy. By measuring the solvent polarity dependence of the quenching in combination with target analysis of the time-resolved data, we were able to show that the mechanism underlying the quenching process is energy transfer from the excited phthalocyanine to the optically forbidden S_1 state of the carotenoid.

Models **2**, **3** and **4** are biased toward energy transfer quenching by structural features of the Pc that lower its reduction potential and thus the driving force for relaxation of the Pc singlet by electron transfer from the carotenoid. Such electron transfer quenching has been observed in Pc-carotenoid constructs having ~300 mV more driving force for electron transfer. In these systems the transient carotenoid radical cation was detected. Selective quenching of the tetrapyrrole singlet state by tuning the number of conjugated carbon-carbon double bonds of nearby carotenoids models the xanthophyll cycle, the energy dissipating (photosynthetic down regulating), non-photochemical quenching (NPQ) process observed in green plants.

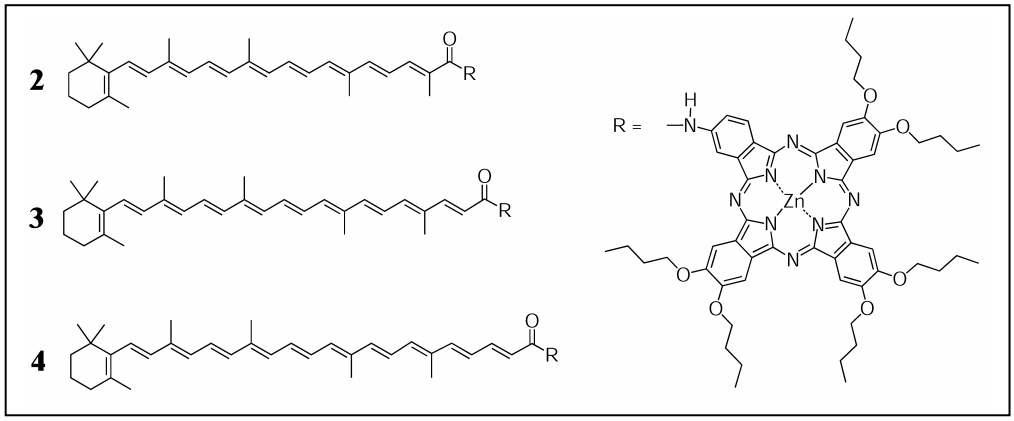

DOE Sponsored Publications 2005-2007

1. "Photoelectrochemical biofuel cells," Sotomura, T.; Gust, D.; Moore, T. A.; Moore, A. L. *Eco Industry*, **2005**, *10*, 19-26.

2. "Bio-inspired energy conversion," Palacios, R. E.; Gould, S. L.; Herrero, C.; Hambourger, M.; Brune, A.; Kodis, G.; Liddell, P. A.; Kennis, J.; Macpherson, A. N.; Gust, D.; Moore, T. A.; Moore, A. L. *Pure & Appl. Chem.,* **2005**, *77*, 1001-1008.

3. "Hybrid photoelectrochemical-fuel cell," Moore, A. L.; Moore, T. A.; Gust, D., in *Nanotechnology and the Environment. Applications and Implications*, Chapter 49 in Symposium Series No. 890, Karn, B.; Masciangioli, T.; Zhang, W.-X.; Colvin, V.; Alivisatos, P., Eds., American Chemical Society, Washington, D. C., **2005**, 361-367.

4. "Enzyme-assisted reforming of glucose to hydrogen in a photoelectrochemical cell," Hambourger, M.; Brune, A.; Gust, D.; Moore, A. L., Moore, T. A. *Photochem. Photobiol.*, **2005**, *81*, 1015-1020.

5. "Mimicking bacterial photosynthesis," Gust, D.; Moore, T. A.; Moore, A. L.; in *Artificial Photosynthesis*, Collings, A. F.; Critchley, C., Wiley-VCH, Weinheim, 2005, pp. 187-210.

6. "Artificial photosynthetic antenna-reaction center complexes based on a hexaphenylbenzene core," Terazono, Y.; Liddell, P. A.; Garg, V. Kodis, G.; Brune, A.; Hambourger, M.; Moore, T. A.; Moore, A. L.; Gust, D. *J. Porphyrins and Phthalocyanines,* **2005**, *10*, 706-724.

7. "Artificial photosynthetic reaction centers with carotenoid antennas," Gould, S. L.; Kodis, G.; Liddell, P.A.; Palacios, R. E.; Brune, A.; Gust, D.; Moore, T. A.; Moore, A. L. *Tetrahedron*, **2006**, *62*, 2074-2096.

8. "Energy and photoinduced electron transfer in a wheel-shaped artificial photosynthetic antenna-reaction center complex," Kodis, G.; Terazono, Y.; Liddell, P. A.; Andréasson, J.; Garg, V.; Hambourger, M.; Moore, T. A.; Moore, A. L.; Gust, D. *J. Am. Chem. Soc.*, **2006**, *128*, 1818-1827.

9. "Characterization of proton transport across a waveguide-supported lipid bilayer," McBee, T. W.; Wang, L.; Ge, C.; Beam, B.; Moore, A. L.; Gust, D.; Moore, T. A.; Armstrong, N. R.; Saavedra, S. S. *J. Am. Chem. Soc.*, **2006**, *128*, 2184-2185.

10. "A simple artificial light-harvesting dyad as a model for excess energy dissipation in oxygenic photosynthesis," Berera, R.; Herrero, C.; van Stokkum, I. H. M.; Vengris, M.; Kodis, G.; Palacios, R. E.; van Amerongen, H.; van Grondelle, R.; Gust, D.; Moore, T. A.; Moore, A. L.; Kennis, J. T. M. *Proc. Natl. Acad. Sci.*, **2006**, *103*, 5343-5348.

11. "Time-resolved EPR investigation of charge recombination to a triplet state in a carotene-diporphyrin triad," Di Valentin, M.; Bisol, A.; Agostini, G.; Moore, A. L.; Moore, T. A.; Gust, D.; Palaciois, R. E.; Gould, S. L.; Carbonera, D. *Molecular Physics*, **2006**, *104*,

1595-1607.

12. "Conductance of a biomolecular wire," Visoly-Fisher, I.; Daie, K.; Terazono, Y.; Herrero, C.; Fungo, F.; Otero, L.; Durantini, E.; Silber, J. J.; Sereno, L.; Gust, D.; Moore, T. A.; Moore, A. L.; Lindsay, S. M. *Proc. Natl. Acad. Sci.*, **2006**, *103*, 8686-8690.

13. "Tetrapyrrole singlet excited state quenching by carotenoids in an artificial photosynthetic antenna," Palacios, R. E.; Kodis, G.; Herrero, C.; Mariño Ochoa, E.; Gervaldo, M.; Gould, S. L.; Kennis, J. T. M.; Gust, D.; Moore,T. A.; Moore, A. L. *J. Phys. Chem. B*, **2006**, *110*, 25411-25420.

14. "Charge separation and energy transfer in a caroteno-C_{60} dyad: Photoinduced electron transfer from the carotenoid excited states," Berera, R.; Moore, G. F.; van Stokkum, I.; Kodis, G.; Gervald, M.; van Grondelle, R.; Kennis, J. T. M.; Gust, D.; Moore, T. A.; Moore, A. L. *Photochem. Photobiol. Sci.*, **2006**, *5*, 1142-1149.

15. "Parameters affecting the chemical work output of a hybrid photobioelectrochemical fuel cell," Hambourger, M.; Liddell, P. A.; Gust, D.; Moore, A. L.; Moore, T. A. *Photochem. Photobiol. Sci*., **2007**, *6*, 431-437.

16. "Photoinduced electron transfer in a hexaphenylbenzene-based self-assembled porphyrin-fullerene triad," Terazono, Y.; Kodis, G.; Liddell, P. A.; Garg, V.; Gervaldo, M.; Moore, T. A.; Moore, A. L.; Gust, D. *Photochem. Photobiol.*, **2007**, *83*, 464-469.

17. "Energy transfer, excited-state deactivation and exciplex formation in artificial caroteno-phthalocyanine light harvesting antennas," Berera, R.; van Stokkum, I. H. M.; Kodis, G.; Keirstead, A.; Pillai, S.; Herrero, C.; Palacios, R. E.; Vengris, M.; van Grondelle, R.; Gust, D.; Moore, T. A.; Moore, A. L.; Kennis, J. T. M. *J. Phys. Chem. B.*, **2007**, in press.

18. "Bio-inspired constructs for sustainable energy production and use," Moore, A. L.; Gust, D.; Moore, T. A. *L'Actualité Chimique*, **2007**, in press.

"ELECTROCHEMICALLY WIRED" DYE-MODIFIED DENDRIMERS AND SEMICONDUCTOR NANOPARTICLES IN SOL-GEL FILMS: TOWARD VECTORIAL ELECTRON TRANSPORT IN HYBRID MATERIALS AND SOLAR-ASSISTED HYDROGEN PRODUCTION

Neal R. Armstrong, Jeffery Pyun, Dominic McGrath, Zhiping Zheng, S. Scott Saavedra,
Department of Chemistry, University of Arizona, Tucson, Arizona 85721

This new project is directed toward the creation of hybrid materials which provide for direct "wiring" of semiconductor nanoparticles (SC-NPs) via a conducting polymer (CP) network to a transparent conducting oxide substrate (ITO). CdSe NPs have been ligand-capped with new electron-rich thiophene ligands, and electropolymerization is used to incorporate the SC-NPs into a poly(3,4-diethyleneoxythiophene) (PEDOT) network. Photoelectrochemical experiments using solution electron acceptors (MV^{++} or C_{60}) show that the PEDOT network can act as an electron donor to the photoexcited NP, at potentials where the CP film is "de-doped" or fully reduced. Photocurrent versus potential is limited by the rate of ET between the PEDOT network and the "wired" SC-NP, showing a Marcus-like I/V relationship. UV-photoelectron spectroscopy (He(II) excitation) has been used on pyridine-capped CdSe NPs tethered to self-assembled monolayers to determine HOMO energies, fully corrected for interface dipole effects. This approach may ultimately allow the characterization of frontier orbital shifts as a result of attachment of new ligands to the NP, a critical measurement to allow the optimization of ET between SC-NPs and electron-rich polymer networks.

Initial efforts have focused on the synthesis of high quality cadmium selenide (CdSe) semiconductor nanoparticles (SC-NPs) and two forms of functional ligands which can be used to stabilize the SC-NP, and introduce electrochemically active (electron-rich) thiophene (PRODOT) monomers to the exterior of the SC-NP: *i)* carboxylic acid-terminated alkyl-PRODOT (PRODOT-CA) and *ii)* second-generation poly(amidoamine) PAMAM dendrimers, decorated with PRODOT monomers. PRODOT pendant groups provide a pathway for electrochemical "wiring" of the SC-NP into a nanocomposite film. PRODOT terminated ligands are under development, with $-NH_2$, and –SH functionality. The approach used for wiring of SC-NPs into a poly-(thiophene) network is based on recent work from our group where "brush-like" PEDOT films were grown on ITO, starting with acid activation of this surface. Optimized versions of these PEDOT films showed rates of heterogeneous electron transfer to solution probe molecules rivaling those

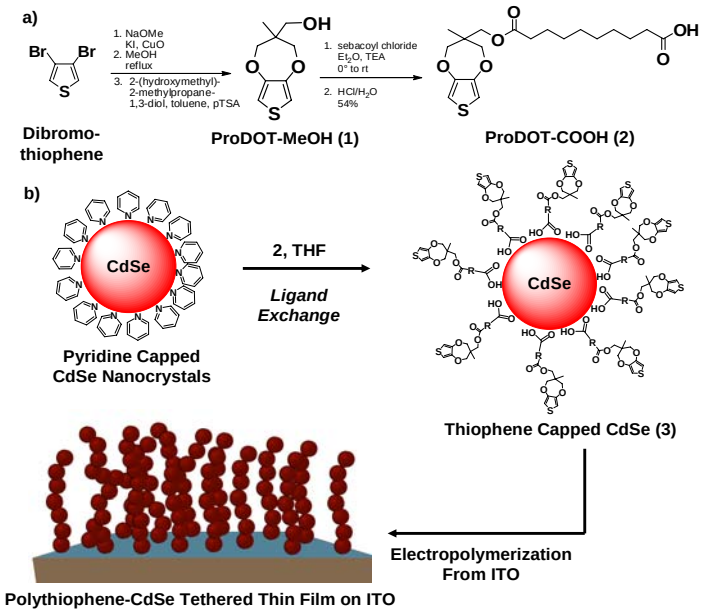

Fig. 1. (a) Schematic view of the synthesis of PRODOT-CA and (b) the addition of this ligand to pyridine-capped CdSe NPs. The resulting PRODOT-capped CdSe NPs are then incorporated into an electrochemically grown network of PEDOT on an activated ITO surface.

seen on bare Au or Pt, a first for any TCO electrode.

PRODOT-CA-capped CdSe NPs have been electrochemically "wired" into a PEDOT network, attached to an activated ITO electrode. Photoexcitation of this hybid thin film results in electron transfer to solution electron acceptors, methyl viologen (MV++) and C_{60} as solution electron acceptors, initiated at potentials where the PEDOT "wire" is in a sufficiently reduced state to allow for hole capture, with minimal back reaction. To our knowledge this is the first report of wiring of a SC-NP into a conducting polymer matrix, providing for control of the rate of photoexcited ET to a solution acceptor. The polymer network also appears capable of protecting the NP from photocorrosion – an essential requirement in future H_2-evolution technologies proposed for these materials.

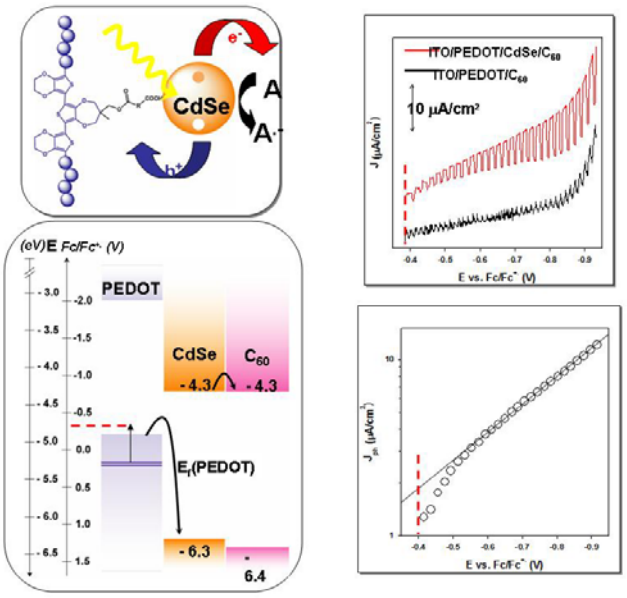

Fig. 2 Schematic view of photoinduced electron transfer from a "wired" CdSe NP, to a solution acceptor (C_{60}), with hole-capture by the reduced PEDOT chain. As anticipated ET from PEDOT to the photoexcited NP is potential dependent, and begins at potentials where the PEDOT film is fully reduced. ET from PEDOT to the photoexcited NP appears to be rate-limiting.

UV-photoelectron spectroscopy have been developed for monolayer-tethered CdSe NPs on Au, using dithiol linkers, to estimate HOMO energies, with full correction of interface dipole effects. These experiments appear capable of providing frontier orbital energies for a wide variety of metal, semiconductor and oxide nanoparticles. We are currently evaluating whether we can attach a variety of ligands to these tethered NPs, and follow energy changes brought about by ligand attachment, ligand cross-linking, and etching (faceting) of the NP.

References:

"Potential-Modulated, Attenuated Total Reflectance Spectroscopy of Poly(3,4 Ethylenedioxythiophene) (PEDOT) and Poly(3,4-Ethylenedioxythiophene Methanol) (PEDTM) Copolymer Films on Indium-Tin Oxide," Walter J. Doherty III, Ronald J. Wysocki Jr., Neal R. Armstrong, and S. Scott Saavedra, J. Phys. Chem. B. *110*, 4900-4907 (**2006**).

"Conducting Polymer Growth in Porous Sol-Gel Thin Films: Formation of Nanoelectrode Arrays and Mediated Electron Transfer to Sequestered Macromolecules," Walter J. Doherty III, Neal R. Armstrong, S. Scott Saavedra, Chemistry of Materials, 17, 3652-3660 (**2005**).

Publications from DOE support:

"Polythiophene-Semiconductor Nanoparticle Thin Films Tethered to Indium Tin Oxide Substrates via Electropolymerization," Clayton Shallcross, Steven E. Bowles, Gemma D'Ambruso, Hank H. Hall, Jeffrey Pyun, Zhiping Zheng, Dominic V. McGrath, Scott S. Saavedra, Neal R. Armstrong, in preparation for submission to JACS.

Characterization of the Frontier Orbital Energies in Tethered CdSe Nanoparticles on Au Using He(II) UV-Photoelectron Spectroscopy, Amy Graham, Clayton Shallcross, Paul A. Lee, Neal R. Armstrong, manuscript in preparation.

"Modification of Indium-Tin Oxide Electrodes with Thiophene Copolymer Thin Films: Optimizing Electron Transfer to Solution Probe Molecules," F. Saneeha Marrikar, Michael Brumbach, Dennis H. Evans, Ariel Lebrón-Paler, Jeanne E. Pemberton, Ronald J. Wysocki, Neal R. Armstrong, Langmuir, 23, 1530-1542 (**2006**).

Session IX

Quantum Particles in Solar Photoconversion

FUNDAMENTAL PHOTOCHEMICAL PROPERTIES OF SINGLE-WALL CARBON NANOTUBES

T.J. McDonald, D. Svedružić, W.K. Metzger, J.L. Blackburn, C. Engtrakul, Y.-H. Kim, M.C. Beard, S. B. Zhang, G.D. Scholes†, G. Rumbles, P.W. King, and M.J. Heben

Energy Sciences, National Renewable Energy Laboratory, Golden, Colorado 80401
†Department of Chemistry, University of Toronto, Toronto, Ontario M5S 3H6 Canada.

This work seeks to understand the basic photochemical properties of carbon single-wall nanotubes (SWNTs) and to develop the design principles for incorporating SWNTs into nanoscale hybrid structures for solar photoconversion. In particular, we wish to: (1) couple SWNTs to other species such as semiconductor nanocrystals and redox or photoactive molecules, (2) elucidate the optical and electronic properties of these assemblies, and (3) tailor the energetics such that the relaxation of photoexcited states can be harnessed to do photochemical work.

Although SWNTs are currently being applied to several different solar energy conversion strategies, many fundamental aspects remain poorly understood. For example, the potentials of the LUMO and HOMO levels for semiconducting tubes relative to vacuum are not known as a function of the (n,m). The absolute potential of the SWNT Fermi level was recently calculated to be insensitive to diameter and bandgap, indicating that the HOMO and LUMO levels move to lower and higher energy, respectively, with decreasing tube diameter.[1] Subsequent experimental studies using organic electron acceptors, however, concluded that the Fermi level position varied strongly as a function of bandgap.[2] Our recent studies found tube-dependent surfactant binding constants and suggested that the apparent Fermi level variation is a consequence of tube-dependent surfactant coverage and related mass transport effects.[3] This year we were able to circumvent these problems by employing the [FeFe] hydrogenase I (*Ca*HydI) from the anaerobic bacterium *Clostridium acetobutylicum*.[4] Under the appropriate conditions, we found that *Ca*HydI

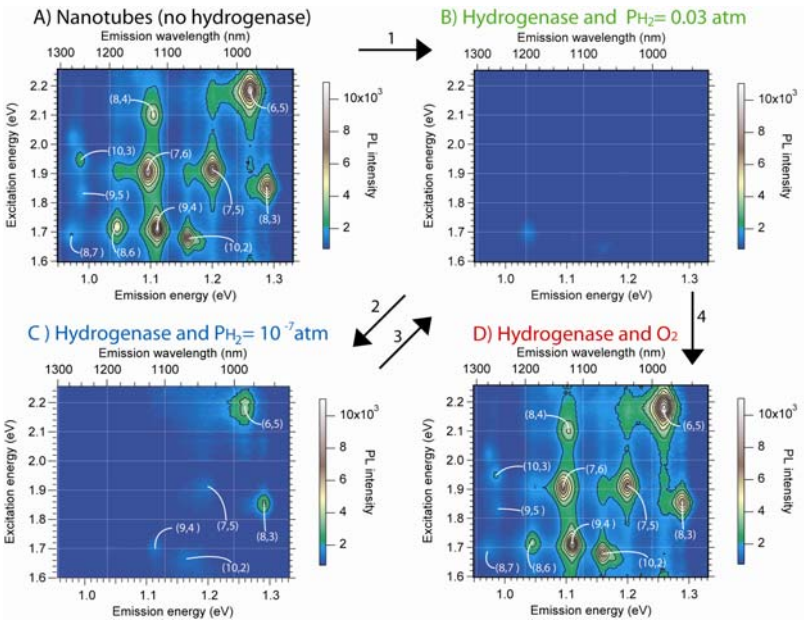

Figure 1: Photoluminescence data for; A) initial SWNT-Na Cholate suspension, B) SWNT- *Ca*HydI suspensions under reducing conditions, C) same as B but with reduced P_{H2}. The small diameter tubes become luminescent. Note that the PL contour map is reversible between B and C with changes in P_{H2}. Part D) shows that the initial spectrum in A is regained upon exposure to air.

in solution displaced surfactant species and adsorbed strongly to the SWNT surfaces. The binding of hydrogenase to the SWNTs rendered the photoluminescence of the tubes reversibly sensitive to changes in the H^+/H_2 redox potential, which was altered by changing the hydrogen partial pressure (see Fig. 1). Evidently, when *Ca*HydI is adsorbed, the catalytic and/or electron transfer FeS-clusters of the enzyme are placed in close proximity to the SWNTs such that facile electron transfer can occur. With this system we were able to measure the absolute position of the SWNT HOMO and LUMO levels as a function of tube diameter in the absence of mass transfer effects. The results were in excellent agreement with theoretical calculations.

The potential to do photochemistry with excited states in semiconducting SWNTs depends on the competing photoexcitation relaxation mechanisms, and these are also poorly understood. To understand the relaxation pathways in more detail we performed steady-state photoluminescence, time-correlated single photon counting, and Raman spectroscopy measurements on isolated single-wall carbon nanotubes from 4 to 293 K. A sample with well-behaved optical properties across the full temperature range of interest was obtained by forming a polymer(AQ55)/SWNT composite. We observed novel photoluminescence spectra that cannot be attributed to vibronic transitions and verified predictions associated with the existence and energy positions of weakly emissive excitonic states. By combining photoluminescence intensity and lifetime data, we determined how nonradiative and radiative excitonic decay rates change as a function of temperature. The analysis afforded a comparison with theoretical predictions. Our results suggest that recombination kinetics are influenced by multiple excitonic states, including a dark lower state.

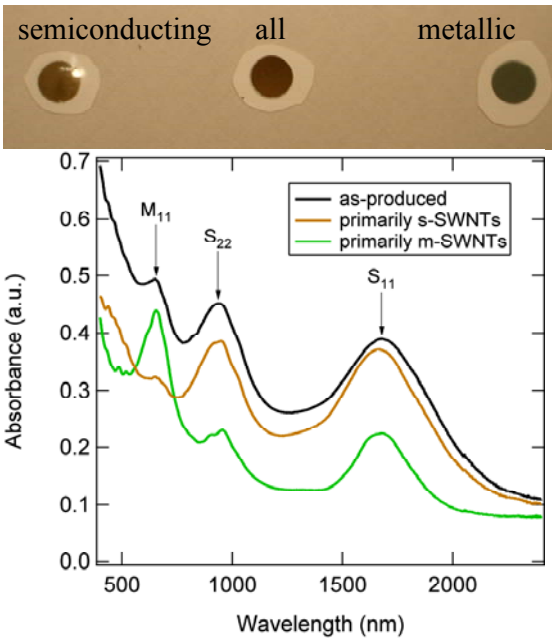

Figure 2: Photographs and absorption spectra of films which contain ~90% semiconducting and ~90% metallic tubes. The data for the as-produced SWNTs is shown for comparison.

Experimental studies to date have been limited to spectral selection of individual species in a distribution or single-tube experiments. Recently, Arnold et al. developed methods to separate SWNTs according to conductivity character.[5] Our understanding of surfactant adsorption on SWNTs has allowed us to rapidly reproduce these results. Figure 2 shows the Vis-Nir absorption spectra for films formed from separated metal and semiconducting tube populations. Note that the M_{11} absorption is nearly absent in the sample which is primarily s-SWNTs, while the absorption associated with the first and second excited states of the semiconducting species (S_{11} and S_{22}) are greatly diminished relative to M_{11} in the m-SWNT sample. Interestingly, the separated films show differences in color reminiscent of size-selected colloid solutions. These samples, in both film and solution form, afford a variety of new studies, some of which will be discussed.

(1) Shan, B. & Cho, K. *Physical Review Letters* **2005**, *94*, 236602-4: (2) O'Connell, et al., *Nature Materials* **2005**, *4*, 412-418; (3) McDonald, T. J., et al., *J. Phys. Chem. B* **2006**, *110*, 25339; (4) King, P. W. et al., *Bacteriol.* **2006**, *188*, 2163-2172; (5) Arnold, M. S., et al., . *Nat Nano* **2006**, *1*, 60-65.

DOE Sponsored Publications 2005-2007

1. "Low-Lying Exciton States Determine the Photophysics of Semiconducting Single Wall Carbon Nanotubes" by G. D. Scholes, S. Tretiak, T. J. McDonald, W. K. Metzger, C. Engtrakul, G. Rumbles and M. J. Heben, submitted, 2007.
2. "Selective Aggregation of Single-Walled Carbon Nanotubes Via Salt Addition" by S. Niyogi, S. Boukhalfa, S. B. Chikkannanavar, T. J. McDonald, M. J. Heben and S. K. Doorn, *Journal of the American Chemical Society* **129**, 1898-1899, 2007.
3. "Temperature-Dependent Excitonic Decay and Multiple States in Single-Wall Carbon Nanotubes" by W. K. Metzger, T. J. McDonald, C. Engtrakul, J. L. Blackburn, G. D. Scholes, G. Rumbles and M. J. Heben, *J. Phys. Chem. C* **111**, 3601-3606, 2007.
4. "Wiring-up Hydrogenase with Single-Walled Carbon Nanotubes" by T. J. McDonald, D. Svedružić, Y.-H. Kim, J. L. Blackburn, S. B. Zhang, P. W. King and M. J. Heben, submitted, 2007.
5. "Chiral-Selective Oxidation of Single-Walled Carbon Nanotubes" by T. J. McDonald, J. L. Blackburn, W. K. Metzger, G. Rumbles and M. J. Heben, *Journal of Physical Chemistry B* in press, 2007.
6. "Extrinsic and Intrinsic Effects on the Excited-State Kinetics of Single-Walled Carbon Nanotubes" by M. Jones, W. K. Metzger, T. J. McDonald, C. Engtrakul, R. J. Ellingson, G. Rumbles and M. J. Heben, *Nano Letters* **7**, 300-306, 2007.
7. "Near-Infrared Fourier Transform Photoluminescence Spectrometer with Tunable Excitation for the Study of Single-Walled Carbon Nanotubes" by T. J. McDonald, M. Jones, C. Engtrakul, R. J. Ellingson, G. Rumbles and M. J. Heben, *Review of Scientific Instruments* **77**, 053104-1, 2006.
8. "Kinetics of Pl Quenching During Single-Walled Carbon Nanotube Rebundling and Diameter-Dependent Surfactant Interactions" by T. J. McDonald, C. Engtrakul, M. Jones, G. Rumbles and M. J. Heben, *Journal of Physical Chemistry B* **110**, 25339-25346, 2006.
9. "Intrinsic and Extrinsic Effects in the Temperature-Dependent Photoluminescence of Semiconducting Carbon Nanotubes" by D. Karaiskaj, C. Engtrakul, T. McDonald, M. J. Heben and A. Mascarenhas, *Physical Review Letters* **96**, 106805, 2006.
10. "Self-Assembly of Linear Arrays of Semiconductor Nanoparticles on Carbon Single-Walled Nanotubes" by C. Engtrakul, Y. H. Kim, J. M. Nedeljkovic, S. P. Ahrenkiel, K. E. H. Gilbert, J. L. Alleman, S. B. Zhang, O. I. Micic, A. J. Nozik and M. J. Heben, *Journal of Physical Chemistry B* **110**, 25153-25157, 2006.
11. "Tribute to Arthur J. Nozik" by R. J. Ellingson and M. J. Heben, *Journal of Physical Chemistry B* **110**, 2125-2125, 2006.
12. "Effect of Removal and Change of Surfactant Upon the Photoluminescence of Carbon Nanotubes" by T. J. McDonald, C. Engtrakul, M. Jones, J. L. Blackburn, G. Rumbles and M. J. Heben, in Proceedings of the SPIE: *Physical Chemistry of Interfaces and Nanomaterials IV*, edited by C. Burda and R. J. Ellingson, **5929**, 169-175, 2005.
13. "Analysis of Photoluminescence from Solubilized Single-Walled Carbon Nanotubes " by M. Jones, C. Engtrakul, W. K. Metzger, R. J. Ellingson, A. J. Nozik, M. J. Heben and G. Rumbles, *Physical Review B* **71**, 115426-115434, 2005.
14. "Self-Organization of Semiconductor Quantum Nanocrystals on Carbon Single-Wall

Nanotubes into Close-Packed Linear Arrays" by C. Engtrakul, J. M. Nedeljkovic, Y.-H. Kim, S. P. Ahrenkiel, K. E. H. Gilbert, J. L. Alleman, S. B. Zhang, O. I. Micic, A. J. Nozik and M. J. Heben, in Mater. Res. Soc. Symp. Proc.: *Functional Carbon Nanotubes*, edited by D. L. Carroll, B. Weisman, S. Roth and A. Rubio, **858E,** HH2.7, 2005.

15. "Protonation of Carbon Single-Walled Nanotubes Studied Using 13C and 1H13C Cross Polarization Nuclear Magnetic Resonance and Raman Spectroscopies" by C. Engtrakul, M. F. Davis, T. Gennett, A. C. Dillon, K. M. Jones and M. J. Heben, *Journal of the American Chemical Society* **127**, 17548-17555, 2005.
16. "Investigation of the Electronic Structure of Carbon Single-Wall Nanotube Hybrid Nanostructures" by C. Engtrakul, M. F. Davis, T. Gennett, A. Dillon, K. M. Jones and M. J. Heben, in Proceedings of the SPIE: *Physical Chemistry of Interfaces and Nanomaterials IV*, edited by C. Burda and R. J. Ellingson, **5929,** 123-128, 2005.
17. "Ultrafast Photoresponse of Metallic and Semiconducting Single Wall Carbon Nanotubes" by R. J. Ellingson, C. Engtrakul, M. Jones, M. Samec, G. Rumbles, A. J. Nozik and M. J. Heben, *Physical Review B* **71**, 115444-115451, 2005.

EXCITON AND CHARGE SEPARATION DYNAMICS IN QUANTUM DOT HETEROJUNCTIONS

David F. Kelley
University of California, Merced
Merced, CA, 95344

GaSe is a layered semiconductor that forms disk-like nanoparticles. The nanoparticles consist of single Se-Ga-Ga-Se tetra-layers and are 2.5 to 12 nm in diameter. They are synthesized in high-temperature coordinating solvents and the diameters are controlled by the synthetic conditions. InSe is a very similar material, and forms similar disk-like nanoparticles. In both cases, polarized transient absorption spectroscopy can be used to elucidate the electron and hole intraband transitions. These spectra are characteristic of electrons and holes in the conduction and valence bands of each type of particle, and are easily assigned. Quantum confinement effects dramatically change the spectroscopy of these particles, compared to bulk semiconductors. The nanoparticle conduction and valence band energetics can be calculated from the energetics in the bulk materials and are shown in figure 1, below.

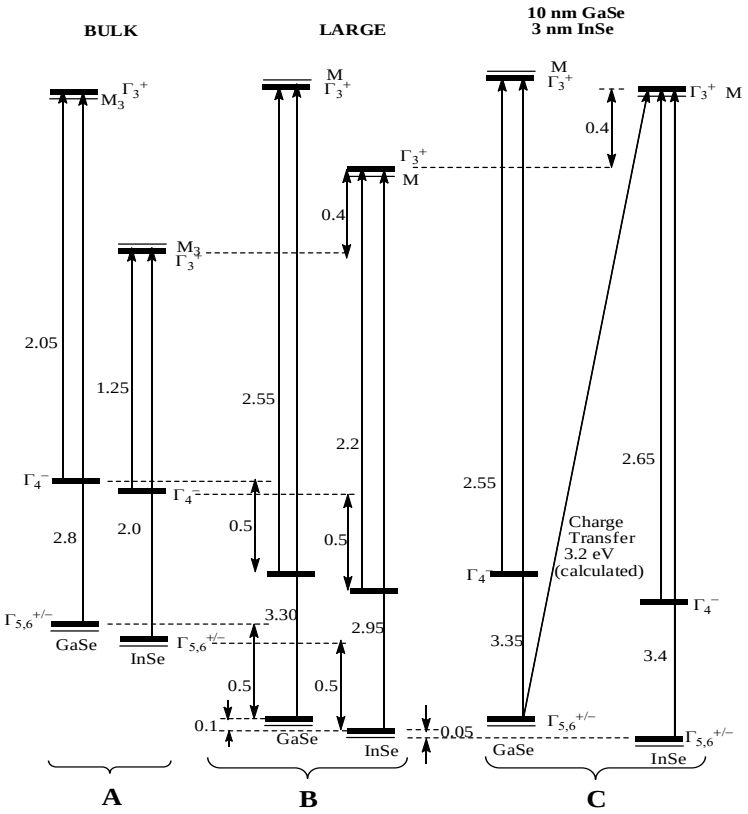

Figure 1. Schematic energy diagram of (A) a bulk GaSe/InSe heterojunction, (B) large, two-dimensional GaSe and InSe particles (z-quantum confinement only), and (C) the GaSe/InSe heterojunction consisting of 10 nm GaSe and 3 nm InSe particles. Allowed transitions are indicated with single-headed arrows. Other energetics are indicated with double-headed arrows. The energetics are based on the bulk energetics (*J. Appl. Phys.* **1996,** 80, 3817) and quantum confinement effects (publications 4 and 8).

Both GaSe and InSe nanoparticles stack to form one-dimensional aggregates in solution. The photophysics of GaSe nanoparticle aggregates and mixed aggregates of GaSe/InSe nanoparticles are studied using static and time-resolved absorption and emission spectroscopies. The aggregate absorption spectra can be modeled using a dipolar coupling model, similar to what is used to describe J-aggregates of organic dyes. The results indicate that excitons in GaSe aggregates are delocalized over several nanoparticles and these excitons can diffuse along the aggregate. Concentration- and time-dependent fluorescence depolarization results indicate that the aggregates are linear over of a distance of about 9 particles. These results also indicate that exciton motion can be characterized by a diffusion constant of about 2 x 10^{-5} cm^2/sec.

Mixed GaSe/InSe nanoparticle aggregates can also be formed. These mixed aggregates exhibit spectroscopic features that are not a simple combination of the constituent nanoparticles, i.e., the low energy static absorption spectrum has a large contribution from the GaSe/InSe nanoparticle heterojunctions. In the case of 10 nm GaSe and 3 nm InSe particles, the transient absorption spectrum obtained following excitation of this feature is characteristic of InSe conduction band electrons and GaSe valence band holes. Thus, the absorption feature due to the heterojunctions is assigned to a direct charge transfer from the GaSe valence band to the InSe conduction band. The energy diagram of the nanoparticle heterojunction is shown in figure 1. The heterojunction spectroscopy is consistent with the band offsets observed in bulk GaSe/InSe heterojunctions and known nanoparticle quantum confinement effects.

Photoexcitation can also produce excitons in the aggregates, away from the heterojunctions. In the case where the GaSe particles are in 10:1 excess, these excitons can undergo diffusion and quench upon reaching a heterojunction. Time-resolved fluorescence kinetics are shown in figure 2. These kinetics are sensitive to the assumed exciton diffusion coefficient and it is therefore possible to accurately extract this value. A diffusion coefficient of 2 x 10^{-5} cm^2/sec is obtained, which is in agreement with values obtained from fluorescence anisotropy decay measurements.

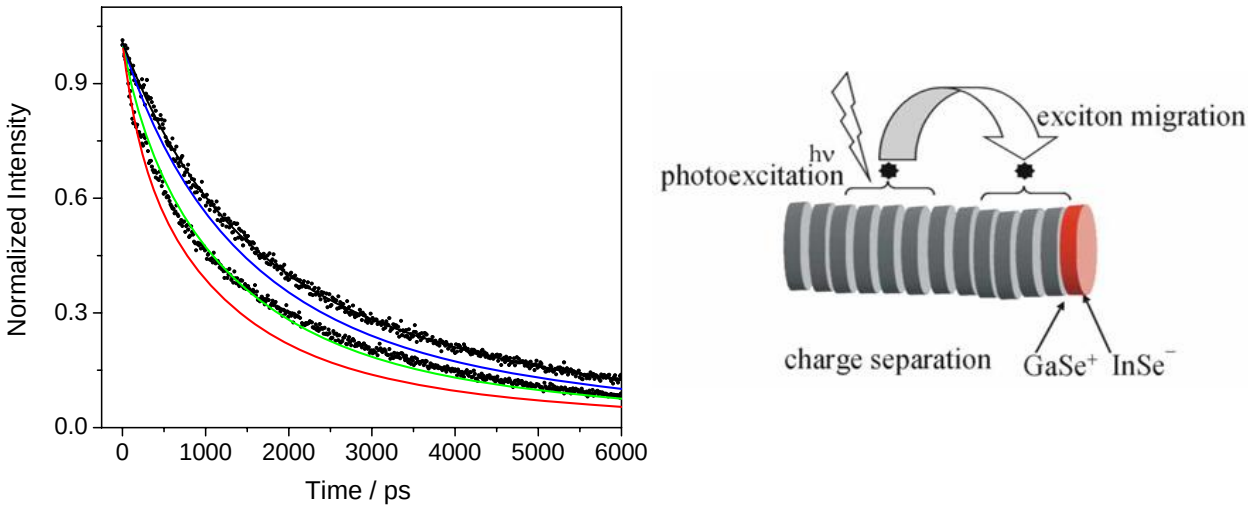

Figure 2. Fluorescence decay kinetics for GaSe aggregates (upper dots) and GaSe/InSe mixed aggregates (lower dots). The calculated fluorescence decay kinetics with diffusion coefficients of 0.0 (black), 0.5 (blue), 2.0 (green) and 5.0 (red) x 10^{-5} cm^2/sec are also shown. A cartoon of this process is shown on the right.

DOE Sponsored Publications 2005-2007

1. Xiang-Bai Chen and David F. Kelley, "Photophysics of GaSe/InSe Nanoparticle Heterojunctions" *J. Phys. Chem. B*, **110**, 25259 (2006).
2. David F. Kelley, Haohua Tu and Xiang-Bai Chen, "Intraband Spectroscopy of GaSe Nanoparticles and InSe/GaSe Nanoparticle Heterojunctions", *Proc. Int'l Conf. Ultrafast Phenomena XV* – in press.
3. David F. Kelley, Haohua Tu, Karoly Mogyorosi and Xiang-Bai Chen, "Electron and hole dynamics in GaSe nanoparticles and GaSe-InSe nanoparticle heterojunctions", *Proc. Soc. Photo-Optic. Inst. Engin.,* **6325**, 63250F (2006).
4. Shuming Yang and David F. Kelley, "Transient Absorption Spectra and Dynamics of InSe Nanoparticles", *J. Phys, Chem. B*, **110**, 13430 (2006).
5. Haohua Tu and David F. Kelley, "Photoinduced direct electron transfer from InSe to GaSe semiconductor nanoparticles", *Nano Letters*, **6**, 116 (2006).
6. Haohua Tu, Karoly Mogyorosi, and David F. Kelley, "Intraband Spectroscopy and Photophysics in GaSe Nanoparticles", *Phys. Rev. B*, **72**, 205306 (2005).
7. David F. Kelley, Haohua Tu, Shuming Yang and Karoly Mogyorosi, "Dynamics of Two-Dimensional Semiconductor Nanoparticle Aggregates and Heterojunctions", *Proceedings of the Electrochemical Society*, Symposium on "Electron Transfer in Nanomaterials" pp. 286 (2005).
8. H. Tu, K. Mogyorosi and D. F. Kelley, "Exciton Dynamics in GaSe Nanoparticle Aggregates", *J. Chem. Phys.* **122**, 44709 (2005).
9. Shuming Yang and David F. Kelley, "The Spectroscopy of InSe Nanoparticles", *J. Phys, Chem. B*, **109**, 12701 (2005).
10. D. F. Kelley, H. Tu, and K. Mogoyrosi, "Photophysics of GaSe Nanoparticles and Nanoparticle Aggregates", *Proc. Soc. Photo-Optic. Inst. Engin.*, **5929,** 59290Q (2005).

MULTIPLE EXCITON GENERATION IN COLLOIDAL SEMICONDUCTOR NANOCRYSTALS AND NANOCRYSTAL ARRAYS FOR EFFICIENT SOLAR ENERGY CONVERSION

R. J. Ellingson, K. P. Knutsen, J. C. Johnson, Q. Song, M. Law, J. M. Luther, K. A. Gerth, M. C. Beard, and A. J. Nozik
Center for Chemical Sciences and Biosciences, Energy Sciences Directorate
National Renewable Energy Laboratory
Golden, CO 80401

In a typical semiconductor, charge carriers photoexcited above the bandgap lose their excess kinetic energy by phonon scattering on the sub-picosecond timescale, relaxing to their respective band edges while heating the crystal lattice. Lattice heating by carrier cooling accounts for the loss of ~49% of the solar power incident on a conventional Si photovoltaic cell. A new very promising route to capturing more electronic energy from the initial photoexcited state has been shown by our recent observations that colloidal semiconductor nanocrystals (NCs) such as quantum dots or quantum rods can efficiently generate two or more electron-hole pairs (excitons) per absorbed photon when excited at an energy above ~3 times the effective bandgap (E_g). Using ultrafast transient absorption optical spectroscopy, we have reported efficient multiple exciton generation (MEG) in NCs of PbSe, PbS, PbTe, and most recently, Si. In each case, we find that the total quantum yield (QY) reaches 2 excitons per absorbed photon at ~3.3E_g. The efficiency of MEG significantly exceeds that of the analogous impact ionization scattering process measured for bulk forms of these semiconductors.

Observation of efficient MEG in Si NCs represents the first such report for indirect-gap semiconductor NCs. We find (Fig. 1) that MEG in 9.5 nm diameter Si NCs ($E_g \approx 1.20$ eV) shows a threshold of ~2.6 E_g ($h\nu_{threshold} = 3.1$ eV), significantly lower than the threshold of ~3.9 eV reported for bulk Si (corresponding to 3.5 $E_{g,bulk\ Si}$). In addition, the MEG QY in Si NCs increases more quickly with photon energy above the threshold than does impact ionization in bulk Si.

Fundamental exciton processes occur in a NC on the following timescales: cooling through phonon scattering, ~1 ps; multiple exciton generation (MEG), ≤ 200 fs; Auger recombination of two excitons, ~100 ps. Therefore, efficient MEG slows the loss of energy from the initial electronic excited state by about two orders of magnitude, substantially improving the prospect for harvesting much of the photon energy in excess of the bandgap. Although substantial barriers must still be overcome, energy-optimized MEG would raise the thermodynamically attainable conversion efficiency for a single-junction solar cell from 32% to 44% "up front", providing ample incentive to understand and harness this novel effect.

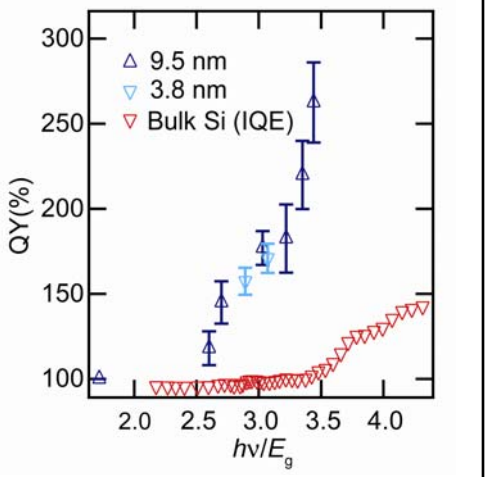

Figure 1. MEG QY values for Si NCs. Red triangles show the impact ionization QY for bulk Si from Wolf *et al.*, *J. Appl. Phys.* 83, 4213 (1998).

The two-exciton Auger recombination time of ~100 ps establishes a target timescale for harvesting energy from the multi-exciton electronic excited state. Ultrafast dissociation of the excitons such that the separated electrons and holes can be efficiently collected external to the NCs represents one possible route. Another example of stabilizing the electronic energy of a single NC's two-exciton excited state consists of exciton (energy) transfer of one exciton to a neighboring NC, such as by Förster resonant energy transfer (FRET). If accomplished, two NCs would each contain one exciton; the ~1 μs single exciton lifetime in isolated PbSe or PbS NCs significantly extends the timescale for separating and harvesting the electron-hole pairs. Thin films provide one possible route to facilitating the harvest of single and multiple excitons, by either charge or energy transport through the NC array.

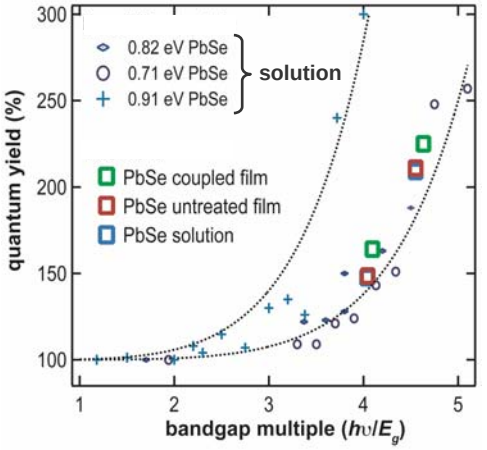

Figure 2. MEG QY values comparing PbSe NCs in solution (blue squares, diamonds, circles, and crosses) and in spin-cast films (green and red squares). QYs for the film studies (green and red squares; blue squares are solution control) utilize R = 2.0 nm NCs.

We have studied MEG in PbSe NC films for varying NC-NC coupling. The solutions used to cast films consist of individual PbSe NCs capped with oleic acid (OA). As-prepared, PbSe NC films cast from this suspension consist of arrays of NCs separated spatially by the ligand shell thickness, ~18 Å. Soaking the film in hydrazine in acetonitrile for ~24 hrs increases NC-NC coupling, as evidenced by a redshifted and broadened first exciton absorption. Increased electronic coupling between NC neighbors reduces the confinement energy for excitons. We expect that for sufficiently strong NC-NC coupling, the size-dependent enhancement of MEG will be reduced.

Our investigations show that the MEG QYs for solution, untreated film, and hydrazine treated film do not differ significantly from one another (Fig. 2). Thus, although the optical properties shift for the treated film, the degree of coupling achieved is not sufficient to alter MEG efficiency. Interestingly, the biexciton lifetime does increase for both the untreated and treated films compared to that of the solution sample. This suggests that while the NCs do not couple strongly in the ground state, the exciton wavefunction clearly samples a larger volume due to NC-NC coupling in the excited state.

We are continuing to study the coupling dependence on MEG in NC films. In order to strengthen the inter-NC coupling, we will anneal films under varying conditions. Higher annealing temperatures and longer annealing times show clear evidence of increased sintering, and increased effective grain size. Using time-resolved terahertz and/or conventional pump-probe spectroscopy, we plan to (1) measure the free carrier yield and/or exciton population, and (2) characterize Auger recombination times for these films. By extending the effective confinement size beyond the bulk Bohr exciton size, we may observe evidence of the size-dependence in the quantum yield as a function of bandgap multiple.

DOE Sponsored Publications 2005-2007

1. J. M. Luther, M. C. Beard, Q. Song, M. Law, R. J. Ellingson, and A.J. Nozik, "Multiple Exciton Generation in Films of Electronically Coupled PbSe Quantum Dots," *submitted*.

2. M. C. Beard, K. P. Knutsen, P. Yu, J. M. Luther, Q. Song, R. J. Ellingson, and A. J. Nozik, "Multiple exciton generation in colloidal silicon nanocrystals," *submitted*.

3. M. Jones, W. K. Metzger, T. J. McDonald, C. Engtrakul, R. J. Ellingson, G. Rumbles, and M. J. Heben, "Extrinsic and Intrinsic Effects on the Excited-State Kinetics of Single-Walled Carbon Nanotubes," *Nano Lett.* **7**, 300 (2007).

4. X. Ai, M. C. Beard, K. P. Knutsen, S. E. Shaheen, G. Rumbles, and R. J. Ellingson, "Photoinduced Charge Carrier Generation in a Poly(3-hexylthiophene) and Methanofullerene Bulk Heterojunction Investigated by Time-Resolved Terahertz Spectroscopy," *J. Phys. Chem. B* **110**, 25462 (2006).

5. A. J. Nozik, R. J. Ellingson, M. C. Beard, J. C. Johnson, J. E. Murphy, Al L. Efros, and A. Shabaev, "Third generation solar photon conversion: multiple exciton generation in semiconductor quantum dots," *PMSE Preprints* **95**, 161 (2006).

6. J. E. Murphy, M. C. Beard, A. G. Norman, S. P. Ahrenkiel, J. C. Johnson, P. Yu, O. I. Micic, R. J. Ellingson, A. J. Nozik, "PbTe Colloidal Nanocrystals: Synthesis, Characterization, and Multiple Exciton Generation," *J. Am. Chem. Soc.* **128**, 3241 (2006).

7. T. J. McDonald, M. Jones, C. Engtrakul, R. J. Ellingson, G. Rumbles, and M. J. Heben, "Near-infrared Fourier transform photoluminescence spectrometer with tunable excitation for the study of single-walled carbon nanotubes," *Rev. Sci. Instr.* **77**, 053104 (2006).

8. R. J. Ellingson, C. Engtrakul, M. Jones, M. Samec, G. Rumbles, A. J. Nozik, and M. J. Heben, "Ultrafast photoresponse of metallic and semiconducting single-wall carbon nanotubes," *Phys. Rev. B* **71**, 115444 (2005).

9. M. Jones, C. Engtrakul, W. K. Metzger, R. J. Ellingson, A. J., Nozik, M. J. Heben, and G. Rumbles, "Analysis of photoluminescence from solubilized single-walled carbon nanotubes," *Phys. Rev. B* **71**, 115426 (2005).

10. R. J. Ellingson, M. C. Beard, J. C. Johnson, P. Yu, O. I. Micic, A. J. Nozik, A. Shabaev, Al. L. Efros, "Highly Efficient Multiple Exciton Generation in Colloidal PbSe and PbS Quantum Dots," *Nano Lett.* **5**, 865 (2005).

11. P. Yu, M. C. Beard, R. J. Ellingson, S. Ferrere, C. Curtis, J. Drexler, F. Luiszer, and A. J. Nozik, "Absorption Cross Section and Related Optical Properties of Colloidal InAs Quantum Dots," *J. Phys. Chem. B* **109**, 7084 (2005).

12. J. L. Blackburn, D. C. Selmarten, R. J. Ellingson, M. Jones, O. Micic, and A. J. Nozik, "Electron and Hole Transfer from Indium Phosphide Quantum Dots," *J. Phys. Chem. B* **109**, 2625 (2005).

Session X

Novel Photoelectrode Morphology

PHOTOELECTROCHEMISTRY OF SEMICONDUCTOR NANOWIRE ARRAYS

Adrian P. Goodey, Sarah Dilts, Paul G. Hoertz, W. Justin Youngblood, Bradley A. Lewis, Emil A. Hernandez-Pagan, Joan M. Redwing, and Thomas E. Mallouk
Departments of Chemistry, Materials Science & Engineering, and Electrical Engineering
The Pennsylvania State University, University Park, PA 16802

Our DOE-supported work has focused on the use of nanoscale inorganic compounds and in particular, semiconductor nanowires and colloidal catalysts in photoelectrochemistry and photocatalysis. The goal of the project is to explore new ways to create efficient multi-junction photoelectrochemical cells and supramolecular water photolysis systems from nanoscale components.

Growth and characterization of semiconductor nanowires. Semiconductor nanowire arrays are an attractive alternative to single crystal semiconductors for photoelectrochemistry. The nanowires can be grown by scalable techniques as arrays of single crystals. Arrays of vertical nanowires separate the length scales of (vertical) light absorption and (horizontal) charge separation. They are also very strain-tolerant relative to larger crystals and therefore are amenable to the growth of axial or radial epitaxial heterojunctions. Single crystal intentionally doped p-type and n-type silicon nanowire (SiNW) arrays were fabricated within the pores of anodic alumina (AAO) templates by vapor-liquid-solid (VLS) growth. Nanowire array resistance was measured as a function of the SiNW length for a series of samples prepared with different dopant/SiH_4 inlet gas ratios and the nanowire resistivity and contact resistance were extracted from plots of array resistance versus nanowire length. The nanowire resistivity measured from the arrays decreased with increasing dopant/SiH_4 ratio and compared favorably with resistivity data obtained from four-point measurements of individual SiNWs grown under identical conditions. Nominally undoped SiNWs grown in the AAO templates were found to be p-type, with a resistivity in the range of 2-6 Ω-cm, indicating the presence of unintentional acceptors in the wires. The resistivity of undoped SiNWs grown under identical conditions but on oxidized (100) Si substrates was much higher, on the order of 10^4-10^5 Ω-cm, suggesting that the AAO templates are the source of the unintentional acceptor impurities.

To circumvent the p-type impurity problem, the VLS growth of SiNW arrays on gold-coated (111) Si substrates was investigated using $SiCl_4$ as the silicon source. Wire orientation was found to be strongly dependent on the growth temperature with ~ 80% of the SiNWs being <111> oriented perpendicular to the substrate at 900°C but dropping to ~18% at 800°C. At low $SiCl_4$ partial pressures (P_{SiCl4}), the growth rate of the wires increases linearly with increasing P_{SiCl4} reaching a maximum of ~ 3 μm/min at P_{SiCl4} of 3.7 Torr. Beyond this point, the growth rate begins to decrease with increasing P_{SiCl4} due to a shift in gas phase equilibrium which promotes the reverse HCl etching reaction. The resistivity of nominally undoped SiNWs was studied using four-point measurements. Nominally undoped SiNWs grown on p-type (111)Si substrates (ρ=1-15 Ω-cm) were determined to be p-type with a room-temperature resistivity on the order of 800 Ω-cm, which was two orders of magnitude

higher than that of SiNWs grown in the AAO templates indicating a reduction in unintentional impurity incorporation.

CdSe nanowire arrays were also grown in AAO templates by two methods. Single crystalline nanowires were obtained by laser-assisted VLS growth at 725°C, again using Au catalyst particles embedded in the AAO channels. CdSe nanowires were also made by lower temperature electrochemical deposition of Se nanowires, which are topochemically converted to Ag_2Se and then to CdSe. The structural and electrical characterization of these nanowires is in progress.

Photoelectrochemistry of Si nanowire arrays. p-Si nanowire arrays grown from SiH_4 and $SiCl_4$ were etched to remove the Au catalyst tips and tested as photoelectrodes in non-aqueous solutions. Using $[Ru(bpy)_3]^{2+}$ as a redox relay, we observed white light photovoltages of 200 and 350 mV, for low-doped and nominally undoped nanowires grown from SiH_4 and $SiCl_4$, respectively. These results are encouraging since electronics grade p-Si single crystal wafers give 500 mV photovoltages uner the same conditions. Overall energy conversion efficiencies for these nanowire cells are now being measured using viologen and $[Ru(bpy)_3]^{2+}$ electron relays in three-electrode cells.

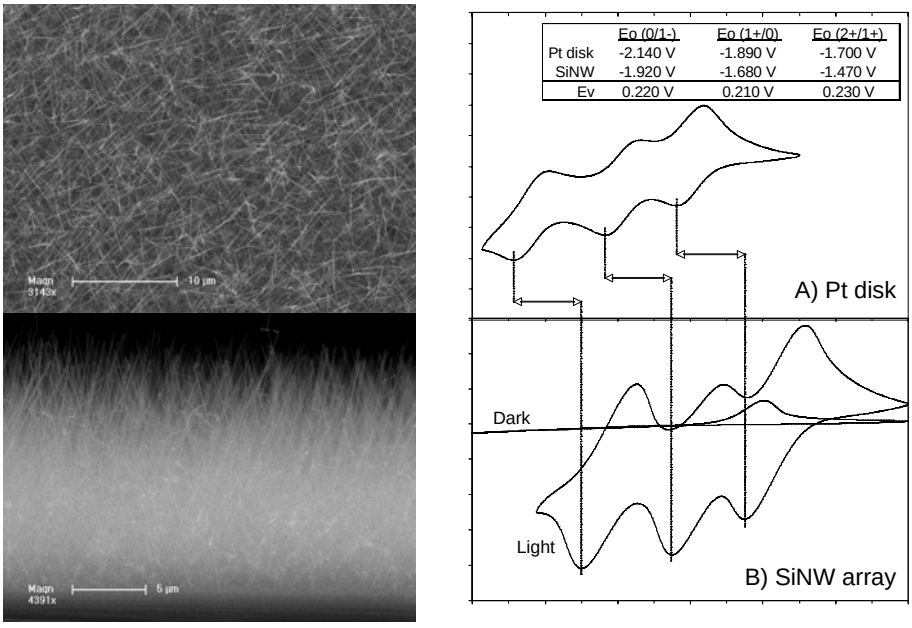

Fig. 1. *Left:* Top and side view scanning electron micrographs of p-SiNW arrays grown from SiH_4/TMB. *Right:* Cyclic voltammetry (CV) of $[Ru(bpy)_3]^{2+}$ at a Pt disk electrode, compared to dark and light CV at a p-SiNW electrode.

IrO_2 nanoparticle water oxidation catalysts. In our continuing work on catalysis for the oxygen evolution reaction (OER), we have studied chelating carboxylate ligands (malonate and succinate derivatives) for stabilizing IrO_2 nanoparticles. These ligands allow us to prepare stable 2 nm diameter colloidal particles, which can be covalently tethered to Ru(polypyridyl) sensitizers. Covalent attachment of the sensitizer allows us to probe the rates of electron transfer directly by transient absorbance techniques. In persulfate solutions, sensitizer bleaching recovery data suggest an OER turnover rate of about 10^2 s^{-1} for surface Ir atoms in these colloids.

DOE Sponsored Publications 2005-2007

1. P. G. Hoertz and T. E. Mallouk, "Light to Chemical Energy Conversion in Lamellar Solids and Thin Films," Inorg. Chem., 44, 6828-6840 (2005).

2. J. A. Schottenfeld, G. Chen, P. C. Ekerdt, and T. E. Mallouk, "Synthesis and Characterization of Layered Perovskite Oxynitride Photocatalysts from Dion-Jacobson Oxide Precursors," J. Solid State Chem. 178, 2313-2321(2005).

3. P. G. Hoertz, Y. I. Kim, W. J. Youngblood, and T. E. Mallouk, "Bidentate Dicarboxylate Capping Groups and Photosensitizers Control the Size of IrO_2 Nanoparticle Catalysts for Water Oxidation," *J. Phys. Chem.,* in press.

4. S.M. Eichfeld, T.T. Ho, C.M. Eichfeld, A. Cranmer, S.E. Mohney, T.S. Mayer and J.M. Redwing, "Resistivity measurements of intentionally doped silicon nanowire arrays," submitted to *Nanotechnology*.

5. A. P. Goodey, S. M. Dilts, K. K. Lew, J. M. Redwing, and T. E. Mallouk, "Silicon Nanowire Array Photoelectrochemical Cells," submitted to *J. Am. Chem. Soc.*

ELECTROCHEMICAL SYNTHESIS OF INORGANIC ELECTRODES WITH CONTROLLED MICRO- AND NANO-STRUCTURES FOR USE IN SOLAR ENERGY CONVERSION

Kyoung-Shin Choi
Department of Chemistry
Purdue University
West Lafayette, IN 47907

When photoelectrochemical devices are built based on *polycrystalline* electrodes that are commercially more viable than single crystal electrodes, particle shapes, sizes, orientations, and interconnections can significantly affect the chemical and physical factors that define the energetics and kinetics of the electrodes. Therefore, (i) precisely controlling micro- and nano-scale structures of inorganic materials that compose polycrystalline films and (ii) understanding the effects micro- and nano-structures have on functional properties are critical for producing highly efficient and cost effective photoelectrode materials. In order to accomplish these tasks, our research project focuses on gaining the new synthetic ability that can rationally and systematically control morphological features of various inorganic electrodes. We achieve this by combining compositionally versatile electrodeposition methods with synthetic concepts that allow for accurate morphological control on various length scales (e.g. supramolecular templating, preferential adsorption).

Electrochemical Construction of Mesoporous Electrodes Incorporating mesoporous structures into inorganic electrodes can generate an enhanced surface area per unit volume and significantly improve the kinetics and mass transport at the interfaces of electrodes. We have developed a new electrochemical method to produce various inorganic films containing uniformly organized mesoporous structures. Our method is based on creating interfacial amphiphilic layers on the working electrode by surface forces and using them as surface templates to electrodeposit inorganic mesoporous films (Figure 1). This method is quite different from and complementary to conventional sol-gel based dip-coating methods where amphiphilic assembly is evaporation-induced and the inorganic wall construction is achieved by the sol-gel process. As a result, this interfacial electrochemical surfactant templating method significantly enhances our ability to assemble various inorganic mesoporous electrodes (e.g. material type, mesostructure type, pore orientation against the substrate) that cannot be produced by previous means. The resulting mesoporous electrodes contain uniform pore sizes and pore connectivities, which allows us to investigate the effect of nanostructural details on photoelectrochemical properties.

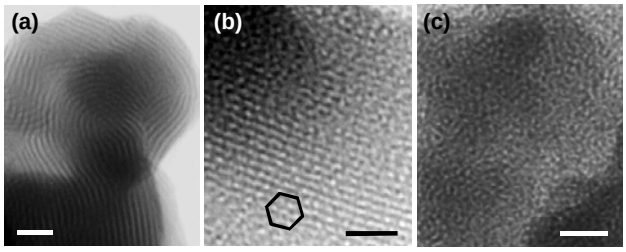

Figure 1. TEM images of (a) ZnO with a lamellar structure, (b) $Ni(OH)_2$ with a hexagonal structure, and (c) SnO_2 with a 3D worm-like structure(scale bar, 20 nm).

Systematic Regulation of Individual Particle Shapes in Polycrystalline Electrodes The shapes of individual crystals that compose polycrystalline electrodes dictate interfacial atomic arrangements and can significantly affect interfacial organic-inorganic interactions (e.g. dye

adsorption), interfacial charge transfer processes, catalytic properties and stabilities of electrodes. Therefore, gaining the ability to uniformly regulate the shape and connectivity of each crystal in polycrystalline electrodes is crucial for identifying optimum interfacial structures that can maximize desired photoelectrochemical properties. Earlier efforts toward controlling crystal shape and branching have been limited to simply stabilizing a few certain shapes instead of providing a general methodology to systematically evolve shapes. Our research specifically focuses on establishing synthetic strategies/conditions that can methodically control habit formation and branching growth processes of inorganic crystals (Figure 2). Homogeneous habit control enables us to study any dependence of physical and chemical properties on different crystallographic planes (e.g. {100} vs. {111} planes) while controlled branching growth provides means to expose highly reactive surfaces at the interfaces. We also investigate formation of dendritic and fibrous architectures in inorganic electrodes. As crystals in dendrites and fibers form physically continuous networks by nature, regulating the details of dendritic growth (e.g. particle sizes, shapes, and degree of branching) allows us to achieve enhanced surface areas while decreasing the rate of charge recombination due to grain boundary problems.

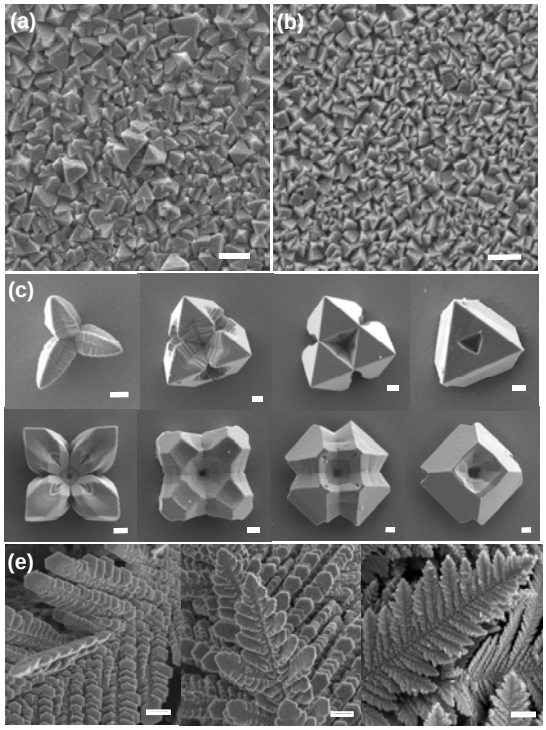

Figure 2. Polycrystalline Cu_2O electrodes composed of micron-size crystals with only (a) {111} planes and (b) {100} planes exposed at the interfaces; (c) Cu_2O crystals with varying degrees of branching; (d) dendritic polycrystalline architecture of zinc/zinc oxide films (scale bar = 1 μm).

Tuning Band Gaps and Doping Types of Semiconducting Electrodes In addition to gaining higher degrees of freedom in controlling morphological features, our research project simultaneously focuses on tuning doping types, compositions, and band positions of semiconducting electrodes. For example, we can now produce Cu_2O as both p-type and n-type electrodes and increase its bandgap energy (E_g) up to 2.6 eV. Bulk Cu_2O (E_g = 1.9 eV - 2.2 eV) cannot photoelectrolyze water to H_2 and O_2 without applying an external bias due to the proximity of its valence band to the oxidation potential of water, leaving little overpotential for the production of O_2. However, the Cu_2O electrode with E_g = 2.6 eV can photoelectrolyze water without applying an external bias due to its lowered valence band position.

Based on our ability to tailor the morphology, composition, and band structure of individual inorganic components, we are now building multi-component, multi-junction photoelectrodes that can enhance photon absorption and interfacial charge transfer processes while diminishing charge recombination and photocorrosion. Considering that the overall efficiency of the multi-component photoelectrodes depends not only on the material-types combined, but also on their junction areas/structures, our synthetic ability will create a multitude of opportunities to assemble and investigate multi-junction photoelectrodes.

DOE Sponsored Publications (2005-2007)

1. Tan, Y.; Steinmiller, Ellen M. P.; Choi, K.-S. "Electrochemical Tailoring of Lamellar Structured ZnO Films by Interfacial Surfactant Templating" *Langmuir* **2005**, *21*, 9618-9624.

2. Siegfried, M. J.; Choi, K.-S. "Elucidating the Effects of Additives on Growth and Stability of Cu_2O Surfaces via Shape Transformation of Pre-Grown Crystals" *J. Am. Chem. Soc.* **2006,** *128*, 10356-10357.

3. Brown, K. E.; Choi, K.-S. "Synthesis and Characterization of Transparent Nanocrystalline Cu_2O Films and Its Conversion to CuO Films" *Chem. Commun.* **2006**, 3311-3313.

4. López, C. M.; Choi, K.-S. "Electrochemical Synthesis of Dendritic Zinc Films Composed of Systematically Varying Motif Crystals" *Langmuir*, **2006**, *22* 10625-10629.

5. Yarger, M. S.; Choi, K.-S. "Electrochemical Synthesis of Cobalt Hydroxide Films with Tunable Interlayer Spacings" *Chem. Commun.* **2007**, 159-161.

6. Santato, C.; López, C. M.; Choi, K.-S. "Synthesis and Characterization of Polycrystalline Sn and SnO_2 Films with Wire Morphologies" *Electrochem. Commun.* **2007**, In press.

7. Spray, R. L.; Choi, K.-S. "Electrochemical Synthesis of SnO_2 Films Containing Three-Dimensionally Organized Uniform Mesopores via Interfacial Surfactant Templating" Submitted, **2007**.

8. Siegfried, M. J.; Choi, K.-S. "Elucidation of a New Overpotential-Limited Branching Mechanism during Electrocrystallization of Cu_2O" Submitted, **2007**.

9. López, C. M.; Choi, K.-S. "Photoelectrochemical Properties of ZnO-Au Composite Electrodes Assembled Based on Fibrous ZnO Architectures" Submitted, **2007**.

10. Steinmiller, Ellen M. P.; Choi, K.-S. "Construction of Lamellar Structured ZnO Films in Basic Media by Electrochemical Generation of Protons" Submitted, **2007**.

Session XI

Hydrogen Evolution at Photocatalytic Surfaces

SUNLIGHT-DRIVEN HYDROGEN FORMATION BY MEMBRANE-SUPPORTED PHOTOELECTROCHEMICAL WATER SPLITTING

Jordan Katz, Josh Spurgeon, and Nathan S. Lewis

Division of Chemistry and Chemical Engineering
California Institute of Technology
210 Noyes Laboratory, 127-72, Pasadena, CA 91125

The simplest solar-derived water splitting system imaginable would consist of a suspension of photocatalytic particles (or a solution of dissolved photoactive dye) in water. The particles (or dye) would absorb sunlight and then directly create chemical fuels as H_2 and O_2 gases, with no need for production of electrical power as an intermediary. However, recombination of the hydrogen and oxygen in periods of weak illumination or darkness, as well as the inherent explosion tendency, will be serious problems with such a system design. A preferred method to avoid generation of hydrogen and oxygen in the same physical space at the same time is therefore to support the photocatalyst assembly in a membrane. This approach is being explored, and developed, as the main focus of this work.

At least three important functions need to be developed to enable such a system to work well as a light-driven water-splitting photoactive assembly. First, the materials must be robust and provide the necessary voltage (1.23 V under standard conditions at 1 atm of pressure) needed to thermodynamically split water into H_2 and O_2. Secondly, the raw materials much be inexpensive and must be useful in an inexpensive form (i.e. not restricted in form to being only used as large area single crystals). Thirdly, the materials must be in a configuration that allows such relatively inexpensive materials to meet a minimum efficiency threshold (typically estimated to be at least 7-10% based on the constraints of the typical insolation flux and land use and balance of systems costs).

To address these issues, we are working on both combinatorial discovery of new photocatalyst materials that are suitable for this purpose, as well as methods for ordering and exploiting nanorod structures of photocatalysts into membranes to allow vectorial charge transport in order to sustain a water-splitting reaction.

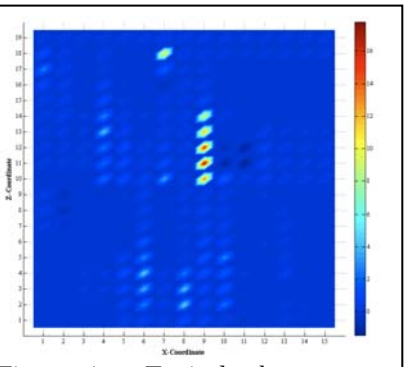

Figure 1: Typical photocurrent map of a slide of metal oxides. The X- and Z-coordinates give each spot's identity, which is correlated with photo-catalytic activity. Here, combinations of Zn and Co in row #9 show photoanodic current.

A novel combinatorial method to print and test thin films of new materials has been developed to quickly and efficiently search for stable photocatalytic materials capable of evolving H_2 gas under visible light illumination. This combinatorial approach relies on a very low-cost commercially available ink jet printer to make microliter quantitatively-controlled mixtures of metal salt solutions. In a matter of seconds, the ink jet printer is able to print up to 256 spots, each with a unique combination of up to eight different metals, directly onto a conductive glass substrate (fluorine doped tin oxide coated glass, or FTO). Once the mixed metal salt solutions are printed and pyrolyzed by baking

in air to form mixed metal oxides, each glass slide is tested under white light illumination in a NaOH electrolyte solution to screen for photocurrent. The great advantage of this method is the combination of the incredible speed and versatility of the printing and screening process, as well as its simplicity and low cost.

To test for photocatalytic activity, a computer-controlled translation stage was used to raster the FTO slide in front of a beam of white light focused down to the size of single metal oxide spot. By chopping the light and using a lock-in amplifier to analyze the photocurrent, it is also possible to measure photocurrents when biasing the sample without any contribution from the dark current. Using a custom automated scanning and data collection program, a FTO slide with over 250 unique photocatalyst materials can be screened in under 30 minutes. For easy interpretation, the data is plotted in a false color image, with the photocurrent plotted versus position on the slide (see **Figure 1**). Positive or negative currents indicate strong photoanodic or photocathodic behavior respectively.

Having developed a robust method for printing and testing materials for photocatalytic activity, we have tested a number of combinations metals, and several combinations appear promising. We have also observed that for some combinations of metals, the measured photocurrents are not constant with time, indicating possible degradation or corrosion of the metal oxide film under illumination. We are currently investigating this effect and are pursuing methods to pre-screen for kinetically unstable species, which are not viable photoelectrodes. Once an appropriate protocol is established, we estimate being able to print and screen some 2,000 materials per day.

In parallel with this effort, we are also developing and investigating the behavior of membrane-oriented nanorods to drive the chemical processes and thereby separate the products. Research has been conducted on the growth of dense, vertical arrays of nanometer-scale semiconductor rods of $CdSe_{0.65}Te_{0.35}$. The motivation for this work comes from theory and modeling which

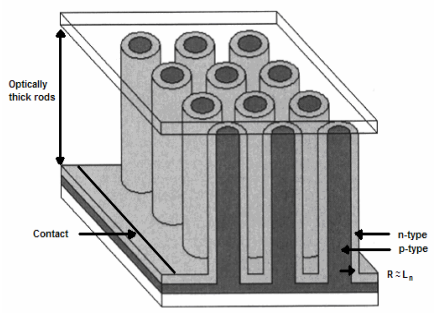

Figure 2 – Nanorod geometry provides sufficient absorption in the vertical dimension while allowing for better carrier collection in the radial dimension

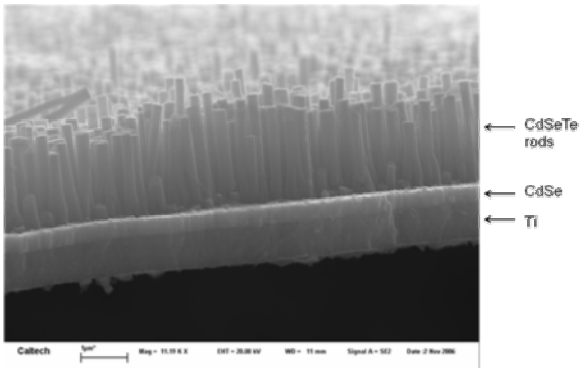

Figure 3 – SEM image of CdSeTe nanorod array

indicate that this novel geometry should lead to improvement in the performance of carrier collection limited semiconductor materials in photovoltaic devices. Commercially available alumina membranes with pores of either 200 nm or 100 nm diameter have been used as a means to control the growth dimensions during CdSeTe electrodepostion. To make the arrays, a very thin layer of CdSe is first sputtered onto one side of the template followed by a thicker layer of Ti. The Ti makes an ohmic back contact and the CdSe layer prevents any possibility of shunting in the photoelectrochemical cell through the metal backing. CdSeTe is then electrodeposited into

the pores and a thick layer of Ni is electrodeposited onto the back of the Ti to serve as a supportive substrate. After the nanorod growth, the constricting template is removed by etching it in a solution of NaOH. The morphology of these structures has been studied using a scanning electron microscope (Figure 2), and their elemental composition has been investigated by an energy dispersive x-ray spectrometer (EDS). The current-voltage properties of the electrodes were measured with a potentiostat in the dark and in the light, and spectral response measurements were conducted as well on both planar and nanorod samples.

Results to date from the current-voltage measurements have shown that these nanorod electrodes are capable of achieving similar short circuit currents to the planar electrodes; however, they have been consistently delivering much lower open circuit voltages (approximately 300 mV for a nanorod electrode compared to about 600 mV for a planar one). Plots of the spectral response have demonstrated that while a planar electrode's quantum efficiency fades as it gets into the red light, a nanorod's quantum efficiency stays mostly flat until it reaches the band gap. This implies that the nanorod geometry is doing a better job of collecting carriers created from light with a greater penetration depth. Future work on this research will include further testing of arrays of various lengths and diameter rods as well as investigating methods to improve the open circuit voltage that these electrodes produce.

DOE Sponsored Publications 2005-2007

Kayes, B.M., Spurgeon, J.M., Sadler, T.C., Lewis, N.S., and Atwater, A.H. "Synthesis and characterization of silicon nanorod arrays for solar cell applications.**"** Conference Record of the 2006 IEEE 4th World Conference on Photovoltaic Energy Conversion (IEEE Cat. No. 06CH37747) 4 pp. 2006

George W. Crabtree and Nathan S. Lewis, "Solar energy conversion", *Phys. Today*, **2007**, *60 (3)*, 37-42.

Nathan S. Lewis, "Toward cost-effective solar energy use" *Science*, **2007**, *315 (5813)*, 798-801.

FUNDAMENTAL INVESTIGATIONS OF WATER SPLITTING ON MODEL TiO_2 PHOTOCATALYSTS DOPED FOR VISIBLE LIGHT ABSORPTION

M. A. Henderson, S. H. Cheung, S. A. Chambers, G. A. Kimmel, P. Nachimuthu, N. G. Petrik and V. Shutthanandan
Chemical and Material Sciences Division and
Environmental Molecular Sciences Laboratory,
Pacific Northwest National Laboratory
Richland, WA 99352

Scope of Project

Development of new energy sources is a major need for the 21st century, and hydrogen has considerable potential as an alternative fuel. In the early 1970s, Fujishima and coworkers discovered that hydrogen could be produced from water electrolysis using electrons photocatalytically generated at TiO_2 electrodes. Their discovery continues to motivate research toward development of TiO_2-based photocatalysts for water splitting, although emphasis is now shifting toward study of visible light active photocatalysts because TiO_2 absorbs little of the solar spectrum. Promising results have emerged recently on a new class of visible-light active TiO_2 photocatalysts doped with anions (C, N, S). This project examines the fundamental properties of heterogeneous photocatalytic water splitting on ion-doped TiO_2 single crystal surfaces. Our objective is to provide fundamental understanding into how doping influences the visible-light absorption properties of TiO_2, how charge carriers from such visible light absorption events participate in surface redox processes, and what is the overall mechanism of the visible light initiated water splitting.

Recent Results

1) Anion doping of TiO_2 by molecular beam epitaxy: We have carried out a detailed study of the epitaxial growth and properties of nitrogen-doped TiO_2 rutile and anatase single crystal films using oxygen plasma assisted molecular beam epitaxy. Highly ordered N-doped TiO_2 films were grown in layer-by-layer fashion on appropriately latticed matched substrates through a surface reaction of sublimed Ti metal with an O_2 plasma seeded with 10-20% N_2. We find that ~1 atomic % N can be incorporated into single crystal anatase films and ~2 atomic % N into single crystal rutile films as substitutional N (labeled 'N_o' to the left in the ball-and-stick model for rutile TiO_2) without accompanied introduction of non-substitutional doping. For example, in the figure below, deuterium nuclear reaction analysis of a 2% N-doped rutile TiO_2(110) film grown on a TiO_2(110) single crystal shows the N to be substitutional for lattice O. These 'rocking curves' are achieved by slight deviations in the D ion beam incident angle. Strong shadowing effects permit near perfect transmission of the D ion beam through the sample along the incident direction ([110]), but collisions occur when the incident angle is deviated. As can be seen, lattice oxygen and the N dopant have the same angular profile about the surface normal. Inclusion of non-substitutional N results in signal along

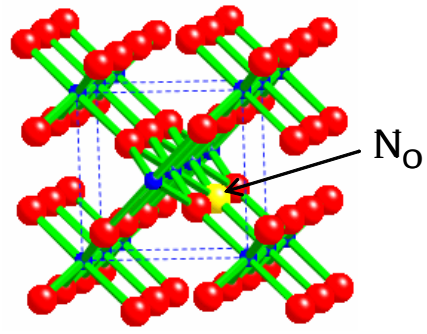

the [110] direction from reaction of the D beam with N. X-ray diffraction also confirms substitution of N for O in the lattice. X-ray photoemission (XPS) establishes that N is present as N^{3-}, and shows evidence for Ti – N hybridization. Ultraviolet photoemission (UPS) and optical absorption reveal that N 2p-derived states fall at the top of the TiO_2 valence band, resulting in an apparent bandgap reduction of ~0.5 eV. Electron paramagnetic resonance shows that N does not act as an acceptor due to compensation by interstitial Ti(III) (Ti_i) which forms during the growth process. Ti_i is a shallow donor in rutile. This methodology for preparing anion doped TiO_2 provide researchers with confidence of the dopant location and properties.

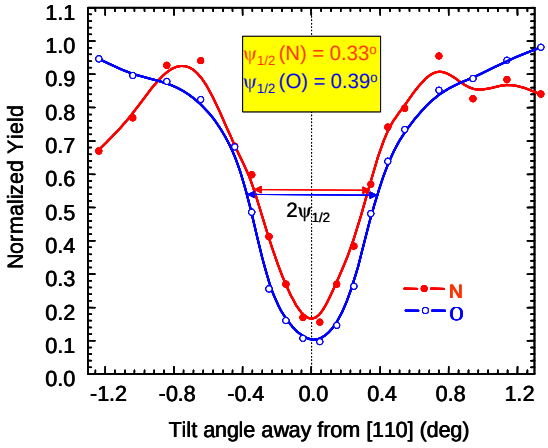

(2) Mechanism of water splitting: We have investigated the electron-stimulated reactions in thin water films on vacuum-annealed rutile TiO_2(110) in order to identify and characterize high energy intermediates that may be associated with water splitting chemistry on TiO_2. The temperature programmed desorption (TPD) spectra of electron-irradiated water films are essentially identical in all respects to those resulting from the reaction of $O_2^{\delta-}$ (formed from O_2 adsorption at surface electronic defects) and water on TiO_2. For coverages less than 1 monolayer (ML), the dominant reaction mechanism is as follows: (i) electronic excitation of an adsorbed water molecule on a Ti^{4+} site leads to (ii) desorption of an H atom leaving OH on the Ti^{4+} site. (iii) This OH readily reacts with a bridging OH, if any are available, to reform water, (iv) otherwise, additional thermal and/or non-thermal chemistry converts these OH groups into O_2, likely through formation of H_2O_2/HO_2 intermediates. Using in-situ scanning tunneling microscopy, we imaged the dissociation of water on the TiO_2(110) surface and the diffusion dynamics of dissociation products at coverages lower than inherent oxygen vacancy concentrations on this surface. Our results confirm that paired hydroxyl groups are the direct product of water dissociation at oxygen vacancies. For the first time, the hydrogens of these hydroxyl pairs are found to spontaneously separate along the (001) direction, indicating hydrogen hopping without the assistance of water molecules. Importantly, it is found that the hydrogens of the hydroxyl pair are not identical; the first hydrogen hop is ~10 times less likely for the hydrogen located at the original vacancy.

Future Plans

(1) Anion doping by molecular beam epitaxy
- Identify precursors that can be used in preparing C-doped TiO_2 films using MBE; carry out C-doping film growth studies and compare to results for N-doping.
- Perform NEXAFS measurements of C- and N-doped TiO_2 films prepared by both MBE and high energy ion implantation.

(2) Mechanism of water splitting

- Begin studies on the UV and visible irradiation of the H_2O+O_2 system on undoped and N-doped TiO_2(110).
- Examine the effect of N-doping on hole-mediated photochemical decomposition of molecules adsorbed on TiO_2(110).
- Prepare and image hydroxylated TiO_2(110) surfaces using neutral and positively charged hydrogen species from direct H atom exposure and organic acid dissociation, respectively.
- Examine with STM the effect of electron and UV irradiation on water and water+oxygen adsorbed on TiO_2(110).

DOE Sponsored Publications 2005-2007

1. Z. Zhang, O. Bondarchuk, J. M. White, B. D. Kay, Z. Dohnálek, "Imaging Water Dissociation on TiO_2(110): Evidence for Inequivalent Geminate OH Groups," *Journal of Physical Chemistry B* 110 (2006) 21840. (Article featured on the journal cover.)

2. S. H. Cheung, P. Nachimuthu, A. G. Joly, M. H. Engelhard, M. K. Bowman, S. A. Chambers, "N Incorporation and Electronic Structure in N-doped TiO_2(110) Rutile", *Surface Science* 601 (2007) 1754.

3. S. A. Chambers, S. H. Cheung, V. Shutthanandan, S. Thevuthasan, M. K. Bowman, A. G. Joly, "Properties of Structurally Excellent N-doped TiO_2 Rutile", submitted to a special issue of *Journal of Chemical Physics* ("Doping and Functionalization of Photoactive Semiconducting Metal Oxides," ed. C. DiValentin, U. Diebold, A. Selloni), in press.

4. C. D. Lane, N. G. Petrik, T. M. Orlando, and G. A. Kimmel, "Electron-stimulated oxidation of thin water films adsorbed on TiO_2(110)," *Journal of Physical Chemistry C*, submitted.

5. Z. Q. Yu, C. M. Wang, S. Thevuthasan, and I. Lyubinetsky, "Toward Improvement of STM Tip Preparation", *Reviews of Scientific Instrumentation*, submitted.

CATALYZED WATER OXIDATION BY SOLAR IRRADIATION OF BAND-GAP-NARROWED SEMICONDUCTORS

Etsuko Fujita, James T. Muckerman, Sergei Lymar, José Rodriguez, Peter Sutter
Chemistry Department and Center for Functional Nanomaterials
Brookhaven National Laboratory
Upton, NY 11973-5000

Coordinated experimental and theoretical studies of water oxidation using direct excitation of band-gap-narrowed semiconductors to absorb a significant fraction of the solar spectrum, together with catalysts that promote four-electron water oxidation to O_2 is being undertaken. This project has three principal thrusts: (1) controllably narrow the band gaps of TiO_2 by replacing oxygen by nitrogen or carbon (or that of GaN:ZnO solid solutions with varying Ga:Zn ratio), and elucidate the resulting electronic properties and stabilities; (2) determine the catalysis of water oxidation by metal oxides, metal hydrous oxides immobilized on titania nanoparticles, and dimeric ruthenium complexes in order to develop a better understanding of the critical four-electron water oxidation catalyst chemistry, and rationally search for improved catalysts; and (3) combine these elements to examine the function of oxidation catalysts on actual band-gap narrowed surfaces. Our integrated approach to solar water oxidation combines experimental and theoretical studies on single crystal surfaces and thin films in interfacial situations ranging from vacuum to vapor to aqueous solution, together with thermodynamic, kinetic and mechanistic studies on catalysts located in solution and at the solid/aqueous interface.

N-doping of TiO_2(110): Photoemission and density functional studies. The electronic properties of N-doped rutile TiO_2(110) have been investigated using synchrotron-based photoemission and density-functional calculations. The doping via N_2^+ ion bombardment leads to the implantation of N atoms (~5% saturation concentration) that coexist with O vacancies. The experimental and theoretical results show the existence of attractive interactions between the dopant and O vacancies. First, the presence of N embedded in the surface layer reduces the formation energy of O vacancies. Second, the existence of O vacancies stabilizes the N impurities with respect to N_2(g) formation. (JR, EF)

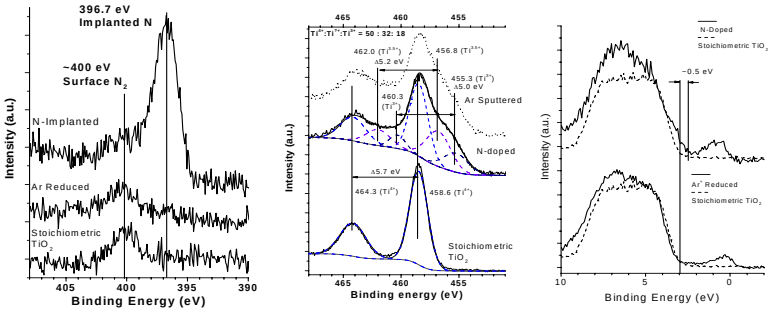

reFigure 1. N 1S core level XPS (left), Ti 2P core level XPS (middle) nd Valence band spectra for Ar^+ reduced and N-implanted rutile TiO_2

Reaction of NH_3 with titania: N-doping of the oxide and TiN formation. The thermal nitridation of TiO_2 has been frequently used for preparation of N-doped TiO_2. Our detailed investigation of this nitridation reaction by time-resolved *in-situ* XRD revealed a smooth transition from the anatase or rutile phase to a cubic TiN phase and incorporation of nitrogen into the interstitial sites of titania. *Ex-situ* characterizations of the synthesized N-doped TiO_2 using XPS and NEXAFS support the interstitial incorporation mechanism, while the substitution mechanism cannot completely be excluded. A comprehensive analysis of the data suggests that

the incorporated nitrogen may form N_2-like species embedded in the titania lattice, which is in agreement with the instability of the incorporated nitrogen atoms found by DFT calculations. We are currently investigating properties and stabilities of N-doped TiO_2 nanoparticles prepared by a sol-gel method toward photochemical water splitting. (JR, EF)

Toward water oxidation by immobilized transition metal hydrous oxides. Synthesis of Co hydrous oxide immobilized on titania nanoparticles has been developed and optimized. Catalytic activity of Co hydrous oxide immobilized on TiO_2 nanoparticles in water oxidation has been characterized using a home-built computerized system with luminescence oxygen detection. With $Ru(bpy)_3^{3+}$ as a one-electron oxidant, essentially stoichiometric oxygen evolution is observed in weakly basic solutions (pH 8.8–10.6) at Co concentrations as low as 5–7 μM, indicating a very efficient catalysis of water oxidation:

$$4\ Ru(bpy)_3^{3+} + 2\ H_2O \xrightarrow{[TiO_2]\text{-}Co} O_2 + 4\ H^+ + 4\ Ru(bpy)_3^{2+}$$

Overall kinetics of water oxidation has been investigated using stopped-flow method and the initial steps of the TiO_2-Co catalytic action has also been investigated by flash photolysis (with V. Shafirovich, NYU) where the $Ru(bpy)_3^{3+}$ oxidant is generated photochemically.(SL)

Theoretical and experimental studies of the mechanism of water oxidation by ruthenium complexes. We are employing a combined theoretical and experimental approach to elucidate the mechanism by which complexes **a**, **c** and **d** catalyze the oxidation of water. H_2O, OH^- and O^- bind to the vacant coordination site on the monomers **b** and **d**, and, in addition, O_2^- binds to the Ru sites in the dimer **a**. These species are involved in proton- and electron-transfer reactions that oxidize water and reduce the catalyst. Here we compare the results of spectroelectrochemical studies of various intermediate species bound to the Ru monomer to DFT and TD-DFT calculations of the electronic structure of each possible species with a given composition, overall charge and spin multiplicity, and their UV-vis spectra, respectively, in order to identify the species observed. See more details about **c** and **d** in the poster given by D. Polyansky. (EF, JM)

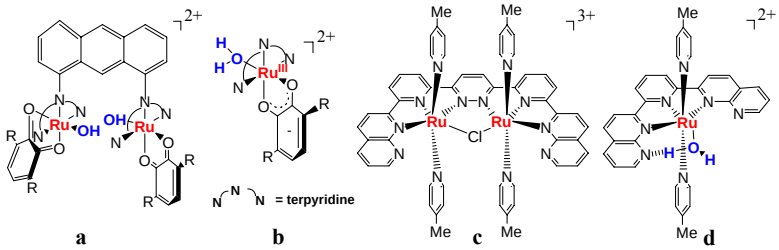

Structural and electronic properties of $(Ga_{1-x}Zn_x)(N_{1-x}O_x)$ solid solution photocatalyst. Recent studies have shown that a solid solution $(Ga_{1-x}Zn_x)(N_{1-x}O_x)$ can decompose water under visible light. We carried out a systematic study of the structural and electronic properties of this solid solution *versus* zinc concentration using the GGA+*U* and the "special quasirandom structures" approaches. Two different periodic supercells were used, and the results obtained from both supercells are in qualitative agreement with available experimental findings, although overall the larger supercell provides a better description of the solid solution. Downward bowing of the band gap over the entire composition range has been observed for both supercells, showing a minimum band gap of the solid solution for some intermediate ZnO concentration. These predictions will be tested experimentally. (JM with M. Newton)

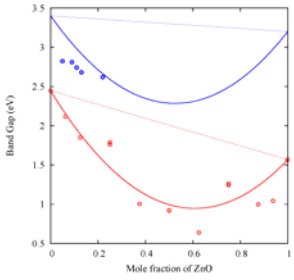

Calculated (red) and experimental (blue) band gap *vs*. ZnO concentration. The calculated bowing parameter has been applied to the experimental BG.

DOE Sponsored Hydrogen Fuel Initiative Publications 2005-2007

N Doping of TiO_2(110): Photoemission and Density-Functional Studies, A. Nambu, J. Graciani, J. A. Rodriguez. Zhong, Q.Wu, E. Fujita, and J. F. Sanz, *J. Chem. Phys*. **2006**, *125*, 094706

Reaction of NH_3 with Titania: N-Doping of the Oxide and TiN Formation, H. Chen, A. Nambu, W. Wen, J. Graciani, Z. Zhong, J. C. Hanson, E. Fujita, and J. A. Rodriguez, *J. Phys. Chem. B*, **2007**, *111*, 1366-1372.

First-principles Studies on the Structural and Electronic Properties of the $(Ga_{1-x}Zn_x)(N_{1-x}O_x)$ Solid Solution Photocatalyst, L. Zhao, J. T. Muckerman, and M. D. Newton, *J. Phys. Chem. C* (submitted).

DOE Sponsored Solar-Photochemistry Publications 2005-2007

Reaction of Hydroxylmethyl and Hydride Complexes in Water: Synthesis, Structure and Reactivity of a Hydroxymethyl-Cobalt Complex, C. Creutz, M. H. Chou, E. Fujita, and D. J. Szalda, *Coord. Chem. Rev.* **2005**, *249*, 375-390.

Carbon-to-Metal Hydrogen Atom Transfer: Direct Observation Using Time-Resolved Infrared Spectroscopy. J. Zhang, D. C. Grills, K.-W. Huang, E. Fujita, and R. M. Bullock, *J. Am. Chem. Soc.* **2005**, *127*, 15684-15685.

Transition State Characterization for the Reversible Binding of Dihydrogen to Bis(2,2'-bipyridine)rhodium(I) from Temperature- and Pressure-Dependent Experimental and Theoretical Studies. E. Fujita, B. S. Brunschwig, C. Creutz, J. T. Muckerman, N. Sutin, D. J. Szalda, and R. van Eldik, *Inorg. Chem.* **2006**, *45*, 1595-1603.

Kinetic Studies of the Photoinduced Formation of Transition Metal-Dinitrogen Complexes Using Time-Resolved Infrared and UV-vis Spectroscopy. D. C. Grills, K.-W. Huang, J. T. Muckerman, and E. Fujita, *Coord. Chem. Rev.* **2006**, *250*, 1681-1695.

Efficient Synthesis of Os-Os dimers: $[Cp(CO)_2Os]_2$, $[Cp^*(CO)_2Os]_2$, and $[(i Pr_4C_5H)(CO)_2Os]_2$, and Computational Studies on the Relative Stabilities of Their Geometrical Isomers. J. Zhang, K. -W. Huang, D.J. Szalda, and R. M. Bullock, *Organometallics* **2006**, *25*, 2209-2215.

Direct Measurements of Rate Constants and Activation Volumes for the Binding of H_2, D_2, N_2, C_2H_4 and CH_3CN to $W(CO)_3(PCy_3)_2$: Theoretical and Experimental Studies with Time-Resolved Step-Scan FTIR and UV-vis Spectroscopy. D. C. Grills, R. van Eldik, J. T. Muckerman, and E. Fujita, *J. Am. Chem. Soc.* **2006**, *128*, 15728-15741.

Characterization of Transit Species and Products in Photochemical Reactions of $Re(dmb)(CO)_3Et$ with and without CO_2, K. Shinozaki, Y. Hayashi, B. S. Brunschwig, and E. Fujita, *Res. Chem. Intermed.* **2007**, *33*, 27-36.

Carbon Dioxide Reduction by Pincer Rhodium η^2-Dihydrogen Complexes: Hydrogen Binding Modes and Mechanistic Studies by Density Functional Theory Calculations. K.-W. Huang, J. H. Han, C. B. Musgrave, and E. Fujita, *Organometallics*, **2007**, 26, 508-513.

Photochemical and Radiolytic Production of Organic Hydride Donor with Ru(II) Complex Containing an NAD^+ Model Ligand, D. E. Polyansky, D. Cabelli, J. T. Muckerman, E. Fujita, T. Koizumi, T. Fukushima, T. Wada, and K. Tanaka, *Angew. Chem. Int. Ed*. **2007**, in press

Theoretical Investigation of the Binding of Small Molecules and the Intramolecular Agostic Interaction at Tungsten Centers with Carbonyl and Phosphine Ligands, J. T. Muckerman, E. Fujita, C. D. Hoff, and G. J. Kubas, *J. Phys. Chem. B* submitted.

Generation of Ru(II)-Semiquinone-Anilino Radical through Deprotonation of Ru(III)-Semiquinone-Anilido Complex, Y. Miyasato, T. Wada, J. T. Muckerman, E. Fujita, and K. Tanaka, *Angew. Chem. Int. Ed*. submitted.

A COMBINATORIAL METHOD FOR DISCOVERY OF WATER PHOTOELECTROLYSIS CATALYSTS

Michael Woodhouse and B. A. Parkinson
Department of Chemistry
Colorado State University
Fort Collins, CO 80523

Direct photoelectrolysis of water using semiconductor electrodes is the "Holy Grail" of photoelectrochemistry. Unfortunately there is no known stable, efficient and inexpensive material that can accomplish this process. We believe that oxide semiconductors are the only materials that have the combination of these required properties, however no such material is currently known. We have been exploiting high-throughput combinatorial methods to begin to screen the potentially millions of possible complex oxide materials for water photoelectrolysis activity. We developed a simple approach that uses ink jet printing to produce overlapping patterns of metal oxide precursors onto conductive glass substrates. When aqueous metal nitrate solutions are printed, subsequent firing at 500°C produces patterns metal oxide phases. Photoelectrolysis activity is screened by measuring photocurrents produced by scanning a laser over the printed patterns in aqueous electrolytes.

Figure 1 shows a scheme for printing mixtures of four metals taken three at a time, borrowed from Mallouk et al, that identified an unexpected composition containing iron, aluminum and cobalt. Photocurrent spectroscopy showed a p-type material with a band gap of about 1.6 eV, a promising value for water photoelectrolysis. Although the off-the-shelf ink jet printers are inexpensive and can easily print any design you can draw they are not very quantitative when the exact printed densities need to be determined so that the stoichiometry of the active compound can be determined. Therefore when a promising composition is identified we use a research level ink jet printer where the printed ink density can be controlled and thus the proportions for preparing a bulk sample can be determined. Figure 2 A and B shows a different printing motif used to more precisely determine the stoichiometry. A further refinement, shown in Figure 2 C and D, reveals that the stoichiometry for a photoactive phase is somewhat forgiving within the narrow boundaries printed ($Co_{0,81\text{-}0,9}Al_{0.05\text{-}0.1}Fe_{0.03\text{-}0.1}$).

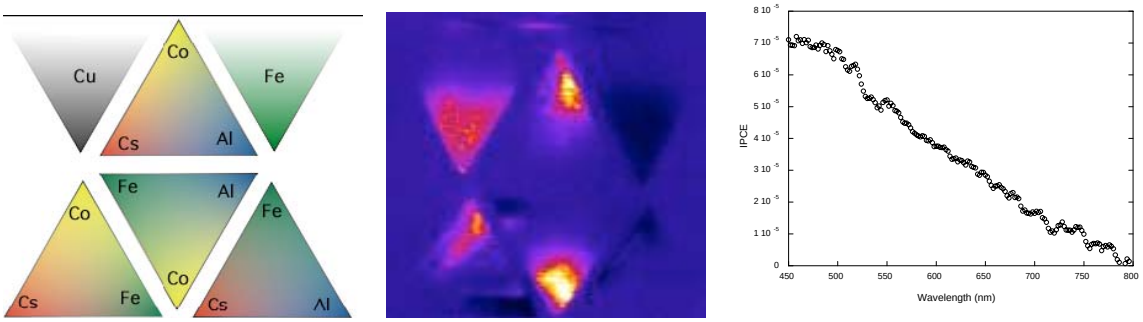

Figure 1 A scheme for high throughput screening of compositional gradients. Pure CuO and α-Fe_2O_3 are printed in triangles at the top as internal standard p and n type oxide materials respectively (left). A false color photocurrent map in 0.1M NaOH that shows a promising p-type material was made in the cobalt rich region of the Fe-Co-Al triangle (middle). A photocurrent spectrum, taken on the high photocurrent region in the middle image, indicates that the material has a band gap of about 1.6 eV.

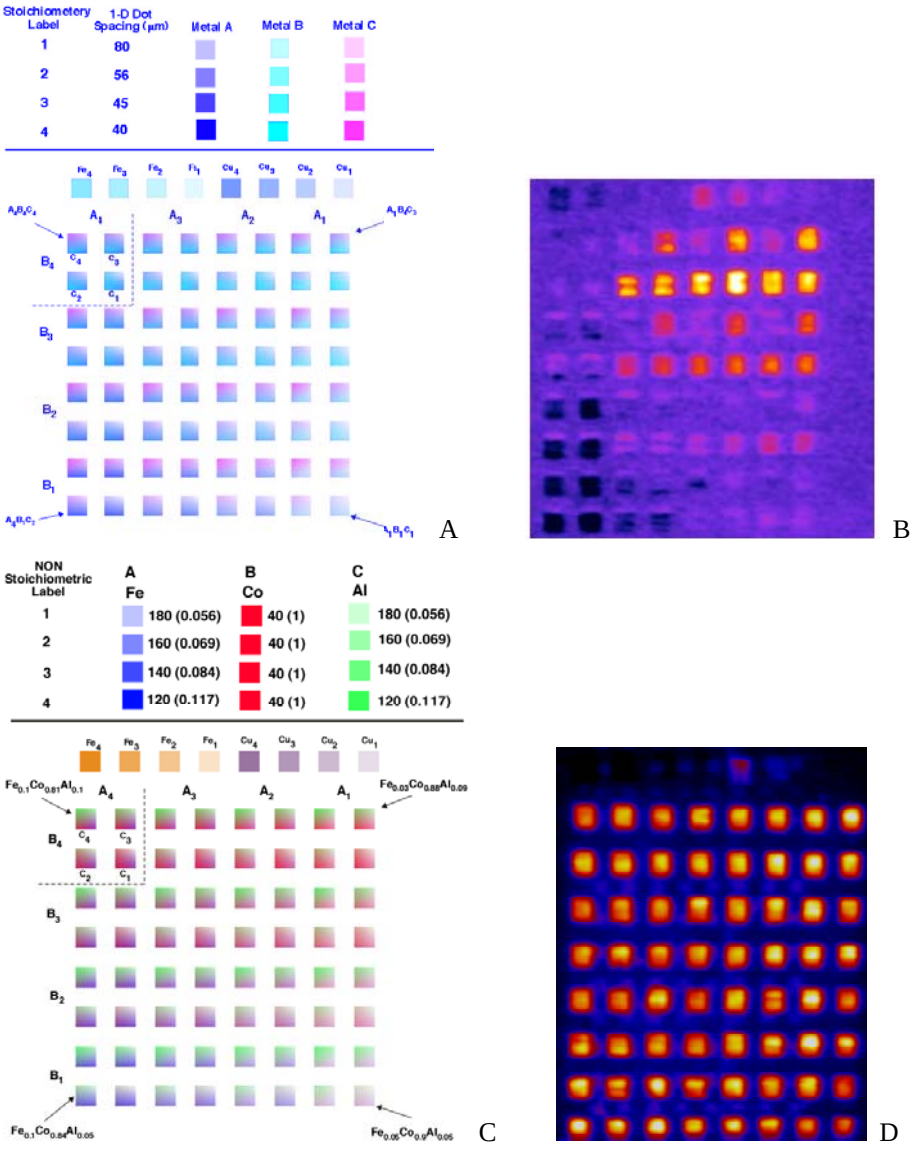

Figure 2 Quantitative printing scheme used for optimizing composition. A-Method for variation of metal stoichiometry from $Co_1Al_1Fe_1$ and $Co_4Al_4Fe_4$ and the photocurrent scan (B). C and D show a much smaller stoichiometric range in the cobalt rich region with the range $Co_{0,81\text{-}0,9}Al_{0.05\text{-}0.1}Fe_{0.03\text{-}0.1}$.

We have been recently printing a mixture of the nitrate salts to prepare films with the near optimum composition to evaluate their efficiency for hydrogen evolution and to add a forth component to the mix. We have also been exploring the role of the substrate in the performance of this material for hydrogen evolution. In addition we are following up on several other new semiconducting oxide compositions that we have identified and are working on expanding the scale of the high throughput initial screening step.

DOE Sponsored Publications 2005-2007

1. Michael Woodhouse, G. S. Herman and B. A. Parkinson, "A Combinatorial Approach to Identification of Catalysts for the Photoelectrolysis of Water", Chemistry of Materials, 17, 4318-4324, (2005)

2. B. A. Parkinson and M. Woodhouse, "A Digital Method for the Identification of Photoelectrolysis Catalysts for Water", Digital Fabrication, R. Mills, Ed., The Society for Imaging Science and Technology: Baltimore, MD, 190-193, (2005)

3. S. Ushiroda, N. Ruzycki, Y. Lu, M. T. Spitler, and B. A. Parkinson, "Dye Sensitization of the Anatase (101) Crystal Surface by a Series of Dicarboxylated Thiacyanine Dyes", J. Am. Chem. Soc., *127*(14), 5158 – 5168, (2005)

4. Laura Sharp, David Soltz and B. A. Parkinson, "Growth and Characterization of Tin Disulfide Single Crystals", Crystal Growth & Design, 6(6), 1523-1527, (2006)

5. Yunfeng Lu, Dae-jin Choi, Jimmy Nelson, O-Bong Yang and B. A. Parkinson "Adsorption, Desorption, and Sensitization of Low-Index Anatase and Rutile Surfaces by the Ruthenium Complex Dye N3", Journal of the Electrochemical Society, 153(8), E131-E137, (2006)

6. Yunfeng Lu, Bengt Jäckel and B. A. Parkinson, "Preparation and Characterization of Terraced Surfaces of Low-Index Faces of Anatase, Rutile, and Brookite". Langmuir, 22(10), 4472-4475, (2006)

7. Yunfeng Lu, Mark T. Spitler and B. A. Parkinson, "Photochronocoulometric Measurement of the Coverage of Surface Bound Dyes on Titanium Dioxide Crystal Surfaces", J. Phys. Chem. B, 110, 25273-25278, (2006)

8. Yunfeng Lu, Mark T. Spitler and B. A. Parkinson, "Regenerator Dependent Photo-Induced Desorption of a Dicarboxylated Cyanine Dye from the Surface of Single Crystal Rutile", Langmuir, in preparation

Poster Abstracts

ZEAXANTHIN RADICAL CATION FORMATION IN MINOR COMPLEXES OF HIGHER PLANT ANTENNA

[1,2]Ahn, T.K., [2,3]Avenson, T.J., [1,2]Zigmantas, D., [1,3]Niyogi, K.K., [1,3]Li, Z. [4]Ballottari, M., [4]Bassi, R., and [1,2]Fleming, G.R.

[1]Physical Biosciences Division, Lawrence Berkeley National Laboratory, Berkeley, CA 94720, [2]Department of Chemistry, Hildebrand B77, University of California, Berkeley, CA 94720-1460, [3]Department of Plant and Microbial Biology, Koshland Hall, University of California, Berkeley, CA 94720-3102, [4]Department of Science and Technology, University of Verona, Italy 37134

During higher plant photosynthesis, photoinhibition of critical energy transducing components within the chloroplast membrane is a natural by-product of light energy conversion. Therefore, various means of photoprotection are essential for survival of plants under conditions when more light energy is absorbed than can be utilized in downstream metabolism. Reversible energy-dependent quenching, or qE, is reported to be the predominant component of the harmless energy relaxation processes that are generally referred to nonphotochemical quenching. qE requires de-epoxidized Xanthophylls (i.e. like zeaxanthin), a trans-thylakoid pH gradient (ΔpH), and the photosystem II antenna-associated protein (PsbS). A previous study in our lab demonstrated, using wild-type spinach thylakoid membranes, that qE is directly related to a charge transfer (CT) process that occurs between zeaxanthin and chlorophyll, a mechanism that was uncovered by combining femtosecond transient absorption (TA) spectroscopy with analyses of various mutant species of Arabidopsis thaliana (Holt et al. Science 307: 433-6). These transient CT species were shown to be correlated with a functional PsbS, supporting the hypothesis that the mechanism is specific to qE. In the work presented herein, we extended this study to investigate where this CT mechanism happens and we found a transient cation signal in isolated CP minor complexes (i.e. CP29, CP26, and CP24), e.g. even in the absence of PsbS, while we couldn't observe any evidence of the cation species in either LHCII trimers or monomers. This transient cation species has a broad absorption centered at ca. 980 nm which is about 20 nm blue-shifted relative to β-carotenoid cation absorption and exhibits 5 ps generation time and 240 ps decay, the latter presumably representing recombination kinetics. We believe that this transient species represents more specifically a zeaxanthin cation radical (Zea•+) by comparison with previous studies. In addition, we demonstrated that all three of the CP monomers (CP29, CP26, and CP24) exhibit evidence of transient Zea•+ formation as implied by their TA spectra. Furthermore, in CP26 we also found evidence of another transient species which absorbs at ~940 nm according to the TA spectra, results which we interpret as evidence of transient lutein cation radical (Lut•+) formation. The role of PsbS is not yet clear, but it most likely contributes in vivo to modulating the conformation of the CP monomers in a manner that facilitates CT state generation and resultant fluorescence quenching. Upon absorption of excess energy in the chloroplast, a functional PsbS, ΔpH and Zeaxanthin conspire to activate CP monomers (CP29, CP26, and CP24) to quench excited chlorophylls by harmless heat dissipation through CT states.

EXCITON AND CARRIER DYNAMICS IN SILICON NANOCRYSTALS AND ELECTRONICALLY COUPLED PbSe NANOCRYSTALS

Matthew C. Beard, Joseph M. Luther, Kelly P. Knutsen, Qing Song,
Matt Law, Randy J. Ellingson, and Arthur J. Nozik
Chemical and Biosciences Center
National Renewable Energy Laboratory
Golden, Colorado 80401

We have studied the exciton dynamics in silicon nanocrystals (NCs) to quantify the efficiency of multiple exciton generation (MEG). We find that at ~2.5 times the effective band gap, E_g, MEG begins to be efficient, and 2.7 excitons are generated for every 1 photon absorbed when the photon energy reaches 3.3 X E_g. We compare this to impact ionization in bulk Si. We have also characterized the Auger dynamics in silicon nanocrystals for three sizes of NCs. Silicon dominates the photovoltaic industry, poses no serious health risk, and is readily available. These results are encouraging and should provide new incentives for understanding interfacial charge separation in nanoscale materials.

These results have important implications for solar energy conversion. The thermodynamic limit for a conventional single junction photovoltaic device is ~33%. The major source of loss is hot carrier cooling, where the excess absorbed energy (photon energy minus the band gap energy) is lost to heat. MEG can partially overcome this limit by converting high energy photons into band gap excitons. This process in NCs is faster than hot carrier cooling and a new mechanism based upon a coherent superposition of excitonic states has been proposed to explain the results. A new thermodynamic limit of ~43% can be achieved with photovoltaic devices employing an MEG active absorber, where the excitons are separated into charge carriers.

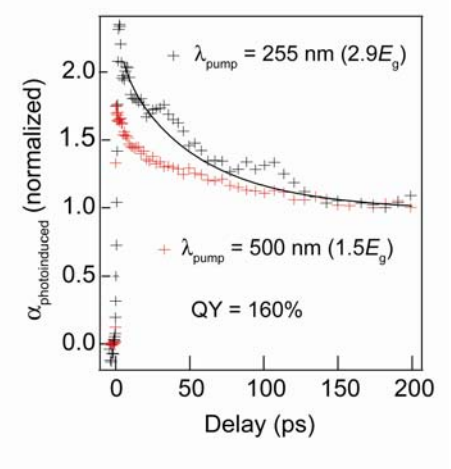

Figure 1. Transient absorption in Si NCs demonstrating MEG.

Certain solar energy approaches utilizing semiconductor NCs are based upon strong inter-NC coupling such that extended electronic states form. A key feature is that the excitons must be dissociated and removed from the individual NCs on a timescale faster than the biexciton lifetime. We have employed both transient absorption and ultrafast pump/probe THz spectroscopy to investigate chemically treated PbSe nanocrystals arrays. The THz response is directly sensitive to the degree of electronic coupling. Carrier trapping rates are also measured simultaneously. We will present THz photoconductivity measurements in ordered arrays of 5.6 nm PbSe NCs with varying inter-NC separation and discuss the various factors that determine efficient long range transport. We compare and contrast the THz photoconductivity results for different chemical treatments.

Transient absorption measurements were employed to investigate MEG in coupleD PbSe NC arrays. We find that under conditions of intermediate coupling the biexciton lifetime increases but the MEG efficiency remains unchanged from isolated NCs.

EXTRINSIC EFFECTS ON THE PHOTOLUMINESCENCE QUANTUM YIELD OF SURFACTANT-DISPERSED SINGLE-WALL CARBON NANOTUBES

J.L. Blackburn, T.J. McDonald, W. Metzger, C. Engtrakul, G. Rumbles, M.J. Heben,
National Renewable Energy Laboratory, Golden, Colorado 80401

The photoluminescence quantum yield (Φ_{PL}) provide a measure of the various radiative and non-radiative recombination rates of a given system. Few reports exist for the quantum yield of single-wall carbon nanotubes (SWNTs) though such information is critical for evaluating nanotube photochemical reactions with donors and acceptors. Within the existing reports in the literature, there is a large spread in the calculated Φ_{PL}. For SWNTs dispersed in aqueous surfactant solutions Φ_{PL} has been estimated at 0.05% - 0.65%,[1] while for long (> 10 μm) SWNTs suspended in air the estimate is much higher, ~7%.[2] This variation suggests a strong dependence of Φ_{PL} on extrinsic environmental factors.

In this report, we discuss extrinsic effects on the quantum yield for commercially obtained HipCo SWNTs dispersed in aqueous surfactant solutions. We find that Φ_{PL} is strongly affected by the surfactant chosen to disperse the nanotubes. Figure 1 demonstrates that Φ_{PL} is a factor of 2-3 higher when SWNTs are dispersed with the bile salt sodium cholate hydrate (cholate) rather than the most commonly used surfactant, sodium dodecyl sulfate (SDS). Additionally, we find that Φ_{PL} is reduced by an order of magnitude when acid-purified HipCo SWNTs rather than as-prepared, unpurified tubes are used. The absolute quantum yield for the SWNT dispersions was calculated by referencing to a known standard, IR26 (Φ_{PL} = 0.14%), and was found to be in the range of 5% for raw tubes dispersed with cholate, higher than has ever been reported for SWNTs in aqueous dispersions.

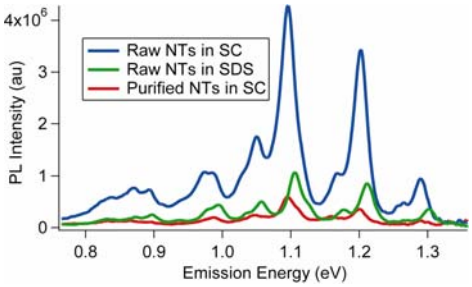

Figure 1 PL spectra of three HipCo dispersions excited at 650 nm.

Raman spectroscopy was used to evaluate the mechanism behind such environmental effects on Φ_{PL}. The quenching of certain vibrational modes, such as the radial breathing modes (RBM) and the Breit-Wigner-Fano (BWF) mode can yield important information on the dielectric environment for SWNTs in the solid-state or in solution.[3] Figure 2 demonstrates that for the acid-purified SWNTs, the RBM modes of larger diameter tubes are significantly quenched, and the BWF modes have narrowed and blue-shifted; similar effects are seen for the SDS surfactant. These effects are typical for SWNTs that have been oxidized by adsorbed protons, and help to explain the observed low Φ_{PL} for purified HipCo SWNTs and SWNTs dispersed with SDS. Detailed mechanistic interpretations will be discussed.

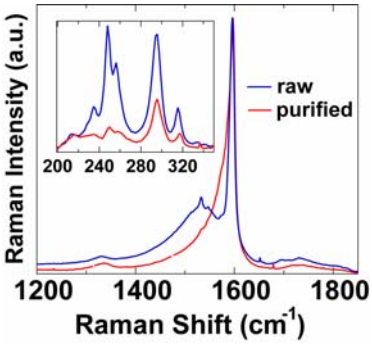

Figure 2 Raman spectra of raw and purified HipCo SWNTs dispersed by cholate.

(1) Jones, M.; Engtrakul, C.; Metzger, W. K.; Ellingson, R. J.; Nozik, A. J.; Heben, M. J.; Rumbles, G. *Physical Review B: Condensed Matter* **2005**, *71*, 115426. (2) Lefebvre, J.; Austing, D. G.; Bond, J.; Finnie, P. *Nano Lett.* **2006**, *6*, 1603.
(3) Blackburn, J. L.; Engtrakul, C.; McDonald, T. J.; Dillon, A. C.; Heben, M. J. *J. Phys. Chem. B* **2006**, *110*, 25551.

REDOX REACTIONS OF THE NON-HEME IRON OF PHOTOSYSTEM II: AN EPR SPECTROSCOPIC STUDY

James P. McEvoy[a] and Gary W. Brudvig

Department of Chemistry, Yale University
PO Box 208107, New Haven, CT 06520-8107
[a]current address: Department of Chemistry, Regis University
Mail Stop D4, 3333 Regis Blvd., Denver, CO 80221

The non-heme Fe^{2+} ion in photosystem II (PSII) lies between the two quinone redox cofactors, Q_A and Q_B, which are linked *via* hydrogen bonds to two of the iron's histidine ligands. The characteristics of the iron are, therefore, relevant to the redox chemistry of Q_A and Q_B, and the metal's coordination sphere has been linked particularly with the operation of redox-coupled proton transfer to Q_B. In this work, we have used EPR spectroscopy to investigate the redox chemistry of the non-heme iron, focusing on the cryogenic photoinduced electron-transfer reactions from the secondary carotenoid, chlorophyll and tyrosine D electron donors to iron and Q_A. Glycolate coordination to the iron was used in combination with potassium ferricyanide to preoxidize the non-heme iron completely and prime it for photoreduction (Figure 1). The oxidized Fe^{3+} and Q_A centers operated essentially as a single, one-electron acceptor site: EPR quantitation of both the oxidized donor yield and the Fe^{2+} Q_A^- yield found no evidence for the formation of more than one oxidized secondary electron donor per PSII. The photooxidized chlorophyll and carotenoid secondary electron donors were shown, for the first time, to be capable of charge recombination with photoreduced Fe^{2+}, oxidizing the iron in a temperature-dependent fashion below 300 K. Two redox populations of Fe^{3+} were revealed at low temperatures. One population was photoreduced at the lowest attainable temperatures, while the other was fully photoreduced only at temperatures above *ca.* 140 K, having an apparent reduction potential below that of the Q_A / Q_A^- couple (–80 mV) at lower temperatures. It is hypothesized that the redox activity of the non-heme iron depends upon the existence of a facile proton-transfer pathway linking the site to the stromal surface of the protein, and that the redox activity of the non-heme iron may be viewed as a probe of physiologically relevant redox-coupled proton-transfer reactions around the Q_B site.

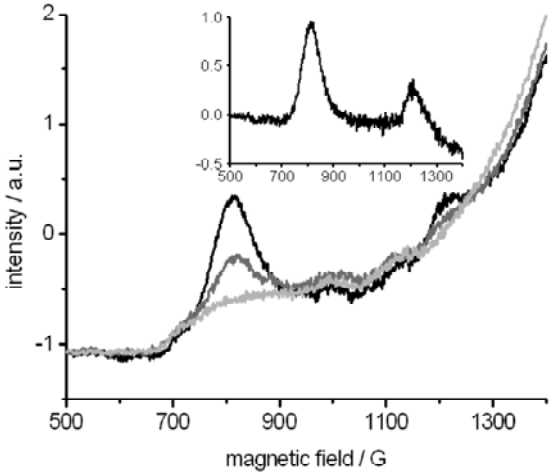

Figure 1. EPR spectra of the non-heme Fe^{3+} before (black) and after illumination at 3.6 K (gray) and 143 K (light gray); Inset: dark-minus-light difference.

"HOT" ELECTRONS IN Ag NANOCRYSTAL PLASMON EXCITED STATES: PHOTOVOLTAGE AND PHOTO-CATALYZED GROWTH

Peter Redmond, Xiaomu Wu and Louis Brus
Chemistry Department
Columbia University
New York, NY 10027

Hot, unrelaxed electrons in particle plasmon excited states cause the near field SERS enhancement. We now explore possible hot electron photochemistry. The photo-catalyzed reduction of aqueous silver ions, by citrate adsorbed on silver nanocrystals, is studied on Formvar/carbon TEM grids and in photoelectrochemical cells. The reaction is characterized by transmission electron microscopy (TEM) monitoring of individual particles throughout the growth process. The photo-initiated growth on the silver particles is uniform and is not dependent upon the laser polarization. The potential of silver particle working electrodes is shown to shift negatively under irradiation in solutions of citrate. Adding silver ions to this system quenches the charging of the particle working electrode. The reaction is hypothesized to result from photo-electron transfer from adsorbed citrate to the silver nanoparticle. The photo charging process is initiated by electronic excitation of the silver particles which causes the oxidation of surface bound citrate ions. Nanocrystal growth occurs when this "stored" charge reduces silver ions in solution. Chronopotentiometry and chronoammperometry methods were used to study the photo charging and electrochemical discharging of silver particle electrodes. In citrate solution, the particles discharge by reducing hydrogen. When silver ions are introduced, the additional discharge pathway of silver reduction increases the rate of discharge. The electrochemical discharging of the particles is modeled using the Butler-Volmer equation. The capacitance of the particle electrode is experimentally determined to be ~2.22×10^{-4} C/V.

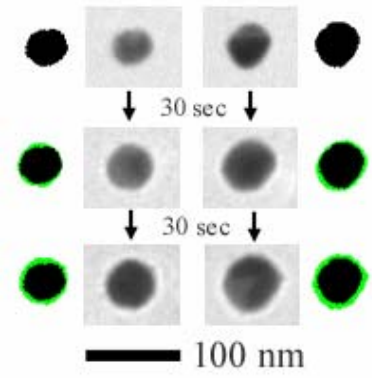

TEM images of silver particles before and after growth. The first row is with no irradiation. The second and third rows are for 30 sec and 60 sec of irradiation respectively.

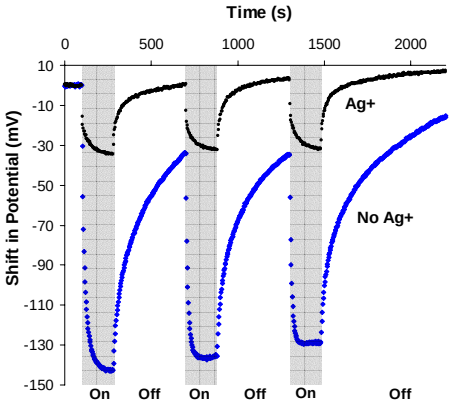

Shift from rest potential of a silver particle working electrode in a solution of 500 uM sodium citrate and 0.1 M potassium nitrate: The black circles have 250 uM silver nitrate in solution. The blue diamonds have no silver nitrate in solution. The shaded areas of the graph = laser is on; unshaded areas = laser off.

TRACKING ELECTRONS AND ATOMS IN A PHOTOEXCITED METALLOPORPHYRIN WITH X-RAY TRANSIENT ABSORPTION SPECTROSCOPY

Lin X. Chen,[a] Xiaoyi Zhang,[a,b] Erik C. Wasinger,[a] Klaus Attenkofer,[b] Guy Jennings,[b] Ana Z. Muresan,[c] Jonathan S. Lindsey[c]

[a]Chemistry Division and [b]X-ray Science Division, Argonne National Laboratory, Argonne, Illinois 60439, USA
[c]Chemistry Department, North Carolina State University, Raleigh, North Carolina 27685, USA

Simultaneously tracking electronic and molecular structures of a photoexcited metalloporphyrin, which are present for only 200 ps in dilute solution, has been realized using X-ray transient absorption spectroscopy (XTA). Combining the laser pulses that generate an excited state metalloporphyrin with X-ray pulses that interrogate the excited state, we were able to simultaneously track the energy levels and electron occupation in molecular orbitals (MOs), as well as the molecular geometry of the short-lived excited state of a nickelporphyrin, in a relatively dilute toluene solution. The experimental results indicate that the excited state has *a*) an electronic configuration with one vacancy in each of $3d_{x2\text{-}y2}$ and $3d_{z2}$ MOs, *b*) an energy gap of about 2.2 eV between $3d_{x2\text{-}y2}$ and $3d_{z2}$ MOs, *c*) energy shifts of $3d_{x2\text{-}y2}$ and $4p_z$ MOs by 0.4 eV and 1.5 eV higher than those of the ground state, and *d*) an expansion of the porphyrin ring characterized by the lengthening of Ni-N and Ni-C bonds by 0.09 and 0.07 Å respectively. Moreover, XTA signals at different X-ray photon energies as functions of the delay time between the laser and the X-ray pulses signify potentials for acquiring the correlation and coherence between different optically excited states using ultrafast X-ray pulses in the future. These results provide references of electronic configurations and molecular geometry for theoretical calculations as well as insightful understanding in control the pathways of optically excited states that play important roles in solar energy utilization, molecular devices, and catalysis.

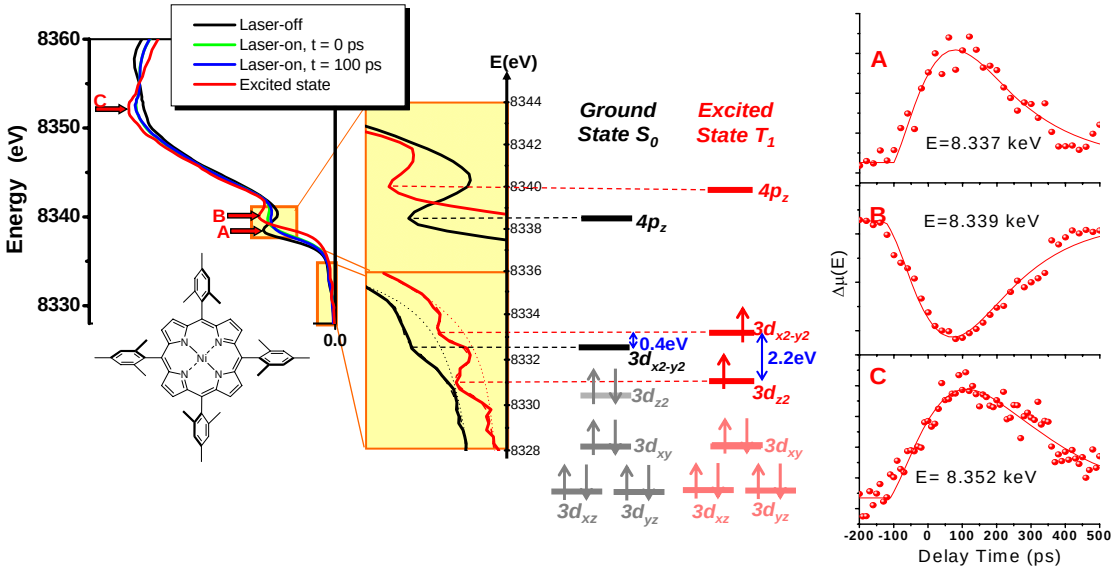

EXCITED STATE GEOMETRY OF MOLECULES EMBEDDED IN COMPLEX FRAMEWORKS AND DEVELOPMENTS OF TECHNIQUES FOR SUB-MICROSECOND DIFFRACTION AT ATOMIC RESOLUTION

Philip Coppens, Chemistry Department, State University of New York, Buffalo, NY 14260-3000

X-ray-laser pump-probe techniques, in which a pulsed laser pump-source is synchronized with probing X-ray pulses, have been successfully used in the determination of excited state geometry.[1] The long-lifetime luminescent state of $\{[3,5\text{-}(CF_3)_2\text{Pyrazolate}]Cu\}_3$,[2] is unique among the compounds studied as it involves an inter- rather than an intra-molecular excitation. We have extended the time-resolved technique to molecules embedded in cavities of supramolecular frameworks, which are a largely untested medium for spectroscopic and photocrystallographic research. The dimeric species $[Cu(NH_3)_2]_2^{2+}$ isolated in a host framework of $THPE^-$ [tris(hydroxyphenyl)ethane],[3] to give $[Cu(NH_3)_2]_2[THPE^-]_2\cdot 3.25H_2O$, is not stable in its isolated state, but, as shown by experiment, is stabilized by Cu^I-Cu^I bond formation on excitation (see figure on right: black lines ground state, open lines excited state. Irradiation of a xanthone dimer in HECR-2xanthone-6MeOH (HECR=hexaethylresorcin[6]arene)[4] similarly leads to increased interaction, in this case the interplanar distance in the dimer contracts from 3.39 to 3.14 Å as predicted but never experimentally observed for excimer formation (see figure on left: full lines ground state, broken lines excited state).[5]

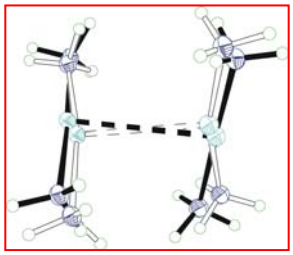

As many photochemical processes relevant for solar-energy capture occur on a timescales faster than those of the above experiments, we have focused our attention on development of methods for submicrosecond diffraction. In ultrafast experiments a large number of reflections must be measured simultaneously, as possible by use of broad bandwidth Laue techniques. We have designed and built a heatload shutter which can absorb the heat load in 'pink-beam' polychromatic experiments.[6] We are testing the integration methods for multi-wavelength diffraction patterns using the *Precognition* software to maximize the accuracy required for atomic-resolution experiments. In the test experiments performed so far at the single-pulse Advanced Ring at the KEK in Japan frames of reflections have been collected with nanosecond exposure, corresponding to a decrease in exposure time of almost three orders of magnitude compared with monochromatic experiments, pointing the way to sub-μs experiments.

---

[1] "The Structure of Short-Lived Excited States of Molecular Complexes by Time-Resolved X-ray Diffraction", P. Coppens, I. I. Vorontsov, T. Graber, M. Gembicky and A. Y. Kovalevsky, *Acta Crystallogr.* A **61**, 162-172 (2005).

[2] "Shedding Light on the Structure of a Photo-Induced Transient Excimer by Time-Resolved Diffraction", I. I. Vorontsov, A. Y. Kovalevsky, Y.-S. Chen, T. Graber, M. Gembicky, I. V. Novozhilova, M. A. Omary, P. Coppens, *Phys. Rev. Lett.*, **94**, 193003/1-193003/4 (2005).

[3] "An Unstable Ligand-Unsupported Copper(I) Dimer Stabilized in a Supramolecular Framework", S.-L. Zheng, M. Messerschmidt and P. Coppens, *Angewandte Chemie, Int. Ed.* **44**, 4614-4617 (2005).

[4] "Syntheses, Structures, Photoluminescence and Theoretical Studies of Xanthone in Crystalline Resorcinarene-Based Inclusion Complexes", S.-L. Zheng and P.Coppens, *Chem. Eur. J.*, **11**, 3583-3590 (2005).

[5] "Supramolecular Solids and Time-Resolved Diffraction", P. Coppens, S.-L. Zheng, M. Gembicky, M. Messerschmidt and P. Dominiak, *CrystEngComm*, **8**, 735–741 (2006).

[6] "On the Design of Ultrafast Shutters for Time-Resolved Synchrotron Experiments." M. Gembicky and P. Coppens, *J. Synchrotron Rad.*, **14**, 133-137 (2006). "A kHz Heat-Load Shutter for White-Beam Experiments at Synchrotron Sources", M. Gembicky, S-I. Adachi and P. Coppens, *J. Synchrotron Rad.*, **14**, 295–296 (2007).

FACILE HYDRIDE TRANSFER TO CARBON DIOXIDE IN WATER

Carol Creutz and Mei H. Chou
Chemistry Department
Brookhaven National Laboratory
Upton, NY 11973

Despite the fact that water is the ideal substrate and medium for photogeneration of fuels, very few studies of carbon dioxide reduction in water have been reported. Interested by a report describing work in organic solvents (Konno et al. *Inorg. Chim. Acta* **2000**, *299*, 155), we have studied the reaction of Ru(terpy)(bpy)H^+ with carbon dioxide in water. The rate of reaction is first order in [Ru(terpy)(bpy)H^+] and [CO_2], 295 K, pH 5.8. k = 8.5 x 10^2 M^{-1} s^{-1}. See Figure 1.)

To establish that the true reactant in water is CO_2 (not bicarbonate or carbonate ions) we carried out a pH jump experiment (Figure 2).

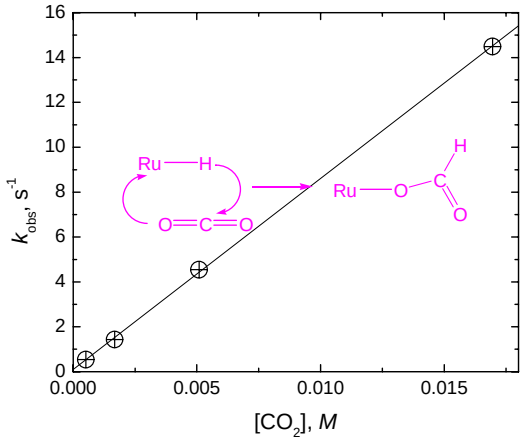

Figure 1. The pseudo first-order rate constant vs. carbon dioxide concentration for reaction in water at 22 °C.

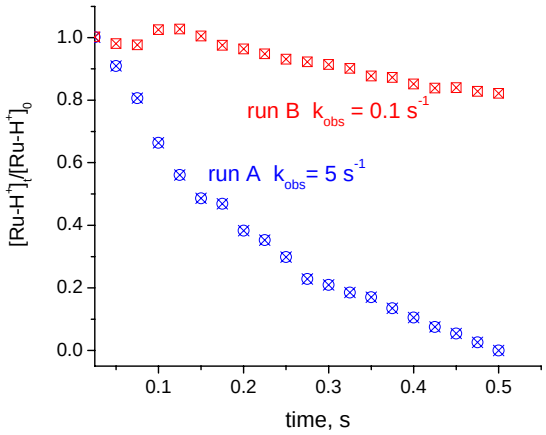

Figure 2. pH Jump.At pH 7 measure rate of reaction of Ru(bpy)(terpy)H^+ with "carbonate" solutions stored at pH 5 (A) and pH 12 (B). See Lymar et al. (*J. Am. Chem. Soc.* **1995**, *117*, 8867)

The rates constants for hydride transfer to CO_2 increase with solvent acceptor number, reminiscent of the behavior of a rhenium hydride studied by Sullivan and Meyer (*Organometallics* **1986**, *5*, 1500) This hydride complex exhibits high field ^{1}H NMR resonance (δ -14.7), a very low M-H stretching frequency (1827 cm^{-1}), and very potent hydride donor (hydricity ≤1.44 eV).

The kinetics of hydride transfer from this complex to protons will also be presented.

PHOTOACTIVE INORGANIC MEMBRANES FOR CHARGE TRANSPORT

Prabir Dutta, Henk Verweij, Bern Kohler
Departments of Chemistry and Materials Science and Engineering
The Ohio State University
Columbus, Ohio 43210

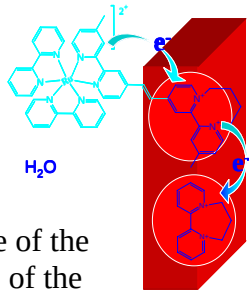

Figure 1

Our approach to long-lived photochemical charge separation is based on thin-film zeolites that function as artificial photosynthetic membranes. As depicted in Figure 1, we are synthesizing ruthenium polypyridine photosensitizer molecules tethered to one side of the membrane along with bipyridinium acceptor molecules within the zeolite. We seek a design that upon photoexcitation, favors unidirectional electron transport from one side of the membrane to the opposite side through the zeolite. The microporous nature of the inorganic zeolite enables the encapsulation of a wide variety of organic molecules, semiconductors, conducting polymers that can act as relays for charge migration.

For synthesis of zeolite L membranes, we have followed a two-step hydrothermal process starting with the deposition of oriented single crystal seeds on alumina supports. The conditions for seed deposition were optimized by varying the zeolite fraction in the deposition dispersion, as well as by tailoring the surface chemistry of the support and the zeolite. The homogeneity and morphology of the membranes, after secondary growth, were characterized by SEM of fracture cross sections of a zeolite L membrane, shown in Figure 2. In addition, the absence of connected meso-defects was confirmed by gas permeation in the non-stationary dead-end mode. The Ar permeance of membranes grown for >40 hr at room temperature and 150ºC was below the detection limit of 10^{-12} mol/(m^2·s·Pa) which is an indication of absence of connected meso-defects.

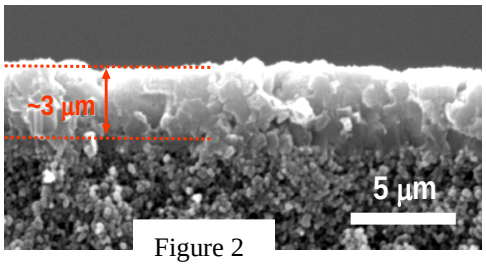

Figure 2

Bipyridinium compounds are attractive electron relay agents and they can be easily incorporated into zeolite voids by ion exchange (Figure 1). By preparing zeolite particles of colloidal size, we have been able to suppress light scattering and greatly improve the optical properties of zeolite nanoparticles suspended in various solvents. With these systems, femtosecond transient absorption signals can be recorded in a conventional transmission geometry with high signal-to-noise ratios. The extreme sensitivity of methyl viologen excited-state dynamics to the solvent in homogeneous solution makes this molecule an excellent probe of the microenvironment within zeolite cavities. Steady-state excitation and emission spectra of zeolite-encapsulated viologens exhibit spectral shifts indicative of quantum confinement effects. Additionally, time-resolved measurements reveal how impediments to molecular motion by the viologen and entrapped solvent molecules affect radiative and nonradiative decay. These results are helping to explain the static and dynamical factors that modulate charge separation, propagation and recombination within zeolite membranes.

PHOTOCATALYTIC GENERATION OF HYDROGEN FROM WATER USING SYSTEMS BASED ON PLATINUM(II) CHROMOPHORES

Pingwu Du, Jie Zhang, Jacob Schneider, Paul Jarosz,
William W. Brennessel and Richard Eisenberg
Department of Chemistry
University of Rochester
Rochester, NY 14627

Photochemical water splitting using visible light represents one of the "grand challenges" in artificial photosynthesis. The reductive side of this reaction is the light-driven generation of H_2 from aqueous protons and an electron source. In this poster, we describe recent efforts relating to this reaction in which platinum(II) diimine and terpyridyl chromophores are employed. These chromophores possess long-lived excited states that correspond to charge transfers to the heterocyclic aromatic ligand and undergo both oxidative and reductive electron transfer quenching. Numerous studies have dealt with the light driven generation of H_2 from aqueous protons, commencing in the 1970s with reports describing systems containing $Ru(bpy)_3^{2+}$ as the chromophore, methyl viologen (MV^{2+}) as both quencher and electron transfer mediator, a metal colloidal catalyst and a sacrificial electron donor. Subsequent studies addressed variation of different system components including attachment of the chromophore to platinized TiO_2. We have found that the acetylide chromophores of types **1** and **2** also lead to light driven H_2 production in multiple component systems containing MV^{2+}, triethanolamine (TEOA) as the sacrificial electron donor and colloidal Pt as the H_2 evolving catalyst. Complexes **1** and **2** undergo both oxidative and reductive quenching at comparable rates, as determined from separate quenching studies, so the full reaction scheme for H_2 production involves both pathways. Initial turnovers for **1** with X=Me numbered 84 after 10 h of irradiation with $\lambda > 410$ nm. Different diquats in place of MV^{2+} were examined and 4,4'-dimethyl-1,1'-trimethylene-2,2'-bipyridinium was found to be most effective with 800 turnovers of H_2 and a lower limit of 67 % yield of H_2 based on TEOA present. When chromophores of type **2** with derivatives of either bipyridine or phenanthroline were attached to platinized TiO_2 without MV^{2+} or diquat present, photogeneration of H_2 was seen (albeit at a lower rate), indicating that TiO_2 was functioning as the electron relay in an integrated system. In order to use lower energy light for H_2 production, the dithiolate chromophores **3** and **4** were employed. Binding studies show that attachment of these chromophores to TiO_2 is complete and irradiation with $\lambda > 455$ nm in the presence of TEOA yields H_2 photogeneration. These systems are photostable under these conditions with no loss of activity after 10 days of irradiation.

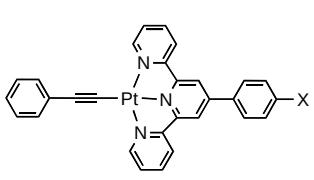

1
X = H, Me, OMe, Cl, Br

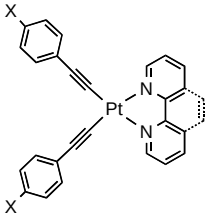

2
X = H, Me, CHO, Cl

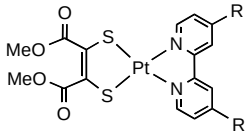

3
R = COOH

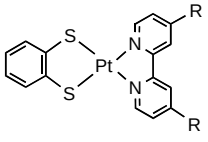

4
R = COOH

ORIENTED TiO_2 NANOTUBE ARRAYS FOR DYE-SENSITIZED SOLAR CELLS: EFFECT OF NANOSTRUCTURE ORDER ON TRANSPORT, RECOMBINATION, AND LIGHT HARVESTING

Kai Zhu, Nathan R. Neale, Alexander Miedaner, and Arthur J. Frank
Chemical and Biosciences Center
National Renewable Energy Laboratory
Golden, CO 80401

In traditional dye-sensitized TiO_2 solar cells (DSSCs or Grätzel cells), photoinjected electrons percolate through a random nanoparticle (NP) network before reaching the charge-collecting electrode. This tortuous conducting pathway leads to slow electron transport. Because the collection of electrons competes with their loss via recombination, high charge-collection efficiencies require that transport is significantly faster than recombination. Films constructed of oriented one-dimensional nanostructures, such as nanotube (NT) arrays, aligned perpendicular to the charge collecting substrate, could potentially improve the charge-collection efficiency by promoting faster transport and slower recombination. In this presentation, we describe the results of our study of the microstructure and the electron dynamics in DSSCs incorporating oriented TiO_2 NT arrays prepared from electrochemically anodizing Ti foils. The morphology of the NT arrays was characterized by SEM (Figure 1), TEM, and XRD. The SEM images show that the arrays consist of approximately hexagonal close-packed NTs, several microns in length, with typical wall thicknesses and inter-tube spacings of 8–10 nm and pore diameters of about 30 nm. The calcined material was fully crystalline with individual NTs consisting of about 30 nm-sized crystallites. The transport and recombination properties of the NT and NP films used in DSSCs were compared. Surprisingly, although both morphologies display similar transport times, recombination was 10 times slower in the NT films, indicating that the NT-based DSSCs have significantly higher charge-collection efficiencies than their NP-based counterparts. Dye molecules were shown to cover both the interior and exterior walls of the NTs. Analyses of photocurrent measurements indicate that the light-harvesting efficiencies of NT-based DSSCs were higher than those found for DSSCs incorporating NPs owing to stronger internal light-scattering effects. The solar cell properties of NT- and NP-based DSSCs were also compared.

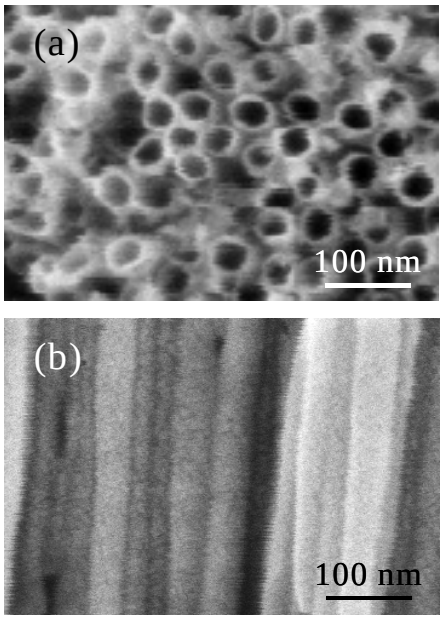

Figure 1. Surface (a) and cross-sectional (b) SEM images of TiO_2 NT arrays.

USING DENSITY FUNCTIONAL THEORY TO MODEL TRANSITION METAL CONTAINING SYSTEMS

Richard A. Friesner, David Rinaldo, Louis Brus, Ying-Reii Chen, Vladimir Blagojevic
Department of Chemistry
Columbia University
New York, NY 10027

We have been proceeding towards our goal of accurately modeling electronic states in TiO_2 nanoparticles (the underlying substrate in the Graetzel cell) by carrying out calculations for TiO_2 clusters, and also by extending our localized orbital correction methodology (B3LYP-LOC) previously developed for second and third row atoms to transition metal containing species. Firstly, we have performed an extensive series of calculations on a wide range of TiO_2 clusters, considering the effects of solvent, and studying ionization potentials and electron affinities. In the Graetzel cell, the key initial issue is the atomic nature of the trapping states which collect electrons from the excited dye molecules on the surface of the TiO_2 nanoparticles, and the ability to accurately calculate the energetics of these states in solution. Achieving this goal will require the ability to converge wavefunctions for large TiO_2 clusters and we have made significant progress in this direction. We have also investigated the effect of using different basis sets, which can have a nontrivial impact on the energetics of the calculations. A picture of a relatively small rutile cluster, capped with hydroxyls, along with the wavefunction of the HOMO, is shown below.

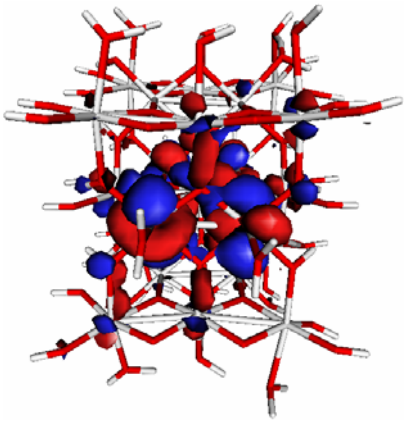

Fig. 1: Ti_{23} rutile cluster capped with hydroxyls; HOMO wavefunction

The cluster calculations described above employ the B3LYP functional, which so far has provided the best performance for transition metal containing systems. However, there are still significant errors in the DFT energetics for metals, in many cases substantially larger than those seen for second or third row containing compounds. We have extended our B3LYP empirical correction scheme to transition metal containing species and demonstrated its validity via applications to the atoms and to ~70 small molecules for which bond energy data is available. A very large improvement in the average error in predicting bond energies as compared to experiment, is obtained, with an acceptable number of fitting parameters. The key issue is assignment of the transition metal bonding orbitals and this will be explained in detail in the poster presentation.

LINKERS FOR SEMICONDUCTOR NANOPARTICLE SENSITIZATION

Artem Khvorostov, Jonathan Rochford, Qian Wei, Piotr Piotrowiak and Elena Galoppini
Department of Chemistry, Rutgers University
Newark, NJ 07041

(1) The sensitization of wide band gap semiconductors by dyes is an interfacial electronic process of fundamental and practical importance. Its applications include the preparation of photoelectrochemical solar cells, photochromic and electrochromic devices, and displays. We have developed rigid linkers (tripods and rigid-rods varying in length and structure) that spatially separate the dye from the semiconductor with a bridge. We have shown that such linkers can be used to prepare model compounds that are useful to study fundamental interfacial electron transfer processes.[1-3] An ultrafast laser system (sub-30 fs independently tunable pump and probe pulses) consisting of two noncollinear optical parametric amplifiers (NOPAs) is now functional in PP's laboratory. This was used to determine photoinduced charge injection rates from molecular tripods terminated with Ru^{II}-bpy chromophores into TiO_2 mesoporous films (**Fig. 1**). A comparison between tripods and rods of different length and conjugation will be presented and how the preparation of the films influences the results will be discussed. To improve the binding we have developed the synthesis of tripodal compounds where the number and position of the COOH anchoring group(s) on the phenyl rings can be changed, **Fig. 2**. Preliminary calculations (Persson, Lund) suggested that COOH groups in meta position will enhance the binding to TiO_2 compared to tripods with the COOH in para position.

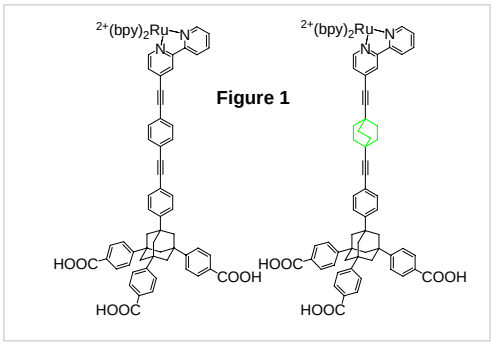

Figure 1

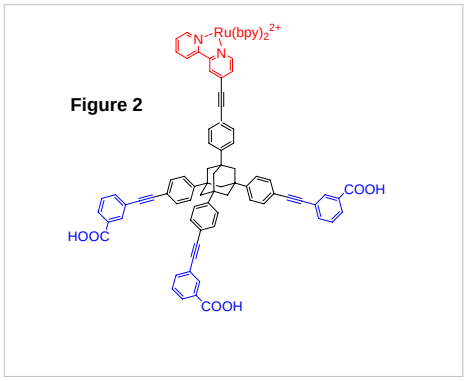

Figure 2

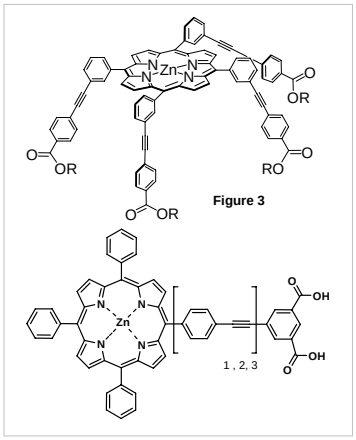

Figure 3

(2) The poster will also discuss the effect of linker length and binding orientation on the efficiency and photophysical properties of novel porphyrin dyes (rigid-rod and tetrachelates) bound to TiO_2, ZnO, and ZrO_2 nanoparticle films and also ZnO nanorods (two examples are shown in **Fig 3**) .[4-6]

Selected DOE-sponsored References: **(1)** *Ru(II)-Polypyridyl Complexes Bound to Nanocrystalline TiO_2 Films Through Rigid-Rod Linkers: Effect of the Linkers Length on Electron Injection Rates* Piotrowiak, P.; Galoppini, E.; Wang D.; Myahkostupov, M. *J. Phys. Chem. C* **2007**, *111*, 2827-2829. **(2)** *Tuning Open Circuit Photovoltages with Tripodal Sensitizers* Clark, C.C.; Meyer, G.J.; Wei , Q.; Galoppini, E. *J. Phys. Chem.B* **2006**, *110*, 11044-11046. **(3)** *Calculated Optoelectronic Properties of Ruthenium tris-bipyridine Dyes Containing OPE Rigid Rod Linkers in Different Chemical Environments* Lundqvist, M. J.; Galoppini, E.; Meyer, G. J.; Persson P. *J. Phys. Chem. A* **2007**, *111*, 1487-1497. **(4)** *Tetrachelate Porphyrin Chromophores for Metal Oxide Semiconductor Sensitization: Effect of the Spacer Length and Anchoring Group Position* Rochford, J.; Galoppini, E.; Chu, D.; Hagfeldt, A.; *J. Am Chem. Soc.* **2007**, *129*, 4655-4665. **(5)** *Fast Electron Transport in Metal Organic Vapor Deposition Grown Dye-sensitized ZnO Nanorod Solar Cells* Galoppini, E.; Rochford, J.; Chen, H.; Saraf, G.; Lu, Y.; Hagfeldt, A.; Boschloo, G. *J. Phys. Chem. B.*, **2006**, 16159 – 16161. **(6)** *Binding Studies of Molecular Linkers to ZnO Nanotips* Taratula, O.; Galoppini E.; Wang, D.; Chu, D.; Zhang, Z.; Chen, H.; Saraf, G. and Lu, Y. *J. Phys. Chem. B* **2006**, *110*, 6506-6515.

HIGHLY ORDERED Ti-Fe OXIDE NANOTUBE ARRAY FILMS: TOWARDS ENHANCED SOLAR SPECTRUM WATER PHOTOELECTROLYSIS

Craig A. Grimes
Department of Electrical Engineering, & Materials Science and Engineering
The Pennsylvania State University, University Park, PA 16802

The material architecture of a semiconductor photoanode plays a critical role in determining the resultant photoconversion efficiencies. The research group of the PI has reported three synthesis generations of highly-ordered TiO_2 nanotube arrays, by anodization of Ti films, and their application to water photoelectrolysis.[1-3] The tubular, vertically oriented, thin-wall architecture appears ideally suited to photoelectrolysis, with the nanotube arrays demonstrating IPCEs of ≈ 90% under bandgap illumination.[2] The first generation TiO_2 nanotube-arrays of up to 500 nm length were fabricated using an aqueous HF based electrolyte.[1] In the second generation, nanotube-array lengths increased to ≈ 7 μm by control of the electrolyte pH.[2] In the third generation, nanotube arrays up to 1100 μm in length have been obtained using various non-aqueous polar organic electrolytes.[3] Under UV spectrum illumination, 320 nm – 400 nm, TiO_2 nanotube arrays several tens of μm in length demonstrate a photoconversion efficiency of ≈ 20%.

We would ideally wish to combine the charge transport and photocorrosion properties of titania with, for example, the 2.2 eV bandgap of α-Fe_2O_3. Since both Ti and Fe can be anodized in a fluoride ion containing ethylene glycol solution,[4] we hypothesized that Ti-Fe metal films could be anodized to obtain highly-ordered, vertically oriented Ti-Fe oxide nanotube arrays showing enhanced visible light water photoelectrolysis properties.

The fabrication and visible spectrum (380 nm – 650 nm) photoelectrochemical properties of self-aligned, vertically oriented Ti-Fe oxide nanotube array films are described. Ti-Fe metal films of variable composition, co-sputtered onto FTO coated glass, are anodized in an ethylene glycol + NH_4F electrolyte; the band gap of the resulting films ranges from UV to visible as dependent upon the Fe content. Ti-Fe oxide nanotube array films 1.5 μm thick demonstrate a sustained 2 mA/cm^2 under AM 1.5. Surface morphology, structure, elemental analysis, optical, and photoelectrochemical properties of the Ti-Fe oxide nanotube array films are considered.

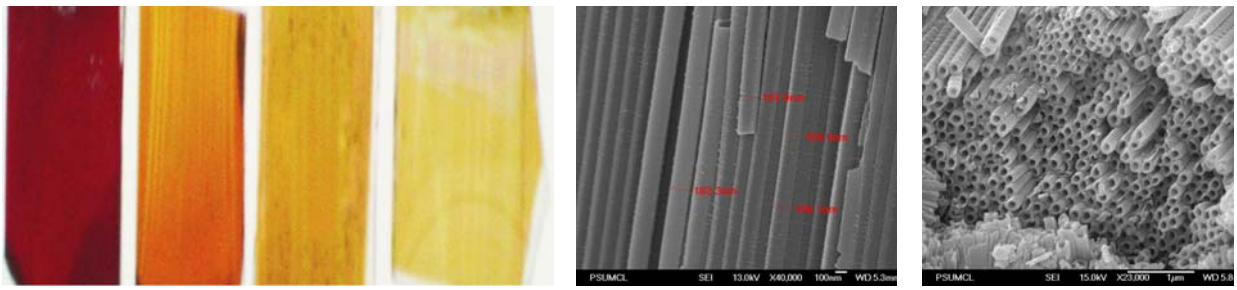

(L) Ti-Fe oxide nanotube array films of varying Ti-Fe composition. (C,R) Vertically oriented, highly ordered nanotube array geometry.

[1] G. K. Mor, K. Shankar, M. Paulose, O. K. Varghese, C. A. Grimes, *Nano Letters*, 2005, **5**, 191.
[2] O.K. Varghese, M. Paulose, K. Shankar, G.K. Mor, C.A. Grimes, *J. Nanosci. Nanotech.,* 2005, **5**, 1158.
[3] M. Paulose, K. Shankar, H. E. Prakasam, O. K. Varghese, G. K. Mor, T. A. LaTempa, A. Fitzgerald, C. A. Grimes, *J. Phys. Chem. B* 2006, **110**, 16179
[4] H. E. Prakasam, O. K. Varghese, M. Paulose, G. K. Mor, C. A. Grimes, *Nanotechnology* 2006, **17**, 4285

SELECTIVE ASSEMBLY OF HETERO-BINUCLEAR UNITS ON THE SURFACE OF NANOPOROUS SILICA

Hongxian Han and Heinz Frei
Physical Biosciences Division, Lawrence Berkeley National Laboratory
Berkeley, CA 94720

Nanoporous oxide materials such as silica are ideal supports for arranging and coupling of inorganic polynuclear photocatalytic sites for multi-electron transfer reactions such as water oxidation or carbon dioxide reduction. Our approach consists of coupling a molecular or well-defined polynuclear catalytic cluster to an all-inorganic binuclear unit on the silica nanopore surface. Metal centers and oxidation states are selected such that the binuclear moiety absorbs in the visible region, and the potentials of the donor and acceptor centers are suitable for driving the desired oxidation or reduction catalysis. In this poster, we will present mild synthetic methods that we have developed in the past two years for the stepwise assembly of binuclear units on silica nanopore surfaces. The methods have allowed us to selectively prepare covalently anchored metal-to-metal charge-transfer chromophores that absorb at photon energies as low as 700 nm and feature metal centers covering a range of redox potentials.

One method exploits the difference in acidity, hence reactivity, of hydroxyl groups of transition metal centers compared to silanol groups of the silica nanopore surface. For the silica material type MCM-41, which has a 1-dimensional channel system (30 Angstrom diameter) the density of SiOH groups on the nanopore surface is between 2 and 3 per nm^2. Reaction of the silanol groups with established organometallic precursors of group 4 metals affords isolated, tripodally anchored Ti or Zr centers featuring TiOH or ZrOH groups. Exposure of TiOH or ZrOH containing silica pore surfaces to non-aqueous solutions of divalent donor metal complexes featuring weakly held CH_3CN ligands (Co^{II}, Mn^{II}, Fe^{II}) results in reaction at the Ti or Zr center at room temperature. Similarly, Ce^{III} precursors react with surface Ti centers with high selectivity. Optical and vibrational spectroscopic analysis indicates preferential formation of oxo-bridged heterobinuclear units over anchoring of isolated metal centers or formation of oxide clusters of the donor metal. We attribute the selectivity to the slightly higher acidity and, therefore, higher reactivity of TiOH or ZrOH groups towards donor metal centers. The higher acidity of these groups compared to SiOH is indicated by a 70 cm^{-1} red shift of the OH stretch mode.

Another synthetic method for binuclear units is based on selective redox reactivity. Examples are the selective attachment of tetrahedral Cr^{VI} centers embedded in the silica pore surface to Ti^{III} or Ir^{III} precursors in non-aqueous solution at room temperature. The coupling is highly selective (no grafting of isolated Ti^{III} centers was detected), which can be rationalized by the redox reactivity of Cr^{VI} ($Cr^{VI} + Ti^{III} \rightarrow Cr^{V} + Ti^{IV}$) compared to the redox inertness of Si. EPR spectroscopy confirms the generation of Cr^{V}, and optical spectroscopy shows the loss of Cr^{VI} and Ti^{III}. The linkage of Ir^{III} to Cr^{VI} centers has similarly been established by EPR, FT-Raman and optical spectroscopy. This is the first step in the assembly of Ir oxide nanoclusters coupled to Cr centers for visible light-driven water oxidation inside the nanopores. Progress in the assembly of $TiOCr^{III}$ units coupled to Ir oxide nanoclusters for achieving water oxidation with a visible binuclear $TiOCr^{III}$ charge transfer pump will be discussed.

TEMPORALLY AND SPATIALLY RESOLVED SOLAR ENERGY FLOW IN PHOTOSYNTHESIS

L. Huang[1,2], G. P. Wiederrecht[1], D. K. Hanson[3], N. Ponomarenko[4], J. R. Norris[4] and D. M. Tiede[2]
Center for Nanoscale Materials[1], Chemistry Division[2], and Biosciences Division[3], Argonne National Laboratory, Argonne, Illinois
Department of Chemistry[4], University of Chicago, Chicago, Illinois

Biological solar energy conversion involves energy transfer processes that span the femtosecond to nanosecond timescales, and involves excitation transfer across a nested hierarchy of chromophores packed within nanometer sized light-harvesting complexes that are in turn organized into variable, quasi-crystalline two dimensional arrays that span hundreds of nanometers. Understanding of short and long-range energy transfer processes in these membranes is crucial for the design of bio-inspired solar cells. Here we will present our preliminary results on directly imaging solar energy flow in photosynthetic architectures with both state-of-the-art time and spatial resolution.

We have performed the first femtosecond time-resolved studies of the primary electron transfer process in single reaction center crystals from wild type strains of *Rhodobacter sphaeroides*. Strong optical dichroism in crystals allowed for selection of individual cofactors within the manifold by polarized excitation and detection. Transient spectra of the crystals exhibit strong polarization dependence and are remarkably different than those in solution. Electron transfer from the bacteriochlorophyll dimer, P, to the bacteriopheophytin acceptor, H, is found to be approximately 2-fold slower in crystals (8 ps) compared to the detergent-solubilized solution state (5 ps). These results will provide opportunities to make direct, quantitative correlation between photosynthetic function and reaction center structure.

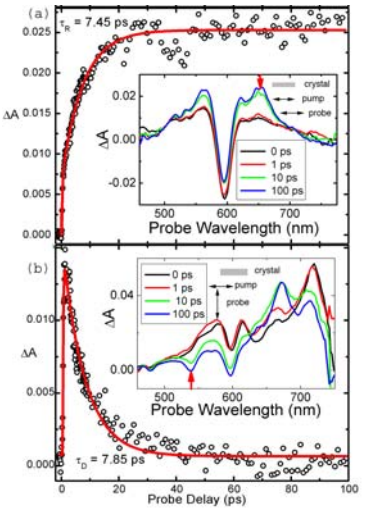

Figure 1: transient absorption spectra (inset) and kinetics of a single RC crystal polarized pump-probe spectroscopy. The polarizations of pump and probe beams are as indicated in the figure. The red arrows in the insets indicate the wavelengths where the kinetics was recorded.

Ultrafast time-resolved spatial imaging of solar energy flow in photosynthetic membranes will be achieved by coupling near-field scanning optical microscope imaging to ultrafast laser excitation and detection. Currently, we have successfully characterized natural membranes by atomic force microscope (AFM), which reveals highly ordered arrays of photosynthetic complexes. This work will ultimately record "snapshots" of energy flow with sub-ps time resolution and 20 nm spatial resolution and directly image distances, timescales, and pathways for solar energy transfer within photosynthetic architectures.

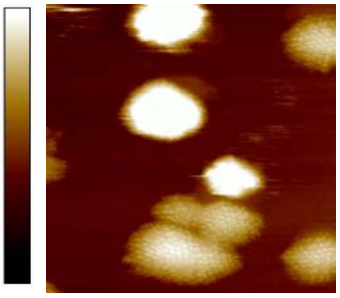

Figure 2: AFM image of *Blastochloris Viridis* membranes. Scan size: 500 nm × 500 nm, full color scale: 30 nm.

PHOTOINITIATED WATER OXIDATION CATALYZED BY RUTHENIUM *cis,cis*--DIAQUADIIMINE μ-OXO DIMERS

Jonathan L. Cape and James K. Hurst
Department of Chemistry
Washington State University
Pullman, WA 99164-4630

Kinetic studies of water oxidation by $[(bpy)_2Ru^{III}(OH_2)]_2O^{4+}$ and structurally related diruthenium ions have usually been made in acidic media using an excess of strong oxidant (e.g., Ce^{4+}, Co^{3+}). Under these conditions, $k_{cat} \approx 10^{-2}$ s^{-1}, which is ~10^4-fold slower than the oxygen-evolving complex (OEC) of photosystem II. This low turnover rate has contributed to the widespread notion that these complexes are ineffective catalysts for water oxidation. However, we find that under neutral conditions (pH 5-9) turnover rates increase by at least 10^2-fold, so that the intrinsic reactivity of the catalytic ions begins to approach that of the OEC. These studies have employed a photocatalytic system initially described by the Grätzel group [Rotzinger, et al., *JACS* **1987**, *109*, 6619], but which had never been quantified. The assumed mechanism is shown in panel a of the accompanying figure, in which we assign **{5,5}** as the O_2-evolving oxidation state of the complex. Rapid oxidation of **{3,3}** through **{3,4}** to a mixture of higher redox states occurs when reactant solutions comprising the sensitizer ($Ru(bpy)_3^{2+}$), oxidant (**{3,3}**), and sacrificial electron acceptor ($S_2O_8^{2-}$) are illuminated (panel b). This spectrum can be deconvoluted to give the steady-state composition of reactive components (panel c), which includes a near-ir band assignable to an hydroxyl-bipyridine adduct. The intensity of this band correlates linearly with the O_2 evolution rate, which is proportionate to the total amount of catalyst present, but independent of the sensitizer concentration. This behavior indicates that the species is a reaction intermediate formed from the catalyst, not an accumulating product. Maximal quantum yields are 40-80% of theoretical limits (panel d). In ongoing studies, we have replaced the sensitizer and electron acceptor components with a pyrylium-based vesicle assembly developed in our lab that is designed when the catalyst is present to drive electroneutral transmembrane reduction of acceptors using water as the electron source.

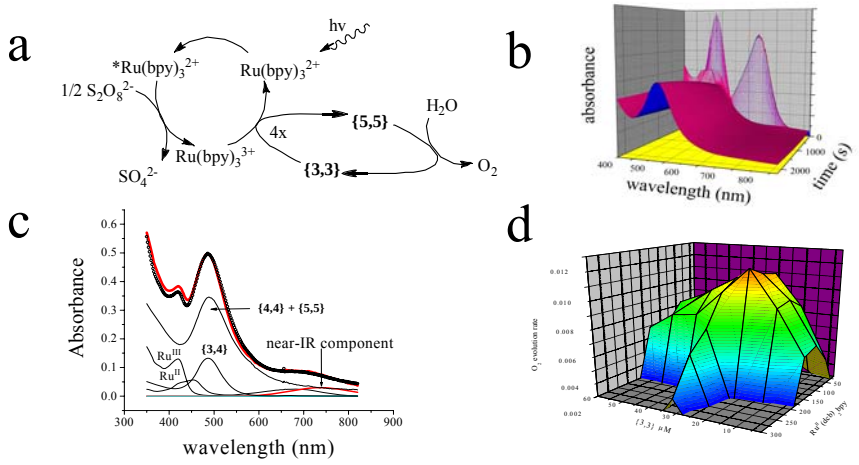

SWCNT-SEMICONDUCTOR ARCHITECTURES FOR PHOTOELECTROCHEMICAL SOLAR CELLS

Prashant V. Kamat and Anusorn Kongkanand
Radiation Laboratory and Department of Chemical & Biomolecular Engineering
University of Notre Dame, Notre Dame, Indiana 46556-0579

A major hurdle in attaining higher photoconversion efficiency in nanostructured semiconductor electrodes is the transport of electrons across the particle network. The photogenerated electrons in a mesoscopic film, for example, have to travel through the network of semiconductor particles and encounter many grain boundaries during the transit. A nanowire or nanotube network if used as a support to anchor semiconductor particles can facilitate the electron transport and further improve light harvesting efficiency (Figure 1). Single wall carbon nanotubes with tailored light harvesting properties can provide new ways to develop next generation solar cells.[1,2]

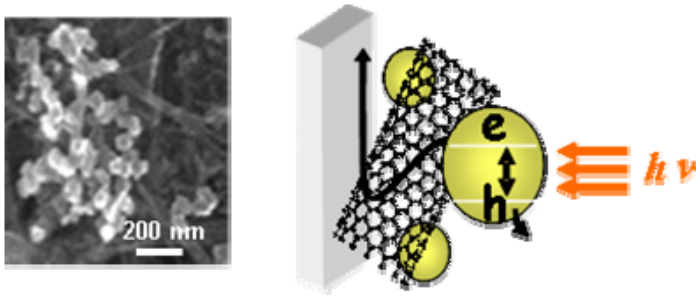

Figure 1. Use of SWCNT network to disperse TiO_2 particles. Left: SEM image of TiO_2 nanoparticles anchored on SWCNT film. Right: A scheme illustrating the principle of charge collection and transport by SWCNT.

By employing single wall carbon nanotube (SWCNT) architecture as conducting scaffolds in TiO_2 semiconductor based photoelectrochemical cell we have now succeeded in boosting the photoconversion efficiency by a factor of two. Titanium dioxide nanoparticles dispersed on single wall carbon nanotube films improved photoinduced charge separation and transport of carriers to the collecting electrode surface. The shift of ~100 mV in apparent Fermi level of the SWCNT-TiO_2 system as compared to the unsupported TiO_2 system indicated Fermi level equilibration between the two systems. Independent charge storage experiments have confirmed the storage of 1 electron per ~32 carbon atoms of the nanotube. The interplay between the TiO_2 and SWCNT in attaining charge equilibration is an important factor for improving photoelectrochemical performance of nanostructured semiconductor based solar cells. Efforts are underway to sensitize SWCNT-TiO_2 composite structures with CdSe quantum dots and dyes.

References:

1. Kamat, P. V. *Meeting the Clean Energy Demand: Nanostructure Architectures for Solar Energy Conversion,* J. Phys. Chem. C, 2007. **111** 2834 – 2860 (Feature Article)
2. Kongkanand, A.; Domínguez, R. M.; Kamat, P. V. *SWCNT Scaffolds for Photoelectrochemical Solar Cells. Capture and Transport of Photogenerated Electrons.*, Nano Lett., 2007. **7** 676-680.

MAGNETIC RESONANCE STUDIES OF PROTON LOSS FROM CAROTENOID RADICAL CATIONS

Lowell D. Kispert[1], A. Ligia Focsan[1], Tatyana A. Konovalova[1], Jesse Lawrence[1], Michael K. Bowman[2], David A. Dixon[1], Peter Molnar[3] and Jozsef Deli[3]
[1]The University of Alabama, Department of Chemistry, Tuscaloosa, AL 35487-0336;
[2]Structural Biology, Pacific Northwest National Lab, Richland, WA 99354;
[3]Department of Biochemistry and Medical Chemistry, University of Pécs, Hungary

Carotenoids, intrinsic components of reaction centers and pigment-protein complexes in photosynthetic membranes, play a photoprotective role and serve as a secondary electron donor. Before optimum use of carotenoids can be made in artificial photosynthetic systems, their robust nature in living materials requires extensive characterization of their electron transfer, radical trapping ability, stability, structure in and on various hosts, and photochemical behavior.

Pulsed ENDOR and 2D-HYSCORE studies combined with DFT calculations reveal that photo-oxidation of natural zeaxanthin **(I)** and violaxanthin **(II)** on silica-alumina produces not only the carotenoid radical cations ($Car^{\bullet+}$) but also neutral radicals (#$Car^{\bullet}$) by proton loss from the methyl groups at positions 5 or 5′, and possibly 9 or 9′ and 13 or 13′. Notably, the proton loss favored in **I** at the 5 position by DFT calculations, is unfavorable in **II** due to the epoxide at the 5, 6 position. DFT calculations predict the isotropic methyl proton couplings of 8-10 MHz for $Car^{\bullet+}$ which agree with the ENDOR for carotenoid π-conjugated radical cations. Large α-proton hyperfine coupling constants (>10 MHz) determined from HYSCORE are assigned from the DFT calculations to neutral carotenoid radicals. Proton loss upon photolysis was also examined as a function of carotenoid polarity [Lycopene **(III)** versus 8′-apo-β-caroten-8′-al **(IV)]**; hydrogen bonding [Lutein (**V**) versus **III]**; host [silica-alumina versus MCM-41 molecular sieve]; and substituted metal in MCM-41.

Loss of H^{+} from the 5(5′), 9(9′) or 13(13′) methyl positions has importance in photoprotection. Photoprotection involves nonphotochemical quenching (NPQ) in which $^{1}Ch1^{*}$ decays via energy transfer to the carotenoid which returns to the ground state by thermal dissipation; or via electron transfer to form a charge transfer state ($\mathbf{I}^{\bullet+\cdots}Chl^{\bullet-}$), lower in energy than $^{1}Chl^{*}$. The formation of $\mathbf{I}^{\bullet+}$ results in bond lengthening, a mechanism for nonradiative energy dissipation. Quenching requires zeaxanthin, a pigment-binding protein PsbS, and low pH in the thylalkoid lumen. Low pH in excess light activates the xanthophyll cycle through the enzyme violaxanthin deepoxidase (VDE) which drives deepoxidation of violaxanthin to zeaxanthin. Also a low thylakoid lumen pH activates binding of zeaxanthin to PsbS by protonating carboxylate chains of VDE and PsbS, facilitating attachment to the membrane and the conversion of violaxanthin to zeaxanthin. The low pH also drives ATP synthesis.

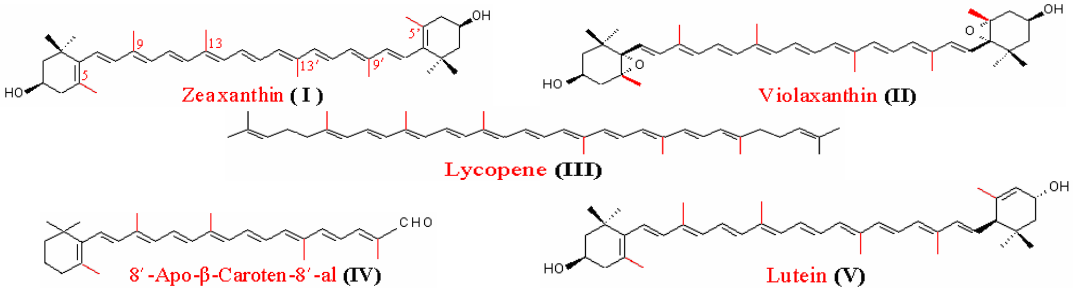

PHOTOPHYSICS OF π-CONJUGATED DENDRIMERS AS DONORS IN ORGANIC DONOR-ACCEPTOR BULK HETEROJUNCTIONS

Nikos Kopidakis, William L. Rance, Muhammet E. Köse, Benjamin Rupert, Jao van de Lagemaat, Sean E. Shaheen and Garry Rumbles

National Renewable Energy Laboratory
1617 Cole Blvd, Golden CO 80401

Bulk heterojunction organic photovoltaic devices are typically based on pi-conjugated polymers as light absorbers and electron donors. However, the presence of intrinsic and extrinsic impurities and the polydisperse nature of polymer samples makes their study at the molecular level difficult. In an effort to understand the photophysics of self-assembled donor-acceptor heterojunctions we have replaced the commonly used polymeric donors with π-conjugated dendrimers that we have synthesized. Dendrimers are soluble molecules that can be synthesized with high purity and monodispersity. The well-defined structure of the dendrimers allows the detailed theoretical understanding of their conformation and properties at the molecular level and makes them advantageous over their polymeric counterparts as model donors for the study of donor-acceptor bulk heterojunctions. We describe the synthesis of a series of phenyl-cored thiophene dendrimers (Figure) and the experimental and theoretical characterization of their optical absorption and emission properties. Time-Resolved Microwave Conductivity and Atomic Force Microscopy measurements in bulk heterojunctions composed of dendrimers with [6,6]-phenyl-C_{60} butyric acid methyl ester (PCBM) show that the rate of recombination of photogenerated carriers correlates to the degree of mixing of the donor and acceptor phase. We discuss how recombination in the bulk heterojunction determines the operating characteristics of complete photovoltaic devices. Finally, we demonstrate that we can further control the conformation and optical absorption properties of dendrimers by adding electron withdrawing groups to the dendrimer core, and investigate what effect that has on the operation of bulk heterojunctions and complete devices.

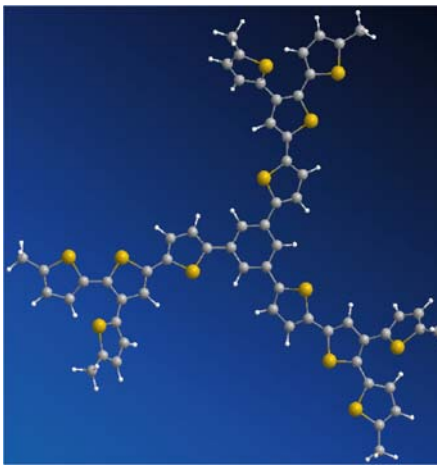

DIRECT MEASUREMENT OF THE FLUORESCENCE QUANTUM YIELD OF INDIVIDUAL SINGLE WALLED CARBON NANOTUBES

Lisa J. Carlson and Todd D. Krauss
Department of Chemistry
University of Rochester
Rochester, New York 14627

Recently, the optical properties of single-walled carbon nanotubes (SWNTs) have been the subject of much interest. Of particular relevance, SWNTs could be attractive as photosensitizers or charge transport materials for applications in photovoltaics. Still, one factor limiting their development has been the absence of an accurate determination of their emissive efficiency. From a fundamental point of view, a molecule's luminescence efficiency is one of its most important photophysical parameters, and often influences whether a system incorporating this molecule is selected for development into a given application.

For an ensemble of nanotubes, the fluorescence quantum yield (QY) is extremely low, typically less than 0.1%. Given that the QY is so low, it is somewhat surprising that fluorescence from individual SWNTs can be detected. Indeed, for a single nanotube suspended in air, recent estimates suggest that the single molecule fluorescence QY is almost two orders of magnitude higher than the ensemble value (~7%). It is clear that a direct and accurate measurement of the fluorescence QY for different nanotube structures (i.e. *(n,m)*) would hold significant fundamental importance and technological relevance.

We will present measurements of the fluorescence QY of single SWNTs, obtained by simultaneously dispersing dilute suspensions of SWNTs and CdTe/ZnS quantum dots (QDs) onto a substrate. Comparisons between the relative fluorescence intensities of the SWNTs and QDs allowed for a direct determination of the SWNT QY given that the QY of single QDs is well defined. We have found that the SWNT QY is ~1± 0.5 %, which is almost two orders of magnitude larger than that determined for an ensemble. The significance of our approach is that we used a straightforward relative quantum yield measurement, as opposed to a very difficult absolute quantum yield measurement. For absolute QY measurements, it is critical to know exactly the amount of excitation received by the sample and difficult to accurately quantify the exact number of photons received by the detector. We will report on whether the measured QY represents an intrinsic property of various nanotube structures, *(n,m)*, or if the QY is influenced by other factors such as the local environment, intertube interactions, and defects.

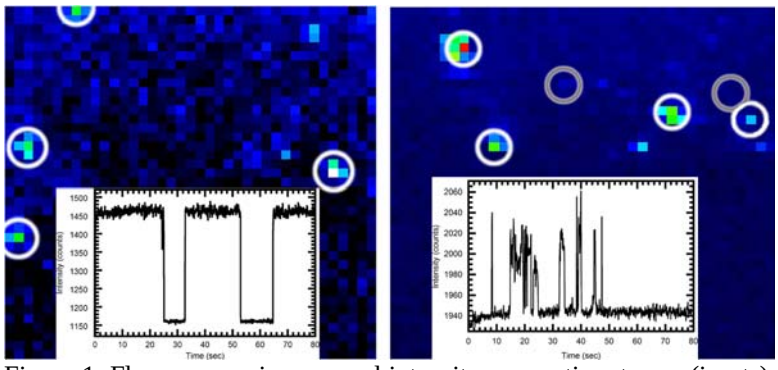

Figure 1. Fluorescence images and intensity versus time traces (insets) from individual SWNTs (left) and CdTe/ZnS QDs (right) co-located on the same substrate. The laser was blocked during the SWNT time trace to produce the "off" intensity periods.

HOLE INJECTION AND TRANSPORT IN DNA

Frederick D. Lewis and Pierre Daublain
Department of Chemistry
Northwestern University
Evanston, IL 60201

The major focus of our research during the current year has been a detailed study of hole injection and hole mobility in capped hairpins possessing stilbenedicarboxamide (SA) electron acceptor and stilbenediether (SD) electron donor separated by a variable number of A-T base pairs (Fig. 1). The integrated application of femtosecond broadband pump-probe spectroscopy, nanosecond transient absorption spectroscopy, and picosecond fluorescence decay measurements permits detailed analysis of the formation and decay of the stilbene acceptor singlet state and of the charge separated intermediates. When the donor and acceptor are separated by either one or two A:T base pairs charge separation occurs via a single step superexchange mechanism. However when the donor and acceptor are separated by three or more A:T base pairs charge separation occurs via a multistep process consisting of hole injection, hole migration, and hole trapping. The rate constant for hole injection is independent of the donor-acceptor distance.

In collaboration with Wasielewski and Cohen, we have determined the time required for hole migration across a stack of A-T base pairs as a function of the length of the stack. Kinetic data are obtained from analysis of the time-dependent change in the transient absorption band shape that results from arrival of the hole at the SD hole trap (Fig. 2). The hole arrival times provide an estimated value for the A-tract hole mobility which is significantly lower than the values for columnar π-stacked discotic materials. The low hole mobilities plausibly result from a combination of weak coupling, static and dynamic disorder, and solvent and ion gating. While our estimated value for the hole mobility is lower than previous estimates, it is still significantly faster than strand cleavage at G-containing sites. The relatively low hole mobility and rapid charge return in our system result in low hole trapping efficiencies in longer A-tracts. Current work is focused on the base sequence-dependence of hole transport dynamics and efficiency.

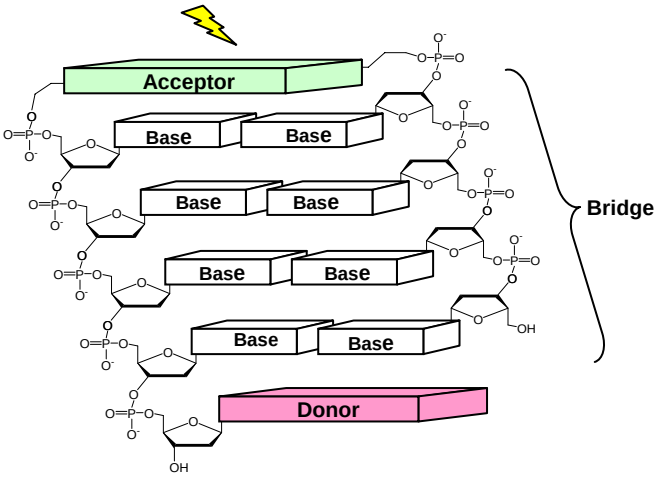

Fig 1. Capped hairpin with hole acceptor and donor separated by four base pairs.

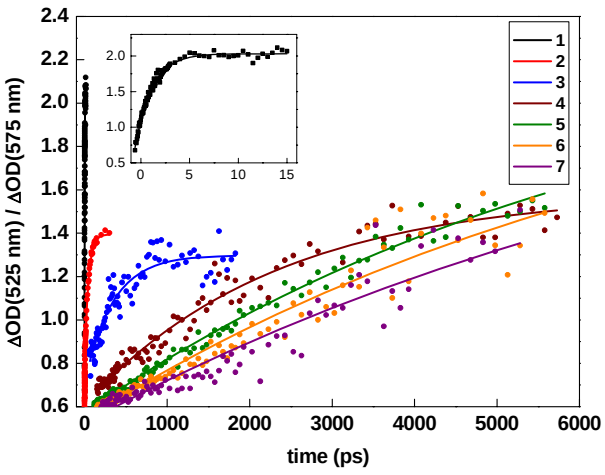

Fig 2. Time-dependent rise in the 525/575 nm band intensity ratios for capped hairpins possessing 1-7 base pairs.

DEPENDENCE OF INTERFACIAL ELECTRON INJECTION RATE ON SOLVENT, ANCHORING GROUP AND SEMICONDUCTOR

Jianchang Guo, Chunxing She, Dave Stockwell, Jier Huang, Baohua Wu, Tianquan Lian
Department of Chemistry
Emory University
Atlanta, GA 30322

Aside from fundamental interest, understanding factors that control interfacial ET is also essential in designing and improving devices that based on semiconductor nanomaterials such as dye-sensitized solar cells. In this paper, we describe our recent investigation of the dependence of injection rates on the solvent environment, anchoring group and the nature of the semiconductor. We will also report the progress in developing vibrational sum-frequency generation spectroscopy as a way to probe adsorbate anchoring geometry and interfacial ET dynamics.

Solvent dependence of interfacial electron transfer. The solvent dependence of interfacial ET was studied by comparing ET rates in dye sensitized TiO_2 nanocrystalline films in different solvent environments. Photoinduced ET rates from $Re(L_A)(CO)_3Cl$ [L_A = dcbpy = 4,4`-dicarboxy-2,2`-bipyridine] **(ReC1A)** to TiO_2 nanocrystalline thin films in air, pH buffer, MeOH, EtOH, and DMF were noticeably different. Origins for the observed difference will be discussed.

Anchoring group dependence. The effects of anchoring groups on electron injection from adsorbate to nanocrystalline thin films were investigated by comparing injection kinetics through carboxylate vs. phosphonate groups to TiO_2 and SnO_2. In the first pair of molecules, ReC1A and ReC1P, the anchoring groups were insulated from the bipyridine ligand by a CH_2 group. Faster injection through the PO_3H_2 than COOH was observed. In the second pair of molecules, $Ru(dcbpyH_2)_2(NCS)_2$ (N3) and $Ru(bpbpyH_2)_2(NCS)_2$ (N3P), [dcbpy = 2,2'-bipyridine-4,4'-biscarboxylic acid, bpbpy = 2,2'-bipyridine-4,4'-bisphosphonic acid], the anchoring groups were directly connected to the bipyridine ligands. The injection rates from N3 and N3P to SnO_2 films were similar. On TiO_2, the injection kinetics from RuN3 and RuN3P were biphasic: carboxylate group enhances the rate of the < 100fs component, but reduces the rate of the slower components. Computational studies of the model complexes were also carried to provide insight into the apparent different effects of anchoring groups in these systems.

Semiconductor dependence. One of the most interesting aspects of interfacial ET is its dependence on the nature of semiconductors. Previous comparison of injection rates to TiO_2, Nb_2O_5, and SnO2, ZnO suggests that the density of conduction band states (DOS) plays an important role in controlling these rates. We have extended similar comparison of injection dynamics to SnO_2 and In_2O_3, which have similar band edge position and DOS. We found that the injection rate to SnO_2 and In_2O_3 were similar for both N3 and Rhodamine B. These results suggest the dominating role of DOS in controlling ET rate. Further comparisons with other dyes are underway.

ULTRAFAST PHOTOPHYSICS OF GROUP 8 METAL COMPLEXES: IMPLICATIONS FOR THEIR USE IN DYE-SENSITIZED SOLAR CELLS

Amanda L. Smeigh, Allison Brown, and James K. McCusker*
Department of Chemistry
Michigan State University
East Lansing, MI 48824

The introduction of the Grätzel Cell has reignited interest in the development of cheaper, more efficient solar energy conversion schemes based on sensitized semiconductors. In spite of considerable effort by a large number of groups around the world, the performance characteristics of these devices still falls short of the cost/efficiency ratio necessary for it to be economically competitive with carbon-intensive technologies. Our research is geared toward developing an alternate approach to this class of solar cells, specifically the feasibility of utilizing first-row transition metal complexes as sensitizers for Grätzel cells.

The project is being developed in three stages: (1) studies of the intrinsic photophysics of target chromophores as it pertains to light capture and interfacial electron transfer; (2) studies of the electron transfer dynamics associated with TiO_2 nanoparticles employing these chromophores as sensitizers; and (3) the development of functional solar cells using first-row metal complexes. Studies by Ferrere and Gregg indicated the production of photocurrent from solar cells sensitized by $Fe(dcbpy)_2(CN)_2$; this, coupled with the fact that Fe(II) is isoelectronic with the Ru(II)-based sensitizers currently employed, compelled us to focus our initial efforts on Fe(II) polypyridyl complexes. Previous work from our group indicated rapid deactivation of the charge-transfer states of this class of compounds. We have now generalized this result across a number of different Fe(II) polypyridyl systems. By combining time-resolved absorption spectroscopy with various steady-state measurements, we have been able to definitively show that deactivation of the charge-transfer manifold occurs on a sub-100 fs time scale (Figure 1); data on Cr(III) compounds suggests that this phenomenon may be general for charge-transfer chromophores of the first transition series. This stands in stark contrast to the behavior of analogous Ru(II) and Os(II) chromophores and underscores the significant impact of low-lying electronic states on the ultrafast dynamics of these compounds. Since population of the charge-transfer state is deemed to be critical for electronic injection into the conduction band of TiO_2, the ultrafast deactivation of charge-transfer states represents a significant hurdle that must be overcome in order to realize the use of first-row compounds in this technology.

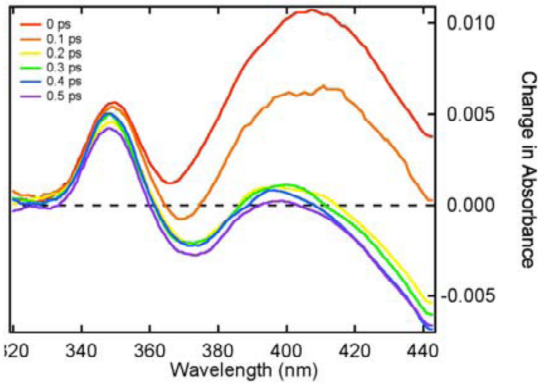

Figure 1. Time-resolved absorption data for $[Fe(terpy)_2]^{2+}$ in CH_3CN solution following ~100 fs excitation into the $^1A_1 \rightarrow {}^1$MLCT absorption at 560 nm. The strong absorption at 405 nm is due to the initially formed MLCT state; its rapid decay to a ligand-field state represents a critically important process in the excited-state dynamics of these compounds in terms of their application to solar energy conversion schemes.

UNIDIRECTIONAL CHARGE TRANSFER FOR ENERGY CONVERSION*

Dan Meisel, [1] T. Sehayek, [2] A. Vaskevich, [2] I. Rubinstein [2]

[1]Radiation Laboratory and Department of Chemistry & Biochemistry, University of Notre Dame, Notre Dame, IN 46556; [2] Department of Materials and Interfaces, Weizmann Institute of Science, Rehovot, 76100 Israel.

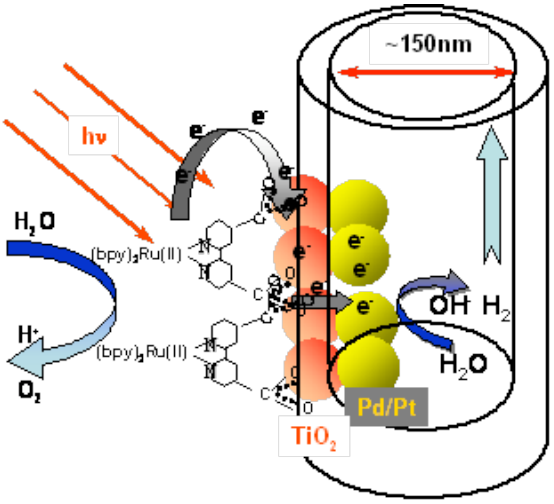

Scheme 1: Schematic presentation of the proposed configuration to achieve photo-induced unidirectional flow of charges. A sensitizing dye is attached exclusively to the external walls of a TiO_2 nanotube, which is internally coated with a nanotube of metallic nanoparticles that serve as the catalyst for hydrogen evolution.

The need to control the direction of the flow of photo-induced redox events, from the initial separation of the electron-hole pair all the way to the final products stage, H_2 and O_2 in the case of water splitting, has been recognized for a long time. Whereas great advances have been made in the initial charge separation stage, not much has been realized in the separation of the products at the later stages. We recently proposed a scheme that could potentially provide unidirectional flow of the photo-induced charge carriers and, in principle at least, maintain the separation to the final redox products. This strategy is outlined in Scheme 1.

Our approach utilizes templates of anodized aluminum as the scaffold to hold the various components during the synthesis of the structure. It relies on the recent demonstration by our collaborators* of the construction of metallic-nanoparticle nanotubes within the template. In the present system we deposit a layer of TiO_2 onto the template followed by a layer of metallic nanoparticles (Figure 1). Sensitizers are then attached exclusively to the outer walls of the TiO_2 layer, following dissolution of the template. Synthesis of every component in this structure has been reported in the literature and binding of each component to its neighboring layer has been demonstrated, but the complete system was not considered in the past. We have already synthesized the complete arrangement and are now studying the photochemistry and photophysics of the system.

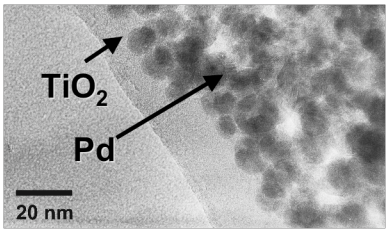

Figure 1: TiO_2 nanotube with attached Pd particles at the tube's internal wall. The Al_2O_3 template has already been dissolved.

* This collaboration is partially supported by the US-Israel Binational Science Foundation.

ELECTRON TRANSFER DYNAMICS IN EFFICIENT MOLECULAR SOLAR CELLS

Aaron Staniscewski and Gerald J. Meyer
Departments of Chemistry and Materials Science and Engineering,
Johns Hopkins University
Baltimore, MD 21218

The realization that photo-induced interfacial electron transfer occurs on ultrafast time scales opens up new opportunities for solar energy conversion. We have recently shown that sensitized ultrafast electron injection into anatase TiO_2 nanocrystals can be used to drive redox reactions that would be thermodynamically uphill from the thermally equilibrated excited state of the sensitizer.[1] The proposed mechanism for this is shown schematically and represents a molecular approach to exceeding the Shockley-Queisser limit.[2]

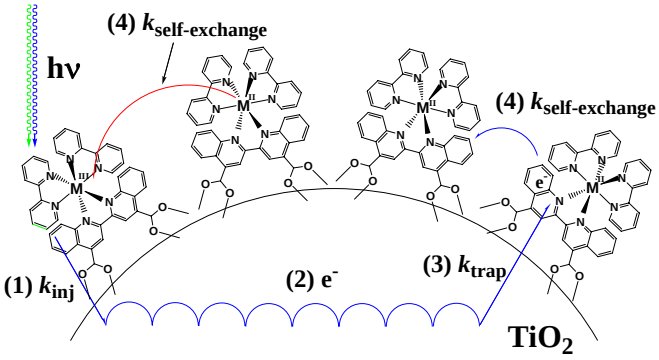

More specifically, nanocrystalline mesoporous TiO_2 thin films were functionalized with $[Ru(bpy)_2(deebq)](PF_6)_2$, $[Ru(bq)_2deeb](PF_6)_2$, $[Ru(deebq)_2bpy](PF_6)_2$, $[Ru(bpy)(deebq)(NCS)_2]$ or $[Os(bpy)_2(deebq)](PF_6)_2$, where bpy is 2,2'-bipyridine and deebq is 4,4'-diethylester-2,2'-biquinoline. These compounds bind to the nanocrystalline TiO_2 films in their carboxylate forms with limiting surface coverages of 8 ($\pm$ 2) x 10^{-8} mol/cm^2. Electrochemical measurements showed that reduction of the coordinated biquinoline ligand (-0.70 V vs SCE) occurred prior to reduction of the TiO_2 nanocrystals. Steady state illumination in the presence of the sacrificial electron donors (such as triethylamine) led to the appearance of the reduced sensitizer. The thermally equilibrated metal-to-ligand charge-transfer (MLCT) excited state and the reduced form of these compounds did not inject electrons into TiO_2. Nanosecond transient absorption measurements demonstrate the formation of an extremely long-lived charge separated state based on equal concentrations of the reduced and oxidized sensitizers. The results are consistent with the mechanism shown schematically where (1) ultrafast excited state injection into TiO_2 is followed transport (2) and interfacial electron transfer (3) to a ground state compound. The quantum yields for this process were found to increase with excitation energy, behavior attributed to stronger overlap between the excited sensitizer and the semiconductor acceptor states. For example, the quantum yields for $Os(bpy)_2dcbq/TiO_2$ were ϕ(417 nm) = 0.18 $\pm$ 0.02, ϕ(532.5 nm) = 0.08 $\pm$ 0.02, and ϕ(683 nm) = 0.05 $\pm$ 0.01. Electron transfer to yield ground state products occurs by lateral intermolecular self-exchange reactions (4). Chronoabsorption measurements indicate that ligand-based reductions were about three orders of magnitude faster than metal-centered intermolecular hole transfer. The conduction band is proposed to mediate the electron transfer reactions. Charge recombination was well described by the Kohlrausch-Williams-Watts model. The generality of these findings will be discussed.

1. Hoertz, P.G.; Staniszewski, A.; Marton, A; Higgins, G.T.; Incarvito, C.D.; Rheingold, A.L.; Meyer, G.J. *J. Am. Chem. Soc.* **2006**, *128*, 8234. 2. Shockley, W.; Queisser, H.J. *J. Appl. Phys.* **1961**, *32*, 510.

PROTON COUPLED ELECTRON TRANSFER (PCET) IN THE OXYGEN EVOLVING COMPLEX (OEC) OF PHOTOSYSTEM II. "WIRED FOR PROTONS"

My Hang Huynh, John Papanikolas, Holden Thorp, and Thomas J.Meyer
Department of Chemistry
University of North Carolina at Chapel Hill
Chapel Hill, NC, 27599-3290

We, and all higher life forms, use oxygen and respiration as our primary energy source. The oxygen comes from water by solar energy conversion in photosynthetic membranes. In green plants, light absorption in Photosystem II (PSII) drives electron transfer activation of the Oxygen Evolving Complex (OEC) where oxygen is evolved. Recent XRD to 3.0 Å resolution and EXAFS measurements have given molecular level insight into structure with a fragment of the $CaMn_4$ cluster in the S_1 state of the Kok cycle illustrated below. We have proposed a model in which PCET and coupled electron-proton transfer (EPT) play major roles in oxidative activation of the OEC. It involves aspartates 61 and 170 and coordinated water molecules, shown but not seen in the structure.

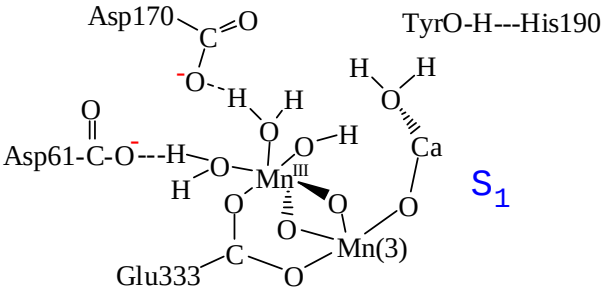

Oxidative activation is initiated by oxidation of tyrosine Y_Z by photoproduced reaction center oxidant P_{680}^+, eq 1. This reaction appears to occur by Multiple Site-Electron Proton Transfer (MS-EPT) with electron transfer to P_{680}^+ and proton transfer to histidine190. MS-EPT is further utilized in oxidative activation of the OEC, eq 2. Subsequently: i) the proton at Asp61 is lost to the lumen through a proton exit channel, and, ii) intra-coordination sphere proton transfer resets the EPT interface at Asp61 giving S_1. Repetition and related cycles build up oxidative equivalents. At the S_3 stage, with three oxidative equivalents stored as $Mn^{IV}(3)Mn^{IV}$, water oxidation occurs by O---O coupling, $Ca\text{-}OH\text{---}O{=}Mn^{IV}Mn^{IV}(3) \xrightarrow{+H_2O} Ca\text{-}OH_2,HOO\text{-}Mn^{III}Mn^{III}(3)$. The intermediate peroxide undergoes further oxidation to $Mn^{III}(O_2^{-\cdot})$ in S_4, which does not build up, finally releasing O_2, $Mn^{III}(O_2^{-\cdot}) \xrightarrow{+H_2O} Mn\text{-}OH_2 + O_2$.

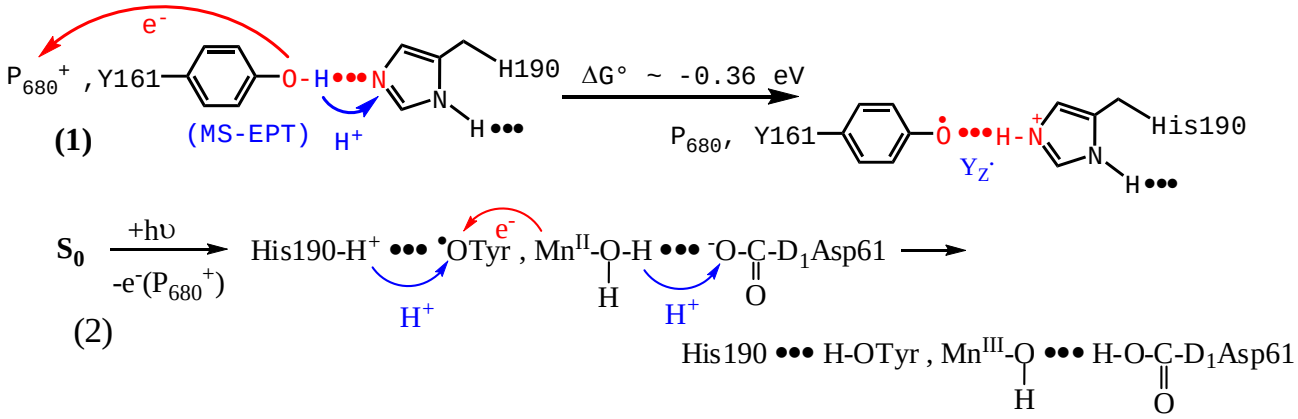

In our model the OEC is an intricate structure that is "wired for protons.

EXCITED STATES OF MOLECULES AND RADICAL IONS

Andrew R. Cook, Sean McIlroy Sadayuki Asaoka and John R. Miller
Chemistry Department
Brookhaven National Laboratory
Upton, New York 11973

Excited singlet states of molecules play an essential role in light-driven energy storage. In addition to fluorescence a valuable property of an excited state is its $S_1 \rightarrow S_n$ absorption spectrum. These bands are useful for investigations of ultrafast charge transfer driven from the excited states and they may contain information about the excitonic nature of those excited states. $S_1 \rightarrow S_n$ transitions were reported for several small molecules in the 1970s; recent interest has focused on materials that can comprise new types of solar cells, including conjugated polymers, which are the essential ingredient in "plastic solar."

Figure 1 shows transient $S_1 \rightarrow S_n$ absorption (blue) for poly(9,9-dihexyl)fluorene in THF solution. The $S_1 \rightarrow S_n$ state has an intense maximum at 780 nm. The spectrum also includes a near infrared band, which appears to be similarly intense, but that band system is not fully observed in the present experiments. Observation of depletion of the ground state absorption, shown in the two insets, aids in, but does not enable complete characterization of extinction coefficients and other quantitative aspects. The well-known $T_1 \rightarrow T_n$ (green) absorption at 760 nm is formed in low quantum yield by intersystem crossing, accounting for its smaller intensity. The $T_1 \rightarrow T_n$ spectrum lacks the near infrared bands seen in the S_1 absorption. The reason for this difference is not yet clear, but the difference could arise if the NIR bands of S_1 involve excitation to charge transfer states.

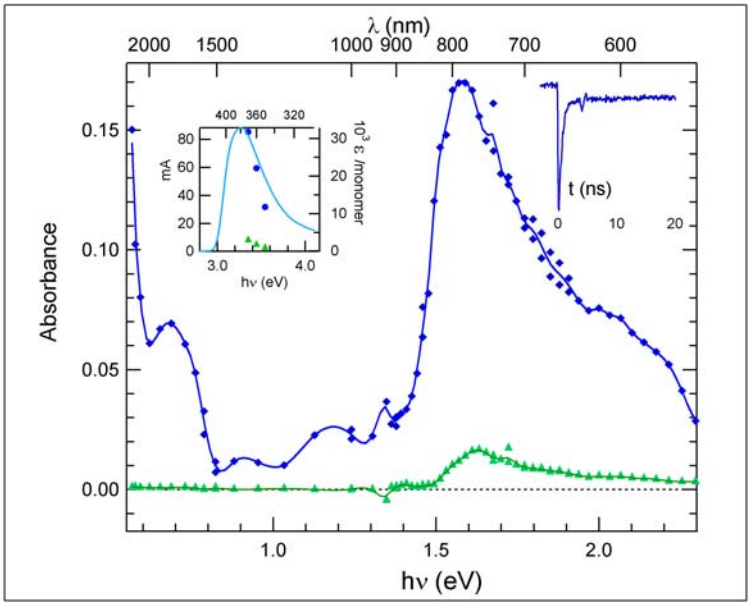

Figure 1 Transient absorption spectra of poly(dihexyl)fluorene in THF: $S_1 \rightarrow S_n$ (◆ τ=0.6 ns) and $T_1 \rightarrow T_n$ (▲). The left inset shows bleaches of the ground state upon formation of S_1 or T_1: the right inset a trace of transient bleaching at 370 nm.

The poster will present similar observations on polythiophene, for which the principal $S_1 \rightarrow S_n$ absorption is further to the red, but for which the low-energy NIR band is not present. Also shown will be spectra for smaller molecules that behave similarly. In each case comparison of the bands of the neutral ($S_0 \rightarrow S_1$, $S_1 \rightarrow S_n$ and $T_1 \rightarrow T_n$) to those of the radical anions and cations will provide insights about the nature of the excited states.

HANGMAN PLATFORMS FOR HYDROGEN AND OXYGEN GENERATION

Daniel G. Nocera

Department of Chemistry
Massachusetts Institute of Technology
Cambridge, MA 02139

Our interest in developing proton coupled electron transfer (PCET) as a mechanism for bond-making and bond-breaking reactions has led us to synthesize and study a series of ligand constructs that poise an acid-base functionality over a redox active metal platform. These "Hangman" ligands utilize the acid-base functionality to form a secondary coordination sphere that can assist proton movement and facilitate substrate assembly within the molecular cleft. We have synthesized both porphyrin and salen "Hangman" systems for oxygen and hydrogen generation.

Key components of oxygen generation are: (1) assembly of water molecules at a redox cofactor by controlling the secondary coordination sphere; (2) activation of water by proton-coupled electron transfer (PCET); (3) the generation of a ferryl proximate to a hydroxide in a controlled microenvironment; (4) oxygen-oxygen bond formation. We have demonstrated (1) – (3) for porphyrin and salen Hangman constructs. Shown below is the graphical juxtaposition of the structurally characterized hydrogen-bonded water channel of P450 (left) and an monomeric iron(III) Hangman heme model system (right). The pendant carboxylic acid of the Hangman system plays a role analogous role of the distal threonine of the enzymatic system, which acts to pre-organize the bound water molecule within the enzymatic-heme cleft.

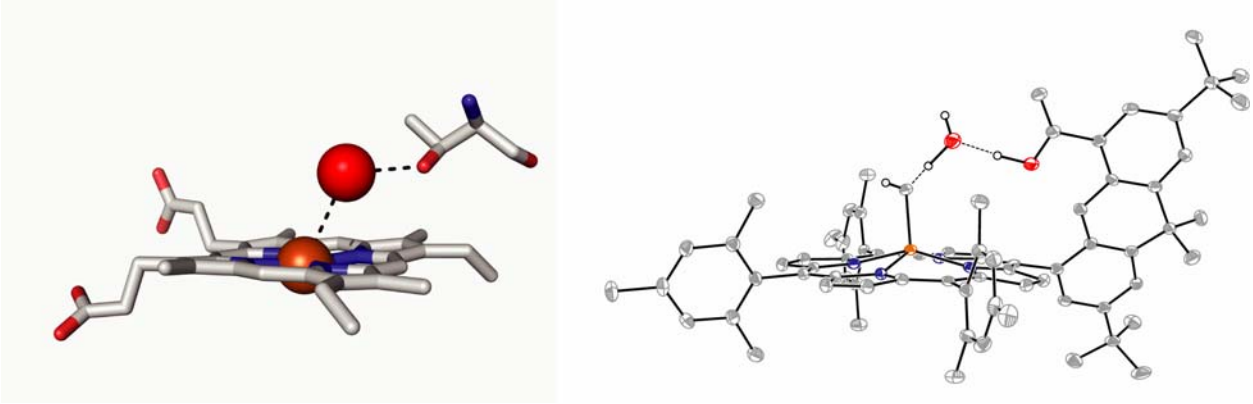

On such Hangman platforms, we have generated the high-valent metal oxo needed for O—O bond coupling. These results will be presented. Strategies to make the oxo electrophilic, and hence more susceptible to nucleophilic attack by hydroxide, step (4), will also be discussed.

Hydrogen generation from Hangman platforms may be achieved by replacing the central metal of the salen or macrocyclic platform with one that can support a hydride. In this case, the hanging group function is to deliver a proton to the hydride, to generate hydrogen. Preliminary results show that the Hangman approach may indeed be exploited for H_2 generation. This preliminary work will be presented and the approach will be generalized to other macrocycle platforms.

INVESTIGATION OF REDOX CENTERS IN GENETICALLY MODIFIED *BLASTOCHLORIS VIRIDIS* REACTION CENTERS

Nina S. Ponomarenko[‡], Oleg G. Poluektov[*], Liang Li[‡], Edward J. Bylina[‖], Rustem Ismagilov[‡], and James R. Norris, Jr.[‡]

[‡]Department of Chemistry
University of Chicago
5735 S. Ellis Avenue
Chicago, IL 60637

[*]Chemistry Division
Argonne National Laboratory
9700 S. Cass Avenue
Argonne, IL 60439

[‖]KAIROS Scientific
10225 Barnes Canyon Road
San Diego, CA 92121.

The reaction centers of *Blastochloris viridis* contain four protein subunits, L–, M–, H– and a cytochrome and constitute a multi component natural molecular wire. To facilitate redox manipulation of this sophisticated electron transport system, oligonucleotide–mediated mutagenesis has been employed to produce two symmetry–related mutants of *B. viridis*. Histidine residues associated with the central Mg^{2+} ions of the two bacteriochlorophylls of the special pair electron donor (His–L173 or His–M200) have been replaced with leucine, resulting in bacteriochlorophyll/bacteriopheophytin L– or M–heterodimers with significantly modified redox potentials. The hemes of the bound cytochrome subunits exhibit new spectroscopic details as characterized by EPR (see Figure 1) and visible absorption spectroscopy. The effects of the amino acid replacements on the optical and EPR properties of the L– and M–mutated reaction centers are similar but different from those of the wild type (WT) strain. To provide the required means for unraveling the complicated spectra associated with the electron transport system of the mutants and WT reaction centers (RCs), X-ray structures determined from single crystals of the WT and M–mutant RCs have been obtained. The availability of single crystals with structures at atomic resolution makes possible a detailed investigation of how these natural molecular wires function.

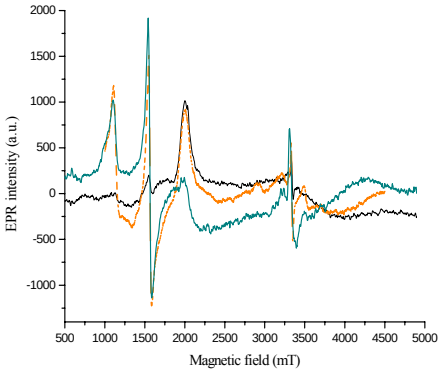

Figure 1.

Low temperature EPR spectra of hemes of *B. viridis* heterodimer mutants
—— WT
—— M
—— L

SOLAR PHOTOCONVERSION EFFICIENCY WITH MULTIPLE EXCITON GENERATION

Mark Hanna and A.J. Nozik
National Renewable Energy Laboratory
Golden, CO 80401

We calculate[1] the maximum power conversion efficiency for conversion of solar radiation to electrical power or to a flux of chemical free energy for the case of hydrogen production from water photoelectrolysis. We consider new types of ideal absorbers where absorption of one photon can produce more than one electron-hole pair that are based upon semiconductor quantum dots with efficient multiple exciton generation (MEG) or molecules that undergo efficient singlet fission (SF). Using a detailed balance model with one sun AM1.5G illumination, we find that for single-gap photovoltaic (PV) devices the maximum efficiency increases from 33.7% for cells with no carrier multiplication to 44.4% for cells with carrier multiplication. We also find that the maximum efficiency of an ideal two-gap tandem PV device increases from 45.7% to 47.7% when carrier multiplication absorbers are used in the top and bottom cells. For an ideal water electrolysis two-gap tandem device, the maximum conversion efficiency is 46.0% using a SF top cell and a MEG bottom cell versus 40.0% for top and bottom cell absorbers with no carrier multiplication. We also consider absorbers with less than ideal MEG quantum yields as are observed experimentally.

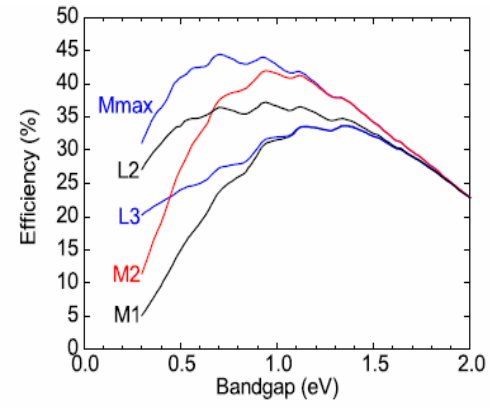

Figure 1. Power conversion efficiencies for cells with a single QD photoconverter vs its bandgap (HOMO-LUMO). Curves labeled M1 and M2 are for multiplication factors resulting from MEG of 1 (none) and 2, respectively, for ideal QD solar cells. Curves labeled L are for results from experimental data with photon energy thresholds at 2Eg and 3Eg.

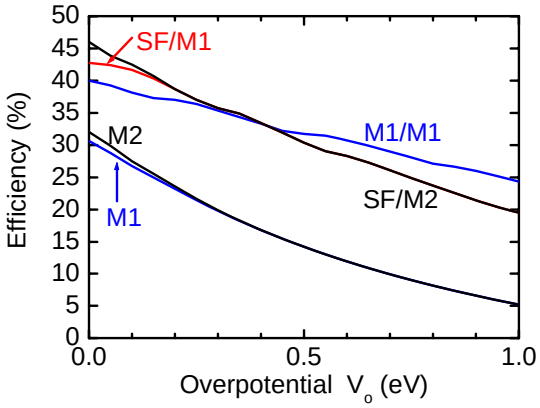

Figure 2. Photoelectrolysis water splitting efficiency vs cell overpotential for a single photoelectrode cell (bottom curve) and for a cell with two photoelectrodes (top curve). The lablkes of M1 and M2 are as previously defined. SF refers to photoelectrodes undergoing singlet fission.

References

1. M.C. Hanna and A.J. Nozik, *J. Appl. Phys.* ***100***, 074510 (2006)

ULTRAFAST KERR-GATED FLUORESCENCE MICROSCOPY

Lars Gundlach and Piotr Piotrowiak
Department of Chemistry
Rutgers University
Newark, New Jersey 07102

Single-molecule (SM) and single nanoparticle spectroscopy provides insights into hidden inhomogeneities and complex distributions that are not discernible in ensemble measurements yet are often crucial in determining the overall behavior of the system of interest. Among the various techniques, time-resolved single-molecule microscopy is especially powerful as it allows one to probe the spatial, temporal and spectral inhomogeneities. At present, its most common implementation, the scanning confocal time correlated single photon counting (TCSPC) microscopy is limited to monitoring one object at a time with maximum resolution of 20 ps. In the wide-field epifluorescence mode the temporal resolution is achieved by the use of intensified CCD cameras and is currently limited to 80 ps. Advanced scanning streak cameras can produce 2D images with time resolution of 20 ps, at a cost that is prohibitive to most individual laboratories. In order to bridge the time domains accessible to ultrafast pump-probe techniques in the bulk and to single molecule fluorescence microscopy, we are constructing a Kerr-gated microscope capable of collecting nearly diffraction limited 2D fluorescence images of sensitized films, nanowires and molecules with sub-100 fs time resolution, *i.e.* at least 100-times better than the current limit.

The core of the approach is simple and involves the insertion of a non-linear optical Kerr gate into the output pathway of an infinity-corrected wide-field microscope. Kerr gating relies on transient birefringence induced by a light pulse in a nonlinear medium placed between crossed polarizers. The collected emission light can pass through the Kerr shutter only when the gating pulse is incident upon the Kerr medium. The transmitted light is detected by a CCD camera, resulting in nearly single photon sensitivity. By delaying the gating pulse with respect to the excitation pulse in the same fashion as in pump-probe experiments, the time evolution of the imaged object, $I(x,y;t)$, can be followed and the corresponding emission decays can be assembled. In addition to the dramatically improved temporal resolution, the wide-field design allows simultaneous tracking of several emitters and fluorescence lifetime imaging (FLIM) of heterogeneous surfaces such as wide-wide bandgap semiconductors films and polymers. The microscope can be also configured in a spectrally dispersed mode and function as an ultrafast fluorescence spectrometer. Preliminary results demonstrating the performance of the instrument in both the imaging and spectrally resolved modes will be shown. The current FWHM time resolution obtained with 20 fs excitation and 70 fs gate pulses while employing fused silica as the Kerr medium is 110 fs.

Fig. 1. The complete Kerr-gate assembly consisting of two Cassegrainian objectives, liquid Kerr medium (benzene), polarizers and the injection mirror.

PROTEIN REGULATION OF THE ELECTRON TRANSFER PROPERTIES IN PHOTOSYNTHESIS

Lisa Utschig[*], Sergey Chemerisov[*], Gerd Kothe[‡], Dave Tiede[*], and Oleg Poluektov[*]
[*]Chemistry Division
Argonne National Laboratory
Argonne, IL 60439
[‡]Department of Physical Chemistry
University of Freiburg
Freiburg, D-79104 Germany

The natural photosynthetic system is an elaborate, highly efficient nano-scale biological machine that carries out solar energy conversion. Although structures for several photosynthetic reaction center (RC) proteins have been determined and the key features of photosynthetic electron transfer are broadly understood, important details of how the synergy between the cofactors and the surrounding protein optimizes electron transfer (ET) reactions have yet to be resolved. It is well established that protein conformational changes play a vital role in biological ET. In the purple bacterial RC, the terminal $Q_A^-Q_B \rightarrow Q_AQ_B^-$ electron transfer is a conformationally gated reaction. The nature of the gate remains unclear. We have recently developed high-frequency (HF) time-resolved (TR) EPR spectroscopic methods that allow us to obtain high quality data on the orientation and distances between active ET cofactors as well as structural information on local protein environments surrounding the cofactors. Results from these HF experiments show that movement of Q_B from the "proximal" to the "distal" site is not a gate for interquinone ET. Interestingly, HF TR EPR spectroscopy predicts a structure for the active Q_A^- site that differs from the geometry determined from X-ray crystallography (Figure 1).

A plausible explanation for this discrepancy is that the quinone geometry obtained from EPR reflects an "active," charge accommodated state of protein and the geometry derived from the crystal structure represents an "inactive" state. Thus, rotation of the quinone is the conformational gate. One concern with this explanation is the possibility that substantial radiation damage to the crystals occurs during X-ray diffraction data collection, resulting in a quinone structure that is irrelevant to the function of the RCs. To check this hypothesis, we are systematically studying the effects of radiation damage to Fe-removed/Zn-replaced RC crystals using HF (130 GHz) EPR spectroscopy. We observe that photolytic activity of the crystals decays at doses at least one order of magnitude lower than doses that result in the accumulation of radical centers and loss of the crystal diffraction ability. Radiation damage first leads to the breaking of bonds in the protein environment and reduction of ET cofactors. Why activity of the crystals is lost long before considerable accumulation of radical species is unclear. Further studies of this issue will provide insight into the role of protein environments in regulating natural photosynthetic ET reactions.

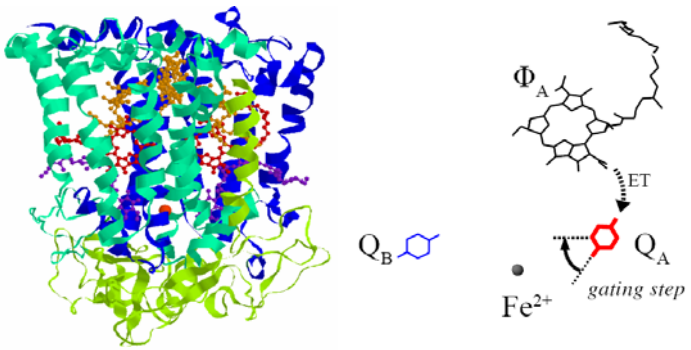

Figure 1. Structure of the photosynthetic protein and the possible conformational gate for ET process.

Ru NAPHTHYRIDYL-PYRIDINE COMPLEXES AS CATALYSTS FOR WATER OXIDATION

Dmitry E. Polyansky,[a] Etsuko Fujita,[a] James T. Muckerman[a] and Randolph Thummel[b]
[a] Chemistry Department, Brookhaven National Laboratory, Upton, NY 11973-5000
[b] Department of Chemistry, University of Houston, Houston, TX 77204-5003

Binuclear trans-[Ru_2(3,6-bis-[6′-(1″,8″-naphthyrid-2″-yl)-pyrid-2′-yl]pyridazine)(4-X-py)$_4$Cl]$(PF_6)_3$ (X= Me, CF_3, Me_2N) and their mononuclear analogs efficiently oxidize water upon treatment with aqueous acidic Ce(IV) solutions. However the mechanism of water oxidation by these complexes is unknown. We have explored water oxidation reactions using different oxidizing reagents (including $[IrCl_6]^{2-}$, $[Ru(bpy)_3]^{3+}$ and Ce(IV) and found that oxygen evolution was observed only with the strong oxidant Ce(IV) (1.35 V vs. SCE). Isotope labeling experiments indicated that water was the only source of evolved oxygen. Electrochemical studies indicate that the first one-electron oxidation is coupled to a proton transfer from the bound water. The one-electron oxidized species $[Ru^{III}(NPM)(OH)]^{2+}$ was observed in pulse radiolysis experiments after oxidation of the starting material with $CO_3^{\bullet-}$ or $[SCN]_2^{\bullet-}$ radicals. The measured UV-vis spectrum matched well the TD-DFT calculated spectrum of $[Ru^{III}(NPM)(OH)]^{2+}$. The two-electron oxidized species $[Ru^{IV}(NPM)(O)]^{2+}$ was produced radiolytically with an excess of $CO_3^{\bullet-}$ radical. Again, good agreement between TD-DFT calculated and experimental spectra was observed. Spin density analysis of DFT calculated structures suggests radical character both on the Ru and O (or OH) centers in $[Ru^{III}(NPM)(OH)]^{2+}$ and $[Ru^{IV}(NPM)(O)]^{2+}$. This radical character of the oxidized species explains their unstable nature, implying the necessity of transient techniques for following the oxidation reactions. In particular, the $[Ru^{III}(NPM)(OH)]^{2+}$ species produced in pulse radiolysis experiments decomposed back to starting material with the rate 2 s^{-1}. The exited-state properties of mononuclear Ru naphthyridyl-pyridine complexes were studied in different solvents. Our preliminary data indicate that a coordinated water ligand causes a substantial decrease in the excited-state lifetime, probably due to fast deactivation through the vibrational manifold of bound water.

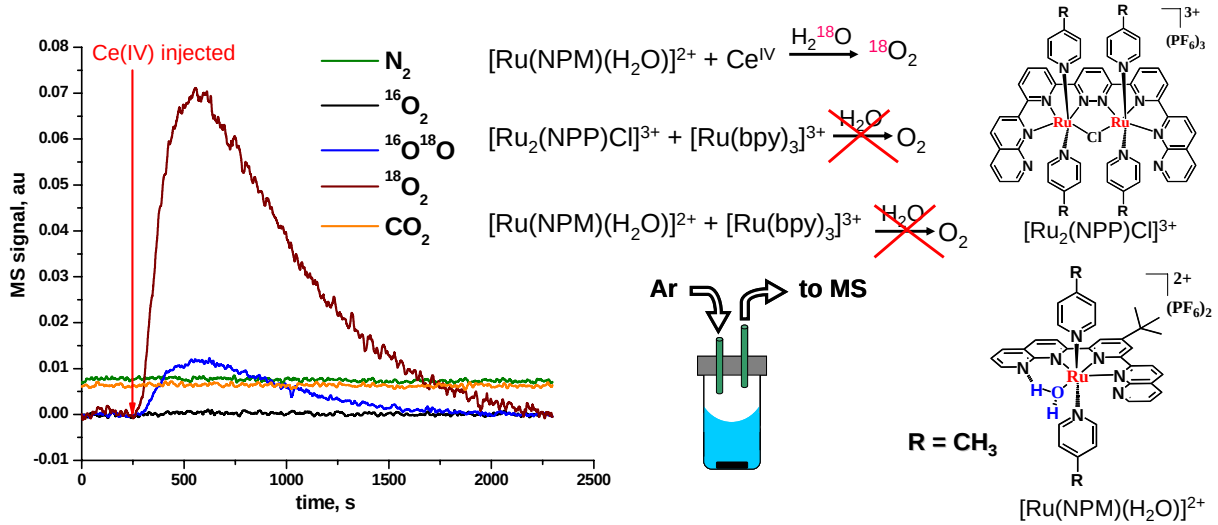

TITANIA NANOTUBES FROM PULSE ANODIZATION OF TITANIUM FOILS

Krishnan Rajeshwar,[1] Wilaiwan Chanmanee,[2] Apichon Watcharenwong,[2] C. Ramannair Chenthamarakshan,[1] Puangrat Kajitvichyanukul,[3] and Norma R. de Tacconi[1]
[1]Center for Renewable Energy Science and Technology (CREST), Department of Chemistry and Biochemistry, The University of Texas at Arlington, Arlington, TX 76019-0065
[2]National Research Center for Environmental and Hazardous Waste Management, Chulalongkorn University, Bangkok, Thailand
[3]Department of Environmental Engineering, King Monkut's University of Technology Thonburi, Bangkok, Thailand

Tailoring the structure and morphology of semiconductor materials on a nanometer size scale has fundamental and practical importance. Nanotubular semiconductor structures are particularly of interest because of their unusual electronic transport and mechanical strength characteristics. In this regard, titania (TiO_2) nanotubes and nanotube arrays have been the subject of many recent studies. An attractive template-free approach for preparing nanotubes, especially aligned arrays of nanotubes, is anodic oxidation of the parent metal in carefully tuned electrolyte environments. Previous anodization studies (including ours) have used either constant potential (potentiostatic) or constant current (galvanostatic) nanotube growth modes. In this poster presentation, pulse anodization is shown to result in better-defined nanotube morphologies than in the constant voltage growth mode. The resultant TiO_2 nanotube arrays will be shown to afford a higher quality of photoresponse. Important mechanistic insights are also furnished by these new data. Careful tuning of the pulse duty cycle and the negative voltage limit point toward the importance of *chemical* (corrosion) processes during the nanotube growth as well as surface passivation effects introduced by the adsorption of the electrolyte species on the growing oxide surface. From a practical process economics perspective, pulse anodization also offers savings in energy consumption relative to the continuous process counterpart. Further, the results from this study provided crucial supporting evidence for existing mechanistic models for anodic growth and self-assembly of oxide nanotube arrays on the parent metal surface. Specifically, adsorption of NH_4^+ species on the TiO_2 surface that is promoted by the negative voltage cycle of the pulse seems to ameliorate the extent of chemical attack of the growing oxide nanoarchitecture by the electrolyte F^- species, resulting in better nanotube morphology. Finally, the effects of the voltage pulse duty cycle and the negative limit values on the nanotube morphology and properties will be described.

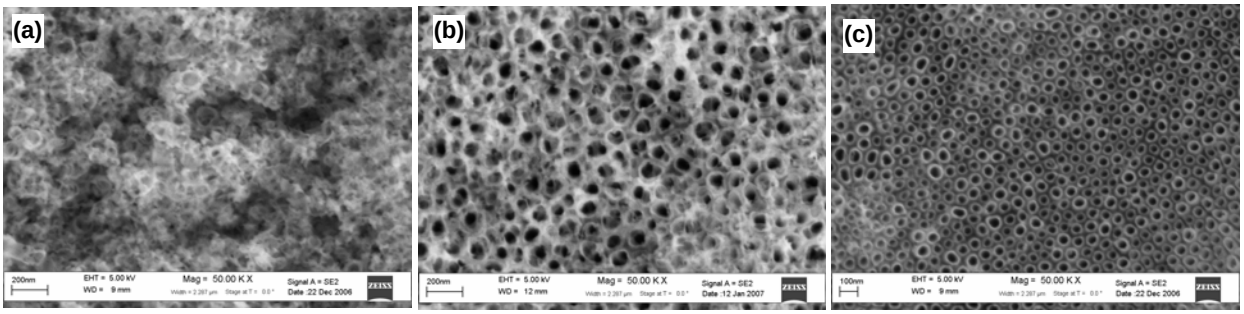

Figure 1. Scanning electron micrographs of TiO_2 films formed from a Ti foil in 0.36 M NH_4F by anodization at constant potential (20 V, 3 h) (a), and by pulse anodization (20 V/-4 V, 3 h) in water (b) and in "wet" glycerol (c).

SOLAR CONVERSION USING CONJUGATED POLYELECTROLYTE/TiO_2 CELLS

H. Jiang, Q. Qiao, P. Taranekar, X. Zhao,
V. D. Kleiman, K. S. Schanze and J. R. Reynolds
Department of Chemistry, University of Florida, Gainesville, FL 32611-7200

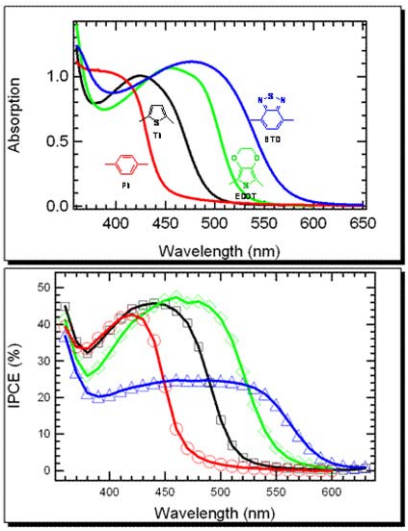

We have demonstrated that a conjugated polyelectrolyte (CPE)/TiO_2 hybrid photoelectrochemical cell operates with good monochromatic quantum efficiency and modest overall solar conversion efficiency. In a continuation of this work, we have fabricated and characterized CPE/TiO_2 hybrid cells using a series of poly(arylene ethynylene) based CPEs with variable band gaps. These polymers feature a backbone consisting of a carboxylated bis(alkoxy)phenylene-1,4-ethynylene unit alternating with a second (arylene ethynylene) moiety (1,4-phenyl, 2,5-thienyl, 2,5-(3,4-ethylenedioxy)thienyl and 1,4-benzo[2,1,3]-thiadiazole). Each of these anionic CPEs adsorbs strongly onto porous nanocrystalline TiO_2. Moreover, they are able to efficiently inject charge into TiO_2 following absorption of visible light. The IPCE and overall power conversion efficiency of the CPE/TiO_2 hybrid cells correlate closely with the polymer's absorption spectra. Transient absorption spectroscopy has been used to gain insight into the dynamics of the charge injection and recombination processes.

In another line of investigation, we have employed hyperbranched CPEs (HB-CPEs) as sensitizers in hybrid TiO_2 photoelectrochemical cells. Both anionic and cationic HB-CPEs can be adsorbed onto porous TiO_2 to produce monolayer and bilayer self-assembled films. Studies have been carried out to explore the effects of deposition sequence (cationic CPE followed by anionic CPE, or *vice versa*) on the film properties and photoelectrochemical cell efficiencies. Results show that both IPCE and overall cell performance are higher for a bilayer configuration compared to monolayer films. Ongoing investigations are exploring the relationship between hybrid film structure and cell performance using electron microscopy and atomic force microscopy.

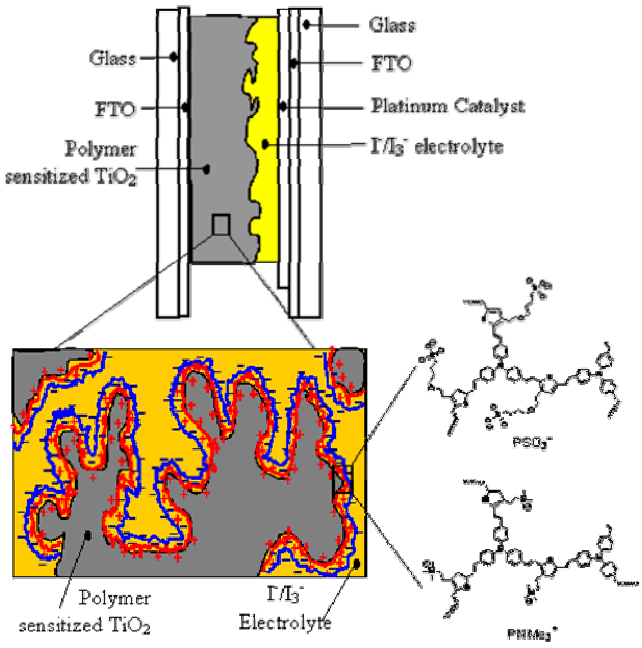

Recent Representative Publications

1. Mwaura, J. K. et al., "Spectral Broadnening in Nanocrystalline TiO_2 Solar Cells Based on poly(p-Phenylene Ethynylene) Sensitizers", *Chem. Mater.* **2006**, *18*, 6109-6111.
2. Taranekar, P. et al., "Hyperbranched Conjugated Polyelectrolytes Bilayer for Solar Cell Applications", submitted.

CONJUGATED POLYELECTROLYTE ARCHITECTURES FOR LIGHT HARVESTING AND ENERGY CONVERSION

R. N. Brookins, L. Hardison, H. Jiang, P. Taranekar, X. Zhao,
V. D. Kleiman, J. R. Reynolds and K. S. Schanze
Department of Chemistry, University of Florida, Gainesville, FL 32611-7200

Conjugated polyelectrolytes (CPEs) based on linear or hyperbranched backbone structures have been synthesized and their photophysical properties characterized. The synthetic efforts are directed towards CPEs with tunable band gaps containing either cationic or anionic side groups. In many cases, we have prepared complementary "pairs" of polymers that feature the same conjugated backbone, but contain either anionic or cationic side groups. In ongoing efforts, we have synthesized linear poly(phenylene ethynylene)- (PPE) and polyfluorene-based polymers. The polyfluorenes have been prepared by a novel approach involving the use of thermally cleavable ester groups as illustrated by graphic **1**. In addition, we are investigating CPE architectures designed to disrupt interchain and/or enhance intrachain interactions. Examples include linear PPEs with dendritic/branched ionic groups (**2**) and hyperbranched conjugated polyelectrolytes (HB-CPEs, **3**).

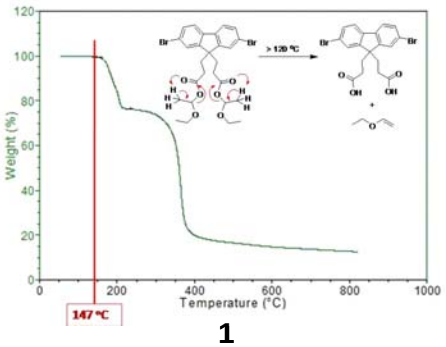

1

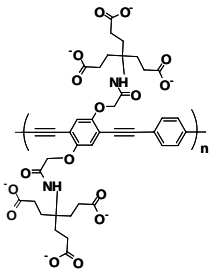

2

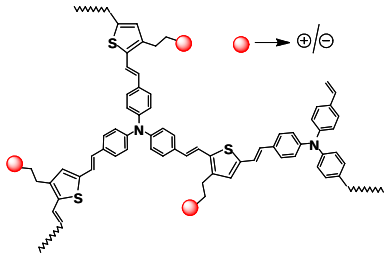

3

The properties of the novel CPEs in solution have been probed using absorption, fluorescence, fluorescence quenching and time-resolved optical spectroscopy. The photophysics of linear CPEs is dependent on both solvent and polymer chain length. Moreover, the fluorescence quenching efficiency is strongly correlated with the degree of CPE chain aggregation, the chain length and the nature and size of the quencher ion. For mono-valent ions the quenching efficiency is enhanced in high molecular weight polymers; by contrast, divalent ions induce polymer chain aggregation, which enhances the quenching efficiency. The solution properties of hyperbranched conjugated polyelectrolytes (HB-CPEs) have been explored. Preliminary results suggest that both anionic and cationic HB-CPEs take on a more "swollen" structure in CH_3OH and a relatively "collapsed" state in H_2O for both cationic and anionic HB-CPEs. The effect of HB-CPE chain solvation on intrachain energy transport and amplified quenching is the subject of ongoing work.

Recent Representative Publications

1. Zhao, X. et al. "Variable Band Gap Poly(arylene ethynylene) Conjugated Polyelectrolytes" *Macromolecules*, **2006**, *39*(19), 6355-6366.
2. Brookins, R. N. et al. "Base-Free Suzuki Polymerization for the Synthesis of Polyfluorenes Functionalized with Carboxylic Acids" *Macromolecules* **2007**, in press.
3. Jiang, H. et al., "Effects of Conjugated Polyelectrolyte Chain Aggregation and Quencher Ion Size on Amplified Quenching", submitted.

A TEMPERATURE-DEPENDENT MECHANISTIC TRANSITION FOR PHOTOINDUCED ELECTRON TRANSFER MODULATED BY EXCITED STATE VIBRATIONAL RELAXATION DYNAMICS

Y. K. Kang, T. V. Duncan, and M. J. Therien
Department of Chemistry
231 S. 34th Street
University of Pennsylvania
Philadelphia, PA 19104-6323

The electron transfer (ET) dynamics of an unusually rigid π-stacked (porphinato)zinc(II)-spacer-quinone (PZn-Q) system, [5-[8'-(4''-[8'''-(2'''',5''''-benzoquinonyl)-1'''-naphthyl]-1''-phenyl)-1'-naphthyl]-10,20-diphenylporphinato]zinc(II) (**2a-Zn**), in which sub van der Waals interplanar distances separate juxtaposed porphyryl, aromatic bridge, and quinonyl components of this assembly, have been measured by ultrafast pump-probe transient absorption spectroscopy over a 80-320 K temperature range in 2-methyl tetrahydrofuran (2-MTHF) solvent. Analyses of the photoinduced charge separation (CS) rate data are presented within the context of several different theoretical frameworks. Experiments show that at higher temperatures, the initially prepared **2a-Zn** vibronically excited S_1 state relaxes on an ultrafast timescale, and ET is observed exclusively from the equilibrated lowest energy S_1 state (CS1). As the temperature decreases, production of the photoinduced charge-separated state directly from the vibrationally unrelaxed S_1 state (CS2) becomes competitive with the vibrational relaxation timescale. At the lowest experimentally interrogated temperature (~80 K), CS2 defines the dominant ET pathway. ET from the vibrationally unrelaxed S_1 state is temperature independent and manifests a subpicosecond time constant; in contrast, the CS1 rate constant is temperature dependent, exhibiting time constants ranging from 4×10^{10} s^{-1} to 4×10^{11} s^{-1}, and is correlated strongly with the temperature-dependent solvent dielectric relaxation timescale over a significant temperature domain. This work not only documents a rare, if not unique example of a system where temperature dependent photoinduced charge separation (CS) dynamics from vibrationally relaxed and unrelaxed S_1 states can be differentiated, but demonstrates a temperature-dependent mechanistic transition of photoinduced CS from the nonadiabatic to the solvent-controlled adiabatic regime, followed by a second temperature-dependent mechanistic evolution where CS becomes decoupled from solvent dynamics and is determined by the extent to which the vibrationally unrelaxed S_1 state is populated.

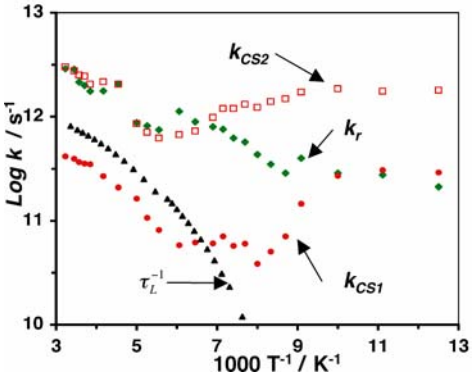

Figure 1. Temperature dependence of the photoinduced charge separation rate constants for vibrationally unrelaxed (red open squares, k_{CS2}) and relaxed (red circles, k_{CS1}) **2a-Zn** S_1 states. The temperature dependent S_1 manifold vibrational relaxation rate constants are shown as green diamonds. The temperature dependent solvent longitudinal relaxation rate constants (τ_L^{-1}) for 2-MTHF are depicted as black triangles.

ELUCIDATING STRUCTURAL DYNAMICS COUPLED TO CHARGE TRANSFER IN DONOR-BRIDGE-ACCEPTOR MOLECULES USING FEMTOSECOND TIME-RESOLVED STIMULATED RAMAN SPECTROSCOPY

Jenny V. Lockard, Annie Butler, and Michael R. Wasielewski
Department of Chemistry
Northwestern University
Evanston, IL 60208-3113

The coupling of structural dynamics to electron transfer in electron donor-bridge-acceptor (D-B-A) molecules is the least well understood part of this fundamental process. In this work, femtosecond time-resolved stimulated Raman spectroscopy (FSRS) is employed to study the changes in molecular structure, especially of the bridge, that occur upon electron transfer in a series of D-B-A systems. The molecules under investigation contain a donor unit consisting of a 3,5-dimethyljulolidine molecule attached to anthracene (DMJ-A). A phenylene-ethynylene unit (PE) serves as the bridge to a naphthalenediimide (NI) acceptor. FSRS spectra of the DMJ-A-PE-NI molecules and the individual components are presented and used to determine the vibrational modes important to the electron transfer process.

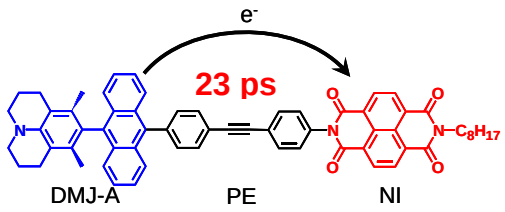

- Ground state PE localized vibrational modes at 1604 and 2241cm^{-1} reach intensity minimum at ~1 ps then regain full intensity by 120 ps
- Intense band at 1450 cm^{-1} is assigned to CN stretch on NI
- Large intensity of the 1450 cm^{-1} band is due to resonance enhancement

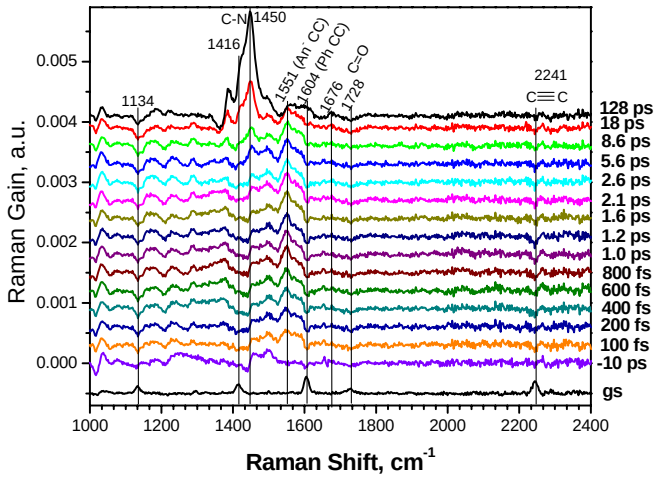

Figure 1. FSRS spectra as a function of time for photoinduced electron transfer within DMJ-A-PE-NI.

We find that the excited state Raman spectrum of the DMJ-A CT state is very similar to that of the known 9-phenylanthracene radical anion, which suggests that the CT state resembles the fully charge-separated state: DMJ$^{+\bullet}$-A$^{-\bullet}$. Following photoexcitation of the corresponding DMJ-A-PE model system, the Raman frequencies observed for PE are localized ground state vibrational modes. Only A$^{-\bullet}$ localized Raman bands are observed, which implies that the PE bridge is weakly coupled to DMJ-A. This implies further that there is no significant change in electron density on PE within DMJ-A-PE in the CT excited state.

In contrast, following photoexcitation of DMJ-A-PE-NI, Figure 1, the ground state PE mode loses intensity at ~1 ps, while the Raman bands assigned to the C=O and C-N stretches of NI$^{-\bullet}$ grow in with τ_{CS} matching that for the formation of DMJ$^{+\bullet}$-A-PE-NI$^{-\bullet}$ obtained from transient absorption measurements. These results show that structural changes to the bridge accompany charge separation.

TOWARD LIGHT DRIVEN WATER OXIDATION IN NANOPOROUS SILICATES THROUGH GRAFTED MANGANESE COMPLEXES

Walter W. Weare and Heinz Frei
Physical Biosciences Division, Lawrence Berkeley National Laboratory
Berkeley, CA 94720

By utilizing metal-to-metal charge-transfer (MMCT) units isolated within a nanoporous silica framework (MCM-41), our lab has recently been able to harness photons to drive the reduction of CO_2 to CO. This poster describes our characterization of the structure and reactivity of possible oxidative units isolated within the same nanoporous structure, with the ultimate goal of utilizing the light-driven oxidation of water to close the photocatalytic cycle.

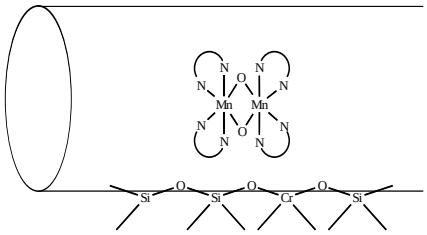

In nature, this demanding reaction is accomplished by four separate single-photon excitation events within the protein complex PSII. The active site contains an isolated Mn_4 core. The quest to structurally and functionally model this manganese core has resulted in a multitude of Mn_xO_y compounds, which we are utilizing as the starting point for our studies. We currently focus on model systems that contain Mn_2O_2 diamond cores, such as $[bpy_4Mn_2O_2][BF_4]_3$, $[phen_4Mn_2O_2][BF_4]_3$, $[terpy_2Mn_2O_2(H_2O)_2][NO_3]_3$, and $[phen_4Mn_3O_4(H_2O)_2][NO_3]_4$. Our initial goal is to gain a detailed structural understanding of the coupling between the Mn cores and visible light charge transfer pumps embedded in the silica pore surface.

We have successfully grafted these compounds onto the surface of MCM-41. To demonstrate that the core remains intact upon grafting, we utilize several techniques which include FT-Raman, EPR, optical DRS, and EXAFS. These techniques are particularly amenable to observation of $Mn_2^{III/IV}O_2$ units, which are conclusively identified with a 16-line EPR signal characteristic of $Mn_2^{III/IV}O_2$ and a Raman resonance at 702 cm^{-1} assigned to the Mn-O stretch of $[bpy_4Mn_2^{III/IV}O_2]$. If the MCM-41 framework contains a redox active metal (such as Cr^{VI}), we observe coupling of the Mn core with the Cr center; EPR (Figure) and Raman spectra indicate the oxidation of $Mn_2^{III,IV}$ to $Mn_2^{IV,IV}$ and reduction of Cr^{VI} to Cr^{V}.

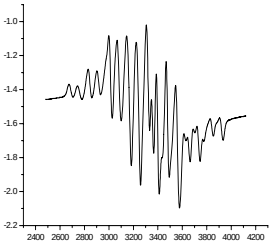

Preliminary results suggest that chemical redox treatment (such as with hydroxylamine or hydrogen) of the manganese grafted nanoporous materials allows control over the oxidation state of the ensemble. Using such strategies, we are attempting to conclusively identify and characterize water oxidation intermediates for each potential catalyst studied, and to understand the structural details of the linkage between grafted manganese complex and charge transfer chromophores on the silica pore surface. Combined with our recent development of binuclear MMCT units with strongly oxidizing donor centers, we anticipate observing light driven oxidation of manganese complexes. This would be an important step toward understanding light driven water oxidation catalysis, and move us closer to our goal of a light driven redox cycle that directly stores energy as a chemical fuel.

List of Participants

Dr. Tae Ahn
Physical Biosciences Division
Lawrence Berkeley National Laboratory
1 Cyclotron Rd
Berkeley, CA 94720
Tel: 510 486 4307
E-mail: taekyuahn@gmail.com

Dr. Neal Armstrong
Department of Chemistry
University of Arizona
Tucson, Arizona 85718
Tel: 520-621-8242
E-mail: nra@u.arizona.edu

Dr. Paul Barbara
Department of Chemistry & Biochemistry
The University of Texas at Austin
1 University Station, A5500
Austin, Texas 78712
Tel: 512-471-2356
E-mail: p.barbara@mail.utexas.edu

Dr. Greg Barber
Materials Research Institute
Pennsylvania State University
104 MRI Building
University Park, PA 16802
Tel: 814-863-9791
E-mail: gdb102@psu.edu

Dr. Victor Batista
Department of Chemistry
Yale University
P.O. Box 208107
New Haven, CT 06520-8107
Tel: 203-432-6672
E-mail: victor.batista@yale.edu

Dr. Matthew Beard
Chemical and Biosciences Center
National Renewable Energy Laboratory
1617 Cole Blvd.
Golden, CO 80401
Tel: 303-384-6781
E-mail: matt_beard@nrel.gov

Dr. Jeff Blackburn
Chemical and Biosciences Center
National Renewable Energy Laboratory
1617 Cole Blvd.
Golden, CO 80401
Tel: 303-384-6649
E-mail: jeffrey_blackburn@nrel.gov

Dr. David Bocian
Department of Chemistry
University of California, Riverside
Riverside CA 92521
Tel: 951-827-3660
E-mail: David.Bocian@ucr.edu

Dr. James Brainard
Chemical and Biosciences Center
National Renewable Energy Laboratory
1617 Cole Blvd.
Golden, CO 80401
Tel: 303 384 6462
E-mail: james_brainard@nrel.gov

Dr. Karen Brewer
Department of Chemistry
Virginia Polytechnic Institute
and State University
Blacksburg, VA 24061-0212
Tel: 450-231-6579
E-mail: kbrewer@vt.edu

Dr. Gary Brudvig
Department of Chemistry
Yale University
P.O. Box 208107
New Haven, CT 06520-8107
Tel: 203-432-5202
E-mail: gary.brudvig@yale.edu

Dr. Louis E. Brus
Department of Chemistry, MS 3125
Columbia University
New York, NY 10706
Tel: 9145482906
E-mail: leb26@columbia.edu

Dr. Ian Carmichael
Radiation Laboratory
University of Notre Dame
Notre Dame, IN 46556
Tel: 574 6314502
E-mail: carmichael.1@nd.edu

Dr. Lin X. Chen
Chemistry Division
Argonne National Laboratory
9700 S. Cass Ave.
Argonne, IL 60439
Tel: 630-252-3533
E-mail: lchen@anl.gov

Dr. Kyoung-Shin Choi
Department of Chemistry
Purdue University
West Lafayette, IN 47907
Tel: 765-494-0049
E-mail: kchoi1@purdue.edu

Dr. Philip Coppens
Department of Chemistry
State University of New York at Buffalo
Buffalo, NY 14260-3000
Tel: 716 645 6800 X2217
E-mail: coppens@buffalo.edu

Dr. Carol Creutz
Chemistry Department
Brookhaven National Laboratory
Upton NY 11973
Tel: 631 344 4359
E-mail: ccreutz@bnl.gov

Dr. Niels Damrauer
Department of Chemistry & Biochemistry
University of Colorado at Boulder
Boulder, CO 80309
Tel: 303-735-1280
E-mail: niels.damrauer@colorado.edu

Dr. Prabir Dutta
Department of Chemistry
The Ohio State University
120 West 18th Avenue
Columbus, Ohio 43210
Tel: 6142924532
E-mail: dutta.1@osu.edu

Dr. Richard Eisenberg
Department of Chemistry
University of Rochester
Rochester, NY 14627
Tel: 585-275-5573
E-mail: eisenberg@chem.rochester.edu

Dr. Randy Ellingson
Chemical and Biosciences Center
National Renewable Energy Laboratory
1617 Cole Blvd.
Golden, CO 80401
Tel: 303-384-6464
E-mail: randy_ellingson@nrel.gov

Dr. C. Michael Elliott
Department of Chemistry
Colorado State University
Ft. Collins, CO 80523-1872
Tel: 970-491-5204
E-mail: elliott@lamar.colostate.edu

Dr. Gregory Fiechtner
Department of Energy
Basic Energy Sciences
19901 Germantown Road
Germantown, MD 20874-1920
Tel: (301)903-5809
E-mail:
gregory.fiechtner@science.doe.gov

Dr. Graham Fleming
Lawrence Berkeley National Laboratory
Mail Stop 50A-4119A
1 Cyclotron Road
Berkeley, CA 94720
Tel: 510 486 6100
E-mail: grfleming@lbl.gov

Dr. Marye Anne Fox
University of California, San Diego
1530 Soledad Ave.
La Jolla, CA 92037
Tel: 858 729 0810
E-mail: chancellor@ucsd.edu

Dr. Arthur Frank
Chemical and Biosciences Center
National Renewable Energy Laboratory
1617 Cole Blvd.
Golden, CO 80401
Tel: 303-384-6262
E-mail: afrank@nrel.gov

Dr. Heinz Frei
Physical Biosciences Division
Lawrence Berkeley National Laboratory
1 Cyclotron Road
Berkeley, CA 94720
Tel: 510 486 4325
E-mail: HMFrei@lbl.gov

Dr. Richard Friesner
Department of Chemistry
3000 Broadway, MC 3110
Columbia University
New York, NY 10027
Tel: 212-854-7606
E-mail: rich@chem.columbia.edu

Dr. Etsuko Fujita
Chemistry Department
Brookhaven National Laboratory
Upton NY 11973-5000
Tel: 631-344-4356
E-mail: fujita@bnl.gov

Dr. Elena Galoppini
Department of Chemistry
Rutgers University
73 Warren Street
Newark, NJ 07102
Tel: 973-353-5317
E-mail: galoppin@rutgers.edu

Dr. Richard Greene
Department of Energy
19901 Germantown Road
Germantown, MD 20874
Tel: 301 903 6190
E-mail: richard.greene@science.doe.gov

Dr. Brian Gregg
Chemical and Biosciences Center
National Renewable Energy Laboratory
1617 Cole Blvd.
Golden, CO 80401
Tel: 303-384-6635
E-mail: brian_gregg@nrel.gov

Dr. David Grills
Chemistry Department
Brookhaven National Laboratory
Upton, NY 11973
Tel: 631-344-4332
E-mail: dcgrills@bnl.gov

Dr. Craig Grimes
Department of Electrical Engineering
Pennsylvania State University
University Park, PA 16802
Tel: 814 8659142
E-mail: cgrimes@engr.psu.edu

Dr. Devens Gust
Department of Chemistry
Arizona State University
Tempe, AZ 85287-1604
Tel: 480-965-4547
E-mail: gust@asu.edu

Dr. Hongxian Han
Physical Biosciences Division
Lawrence Berkeley National Laboratory
1 Cyclotron Rd
Berkeley, CA 94720
Tel: 510 486 4307
E-mail: hhan@lbl.gov

Dr. Alex Harris
Chemistry Department
Brookhaven National Laboratory
Upton, NY 11973-5000
Tel: 631-344-4301
E-mail: alexh@bnl.gov

Dr. Michael Heben
Chemical and Biosciences Center
National Renewable Energy Laboratory
1617 Cole Blvd.
Golden, CO 80401
Tel: 303.641.8476
E-mail: michael_heben@nrel.gov

Dr. Michael Henderson
Chemical Sciences Division
PO Box 999, MS K8-93
Pacific Northwest National Laboratory
Richland, WA 99352
Tel: 509-376-2192
E-mail: ma.henderson@pnl.gov

Dr. Dewey Holten
Department of Chemistry
Washington University
St. Louis, MO 63130
Tel: 314-935-6502
E-mail: holten@wustl.edu

Dr. Michael Hopkins
Department of Chemistry
University of Chicago
Chicago, IL 60637
Tel: 773-702-6490
E-mail: mhopkins@uchicago.edu

Dr. James Horwitz
Department of Energy
19901 Germantown Road
Germantown, MD 20874
Tel: 301 903 4894
E-mail: james.horwitz@science.doe.gov

Dr. Libai Huang
Chemistry Division
Argonne National Lab
Argonne, IL 60439
Tel: 630-252-6069
E-mail: huang-stevenson@anl.gov

Dr. Joseph Hupp
Department of Chemistry
Northwestern University
Evanston, IL 60208
Tel: 847-491-3504
E-mail: j-hupp@northwestern.edu

Dr. James Hurst
Department of Chemistry
Washington State University
Pullman, WA 99164-4630
Tel: 509-335-7848
E-mail: hurst@wsu.edu

Dr. Prashant Kamat
Radiation Laboratory
University of Notre Dame
Notre Dame, IN 46556
Tel: 574-631-5411
E-mail: pkamat@nd.edu

Dr. David Kelley
Department of Chemistry
University of California, Merced
Merced, CA 95344
Tel: 209 228 4354
E-mail: dfkelley@ucmerced.edu

Dr. Lowell Kispert
Department of Chemistry
The University of Alabama
Tuscaloosa, Alabama 35487-0336
Tel: 205 348 7134
E-mail: lkispert@bama.ua.edu

Dr. Valeria Kleiman
Department of Chemistry
University of Florida,
Gainesville, Fl 32611-7200
Tel: 352-392-4656
E-mail: kleiman@chem.ufl.edu

Dr. Bern Kohler
Department of Chemistry
The Ohio State University
Columbus, OH 43210
Tel: 614-688-3944
E-mail: kohler@chemistry.ohio-state.edu

Dr. Nikos Kopidakis
Chemical and Biosciences Center
National Renewable Energy Laboratory
1617 Cole Blvd
Golden, CO 80401
Tel: (303) 384-6222
E-mail: nikos_kopidakis@nrel.gov

Dr. Todd Krauss
Department of Chemistry
University of Rochester
Rochester, New York 14627-0216
Tel: 585-275-5093
E-mail: krauss@chem.rochester.edu

Dr. Frederick Lewis
Department of Chemistry
Northwestern University
Evanston, IL 60208
Tel: 847-491-3441
E-mail: fdl@northwestern.edu

Dr. Nathan Lewis
Department of Chemistry
California Institute of Technology
Pasadena, CA 91125-7200
Tel: 626-395-6335
E-mail: nslewis@caltech.edu

Dr. Tianquan Lian
Department of Chemistry
Emory University
Atlanta, GA 30322
Tel: 404-7276649
E-mail: tlian@emory.edu

Dr. Jonathan Lindsey
Department of Chemistry
North Carolina State University
Raleigh, NC 27695-8204
Tel: 919-515-6406
E-mail: jlindsey@ncsu.edu

Dr. Paul Maggard
Department of Chemistry
North Carolina State University
Raleigh, NC 27695-8204
Tel: 919-515-5079
E-mail: Paul_Maggard@ncsu.edu

Dr. Thomas Mallouk
Department of Chemistry
Pennsylvania State University
University Park, PA 16802
Tel: 814-863-9637
E-mail: tom@chem.psu.edu

Dr. Mark Maroncelli
Department of Chemistry
Pennsylvania State University
University Park, PA 16802
Tel: (814) 865-0898
E-mail: maroncelli@psu.edu

Dr. James McCusker
Department of Chemistry
Michigan State University
East Lansing, MI 48824
Tel: 517-355-9715 ext. 106
E-mail: jkm@cem.msu.edu

Dr. Daniel Meisel
Radiation Laboratory
University of Notre Dame
Notre Dame, IN 46556
Tel: 574 631-5457
E-mail: dani@nd.edu

Dr. Thomas Meyer
Department of Chemistry
University of North Carolina, Chapel Hill
Chapel Hill, NC 27599-3290
Tel: 919-843-8312
E-mail: tjmeyer@unc.edu

Dr. Gerald Meyer
Department of Chemistry
Johns Hopkins University
Baltimore, MD 21218
Tel: 410-516-7319
E-mail: meyer@jhu.edu

Dr. John Miller
Chemistry Department
Brookhaven National Laboratory
Upton, NY 11973
Tel: 631 344 4354
E-mail: jrmiller@bnl.gov

Dr. Thomas Moore
Department of Chemistry & Biochemistry
Arizona State University
Tempe, AZ 85287-1604
Tel: 480 965 3308
E-mail: tmoore@asu.edu

Dr. Ana Moore
Department of Chemistry & Biochemistry
Arizona State University
Tempe, AZ 85287-1604
Tel: 480 965 2953
E-mail: amoore@asu.edu

Dr. James Muckerman
Chemistry Department
Brookhaven National Laboratory
Upton, NY 11973-5000
Tel: 631-344-4368
E-mail: muckerma@bnl.gov

Dr. Marshall Newton
Chemistry Department
Brookhaven National Laboratory
Upton, New York 11973
Tel: 631 344 4366
E-mail: newton@bnl.gov

Dr. Daniel Nocera
Department of Chemistry
Massachusetts Institute of Technology
Cambridge, MA 02139
Tel: 617-253-5537
E-mail: nocera@mit.edu
Dr. James Norris
Department of Chemistry
University of Chicago
Chicago, IL 60637
Tel: 773-702-7864
E-mail: jrnorris@uchicago.edu

Dr. Arthur Nozik
Chemical and Biosciences Center
National Renewable Energy Laboratory
1617 Cole Blvd.
Golden, CO 80401
Tel: 303 384 6603
E-mail: anozik@nrel.gov

Dr. John Papanikolas
Department of Chemistry
University of North Carolina, Chapel Hill
Chapel Hill, NC 27599
Tel: 919 962-1619
E-mail: john_papanikolas@unc.edu

Dr. Bruce Parkinson
Department of Chemistry
Colorado State University
Fort Collins, CO 80523
Tel: 970 491-0504
E-mail: Bruce.Parkinson@colostate.edu

Dr. Piotr Piotrowiak
Department of Chemistry
Rutgers University
Newark, New Jersey 07102
Tel: 973-353-5318
E-mail: piotr@andromeda.rutgers.edu

Dr. Oleg Poluektov
Chemistry Division
Argonne National Laboratory
Argonne, IL 60439
Tel: 630 2523546
E-mail: Oleg@anl.gov

Dr. Dmitry Polyansky
Chemistry Department
Brookhaven National Laboratory
Upton, NY 11973
Tel: (631)344-4357
E-mail: dmitryp@bnl.gov

Dr. Oleg Prezhdo
Department of Chemistry
University of Washington
Seattle, WA 98195
Tel: 206 221-3931
E-mail: prezhdo@u.washington.edu

Dr. Jeffrey Pyun
Department of Chemistry
University of Arizona
Tucson, AZ 85721
Tel: 520-626-1839
E-mail: jpyun@email.arizona.edu

Dr. Krishnan Rajeshwar
Department of Chemistry & Biochemistry
The University of Texas at Arlington
Arlington, TX 76019
Tel: 817 272 3492
E-mail: rajeshwar@uta.edu

Dr. Joan Redwing
Department of Materials Science
and Engineering
Pennsylvania State University
University Park, PA 16802
Tel: 814-865-8665
E-mail: jmr31@psu.edu

Dr. John Reynolds
Department of Chemistry
University of Florida
Gainesville, FL 32611
Tel: 352-392-8544
E-mail: borrero@chem.ufl.edu

Dr. Eric Rohlfing
Department of Energy
19901 Germantown Road
Germantown, MD 20874
Tel: 301 903-8165
E-mail: eric.rohlfing@science.doe.gov Dr.

Garry Rumbles
Chemical and Biosciences Center
National Renewable Energy Laboratory
1617 Cole Blvd.
Golden, CO 80401
Tel: 303 384 6502
E-mail: garry_rumbles@nrel.gov

Dr. Kirk Schanze
Department of Chemistry
University of Florida
Gainesville, FL 32611-7200
Tel: 352-392-9133
E-mail: kschanze@chem.ufl.edu

Dr. Russell Schmehl
Department of Chemistry
Tulane University
New Orleans, LA 70118
Tel: 504-862-3566
E-mail: russ@tulane.edu

Dr. Mark Spitler
Department of Energy
19901 Germantown Road
Germantown, MD 20874
Tel: 301 903 4568
E-mail: mark.spitler@science.doe.gov

Dr. Michael Therien
Department of Chemistry
University of Pennsylvania
Philadelphia, PA 19104-6323
Tel: 215-898-0087
E-mail: therien@sas.uPennsylvania.edu

Dr. Randolph Thummel
Department of Chemistry
University of Houston
Houston, TX 77204-5003
Tel: 713 743-2734
E-mail: thummel@uh.edu

Dr. David Tiede
Chemistry Division
Argonne National Laboratory
Argonne, IL 60439
Tel: 630-252-3539
E-mail: tiede@anl.gov

Dr. Lisa Utschig
Chemistry Division
Argonne National Laboratory
Argonne, IL 60439
Tel: 630-252-3544
E-mail: utschig@anl.gov

Dr. Jao van de Lagemaat
Chemical and Biosciences Center
National Renewable Energy Laboratory
1617 Cole Blvd.
Golden, CO 80401
Tel: 303-3846143
E-mail: jao_vandelagemaat@nrel.gov

Dr. Hendrik Verweij
Department of Materials Science
and Engineering
The Ohio State University
Columbus, OH 43210
Tel: 614-247-6987
E-mail: Verweij.1@osu.edu

Dr. Albert Wagner
Chemistry Division,
Argonne National Laboratory
Argonne, IL 60439
Tel: 630-252-3570
E-mail: wagner@tcg.anl.gov

Dr. Michael Wasielewski
Department of Chemistry
Northwestern University
Evanston, IL 60208-3113
Tel: 847-467-1423
E-mail: m-wasielewski@northwestern.edu

Dr. Walter Weare
Physical Sciences Division
Lawrence Berkeley National Laboratory
1 Cyclotron Road
Berkeley, CA 94720
Tel: (617)312-2911
E-mail: wwweare@lbl.gov

Dr. James Whitesell
University of California, San Diego
1530 Soledad Ave.
La Jolla, CA 92037
Tel: 858 729 0810
E-mail: jkwhitesell@mac.com

Dr. Frank Willig
Fritz-Haber-Institut der MPG
Department TH
Faradayweg 4-6
14195 Berlin
Germany
Tel: 30 49 8413
E-mail: willig@fhi-berlin.mpg.de

Author Index